Emulsion-based delivery systems to improve gut and brain bioaccessibility of curcumin in relation to Alzheimer's disease prevention

A thesis presented in partial fulfilment of the requirements for the degree of

Doctor of Philosophy in Food Technology

at Massey University, Palmerston North, New Zealand

Taciana Lunelli

2023

Para os meus amados pais,

For your constant support

I dedicate this thesis to you.

Abstract

Medium chain triglycerides (MCT) from coconut oil, omega-3 polyunsaturated fatty acids from fish, phospholipids from dairy milk, and curcumin from turmeric all have been recognized for their anti-inflammatory and antioxidant properties. Curcumin is also a potential candidate for Alzheimer's disease (AD) prevention; however, curcumin is poorly bioavailable unless emulsified. The milk fat globule membrane (MFGM) has natural emulsifying properties. I aimed to design an emulsion-based delivery system containing functional oils to encapsulate and deliver curcumin to the brain. I evaluated three commercial MFGM components with coconut and fish oils to produce emulsions with improved curcumin bioavailability. The emulsion structures were characterised by particle size, zeta-potential at the surface, microscopic structure, curcumin loading efficiency, and phospholipid distribution. All emulsions showed stable to particle size changes over 40 days at 4°C. Emulsion particle size decreased significantly with increasing concentrations of emulsifier, and presented negative zeta-potential varying from -50 to -20 mV, with the MFGM fractions creating significantly different charges and curcumin loading efficiency based on phospholipid and protein composition. All MFGM fractions efficiently created stable emulsions with small particle size and encapsulated curcumin. After simulated *in vitro* digestion, the emulsion with the highest phospholipid content had significantly higher curcumin bioaccessibility compared to the others. Fresh and digested emulsions and their components were assessed in the BE(2)-M17 neuroblastoma cell model for amyloid-β (Aβ) toxicity. Emulsions composed of both fish and coconut oils provided greater protection against Aβ toxicity compared to coconut oil alone. Curcumin was transported *in vivo* across the intestinal wall to the bloodstream and across the blood-brain barrier to the brain in rats fed all curcumin delivery formats. The kinetics of curcumin in blood and brain varied depending on the emulsion format. MFGM emulsions significantly reduced the curcumin and its metabolites peak time in blood and brain compared to the commercial curcumin preparation Meriva®, and all emulsions improved overall curcumin bioavailability and accumulation in the brain compared to free curcumin. A novel *ex vivo* approach using rat plasma samples directly in the neuroblastoma cell model requires further optimisation but demonstrated a significant interaction between gender and treatment on cell viability.

Acknowledgment

What a journey this research has been and how important it was to have people to provide support, help and share the good moments. Firstly, I would like to thank my supervisory team, Distinguished Professor Harjinder Singh, Dr. Fran Wolber, Professor Aiqian Ye, Professor Ralph Martins and Professor Manohar Garg. I enjoyed all our meetings and their efforts to make me move forward, for the scientific and personal support I am grateful. I want to thank Harjinder for his scientific inputs and advice and diligent support throughout my PhD. Having the opportunity to work with him is solely a motive for immense appreciation. I can't thank Fran enough for her feedback, constant scientific and personal support, kindness and above all for seeing my potential and helping me move towards a good career, I am so deeply thankful. To Aiqian for his scientific insights, helpful discussions, and feedback. To Manohar for his valuable contributions and help with samples. A big and warm thank you to Ralph, who hosted me in Perth for six months and was so very kind and supportive of me being there during the COVID-19 pandemic, his support made my time easier and more enjoyable, despite the uncertainties and fears of that period.

In memory of Harjot Khaira, who started this research, but whose life was taken too early, I too say thank you. She idealized this research project and left a draft of the literature review, which has been updated and adjusted, while the critical concepts and ideas outlined were kept as much as possible. Harjort's sad ending was the start of a new life journey for me, which makes me believe that God has a purpose that goes beyond our humane understanding.

I am grateful to the Riddet Institute for funding my research and for providing me with a grant to take on an Overseas placement at Edith Cowan University. I am also immensely grateful to have had the opportunity to work closely with Fonterra. Alastair McGibbon was the greatest mentor and advisor; his vast knowledge and kindness were a gift to me. I also liked to thank Kevin Ma for the hours in the lab teaching me how to extract and analyse phospholipids, I am grateful for his kindness to share knowledge and for the help running my samples. To the whole team in Perth who received me with warmth and supported my experiments, in special Pamoda Jayatunga, Prashant Bharadwaj, Eugene Hone and Kitya Dufall; they were all amazing and I missed the catch ups and chats we had. I am also grateful to the team at the Manawatu Microscopy and Imaging Centre (MMIC) at Massey University for their help with the images.

A huge thank you to Carlos Montoya for his help with statistical analysis using SAS. Thanks to Maheeka Weerawarna, which was not only the best office mate but also helped me

with statistical analysis right at the final stages of my data analysis. To Karl Fraser for helping me develop and run the curcumin analysis; he not only helped me, but thought me so much about chemistry, which is not an easy task, I really appreciate that. To Maggie Zou and Peter Zhu at the Riddett lab for so many things they helped me with; they were patient, supportive and always willing to give some of their time and knowledge, thank you. Thanks to Anant Dave for providing feedback, for sharing his experience in the lab and for being prompt to help when I needed. An enormous thank you to the cell culture lab team, Gabrielle Plimmer, Shampa De, and Louise Shaw; they accommodated my needs and thought me so much. I also like to thank Aimee Hamlin for her help during my animal trial at the SAPU. The rat and cell trials of my research would not have been possible to conduct without their support. Thanks to the ethics animal committee for assessing and approving my experiment.

To Carol Thum and Juliana Leite for being there for me when I had trouble coping, being great scientist friends who understood my journey and gave me precious advice. To Mariza for her friendship and for checking my calculations and helping with all that chemistry, I appreciate you sharing your knowledge and supporting me when I needed. Many thanks to my office and lab mates throughout the years, they made the PhD process more enjoyable. A special thanks to Marina Marinea, Esther Onguta, Akashdeep Beniwal, Murali Van Der Zeist, Marit Van Der Zeijden, JieHong Chiang, Feng-Ming Chuang, Giovanna Castillo, Umani Walallawita, Maryam Abshrini, Natasha Nayak and Nikhila Mary Vijay.

I also want to express my gratitude to my family back in Brazil for their constant support, especially my father and my mother, Nelson and Elenita Lunelli. They always supported me in any decisions I made, including moving to New Zealand to pursue an overseas life/career. I know that was not an easy request, but they never discouraged me, despite suffering from my absence. I thank them for believing in me and for making me feel that independent of any outcomes in life, I am enough.

Last but most important, I want to thank my partner, Kambiz Esfandi, for his constant support, patience, and guidance. He always believed in my capabilities and push me through the moments I felt I could not move forward. He was my strength, my motivation, and my example. His experience in living overseas and in science facilitated my adaptation to many situations I faced during my PhD, and for that I am immensely grateful. He made my journey easier, more relaxed and fun. Thanks to him I am becoming a better scientist and person every day.

Table of Contents

Abstract iii
Acknowledgment iv
List of figures x
List of tables xiii
List of abbreviations xviii
Chapter 1 - Introduction 1
Chapter 2 - Literature review 3
2.1 Introduction 3
2.2 Alzheimer's disease 4
2.2.1 Aging 4
2.2.2 Alzheimer's disease pathology 6
2.2.3 Risk factors 9
2.3 The role of diet in late-onset of Alzheimer's disease 9
2.4 Dietary risk factors for AD 14
2.4.1 Saturated fat 14
2.4.2 High carbohydrate diet 15
2.5 Bioactive food components beneficial for AD 16
2.5.2 Curcumin 20
2.5.3 Coconut oil 28
2.5.4 Milk fat globule membrane 29
2.6 Delivery systems for bioactive compounds beneficial for AD 30
2.6.1 Emulsion-based delivery systems 31
2.7 Emulsion digestion 33
2.8 Prospects on delivery of bioactive compounds 36
Chapter 3 - Materials and equipment 37
3.1 Materials 37
3.1.1 Milk Fat Globule Membrane derived material 37
3.1.2 Curcumin 37

3.1.3 Coconut oil (CO)/Medium Chain triglyceride oil (MCT) 37
3.1.4 Fish oil (FO) 38
3.1.5 Phospholipid standard 38
3.1.6 Curcumin Standard 38
3.1.7 Chemicals 39
3.2 Equipment 39
3.2.1 Water bath 39
3.2.2 pH meter 40
3.2.3 High-performance liquid chromatography (HPLC) 40
3.2.4 Centrifuges 40
3.2.5 Handheld homogeniser 40
3.2.6 Homogeniser 41
3.2.7 Mastersizer 41
3.2.9 Zetasizer 42
3.2.10 HPLC-LC/MS 43
3.2.11 Confocal Laser Scanning Microscopy 43
Chapter 4 - Milk fat globule membrane derived material as an emulsifying agent in the preparation of curcumin loaded oil-in-water emulsions 44
Abstract 44
4.2 Introduction 45
4.3 Materials and Methods 47
4.3.1 Materials 47
4.3.2 Methods 48
4.4 Results and discussion 53
i) Selection of emulsions components 53
ii) Selection of emulsifier concentrations based on particle size and stability over time 54
iii) Characterization of emulsions prepared using selected MFGM concentrations 58
iii) Curcumin and phospholipid distribution between the oil and aqueous phase 68
4.5 Conclusions 73

Chapter 5 - Behaviour of curcumin loaded oil-in-water emulsions prepared using milk fat globule membrane material under *in vitro* gastrointestinal conditions 75

Abstract 75

5.1 Introduction 76

5.2 Materials and Methods 80

5.2.1 Materials 80

5.2.2 Methods 80

5.3 Results and discussion 84

a) Particle size and zeta-potential during in vitro gastrointestinal digestion 84

5.5 Conclusions 107

Chapter 6 - *In vivo* delivery of curcumin and its metabolites to the brain and plasma of male and female Sprague-Dawley rats.....109

Abstract 109

6.1 Introduction 110

6.2 Materials and Methods 114

6.2.1 Materials 114

6.2.2 Methods 114

6.2.2.1 Emulsion preparation 114

6.2.2.2 *In vivo* assay using Sprague-Dawley rats 115

6.2.2.3 Preparation of rat feed 117

6.2.2.4 Sample preparation and HPLC-LC/MS analysis 118

6.2.2.5 HPLC-LC/MS 120

6.2.2.6 Statistical analysis 121

6.3 Results and discussion 121

6.4 Conclusions 135

Chapter 7 Effect of *in vitro* digested emulsions and *ex vivo* post-prandial serum on neuronal cell viability and protection against amyloid-beta toxicity *in vitro* 136

7.1 Abstract 136

7.2 Introduction 136

7.3 Materials and methods 138

7.3.1 Materials 138
7.3.2 Methods 138
7.4 Results and discussion 142
7.4.1 Effect of non-digested and digested emulsions on cell proliferation 142
7.4.2 Effect of non-digested and digested emulsions against Aβ-induced toxicity 146
7.4.3 Effect of serum of rats fed formulations on cell proliferation 152
7.4.4 Effect of serum from rats fed formulations against AB-induced toxicity 156
7.5 Conclusions 161
Chapter 8 Discussion and future research prospects 163
8.1 General discussion 163
8.2 Future research prospects 166
References 168
Appendixes 200

List of figures

Figure 2.1. Global population by broad age groups, 1980, 2017, 2030, 2050. Data source: United Nations (2017).....5
Figure 2.2. Illustration of the amyloidogenic pathway. 7
Figure 2.3. Curcumin chemical structure (PubChem, 2004) and illustration of turmeric (Curcuma longa) plant 21
Figure 2.4. Mechanisms of curcumin action in AD.....22
Figure 3.1. Two valve homogenizer APV 2000, Silkeborg, Denmark.....41
Figure 3.2. Mastersizer 2000 E (Malvern Instruments, Malvern, Worcestershire, UK) 42
Figure 3.3. Zetasizer nano ZS (ZEN3600, Malvern Instruments Ltd. Malvern, Worcestershire, UK) 43
Figure 4.1. Mean particle size ($d_{3,2}$) of emulsions prepared using varying concentrations of three MFGM materials.....55
Figure 4.2. Particle size distribution of emulsions prepared using varying concentrations of three MFGM materials.....57
Figure 4.3. Particle size distribution of emulsions at day 0 (square), day 7 (diamond), day 20 (triangle) and day 40 (circle) of storage at 4°C (a=MFGM1, b=M2FGM, c=MFGM3).....60
Figure 4.4. Zeta-potential of emulsions prepared using selected emulsifier concentrations. .62
Figure 4.5. Particle size distribution of emulsions prepared using selected emulsifier concentrations. 63
Figure 4.6. CLSM images of emulsions prepared using selected emulsifier concentrations .64
Figure 4.7. Loading efficiency (LE - total emulsion basis) of emulsions prepared using selected emulsifier concentrations. 65
Figure 4.8. Phospholipid class distribution in emulsions prepared using selected emulsifier concentrations 68
Figure 4.9. Curcumin concentration in cream phase (green) and aqueous phase (pink) of emulsions prepared using selected emulsifier concentrations 69
Figure 4.10. Total phospholipid concentration in surface and aqueous phases of emulsions prepared using selected emulsifier concentrations after phase separation by centrifugation.. 73
Figure 5.1 Schematic representation of lipid digestion and the possible changes in emulsion structure as it passes through the GIT from mouth to small intestine. Adapted from Singh, Ye & Horne, 2009. 78

Figure 5.2. Confocal images and particle size distribution of emulsion systems stabilized by MFGM derived materials.....88
Figure 5.3. Kinetics of Free Fatty Acid (FFA) release from emulsions prepared using MFGM 92
Figure 5.4. Representation of sample phase separation after high speed centrifugation (left) and an emulsion system centrifuged (15000g) after simulated *in vitro* gastric digestion. 97
Figure 5.5 Phospholipid distribution in the cream and aqueous phase of emulsions (a) prepared using MFGM.....98
Figure 5.6. Phospholipid concentration and absolute class distribution in emulsion systems prepared using MFGM fractions and their respective gastric and intestinal digesta. 102
Figure 5.7. Relative phospholipid class distribution in emulsion systems prepared using MFGM fractions and their respective gastric and intestinal digesta.....103
Figure 6.1 Curcumin dissolved in MCT oil (5 mg/ml) on the left and curcumin solubilised in oil in emulsified state after high pressure homogenisation on the right (A); Dried emulsion after freeze-drying on the left, and example of treatment treats on the right (B),.....115
Figure 6.2. Schematic representation of rat trial 116
Figure 6.3. A) Rat eating a solid treat; B) Rat voluntarily grabbing treat after training period; C) Syringe administration applied to rats that were not accepting treat eating 117
Figure 6.4. Curcumin peaks detected by HPLC-LC/MS. 122
Figure 6.5. Curcumin metabolite peaks detected by HPLC-LC/MS.. 123
Figure 6.6. Kinetic differences in the appearance of curcumin + metabolites in plasma after oral administration of treats containing free curcumin (free Curc), bioavailable curcumin formulation (Meriva®), emulsion system 1 (EM1) and emulsion system 2 (EM2).....124
Figure 6.7. Kinetic differences in the appearance of curcumin in plasma after oral administration of treats containing free curcumin (free Curc), bioavailable curcumin formulation (Meriva), emulsion system 1 (EM1) and emulsion system 2 (EM 2).....126
Figure 6.8. Kinetic differences in the appearance of CG in plasma after oral administration of treats containing free curcumin (free Curc), bioavailable curcumin formulation (Meriva), emulsion system 1 (EM1) and emulsion system 2 (EM 2)......127
Figure 6.9. Kinetic differences in the appearance of CS in plasma after oral administration of treats containing free curcumin (free Curc), bioavailable curcumin formulation (Meriva), emulsion system 1 (EM1) and emulsion system 2 (EM 2)......128

Figure 6.10. Normalised kinetics for Curc, CG and CS in plasma after oral administration of treats containing free curcumin (a), bioavailable curcumin formulation Meriva (b), emulsion system EM1 (c) and emulsion system EM2 (d).. 129
Figure 6.11. Kinetics of Curc in brain of rats after 15, 30, 60 and 120 minutes of oral administration of treats containing free curcumin (free Curc), bioavailable curcumin formulation (Meriva), emulsion system 1 (EM1) and emulsion system 2 (EM 2). 132
Figure 6.12. Phospholipid distribution in plasma. 135
Figure 7.1. Effect of emulsion systems on M17 cell viability after 72 hours incubation at 0.5 and 1% concentration in DMEM/F12 as a replacement for FBS.. 143
Figure 7.2. Effect of oil and emulsifier on M17 cell viability after 72 hours incubation in DMEM/F12 as a replacement for FBS.. 145
Figure 7.3. Cell viability for *M17* cells treated with Aβ at different concentrations (15, 20, 25uM) over 72 hours incubation. Viable cells expressed in percentage of control.. 147
Figure 7.4. Graphical representation of data above and under toxicity threshold.. 149
Figure 7.5. Effect of emulsion systems on cell viability after Aβ-induced toxicity over 72 hours incubation at 0.5 and 1% concentration in DMEM/F12 as a replacement for FBS.....150
Figure 7.6. Effect of oil and emulsifier on cell viability after Aβ-induced toxicity over 72 hours incubation in DMEM/F12 as a replacement for FBS.. 151
Figure 7.7. The optical density, equating to cell viability, after FBS or serum treatment with control and emulsion 2 treatment rat serum samples, was assessed to determine optimal working concentrations in M17 cells.. 154
Figure 7.8. Effect of treatment and gender on the viability of M17 cells treated with serum from rats fed free or encapsulated curcumin.....155
Figure 7.9. Cell viability normalised to FBS treated control wells, which were set at 100% (black horizontal line), for test wells with rat serum samples collected 15 – 120 minutes after ingestion of different curcumin treatments. 156
Figure 7.10. Cell viability as a percentage of FBS treated cells over time for different treatments added at 1% concentration to DMEM/F12 cell culture media.. 158
Figure 7.11. Loss in viability induced by Aβ. a) Effect of treatment and time on cell viability. b) Effect of gender and treatment on cell viability. 159

List of tables

Table 2.1. Summary of natural bioactive compounds tested against AD biomarkers in vitro/in vivo and their primary outcomes 13
Table 2.2. Composition of Milk Fat Globule Membrane. Adapted from (Singh, 2006) 30
Table 3.1. MFGM composition.....37
Table 3.2. Fatty acid composition of Essente and CocoMCT® oils used for emulsion preparation 38
Table 3.3. List of general chemicals used throughout the experiments. Chemicals used for specifically for each individual set of experiments are described in each chapter and were purchased from Sigma Aldrich Chemical Co., St. Louis, MO, USA unless otherwise specified. 39
Table 4.1. Emulsions coding and composition. CO = virgin coconut oil; FO = Fish oil.....49
Table 4.2. HPLC elution gradient 52
Table 4.3. Ion source conditions 52
Table 4.4. Precursor Ion (PIS) and Neutral loss (NL) scanning conditions.....52
Table 4.5. Mean ± SEM (N=3) phospholipid concentrations of MFGM fractions.....54
Table 4.6. Mean particle size ($d_{3,2}$) of emulsions prepared using selected emulsifier concentrations 59
Table 4.7. Phospholipid class distribution in emulsions prepared using selected emulsifier concentrations 67
Table 4.8. Mean phospholipid concentration of emulsions prepared using selected emulsifier concentrations 71
Table 5.1. Emulsions coding and composition. MCT = Medium chain triglyceride oil; FO = Fish oil 81
Table 5.2. Mean particle size (d_{43}) and zeta-potential of fresh emulsions systems stabilized by MFGM and corresponding gastric and intestinal digestion.....86
Table 5.3. Lipolysis kinetic data of in vitro intestinal digestions of various emulsions prepared using MFGM-derived materials.....94
Table 5.4. Curcumin bioaccessibility after *in vitro* gastric and intestinal digestion of emulsions stabilized by MFGM. 96
Table 5.5. Phospholipid distribution in emulsions prepared using MFGM and their correspondent cream and aqueous phase and gastric and intestinal digesta. 105

Table 5.6. Statistical findings based on 3-wayANOVA on the effects of MFGM fraction, oil type and digestion on the distribution of individual phospholipid groups across emulsions and their corresponded cream phase.....107
Table 6.1. Pre-clinical and clinical studies using various formats, doses and administration routes for curcumin.....113
Table 6.2. Final composition of rat treats used to deliver curcumin.....118
Table 7.1. Composition of emulsions systems.....140
Table 7.2. Composition of cell treatment media.....141

List of abbreviations

CO	Virgin coconut oil
FO	Fish oil
MCT	Medium chain triglycerides
ω-3	Omega-3
PUFA	Polyunsaturated fatty acids
C	Curcumin
DMC	Desmethoxycurcumin
BDMC	Bisdemethoxycurcumin
CG	Curcumin β-D-glucuronide
CS	Curcumin sulphate tetrabutylammonium
D6C	$_2H^6$-curcumin
BPAG-d6	A-d6 β-D-glucuronide
(O/W)	Oil in water emulsions
MFGM	Milk fat globule membrane
MFGM1	Milk fat globule membrane fraction one (Lipid700)
MFGM2	Milk fat globule membrane fraction two (BPC50 GU09)
MFGM3	Milk fat globule membrane fraction three (HFWPC70)
PE	Phosphatidylethanolamine
PC	Phosphatidylcholine
SMP	Sphingomyelin
PS	Phosphatidylserine
PI	Phosphatidylinositol
TPL	Total phospholipids
LPE	Lyso-Phosphatidylethanolamine,
LPC	Lyso-Phosphatidylcholine
EFA	Essential fatty acids
EPA	Eicosapentaenoic acid
DHA	Docosahexaenoic acid
TAG	Triacyl glycerol
SCT	Short chain triglycerides
LCT	Long chain triglycerides
MAG	Monoacylglycerol
DAG	Diacylglycerol
FFA	Free fatty acids

GIT	Gastrointestinal tract
$d_{3,2}$	Surface weighed particle size
$d_{4,3}$	Volume weighed particle size
LE	Loading efficiency
ANOVA	Analysis of variance
SSF	Simulated salivary fluid
SGF	Simulated gastric fluid
SIF	Simulated intestinal fluid
FBS	Foetal bovine serum
DMEM	Dulbecco's Modified Eagle Medium
F12	Nutrient Mixture F-12
MTS	3-[4,5-dimethylthiazol-2-yl]-2,5 diphenyl tetrazolium bromide assay
M17	BE(2)-M17 human neuroblastoma cells
BBB	Blood-brain barrier
AD	Alzheimer's disease
ROS	Reactive oxygen species
Aβ	Amyloid-β peptide
MCI	Mild Cognitive Impairment
APP	Amyloid Protein Precursor
BACE1	β-secretase
ApoE4	Apolipoprotein E
MMSE	Mini-Mental State Examination

Chapter 1 - Introduction

Alzheimer's disease (AD) is the most common form of dementia in people aged 65 or over, and accounts for 60 to 80% of neurodegenerative disease cases worldwide (World Health Organization [WHO], 2022). AD is a progressive neurodegenerative disease that causes impaired judgement, memory dysfunction, temporal and spatial disorientation and loss of lexical access (Sahni et al., 2011). The disease is believed to start years before symptoms appear, with a lengthy preclinical stage where pathological changes occur without symptoms. Before the development of clinical dementia, a stage characterized by memory complaints and mild cognitive impairment is observed (Gerstenecker and Mast, 2015). Pathologically, AD is characterized by the accumulation of intracellular neurofibrillary tangles and extracellular senile plaques of amyloid-β peptides (Aβ) (Sennvik et al., 2000). Its exact cause is still uncertain, but a series of factors can contribute to its onset, and despite years of extensive investigations, no curative treatments are available yet (Belkouch et al., 2016).

The search and use of potential natural agents with efficient therapeutic effects against neurodegenerative disorders is essential and many researchers have focused on the role of diet and nutrition for prevention of AD. The food sector is concerned with developing functional foods with benefits for health and well-being. Some of the most important groups of foods pointed to be beneficial include polyunsaturated fatty acids and polyphenols, due to their antioxidant and anti-inflammatory activities. In general, foods containing bioactive compounds are related to the decline in the risk of important chronic diseases (Hernández-Ledesma et al., 2017).

The pathological processes in AD, as in many chronic diseases, are driven partly by oxidative stress. Regular intake of dietary antioxidants, such as curcumin, therefore may reduce the risk of AD development. However, many bioactive antioxidants are poorly bioavailable, often due to their hydrophobic nature. This presents a challenge to researchers: to retain bioactivity while increasing bioavailability, while simultaneously presenting the bioactive compound in a food format that consumers are willing to eat on a daily basis. For curcumin, improved delivery formats that can increase its effects are still not available and fully validated, suggesting that more research is needed to improve the bioavailability of curcumin and to create a suitable product for clinical trials. However, improved delivery formats that can increase its effects are still not available and fully validated, suggesting that more research is

needed to improve the bioavailability of curcumin and to create a suitable product for clinical trials.

Research objectives

The overall aim of this research is to design food formulations that can deliver bioactive compounds for prevention of Alzheimer's disease.

Objective 1. To identify food or food-derived bioactive compounds that are known to be beneficial for brain health, particularly Alzheimer's Disease, from published literature and human clinical data (Chapter 2).

Objective 2. To develop an oil-in-water emulsion for delivery of bioactive compounds identified in objective 1 (omega-3 fatty acids, MCT and curcumin), using milk fat globule membrane (MFGM) derived material as an emulsifier (Chapter 4).

Objective 3. To determine the behaviour of MFGM stabilised emulsions under *in vitro* digestion conditions, with a focus on bioaccessibility of curcumin (Chapter 5).

Objective 4. To assess the *in vivo* delivery, bioavailability, and metabolism of curcumin encapsulated in emulsions prepared using MFGM material rich in phospholipids (Chapter 6).

Objective 5. To assess the effect of *in vitro* and *ex vivo* digested curcumin loaded emulsions against amyloid-β toxicity *in vitro* using the M17 neuroblastoma cell line (Chapter 7).

Chapter 2 - Literature review

This review aims to provide current information on functional foods and discuss the relationship between diet and lifestyle in Alzheimer's disease (AD.) An outline of the disease mechanisms and the main risk factors will be presented, and the effects of different food groups and lifestyle on AD risk will be discussed. The impact of individual functional components of foods will also be discussed, along with the potential for their use as a preventative approach to delay disease onset.

2.1 Introduction

AD accounts for 60 to 80% of cases worldwide and affects mostly people aged 65 or over (WHO, 2022). AD is a devastating neurodegenerative disease. Once the symptoms appear it is often too late for interventions as pathological changes precede the clinical symptoms. First observed signs are characterised by memory complaints and confusion and followed by mild cognitive impairment. As the disease progresses the memory impairment worsens to moderate and severe, causing memory loss, loss of verbal communication abilities, disorientation, and impaired judgment (Dubois and Albert, 2004, Sahni et al., 2011). Evidence suggests that pathologically, AD is characterized by the accumulation of intracellular neurofibrillary tangles inside neurons and extracellular senile plaques of amyloid-β peptides (Aβ) that can be observed in the brain, central nervous system, and also blood stream (Bateman et al., 2012, Atwood et al., 2003b). Its exact cause is still uncertain, but a number of genetic and environmental factors can contribute to its onset, such as age, genetic predisposition, level of education, presence of other non-communicable disease and lifestyle (Baumgart et al., 2015). Despite 100 years of extensive investigations, no curative treatments are available yet.

A recent guideline published in the *Lancet* (Livingston et al., 2020) suggests that up to 35% of dementia cases could be potentially prevented through changes in lifestyle. Obesity, hypertension, diabetes and dyslipidaemia have all been associated with increased incidence of dementia and are all directly related to diet. Considering the strong impact food can have on AD, the search and use of potential natural agents with efficient therapeutic effects against neurodegenerative disorders is an important and growing field among researchers. Thus, the food sector is concerned with developing functional foods with positive benefits for health and well-being. Some of the most essential food groups shown to be beneficial include polyunsaturated fatty acids (PUFA) and polyphenols due to their antioxidant and anti-

inflammatory activities. In general, foods containing bioactive compounds are correlated with a decline in the risk of chronic diseases (Hernández-Ledesma et al., 2017).

The primary way bioactive compounds can prevent and treat some diseases is to act as antioxidants, especially in AD, where oxidative stress plays an important role. Curcumin, a natural phenolic compound isolated from the spice herb *Curcuma longa,* has been pointed as an effective natural treatment for AD. In AD, curcumin acts by inhibiting acetylcholinesterase (AChE) activity and protecting cells against Aβ toxicity (Ono et al., 2004). AChE is a crucial enzyme in the nervous system that regulates the neurotransmitter acetylcholine (Ach). By rapidly breaking down acetylcholine into its components, AchE terminates its action in the synaptic cleft, where nerve signals are transmitted. This ensures precise and controlled signal transmission, preventing prolonged excitation of neurons or muscle cells. AchE's role in regulating acetylcholine levels is vital for maintaining normal nerve function and preventing overstimulation, contributing to the delicate balance in the nervous system (Massoulié, 2002, Soreq and Seidman, 2001).

Curcumin also presents antioxidant activity and effectiveness in the inhibition of Aβ1-42 fibrillogenesis (Serafini et al., 2017). However, it shows low bioavailability, which means that it cannot reach the therapeutic target at the desired dose even when consumed in high amounts (Naksuriya et al., 2014). The best way to overcome this challenge is to develop delivery systems to encapsulate curcumin and protect it from the gastrointestinal digestive system, thus increasing its delivery to blood and to the desired site of action. Due to curcumin's high hydrophobicity and human physiology being essentially an aqueous-based system, oil-in-water emulsions are suggested as the most prominent and effective choice to deliver curcumin and improve its use as a therapeutic compound (Araiza-Calahorra et al., 2018).

Prevention strategies, such as diet and lifestyle, are considered necessary in the fight against AD. They can potentially reduce the risk, delay disease onset, and act as a preventative treatment against this devastating disease (Hooijmans and Kiliaan, 2008).

2.2 Alzheimer's disease

2.2.1 Aging

Ageing is a global occurrence that significantly impacts the structure of populations and has become one of the most remarkable social transformations of the twenty-first century. The number of older people is growing faster than the number of people in any younger age

group. This tendency is due to falls in fertility, declining mortality and medical advances (United Nations, 2017). As a result, the number of people aged 60 years or more has shown a considerable increase in the last few years in most countries around the globe (Figure 2.1). According to projections, this growth will be even more accelerated in the following decades (United Nations, 2017). In 1980 the global population aged 60 years or more was 382 million; in 2017 it had more than doubled to 962 million older people worldwide. This number is projected to reach nearly 2.1 billion in 2050.

Along with the increase in life expectancy, age-related health conditions are expected to rise. The body's cellular functions and resistance to stress drops dramatically with ageing, becoming one of the main risk factors for cardiovascular diseases (CD) and neurodegenerative diseases (ND) (García-Serrano et al., 2020). It is important to note that a series of risk factors and biomarkers for CD overlap with those for ND, such as oxidative damage and microglial inflammation. This suggests that preventative strategies currently applied for CV disease could be relevant and replicated for ND including AD (Cole et al., 2005b).

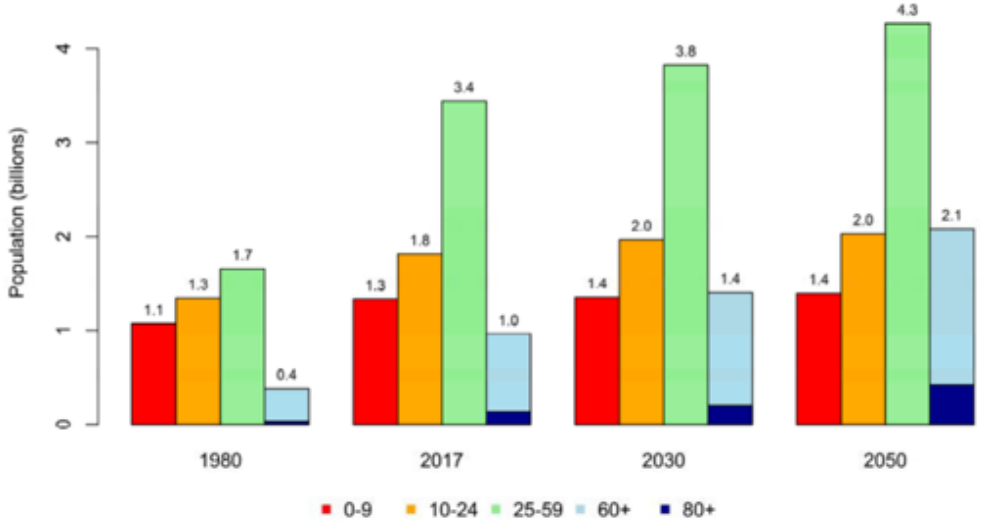

Figure 2.1. Global population by broad age groups, 1980, 2017, 2030, 2050. Data source: United Nations (2017)

To date, around 50 million people are living with dementia worldwide, and this number is projected to reach 152 million in 2050 (WHO, 2022). The onset of neurodegenerative disorders in a population brings consequences for many sectors, such as labour, financial markets, demand for goods, transportation, housing, health care and medical support (Serafini et al., 2017). In New Zealand, 70,000 people have dementia today, and this number is estimated to more than double by 2050, reaching a total of 170,000 patients in the country. The associated costs with dementia were $1.676 billion in 2016, representing a 75% increase since 2011 and

a projection to reach $4.6 billion by 2050 (Alzheimer's New Zealand, 2021). Immediate efforts are needed to prevent and delay the onset of AD to minimize its impacts for individuals, their families and whanau, and society.

2.2.2 Alzheimer's disease pathology

AD is a progressive neurodegenerative disease that causes loss of memory and cognitive function. The most accepted pathological characteristic of AD is the extracellular accumulation of the Aβ peptide as senile plaques primarily in the brain; however, Aβ can also be observed in lower levels outside of the brain, in the peripheral nervous system and in blood vessels in the brain (Bateman et al., 2012, Atwood et al., 2003a). The disease was named after Dr. Alois Alzheimer. His ground-breaking discovery in the early 20th century laid the foundation for understanding the disease's pathology. The original disease description highlighted the presence of abnormal protein aggregates, specifically Aβ plaques and tau tangles, in the brains of affected individuals. These hallmark pathological features have become central in the study of Alzheimer's disease (Verhey, 2009). Research has since expanded our understanding of the disease's underlying mechanisms, revealing the involvement of neuroinflammation (Amoretti et al., 2002), gut microbiota alterations (Liu et al., 2020a), and oxidative stress (Behl, 1999) as potential contributors to Alzheimer's pathogenesis.

In healthy individuals, the Amyloid-β Protein Precursor (APP) is broken down by the action of the enzymes α-secretase and γ-secretase, generating a soluble peptide that is easily eliminated by the body. In AD, γ-secretase interacts with β-secretase (BACE1) instead of α-secretase, creating an insoluble Aβ peptide (40-42 amino acids), which tends to bond together and form plaques known as senile plaques mostly in the brain, outside of the neurons (Figure 2.2), infiltrated by reactive microglia and astrocytes that create inflammation. This irregular folding and aggregation of peptides into senile plaques is associated with the initial development of neurodegeneration in AD (Kumar et al., 2015). The events that progressively develop following plaque development include increased calcium influx, oxidative stress, inflammatory processes, activation of kinase and phosphatase activities, cytokines, irregular regulation of transcription factors, and disruptions in ion channel and receptor gene expression (Park and Kim, 2002, Thapa et al., 2013).

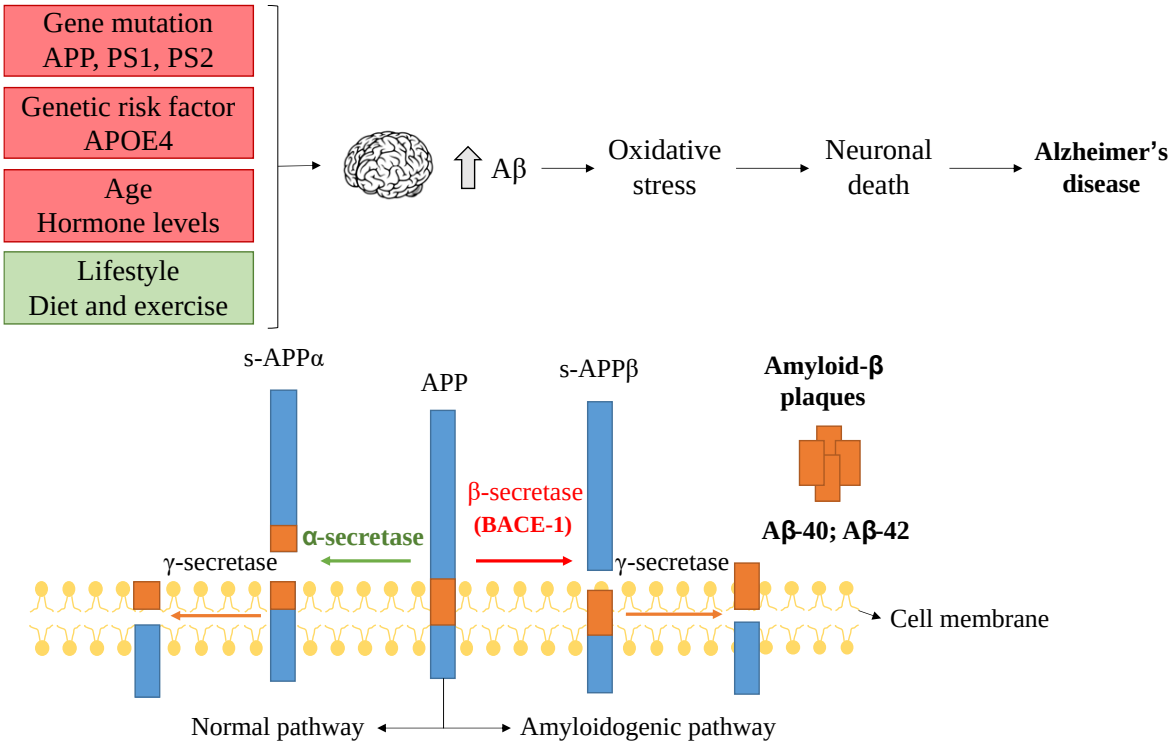

Figure 2.2. Illustration of the amyloidogenic pathway. Amyloid precursor protein (APP) undergoes cleavage primarily by beta-secretase (β-secretase or BACE1), leading to the release of a soluble fragment and leaving a membrane-bound C-terminal fragment. Subsequently, gamma-secretase cleaves the C-terminal fragment, generating beta-amyloid peptides of varying lengths, with Aβ40 and the more toxic Aβ42 being prominent. The accumulation of Aβ42 promotes aggregation, forming amyloid plaques. Adapted from (Cole and Vassar, 2007)

In addition to Aβ plaques, intracellular tau tangles may initiate the disease cascade in AD. Tau is a microtube-associated protein found in the central nervous system (CNS) and peripheral nervous system, primarily located in healthy neurons' axons (Neddens et al., 2018). Tau preserves the microtubules' stability and monitors intracellular traffic (Li et al., 2019). The activation of the enzyme kinase transfers phosphate groups to tau, changing its shape to a hyperphosphorylated state and decreasing its affinity for microtubules. Consequently, a decrease in overall tubulin assembly destabilizes the microtubules and disrupts the intracellular transport system. In AD, the interruption of normal tau function leads to a cascade of events culminating with large amounts of phosphorylated tau accumulated inside the neurons, specifically in the cytoplasm. Accumulated tau forms intraneuronal neurofibrillary tangles (NFTs) culminating with neuronal death (Novak et al., 2018). The consequent impairment of tau function leads to an increase in mitochondrial function burden, followed by mitochondrial dysfunction and ends with releasing reactive oxygen species (ROS) (Lin and Beal, 2006). c-Jun N-terminal kinases (JNK) are protein kinases involved in stress signalling pathways. Stressing elements, such as those formed in AD pathology including pro-inflammatory

cytokines, oxidative stress, growth factors, and Aβ peptides activate the JNK pathway, thereby contributing to the damage caused by AD (Yarza et al., 2016).

In the pursuit to understand the mechanisms of AD, a number of models, both *in vitro* and *in vivo*, have been used to simulate and understand the complexities of this neurodegenerative disorder. *In vitro* models involve the use of neuronal cells, often derived from human pluripotent stem cells, exposed to various stimuli to induce pathological features of AD. These models provide a controlled environment to study molecular and cellular aspects of disease progression, enabling the investigation of specific cellular responses, such as amyloid-beta aggregation and tau hyperphosphorylation (Hardy and Selkoe, 2002, Takashima, 2006). On the other hand, *in vivo* models aim to mimic the complex relationship of cellular, anatomical, and systemic factors present in the living organism. Transgenic mouse models expressing mutated forms of human amyloid precursor protein (APP) and tau protein have been key in the understanding of AD pathology. These models allow researchers to study the effects of potential therapeutic interventions on cognitive decline and neuropathology in a more complete context (Games et al., 1995, Götz et al., 2004).

Both *in vitro* and *in vivo* models have their respective strengths and limitations. While *in vitro* models offer control over experimental conditions and facilitate high-throughput screening, they may oversimplify the complex interactions present in the brain. In contrast, *in vivo* models capture the systemic and physiological aspects of AD but can be resource-intensive and time-consuming . The synergy between *in vitro* and *in vivo* models contributes to a comprehensive understanding of Alzheimer's disease, offering insights into cellular and molecular mechanisms while also considering the systemic context in which the disease develops. By utilizing a combination of these models, researchers can uncover novel insights into the processes underlying AD and pave the way for the development of effective therapeutic strategies (Heneka et al., 2015, Ransohoff, 2016). A more in depth discussion on the use of cellular and animal models has been published elsewhere and can be referred too for further details. The authors highlighted several major pathogenic mechanisms of AD that were discovered using mutated mice, and discussed the shortcomings of animal models and the need for more reliable cellular models (Trujillo-Estrada et al., 2022).

2.2.3 Risk factors

The disease involves genetic and non-genetic risk factors. It can present an early (congenital) onset and a late (sporadic) onset. Only about 5- 10% of cases are congenital, being mainly correlated to mutations in three different genes (APP, PSEN-1, and PSEN-2) that alter the production of Aβ and cause an overabundance of the peptide. The more common late-onset AD is responsible for 90-95% of the cases. Inheritance of the ε4 allele of apolipoprotein E (ApoE4) is considered as a genetic risk factor; it will not necessarily be responsible for the disease onset, but it might increase the probability for those who carry the allele. This allele can affect the disease progression, the degree of neuronal loss, the accumulation of Aβ plaques and cholinergic activity (Sahni et al., 2011). The non-genetic factors involved in the late-onset disease variant are advanced age, diabetes, obesity, traumatic brain injury, hormone levels, cardiovascular disease, air pollution, level of education, level of physical exercise and dietary choices (Livingston et al., 2020, Barnett et al., 2013). Age is the highest risk factor, with incidence and prevalence of the disease increasing dramatically after 60 and practically doubling every five years after 65 (Esposito et al., 2002). In this sporadic form of AD, the primary pathological aspects of the ageing process are the damage that oxidation causes to neuronal molecules, the accumulation of iron molecules in specific areas of the brain, and the inflammation processes that lead to a proliferation of reactive microglia (Gerlach et al., 2003).

The majority of the AD risk factors, such as age and hormone levels, are not modifiable. However, diet and lifestyle can be adjusted and applied as a preventative strategy to reduce or delay the disease onset (Hooijmans and Kiliaan, 2008). Presently the number of synthetic drugs available to manage this disease is limited, and none are a true preventative or cure. Several natural compounds, such as bioactive food compounds, have been investigated to prevent and delay the onset of AD. Early intervention through changes in food habits could potentially reduce the incidence or delay the onset of this devastating disease.

2.3 The role of diet in late-onset of Alzheimer's disease

Diet and health are strongly connected. More than ever, food has been designed for its functional properties and aims to reach specific groups, such as infants, the elderly, athletes and people with particular health conditions. Furthermore, the increase in life expectancy has increased the need and request from consumers for healthier diets to provide better life quality for the ageing population. (Heinrich and Prieto, 2008).

Inflammation and oxidative stress are two of the main factors acting in the early stages of AD. By reinforcing the disease cycle, they can amplify the damaging effects. Thus, epidemiologic studies suggest that antioxidant, anti-inflammatory, and neuroprotective agents derived from plants and healthy food might protect against AD. The most accepted way these components can positively affect the disease progression is by scavenging reactive oxygen species (ROS), downregulating the production of pro-inflammatory cytokines, and strengthening antioxidant defence in neurons. Furthermore, specific diets, such as the Mediterranean Diet (MeDi), have been correlated with a lower occurrence of AD (Steele et al., 2007). The MeDi diet is composed primarily of vegetables, fruits and fish, all rich sources of antioxidants.

The brain consumes 20% of the oxygen inhaled, providing the necessary elements for brain function but increasing free radicals and oxidation within the tissue. It also contains elevated concentrations of iron and polyunsaturated fatty acids, both of which are easily oxidized. In addition, the brain's metabolism is mainly glucose-based, and the respiratory turnover is high. Altogether, those factors make the brain vulnerable to oxidative damage (Prasad et al., 1999). Furthermore, most other tissues in the body are equipped with antioxidant defence enzymes that help with the clearance of free radicals. However, in the brain, the levels of those enzymes are low and consequently not as efficient at free radical clearance. The increased production and reduced clearance cause a disparity between prooxidants and antioxidants, leading to a state of oxidative stress in the brain (Behl, 1999).

Food is an essential source of nutrients and energy to the body. It is through the delivery of essential nutrients that cells receive the energy needed to maintain body function. However, the components of food can extend beyond essential nutrition. A series of foods and food groups have been classified as functional foods. The term can be broad and is often misinterpreted or misused. Still, the category of 'functional foods' was recently defined as food, in either its natural or industrially processed state, that can provide potential non-nutritive health benefits when consumed regularly and at sufficient levels (Granato et al., 2017).

Neuroprotection is one of the many potential health benefits of functional foods. It can occur through a variety of mechanisms, including that of antioxidant activity and the prevention of neuronal death (Drukarch and van Muiswinkel, 2001). Fruits and vegetables are a rich source of essential vitamins that have been positively correlated with cognition. When consumed in high amounts, vitamin C, vitamin E, and carotenoid-rich sources such as fruits and vegetables, have been positively associated with improvements in cognition and reduced risk of dementia

in the elderly (Ferrari, 2001). Vitamins act as natural antioxidants, protecting the brain from oxidation. In addition, tea polyphenols and lipoic acid are known to protect the brain from neurodegeneration (Ferrari, 2007). Antioxidant-rich diets containing caffeine from coffee and tea, epigallocatechin-gallate esters from green tea, anthocyanins from plum juice, resveratrol from red wine, and components of *Ginkgo biloba* have been shown to inhibit Aβ production or aggregation and slow down cognitive decline in animal models (von Arnim et al., 2010).

The relationship between nutrition and cognition is associated with individual food components and nutrients as well as dietary patterns. The interaction of different nutrients in a diet may increase possible benefits through additive or even synergistic effects (van den Brink et al., 2019). The intake of antioxidant-rich food groups, such as fruits and vegetables, and those rich in omega-3 (ω-3) fatty acids, such as nuts, vegetable oil, and fish, have been related to reduced AD risk. Conversely, diets rich in refined sugar and saturated fats from meat and dairy sources have been associated with increased risk of AD (Otaegui-Arrazola et al., 2014). In dietary patterns, reduced risk of AD has been linked to the MeDi, a diet composed mainly of a high intake of vegetables, fruits, nuts, seeds, legumes, potatoes, whole grains, fish, seafood and extra virgin oil; medium intake of poultry, eggs, yoghurt and cheese; low intake of red meat, sweets and saturated fats; and moderate consumption of red wine (Davis et al., 2015). A recent study by Rayne-Smith and collaborators examined for the first time the relationship between adherence to the MeDi and the accumulation of Aβ. Their findings indicated a potential beneficial effect of high adherence to the Medi on cognition and reducing Aβ in older adults with cognitive impairment (Rainey-Smith et al., 2018). In addition to neuroprotective effects, the high and regular intake of fruits and vegetables is strongly associated with reducing cardiovascular and coronary heart disease (Keys, 1995) (Liu, 2003).

Similar to the MeDi, the Dietary Approaches to Stop Hypertension (DASH) diet consists mainly of vegetables, fruits, lean meat and whole grains. The key daily food components of the DASH diet are approximately: five servings of vegetables, five servings of fruit, less than six small servings of lean meat, two servings of low-fat dairy products, seven servings of whole grain carbohydrates, and two to three servings of fats and oils. In addition to daily recommendations, a weekly intake of nuts and seeds four to five times and fewer than five servings of sweets is suggested. It is important to note that the carbohydrates indicated in the diet are healthy ones, such as root vegetables (potatoes), cucurbits (pumpkins) and whole grains, rather than processed carbohydrates. The quality of the fat consumed in this diet is also crucial to ensure beneficial effects and should be sourced from olive oil, nuts, avocado, hemp

seed, flaxseed and fish rich in ω-3 fats (Challa HJ, 2021). The DASH diet is designed to improve cardiovascular conditions by reducing blood pressure and serum uric acid levels in people suffering from hyperuricemia (Rai et al., 2017).

In 2015, Morris and collaborators proposed a new diet combining the MeDi and the DASH diet and called it Mediterranean-DASH Diet Intervention for Neurodegenerative Delay (MIND). This diet consists of MeDi and DASH diets adjustments according to relevant findings from previous research in dementia. The adjustment that makes the MIND diet exclusive is the suggested consumption of green leafy vegetables and berries specifically, but not other fruits (Morris et al., 2015). High adherence to the MIND diet slowed cognitive decline after stroke in a community cohort of 106 people. The study has a follow up of 5.9 years and adjusted the scores of cognitive tests for sex, education, age, and the APOE-4 allele (a genetic AD risk factor), smoking, caloric intake and physical and mental stimulation (Cherian et al., 2019). An ongoing study will analyse the effect of the MIND diet over three years of intervention in a cohort of 604 people aged 65 to 84 years old and at risk for AD. The findings from this study is expected to provide a better understanding of dietary patterns and their link with cognitive health (Liu et al., 2021b).

Table 2.1 provides a comprehensive list of studies that assessed the role of food or dietary patterns in AD. It is important to reinforce that besides diet, physical activity has also been associated with healthy ageing. Regular moderate exercise is believed to reduce the risks of dementia and cognitive decline, and that was observed in the Canadian Study of Health and Aging, where a 42% reduction in the risk of cognitive decline and a 50% reduction in risk of dementia were observed in a cohort of people aged 65 years or older (Ferrari, 2007). In a study by Liang and collaborators, the levels of AD biomarkers (Aβ and tau) in cerebrospinal fluid were analysed in a cohort aged 55 to 88 years old who self-reported their levels of physical exercise. They observed a positive correlation between high levels of exercise and lower AD biomarkers in cognitively normal older adults (Liang et al., 2010). Even though physical activity has been suggested as a potential intervention for preventing AD, this review will focus on the effects of diet and possible food-based interventions.

Table 2.1. Summary of natural bioactive compounds tested against AD biomarkers *in vitro/in vivo* and their primary outcomes

PUBLICATION	HYPOTHESIS TESTED	RESEARCH FINDINGS
(Barberger-Gateau et al., 2007)	Relationship between dietary patterns (**fruits, vegetables and ω-3**) and risk of dementia and AD in 8.085 non-dement participants ager 65 or more	Decreased risk of dementia after daily consumption of fruits and vegetables, reduced risk of AD and dementia after weekly consumption of fish (ω-3 PUFA) in ApoE4 noncarriers
(Krikorian et al., 2010)	Effects of daily consumption of wild **blueberry juice** in a sample of nine older adults with early memory changes	Improved word list recall and paired-associate learning; reduced depression symptoms after 12 weeks of intervention
(Patil et al., 2013)	Effect of **curcumin, EGCG** and **resveratrol** on the upregulation of BAG2 and LAMP1 proteins (involved in tau clearance) in rat cortical neurons	Different concentrations of compounds up-regulated BAG2; EGCG upregulated LAMP1 levels at higher concentrations; curcumin doubled BAG2 levels at low concentrations and downregulated levels of phosphorylated tau
(Nafar, 2014)	Effect of **coconut oil** on cortical neurons treated with Aβ *in vitro*	Improvement in cell survival in cultures exposed to Aβ and treated with coconut oil compared to those exposed only to Aβ; attenuated mitochondrial alterations induced by Aβ
(Chang et al., 2015)	Effect of **caffeic acid** in memory improvement of rats fed with a high-fat diet (HFD)	Caffeic acid significantly improved memory impairments in HFD rats
(Hu Yang et al., 2015)	Effect of coconut oil on memory of patients with AD	Coconut oil significantly improved memory in the treatment group compared to the control; the improvement was dependent on gender, diabetes and degree of dementia
(Morzelle et al., 2016)	Effect of **pomegranate** peel extract (PPE) on spatial memory, neuroplasticity, oxidative stress and inflammation in a mouse model for AD	PPE improved spatial memory compared to control in Barnes maze; reduced Aβ plaques; reduced acetylcholinesterase activity; increased the expression of brain-derived neurotrophic factor
(Jeyapriya Raja Sundaram, 2017)	Effect of **curcumin** on neuroinflammation (cyclin-dependent kinase 5-Cdk5) and neurodegeneration in p25Tg mice	Curcumin prevented p25-mediated glial activation and pro-inflammatory cytokines and chemokines production in p25Tg mice; reduced p25-induced tau/ Aβ pathology
Rho et al. (2019)	Inhibitory effects of phenolic compounds from fermented tea (*Camellia sinensis L.*) against Aβ aggregation	Catechin gallate (CG), epicatechin gallate (ECG), and epigallocatechin gallate (EGCG), significantly decreased Aβ aggregation at a concentration of 10 μg/mL, compared to the positive control, Aβ alone

Abbreviations: Omega-3 (ω-3); Alzheimer's disease (AD); Polyunsaturated fatty acids (PUFA); Apolipoprotein allele-4 (ApoE4); Bcl-2-associated athanogene 2 (BAG2); Lysosomal-associated membrane protein 1 (LAMP1); Epigallocatechin gallate (EGCG); Amyloid-β (Aβ); High-fat diet (HFD); Pomegranate peel extract (PPE); cyclin-dependent kinase 5(Cdk5); Catechin gallate (CG), epicatechin gallate (ECG).

2.4 Dietary risk factors for AD

2.4.1 Saturated fat

As much as food can positively impact health, it can also be one of the main risk factors for many conditions and cause severe damage to the body. High intake of fat, refined sugar, and processed food often culminates in obesity, leading to hypertension, high cholesterol, and diabetes (Sinha and Haque, 2022). Type 2 diabetes is strongly correlated with mild cognitive impairment and dementia and is caused by insulin resistance and pancreatic β-cell dysfunction (Koekkoek et al., 2015, Groeneveld et al., 2018, Qiu et al., 2014, Biessels et al., 2014).

Among food groups, saturated and trans fats have been associated with increased risks of dementia and AD (Laitinen et al., 2006, Luchsinger et al., 2002). A regression analysis was perform by Grant (1997) to identify the correlations between fat intake and AD in 18 community-wide studies from 11 different countries. The main finding was that the total calories and fat consumed in different countries had the highest correlation to the prevalence and incidence of AD (Grant, 1997).

A meta-analysis of four prospective cohort studies concluded that a higher intake of saturated fats increased the risk of AD by 39% and the chance for dementia by 105%. They also analysed the dose-dependent risk and observed a 15% increase in the risk for AD with an intake of saturated fats of 4g/day (Ruan et al., 2018). Some animal trials have proved that a high intake of saturated fats can increase Aβ deposition. In a transgenic mouse model for AD, Aβ deposition was significantly higher for animals fed only with saturated fats but lower when the ω-3 PUFA DHA was incorporated into the diet (Oksman et al., 2006). However, a clinical trial conducted by Hooper and co-workers could not find an association between erythrocyte membrane saturated fatty acids and Aβ deposition in the cortex of a human cohort aged 70 years or older (Hooper et al., 2017), suggesting that dietary fats may act or be deposited selectively in organ systems rather than in a systemically equivalent fashion.

The Rotterdam Study is an ongoing long-term study that started in the mid-1980s. It arose from the increase in life expectancy, changes in the population's demography and the possibility of a population suffering from age-related conditions. The study aimed to evaluate an extensive cohort for psychiatric, neurological, locomotor, cardiovascular, respiratory, endocrine, hepatic and ophthalmological diseases (Oeppen and Vaupel, 2002, Hofman et al., 2007, Ikram et al., 2020a). The selection of the cohort started in 1989 and recruited people aged

55 years or more, with no exclusion criteria. Since the first recruitment, extensions of the cohort have been added; in 2000, people aged 45 to 54 years were added and in 2016, people aged 40 or more were allowed to join the cohort bringing the total number of subjects to 14,926 subjects. This selection was expected to be completed by 2020 and yield approximately 3000 new participants (Ikram et al., 2020b).

A high intake of saturated dietary fat seems to be associated with cognitive decline. A study looked into dementia development over 26 years of follow-up (1990-2016), and found that 1489 subjects (~1%) from 156,088 were diagnosed with dementia (Licher et al., 2019, Wolters et al., 2019). In an earlier update, around two years after the baseline assessment, 1.1% of the cohort developed dementia, from which 72% were diagnosed with AD, 12% with vascular dementia and 16% with other types of dementia. Subjects that had a high intake of total fat, saturated fat and cholesterol presented an increased risk of dementia and were strongly associated with vascular type dementia (Kalmijn et al., 1997). The Chicago Health and Aging Project study also identified a positive correlation between saturated and trans-fat intake and the risk of developing AD. Using mixed models to analyse the data after adjustment for demographics, intake of antioxidants and other dietary fats and cardiovascular risk, authors observed that higher intake of saturated fat and trans-unsaturated fat were linearly associated with greater decline in cognition over 6 years (Morris et al., 2004).

2.4.2 High carbohydrate diet

The intake of highly processed carbohydrates with a high glycaemic index promotes a rapid rise in blood glucose levels following meals. The continuous consumption of diets rich in processed carbohydrates can lead to insulin resistance and diabetes (Seneff et al., 2011a). Diabetes mellitus and cardiovascular disease are the main concerns for those suffering from metabolic syndrome, a combination of metabolic imbalances in the body that can lead to increased risk of dementia and AD. According to clinical studies, patients with type-2 diabetes have a two to five times increase in the risk of AD (Ott et al., 1999, Nicolls, 2004). A more recent study observed a correlation between mild cognitive impairment and early dementia with type-2 diabetes, where authors used advanced multimodal magnetic resonance imaging (MRI) and found grey matter atrophy to be the main correlation between the conditions (Groeneveld et al., 2018).

Fructose, a common sugar used in processed foods, is believed to be ten times more reactive than glucose in inducing glycation, a non-enzymatic and spontaneous reaction between

free reducing sugars and free amino groups of proteins, DNA, and lipids. This reaction creates Amadori products that are dehydrated and rearranged in a series of irreversible reactions, culminating with the formation of advanced glycation end products (AGEs) that are not eliminated and contribute to oxidative stress in ageing (Kim et al., 2017, Seneff et al., 2011b). A high carbohydrate diet is proposed to disturb the homeostasis of lipids in the central nervous system, mainly by reducing the delivery of essential fatty acids. This mechanism is responsible for compromising cellular membrane integrity and consequently decreasing the functions of membrane proteins such as APP. In addition, elevated insulin/insulin growth factor signalling can accelerate cellular damage. Those mechanisms are responsible for a disturbance in cholesterol metabolism that promotes increased processing of APP, decreased cellular trafficking, and the generation of Aβ peptide (Henderson, 2004). Therefore, it has been proposed that a reduced intake of carbohydrates and increased intake of essential fatty acids (EFA) might effectively prevent AD.

2.5 Bioactive food components beneficial for AD

2.5.1 Omega-3 polyunsaturated fatty acids

The three major dietary ω-3 PUFA are α-linolenic acid (ALA; C18:3), eicosapentaenoic acid (EPA; C20:5) and docosahexaenoic acid (DHA; C22:6) (Riediger et al., 2009). PUFA are often categorized as EFA, or those that the body cannot produce and need to be obtained from the diet. They are responsible for the mediation of brain functions from infancy to ageing and are involved in a series of brain-related disorders (Yehuda et al., 2005b). These fatty acids are constituents of cell membranes and as such are key components for membrane fluidity.

EFA play important role in the transfer of oxygen from the air in the lungs to the bloodstream, the manufacture of haemoglobin and the production of energy. They are found in high concentrations in the brain, and are crucial for its proper function including the normal transmission of nerve impulses, cell growth and division, and nerve function (Yehuda et al., 2002). The effects of PUFA in particular on brain functions include modifications of membrane fluidity, the activity of membrane-bound enzymes, the number and affinity of receptors, the function of ion channels, the production and activity of neurotransmitters and signal transduction (Yehuda et al., 2002). They have been shown to regulate cell survival, neurogenesis, brain inflammation and synaptic function (Bazinet and Layé, 2014). In AD, the levels of total PUFA are reduced, altering the membrane structure and contributing to oxidative stress (Yehuda et al., 2005a). An increase in dietary consumption of those fatty acids is

associated with improvements in brain health and membrane fluidity. Studies suggest that a high intake of ω-3PUFA from fish and marine oils may lower AD risk (Boudrault et al., 2009).

With the inclusion of ω-3 PUFA into neuronal membranes, the total cholesterol is reduced, strongly affecting membrane fluidity, viscosity and permeability, all essential properties for synaptic plasticity and neurotransmission of complex cognitive processes (Yehuda et al., 2005a, Wassall et al., 2004). The period of infancy, when the brain is developing, and of ageing, when the brain is more vulnerable to oxidation damage, are the two more critical life stages for brain function, and adequate EFA and PUFA is crucial (Yehuda et al., 2005b). The blood-brain barrier (BBB) is key to the delivery and bioavailability of PUFA to the brain, as fatty acids whether produced by the body or obtained from the diet are perceived and used in the same way by the brain. Phospholipids are important cell membrane components that contain fatty acids, and the lipid component in the brain has a relatively high turnover rate. (Yehuda et al., 2000). Among AD patients, the decrease in EFA and PUFA is severe and contributes to cognitive decline and synaptic loss (Yehuda et al., 2002). Some studies (Yehuda et al., 2002) looked into the supplementation with EFA and PUFA and showed that it could correct the deficiency.

A series of authors have suggested that moderate fish consumption as a source of ω-3 PUFA can reduce the risk of cognitive impairment (Fotuhi et al., 2009, Conquer et al., 2000, Hooijmans and Kiliaan, 2008, Cherian et al., 2019, Morris et al., 2015). The neuroprotective effects of ω-3 PUFA depend on distinct and interconnected molecular mechanisms (Florent-Béchard et al., 2009). Membrane fluidity is increased with increased ω-3 PUFA consumption, generating improvement in neurotransmission through the enhancement in functionality and affinity of ion channel receptors and the signalling due to increased binding receptors (Farkas et al., 2002). In addition, they can promote increased fluidity by replacing the more pro-inflammatory omega-6 fatty acids and cholesterol from the membranes (Yehuda et al., 1998, Heron et al., 1980). The brain is a lipid-rich organ, and phospholipids compose around 25% of its dry weight. It appears that the health benefits of ω-3 PUFA are related to the incorporation of these fatty acids into the membrane phospholipids (Clandinin et al., 1994). As in other tissues, ω-3 PUFA in the brain act by producing fewer inflammatory and aggregatory eicosanoids, and the absence of these may enhance and preserve brain function (Uauy Dagach-Imbarack and Dangour, 2006). To better understand the relationship between ω-3 PUFA, specifically DHA, in AD patients, Tully and collaborators conducted a case-control study using a cohort of 148 people, separated into 4 groups, diagnosed with AD based on the Mini-Mental

State Examination (MMSE) compared to a control group. The serum cholesteryl ester-fatty acids were used as a biomarker, and they observed significantly lower levels of the biomarker in the AD groups compared to control (Tully et al., 2003).

DHA is the major ω-3 PUFA in neuronal membranes as it comprises 30–40% of the neuronal phospholipids, mostly as phosphatidylethanolamine and phosphatidylserine (Yuen et al., 2005, Lauritzen et al., 2001). DHA and EPA can affect brain function through the production and operation of neurotransmitters such as serotonin and dopamine, inhibition of phospholipase A2, and inhibition of protein kinase C (Riediger et al., 2009). ω-3 PUFA are known for their anti-inflammatory properties, and it has been suggested that they may delay the onset of AD by reducing inflammation in the brain; this correlation was strengthened by the finding of inflammatory markers in the brains of patients with AD (Honig, 2000). DHA has a flexible structure that can undergo inter-conversion, twisting its structure into different states, such that the terminal methyl end often approaches the membrane surface. That results in increase fluidity and reduced membrane thickness, which modulates the activity of proteins and vesicle fusion/formation (Marszalek et al., 2005, De Wille and Farmer, 1992, Poling et al., 1996).

The amount of DHA present in the brain membrane can be altered by diet and life stage (e.g. infancy and ageing) (Uauy and Dangour, 2006). In AD, the accumulation of Aβ is related to an inflammatory response that leads to activation of microglia and recruitment of astrocytes (Sastre et al., 2006). The incorporation of DHA and EPA in the diet can impact inflammatory diseases, such as asthma or atherosclerosis, suggesting that those ω-3 PUFA have an essential role in the regulation of inflammatory processes. A study using primary co-cultures of human neurons and glial cells to assess the effect of nanomolar concentrations of DHA found that cells treated with DHA reduced 20-25% of Aβ production and 50% of Aβ-induced cell apoptosis (Fifre et al., 2006).

In AD, the abnormal cleavage of the APP protein leads to the creation of Aβ peptides through the amyloidogenic pathway. It has been demonstrated that DHA can promote the non-amyloidogenic path (Figure 2.2), promoting reduced levels of Aβ in a cellular model for AD (Sahlin et al., 2007). In the non-amyloidogenic path, the activity of β and γ-secretase are reduced, preventing the interaction with APP to generate Aβ. DHA might facilitate the activity of α-secretase, consequently promoting the nonamyloidogenic processing of APP (Lim et al., 2005). Florent and collaborators used rat cortical neurons to understand better the molecular basis of the effects of DHA treatment against Aβ oligomers and survival pathways. They

concluded that DHA protected cortical neurons from Aβ's cytotoxic effect *in vitro* through the prevention of cytoskeleton perturbation and caspase activation, both of which are apoptosis biomarkers.

Many animal, epidemiological, and clinical studies showed that DHA consumption is associated with reduced AD risk (Bourre, 2007, Freemantle et al., 2006, Green et al., 2007, Lukiw et al., 2005, Schaefer et al., 2006). In adult rats, learning and cognitive behaviour were related to DHA status/levels in the brain, which is believed to be associated with the amount of ω-3 fatty acids in the diet (Moriguchi et al., 2000). DHA in the form of fish oil supplementation in an AD rat model showed antioxidant effects in the rat's brain corpus striatum, hippocampus and cortex (Florent-Béchard et al., 2007). Dietary PUFA has also been reported to induce differential gene expression pattern in the brain related to the myelination process. Aged rats fed with fish oil using a nutrigenomic approach revealed that the expression of several genes changed significantly, including the gene encoding the Aβ-scavenger transthyretin in the hippocampus (Florent-Béchard et al., 2009). Overall, DHA supplementation in rat and mouse models of AD seem to improve learning ability, protect against Aβ production, decrease neuronal apoptotic neurons, protect against dendritic pathology and increase synaptic protein and phospholipid densities (Hashimoto et al., 2005a, Hashimoto et al., 2005b, Hashimoto et al., 2002, Hooijmans and Kiliaan, 2008, Pepe et al., 1999). It is important to note that rodent AD models have been designed to mimic an overproduction of Aβ, which is observed in the familial cases of dementia rather than the sporadic form of the disease, and thus may be an ineffective model to represent the early stages of the more widespread form of AD.

Based on positive outcomes previously obtained from cell and animal studies, Quinn and collaborators conducted a randomized, double-blind, placebo-controlled trial to assess the effects of DHA supplementation in individuals with mild to moderate AD (MMSE scores, 14–26). Participants were given 2g of either DHA or placebo, divided into two doses daily for 18 months; this dose met the recommended daily intake for DHA [2 g to 4 g of EPA and DHA are recommended by the American Heart Association (Kris-Etherton et al., 2003)]. No reduction in the rate of cognitive and functional decline was observed in this cohort that received supplementation with DHA (Quinn et al., 2010). Conversely, a randomized, double-blinded, parallel-group comparative study found that ω-3 activated cognitive function in a cohort of 45 participants 61-72 years old (Konagai et al., 2013). This group compared krill oil containing ω-3 PUFA incorporated in phosphatidylcholine, sardine oil containing ω-3 PUFA incorporated

in triglycerides, and medium-chain triglycerides as control. They found that ω-3 oils significantly improved cognition over 12 weeks as assessed by oxyhaemoglobin levels and P300 component concentrations in the cortex during memory and calculation tasks compared to the triglyceride placebo. It was hypothesised that between the two forms of ω-3 intervention, the phospholipids-incorporated format improved the delivery and effects in cognition, suggesting that phospholipid conjugation can improve bioavailability (Konagai et al., 2013).

Another pilot trial evaluated the effects of ω-3 PUFA alone vs ω-3 plus alpha-lipoic acid (LA) vs placebo on oxidative stress biomarkers in 39 AD patients over 12 months. They found no difference in an oxidative stress biomarker (F2-isoprostane levels) between groups at the end of the study period and no difference between ω-3 alone and in combination with LA against placebo in the AD Assessment Scale-cognitive subscale or Activities of Daily Living. However, ω-3+LA showed a significantly reduced decline in the Mini-Mental State Examination and Instrumental Activities of Daily Living. The cohort used in this study was small and the authors suggested further investigations on the effects of ω-3 alone or in combination with LA were warranted (Shinto et al., 2014). Overall, the human data available presents some controversy and does not correlate with the apparent positive effects observed in *in vitro* and animal data, suggesting that there is still the need to investigate the impact of ω-3 in AD. Perhaps the form of administration, such as conjugated, encapsulated or incorporated to a food product, would provide more palatability and could be used in clinical trials for more extended periods, in bigger cohorts and potentially provide significant health benefits and improvements in cognition. It is also likely that digestive and metabolic processes differ sufficiently across mammalian species to be part of the cause of the conflicted findings; it is not unusual for findings in rat and mouse models to fail to extrapolate to humans.

2.5.2 Curcumin

Curcumin is the main polyphenolic compound found in the rhizomes of the herb turmeric (*Curcuma longa* L.). Turmeric is comprised of 2–10% curcuminoids, with the three main types being curcumin (C, 40-80%), desmethoxycurcumin (DMC, 7-30%) and bisdemethoxycurcumin (BDMC, 1-30%). The amount of each curcuminoid can vary considerably according to seasonal and geographical changes as well as soil conditions; however, curcumin is invariably present in a higher amount than DMC or BDMC (Heger et al., 2014, Serafini et al., 2017). Curcumin has a molecular weight of 368.38 g/mol and a melting

point of 183°C (PubChem, 2004). The chemical structure of curcumin is composed of three bodies: two o-methoxy aromatic rings connected by a bridge that has seven carbons of α,β-unsaturated β-diketone moiety (Figure 2.3). Due to its structure, curcumin can present three possible forms: two isomers in a keto-enol tautomeric form and one β-diketonic tautomeric form (Payton et al., 2007). The different structure conformations occur based on the pH in which curcumin is dispersed; the keto-form is prevalent under acidic and neutral conditions, while under basic (pH > 8) aqueous conditions or when dispersed in ethanol in the dark it presents the enolic form (Jovanovic et al., 1999, Kolev et al., 2005). The enol (hydrogen-bonding) configuration is predominant in the crystal form, resulting in loss of molecule planarity (Tønnesen H.H., 1982, Kolev et al., 2005). The fact that curcumin has a neutral hydrophobic carbon bridge attached to either enol of keto polar forms facilitates the permeation across biological membranes including the BBB, and therefore this is a key mechanism for curcumin's penetration and action in the brain (Balasubramanian, 2006).

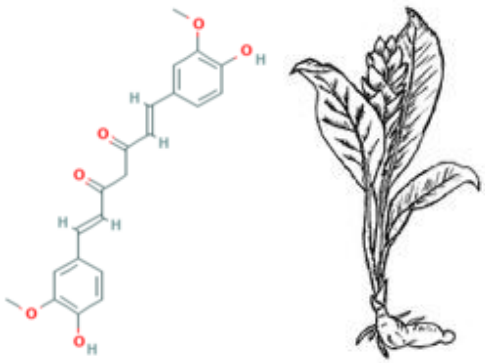

Figure 2.3. Curcumin chemical structure (PubChem, 2004) and illustration of turmeric *(Curcuma longa)* plant

Turmeric has been used for centuries as a dye, culinary spice and food preservative. In addition, curcumin has a long history of use in traditional medicines of China and India due to a series of health-promoting properties, such as anti-tumour, anti-oxidant, anti-microbial and anti-inflammatory (Ammon, 1991, Takahashi et al., 2009, Yan et al., 2011, Ahmed and Gilani, 2009, Bandyopadhyay, 2014, Bengmark, 2006). One of the first scientific reports related to the medicinal uses of curcumin was published in 1748 (Loeber, 1748). Since then, the interest in the investigation of curcumin's health benefits has remained strong. A *Lancet* report published in 1937 explored findings by previous authors in the successful use of turmeric extract as a treatment for hepatic and biliary diseases (Oppenheimer, 1937). There remain gaps in understanding the health effects of curcumin, especially in humans, hence many studies are being conducted to investigate its protective properties against a series of conditions in *in vitro*,

animal and human studies. Turmeric has been administrated in a wide range of forms and formulations, such as fresh turmeric roots, pure curcumin powder and encapsulated through oral, intra-nasal, intravenous or topical creams delivery (Baek and Cho, 2017, Brouet and Ohshima, 1995, Huang et al., 1994, Lao et al., 2006, Marczylo et al., 2007, McClements and Xiao, 2017, Pan et al., 1999b, Wahlstrom and Blennow, 1978, Sharma et al., 2005, Lin et al., 2009).

One of the many benefits of curcumin is that it presents neuroprotective effects provided by different mechanisms acting on Aβ formation. These include low cholesterol levels, metal chelation, lipid peroxidation, reduced expression of BACE 1 and c-Jun N-terminal kinase (JNK)-mediated transcription (Figure 2.4) (Cole et al., 2005b). Researchers have observed that the incidence of AD is 4.4-fold lower in countries where curcumin consumption is high, such as India and China, compared to those where curcumin is not part of the diet such as the United States (Ganguli et al., 2000).

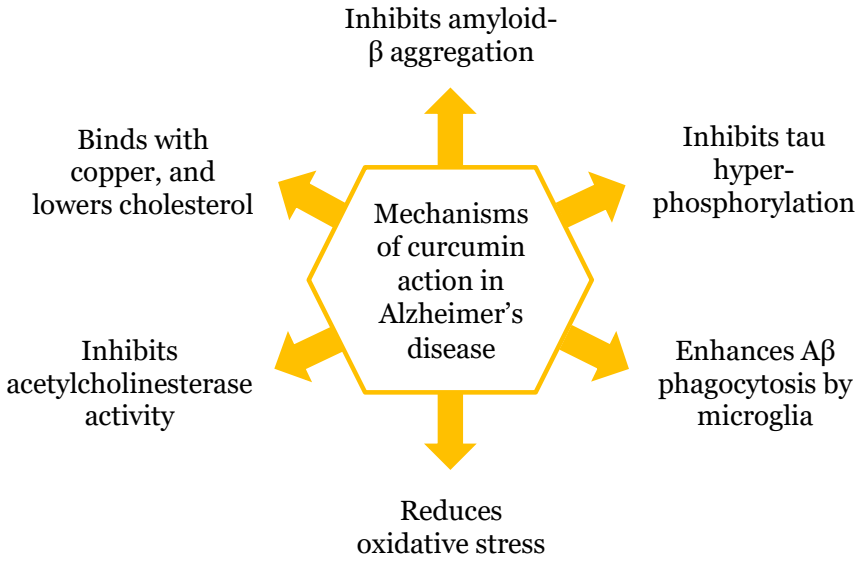

Figure 2.4. Mechanisms of curcumin action in AD

Curcumin is believed to modulate a series of molecular targets, cell signalling proteins, cytokines, chemokines, cycle proteins, enzymes, surface adhesion molecules and receptors (Jäger et al., 2014). It exhibits potent antioxidant effects through increasing the production of antioxidant enzymes, leading to the scavenging of excess ROS and inhibition of lipid peroxidation (Hewlings and Kalman, 2017). A study using rat liver mitochondria was used to assess the antioxidant effect of curcumin and its synthetic analogues on lipid peroxidation and protein oxidative damage. From seven tested analogues, including the intact molecule, five

were effective in inhibiting free radical-induced oxidation of phenolic groups (Wei et al., 2006).

In the inflammatory cascade, curcumin activates protein-1 transcription. It also inhibits the formation of pro-inflammatory cytokines such as IL-β, IL-8, TNF-α and reactive Glial fibrillary acidic protein, eventually promoting inhibition of the inflammation pathway. Lipoxygenase and COX-2 enzymes are involved in the synthesis of pro-inflammatory prostaglandins, thromboxanes and leukotrienes. Another enzyme involved in this process is inducible nitric oxide synthase (iNOS) that releases nitric oxide in addition to pro-inflammatory cytokines. In addition, the inducible nuclear transcription factor-κB (NF-κB), is responsible for the regulation of genes involved in the immune and inflammatory responses. Those factors are directly related to the production and accumulation of Aβ and its consequent toxicity to the brain. Curcumin's anti-inflammatory effects are mainly attributed to its powerful ability to inhibit those enzymes, alleviating the production of inflammation and toxicity-inducing signalling molecules (Bengmark, 2006, Rao, 2007, Sandur et al., 2007, Liu et al., 2017).

The molecular structure of curcumin has been associated with its ability to bind with Aβ *in vitro*, suggesting that it could inhibit aggregation or even act on disaggregating Aβ fibrils or plaques in the brain. Yan and collaborators used an AD mouse model assess the efficacy of curcumin on Aβ clearance. They found that 0.8 μM of curcumin was sufficient to inhibit Aβ aggregation and that 1 μM was sufficient to disaggregate Aβ-40 *in vitro* (Yang et al., 2005). Besides preventing Aβ aggregation, curcumin can reduce plaque burden due to its anti-inflammatory and antioxidant activities that inhibit cell signalling pathways, promoting cellular functions that protect against Aβ toxicity (Sharma et al., 2007). Curcumin's strong ability to inhibit cytokines is believed to limit oxidative damage and inflammation induction of BACE1, the enzyme responsible for the initial steps of Aβ production (Kakar and Roy, 1994, Strimpakos and Sharma, 2007). The above factors have been validated in Aβ toxicity in different AD models, suggesting curcumin's potential use as a multi-target intervention.

Metals have been related to Aβ toxicity and aggregation. The chemical structure of curcumin, composed by two phenolic groups separated by a carbon bridge, promotes chelating activity of metals such as iron. Thus, curcumin also acts as an anti-oxidant by inhibiting metal catalysed peroxidation (Venkatesan and Rao, 2000). It has been shown that curcumin can reduce BACE1 expression in animal models submitted to elevated oxidative stress and inflammation. Curcumin inhibits cytokine and microglial activation related to neurotoxicity

through immunosuppression and immunomodulation. It also increases mRNA and immunostaining for the microglial phagocytosis markers CD11c and macrosialin, which are related to Aβ clearance (Cole et al., 2005b). The JNK-mediated Aβ aggregation and the tau protein aggregation are also supressed by curcumin (Cole et al., 2007).

Curcumin has been tested against Aβ in a series of cell line models. Kim and collaborators used rat (PC12) and human (HUVEC) cells to assess the effect of curcumin, desmethoxycurcumin, and bisdemethoxycurcumin against Aβ toxicity. Doses of 3-7 μg/ml of curcuminoids promoted an effective response in 50% of the cultured cells for both models (ED50), providing protection from Aβ toxicity. In addition, curcuminoids were more effective antioxidants than α-tocopherol as assessed using a DPPH radical trapping assay (Kim et al., 2001). In an animal study, Lim and collaborators used a mouse model (Tg2576) that overproduces Aβ. They observed reductions in inflammation, oxidative damage and formation and accumulation of Aβ after curcumin treatment at low (160ppm) and high doses (500ppm) added to their chow and administered for 6 months. They hypothesised that the positive outcomes provided by curcumin were related to the suppression of microglia activation and reduction of glial fibrillary acidic proteins (GFAP). The lower dose tested in this study was enough to present the beneficial improvements of curcumin treatment (Lim et al., 2001b). Similar outcomes, including improvement in cognition, were observed in another study in 19 month old female rats Sprague-Dawley rats infused with Aβ using and fed diets containing curcumin at 200 and 500 ppm in diet over three months (Frautschy et al., 2001).

The Tg2576 mouse was also used as a model to assess curcumin's BBB crossing and ability to bind with Aβ *in vivo*. Curcumin was injected (200 μL of a 500 ppm solution) to reach around 2 μM in the bloodstream. *In vivo* assays showed that curcumin crossed the BBB and bound with Aβ. *In vitro* assays using mouse brain as well as synthetic Aβ showed that curcumin inhibited aggregating (IC50 = 0.8 μM) as well as disaggregated fibrillar Aβ40 (IC50 = 1 μM). Curcumin proved to be more effective against Aβ40 aggregation than naproxen and ibuprofen and prevented Aβ42 oligomer formation and toxicity between 0.1 and 1.0 μM (Yang et al. (2005).

Animal studies have shown that mammals have a high tolerance to curcumin even when administered in high doses. For instance, a study on rats assessed a single dose of 30% turmeric in diet and observed no toxic effects. In another study curcumin presented no adverse effects in rats and monkeys fed 1.8 g/kg per day and 0.8 mg/kg per day, respectively for 90 days

(Majeed et al., 1995). As curcumin proved to be safe in a series of animal trials and beneficial for cognition, subsequent clinical trials have been conducted to test the same effects in humans (Hamaguchi et al., 2006, Hamaguchi et al., 2010). Because of its potent anti-carcinogenic activity, curcumin has already been through extensive preclinical toxicology and clinical testing and has a very favourable safety profile (Kelloff et al., 1996).

The metabolism of curcumin in humans promotes tolerance to high doses of curcumin with no significant side-effects. It is important to note that the metabolism of humans is different from other mammals and understanding those differences is therefore key in the development of delivery systems. Ireson et al. (2022) used subcellular fractions of human and rat intestinal and hepatic tissue as well as intact rat intestinal sacs to better understand curcumin metabolism. The authors found that curcumin conjugation was greater in intestinal fractions from humans as compared to rats, while in hepatic fractions the opposite was observed. They concluded that there is more metabolic activity in human intestinal tissue than rat intestinal tissue, with extensive conjugation and reduction of curcumin occurring in the former (Ireson et al., 2002).

A phase 1 clinical trial recruited 25 individuals who were given 8g of curcumin per day and observed no toxic effects. The maximum curcumin concentration in serum was found at 1 to 2 hours after oral administration and declined gradually within 12 hours (Chen et al., 2001). Although curcumin has been showed to be safe, some gastrointestinal discomfort in humans can be observed. For instance, one study found minor adverse effects after administration of high doses of curcumin. The study used 12 healthy human volunteers to assess the pharmacokinetics of a curcumin preparation after a single administration. Curcumin was given at dosages of 10g and 12g (n=6 per dose) and plasma concentration assessed for free curcumin and metabolites from 0.25 to 72 hours after ingestion. The adverse effects observed included headache, sore arms (unlikely to be related to treatment but possibly due to cannulation and posture) and yellow, loose stool one day after consumption. Those effects were reported by the authors as grade 1 following the National Cancer Institute Common Toxicity Criteria (version 2.0) (Vareed et al., 2008). More details and studies on the safety and anti-inflammatory activity of curcumin have been reviewed elsewhere (Chainani-Wu, 2003).

Even when administered in higher doses or in products formulated to increase bioavailability, curcumin concentration found in plasma is low and often unlikely to reach physiological concentrations capable of inhibiting inflammation. Cuomo et al. (2021) assessed the delivery of curcumin in a bioavailable lecithin formulation (Meriva®) to healthy humans

and found 29-fold higher absorption for Meriva® compared to unformulated curcumin. However, only phase-2 metabolites (submitted to conjugation reaction to convert the molecule to a more polar format through glucuronidation and sulfation) were detected, and plasma concentrations were still significantly lower than the required dose for anti-inflammatory activity (Cuomo et al., 2011).

As a highly lipophilic compound, curcumin has the ability to cross the BBB (Wang and Pantopoulos, 2005). However, curcumin is rapidly metabolized by conjugation before reaching the BBB, and as a result, the brain bioavailability is very low (Kelloff et al., 1996). Despite being safe when administered at high doses, the low bioavailability due to high hydrophobicity, poor gut absorption, degradation at alkaline pH and rapid systemic elimination impose limitations to its pharmaceutical use and health benefits (Anand et al., 2007, Wahlström and Blennow, 1978). A study assessing curcumin bioavailability after administration of a very high daily dose (12g) to humans have detected only conjugated forms of curcumin in plasma, supporting the observations described above (Cuomo et al., 2011).

To overcome its low bioavailability, researchers have been exploring alternatives ways to administer curcumin and reduce its excretion and metabolism. It has been suggested that adjuvants such as piperine, quercetin and turmeric oil could increase curcumin absorption (Wang et al., 1997). Due to the lipophilic nature of curcumin, its inclusion in lipophilic matrices has also been suggested and extensively explored, for example through the encapsulation in liposomes, emulsions, nanoparticles, solid-lipid nanoparticles and micelles (Yallapu et al., 2012). Another proposed strategy that has been gaining attention and has demonstrated efficacy in increasing curcumin bioavailability is its complexation with phospholipids. It is believed that curcumin's polar groups can bond via hydrogen bonding and dipole interactions to the polar head groups of phosphatidylcholines. Semalty et al. (2010) found that curcumin strongly bonded to phospholipid micelles, which promoted a shield from hydrolytic activity, therefore protecting it against degradation in aqueous solution. Additionally, phospholipid complexation could directly increase the absorption of curcumin as they are rapidly absorbed to membranes (Semalty et al., 2010).

It has been hypothesised that the majority of orally ingested curcumin is eliminated unmetabolized through faeces, while the absorbed minority is quickly converted to the water-soluble metabolites curcumin glucuronide and curcumin sulphate. For instance, a study assessed the effect of curcumin and piperine co-administration through oral administration at 2 g/kg body weight in rats and humans. The authors used the 20 mg/Kg body weight piperine

in an attempt to reduce curcumin conjugation and consequently increase bioavailability. They found a maximum concentration in serum of 1±0.26 μg/ml for curcumin alone and 1.5±0.25 μg/ml for curcumin-piperine in rats. In humans the maximum curcumin concentrations were 0.006±0.005 for curcumin alone and 0.18±0.03 μg/ml when administered in combination with piperine (Shoba et al., 1998). Curcumin alone was observed in higher concentrations in rats than humans, yet for both species the curcumin-piperine complex provided much higher concentrations and a significant increase in curcumin bioavailability.

A study using mouse which used a much smaller dose (0.1 g/kg body weight) compared to the study by Shoba et al. (1998) (2 g/kg body weight), found 0.4 μg/ml in brain tissue (Pan et al., 1999a). Another study evaluated curcumin's tissue distribution using tritium labelled drug and found detectable radioactivity in blood, liver and kidney after administration of 3 different doses (10, 80 and 400 mg curcumin-tritium complex). The authors interestingly observed that more curcumin did not necessarily result in higher absorption, with a rate of 60-66% of the given dose being absorbed for all doses (Ravindranath and Chandrasekhara, 1982). On the other hand, intraperitoneal or intravenous routes have shown better results. Yang et al. (2007) compared oral and intravenous curcumin routes in rats, and found that a dose of 10 mg/kg given intravenously resulted in a maximum circulating concentration of 0.36 μg/ml, compared to only 0.06 μg/ml when given orally at 50-fold higher dose (Yang et al., 2007). Marczylo et al. (2007) found a 20-fold increase in curcumin bioavailability in a rat study in which a curcumin-phosphatidylcholine complex (Meriva®) was given at a dose of 340 mg/kg compared to unformulated curcumin. Another study found a 3.4-fold increase in curcumin absorption in the Meriva format against unformulated curcumin (Liu et al., 2006). Overall, the variations in products, doses, delivery formats, species utilised, and outcomes measured in these studies make them difficult to compare or draw overall conclusions from as to the optimal way to provide curcumin to humans.

Several models have been developed to increase curcumin's bioavailability by encapsulation and binding with other molecules to protect this compound through digestion or to increase its BBB crossing. Most of the studies in the literature have found beneficial effects using *in vitro* models and animal disease models; however, only a few of those escalated to human trials and even fewer found the effects in animal models extrapolated to humans. The reasons attributed to the difficulty in translating the effects from animal to human models are the differences in metabolic rates and digestion, the diversity of doses and forms of administration. These factors indicate that there is still a need to better investigate curcumin's

metabolism and effects *in vivo,* as well as the need for development of technologies that enable curcumin to be incorporated in long-term clinical trials.

2.5.3 Coconut oil

Coconut oil is derived from the seeds of coconut palm (*Cocos nucifera)*. It is composed of vitamin E, polyphenols and several medium chain triglycerides such as lauric acid and caprylic acid (Wallace, 2019). Virgin coconut oil (CO) is found and sourced from the fresh kernel of coconut fruit. It can be obtained through mechanical or natural ways, with the use of heat or cold and without the need for chemical treatment (Villarino et al., 2007). Since its appearance in the market, CO has been well accepted by consumers as a functional food oil and the demand for the product continues to increase (Marina et al., 2009).

CO is composed by a mixture of medium-chain triglycerides (MCT) and long-chain triglycerides (LCT) at a ratio of 3:1 (Liau et al., 2011). Approximately half of the fatty acid content in CO is lauric acid, a substance with broad-spectrum antimicrobial activity against bacteria, fungi and viruses (M.A. Hamid, 2011). MCT are easy to digest, absorb and oxidize in comparison to long-chain fatty acids. Short-chain fatty acids and MCT are easily solubilized in the aqueous phase of the intestinal contents as long as lipase is available for digestion, absorbed readily and carried to the liver where they release energy. They also present less deposition in adipose tissue (less obesity), decrease protein catabolism, and raise thyroid function (Srivastava et al., 2017). CO could help to reduce total blood cholesterol, triglycerides, and phospholipid in serum and tissues (Nevin and Rajamohan, 2004). Additionally, they elevate energy expenditure and metabolism, and are converted to energy in the liver directly instead of being store in adipose tissue (Liau et al., 2011).

Nevin and collaborators used Sprague–Dawley rats to assess the effect of CO consumption on lipid parameters compared with copra oil consumption. They found that CO has positive effects in reducing lipid levels in serum and tissues of rats. CO reduced triglycerides, total cholesterol, LDL, phospholipids, and VLDL cholesterol levels and increased HDL cholesterol (Nevin and Rajamohan, 2004). A recent study used an AD animal model (receiving Aβ) and high-fat diet (HFD) to determine the effects of CO on inflammation and oxidative stress. CO reduced Aβ plaques and phosphorylated tau and improved hippocampus histological changes (Mirzaei et al., 2018). Another study examined the impact of coconut oil on APP gene expression and secretion of Aβ in a mouse neural crest-derived cell line(N2a cells) expressing the human APP gene (N2a/APP695). They found that coconut oil

treatment decreased APP expression in N2a cells and reduced the secretion of Aβ40 and Aβ42. The results suggest that coconut oil promotes inhibition of APP and Aβ secretion (Bansal et al., 2019).

Although CO has been used in cooking and baking, the consumption of pure oil in clinical trials can impose issues of dropout due to poor palatability. Based on the benefits of CO and the intertest in long clinical trials, the formulation of oil-in-water emulsions might increase palatability and facilitate consumption. Additionally, CO can be used in the encapsulation of lipophilic bioactive compounds increasing the beneficial effects against diseases. To elaborate a stable emulsion system using coconut oil, it is necessary to select an appropriate emulsifying agent.

2.5.4 Milk fat globule membrane

The milk fat globule membrane (MFGM) is a membrane surrounding the fat globules in mammalian milk. It is a complex system composed by several layers of proteins and lipids (Table 2.2) (Walstra, 2005). MFGM acts as a natural emulsifier to prevent flocculation and coalescence of the fat globules in milk and protects the fat against enzyme action (Singh, 2006). The proteins and phospholipids present in MFGM have gained interest due to their potential for nutraceutical applications and use as functional foods for the prevention or treatment of chronic diseases such as obesity, cancer, cardiovascular disorders and diabetes (Spitsberg, 2005b). Along with their health-promoting properties, the emulsifying property of the MFGM components has attracted research interest for exploring their isolation and application as functional foods (Singh, 2006).

Table 2.2. Composition of Milk Fat Globule Membrane. Adapted from (Singh, 2006)

MFGM composition	
Protein	**Lipids**
Mucin I (MUC1)	Triglycerides
Xanthine oxidase	Diglycerides
PAS III	Sterols
CD36 or PAS IV	Free fatty acids
Butyrophilin	Phospholipids
Adipophilin (ADPH)	Sphingomyelin
PAS 6/7[a]	Phosphatidylcholine
Fatty acid binding protein (FABP)	Phosphatidyl ethanolamine
BRCA1[b]	Phosphatidyl inositol
	Phosphatidyl serine
	Lysophosphatidylcholine

[a]Periodic acid/Schiff 6 and 7 (PAS6 and PAS 7); [b]Fatty acid binding protein BRCA1 and BRCA2 are involved in the inhibition of breast cancer.

The use of MFGM as emulsifier and for encapsulation of nutraceuticals has been studied. For instance, Phan et al., (2013) compared the emulsifying properties of MFGM fragments concentrated from reconstituted buttermilk with those from buttermilk powder (BMP), skim milk powder (SMP) and sodium caseinate (SC). They found that emulsions prepared with MFGM material were more stable and presented smaller particle sizes compared to BMP, SMP and SC (Spitsberg, 2005b). The use of phospholipids and proteins derived from MFGM has also been studied. It is possible that the combination of both could create stable emulsions which may be of interest for use in the food industry. In one study, MFGM proteins and polar lipids (phospholipids) were use separately and in combination to examine their efficiency as emulsifiers. The authors found an interactive effect on droplet size of proteins and phospholipids at emulsifier concentrations lower than 2.3%. Proteins were found to preferentially adsorbed at the emulsion droplet surface compared with phospholipids (Phan et al., 2016).

2.6 Delivery systems for bioactive compounds beneficial for AD

Despite the numerous beneficial properties that curcumin offers, its low solubility in physiological fluids and limited bioavailability need to be addressed. The most accepted strategy is the development of efficient and effective delivery systems. Delivery systems offer the advantages of encapsulating bioactive components, protecting them through the gastrointestinal digestion and increasing their delivery to the desired site of action. They can

be tailored to achieve different physico-chemical properties, to promote palatable attributes and specially to control the release of the bioactive component of interest. The compatibility between the components of a system, as well as the feasibility and costs of large-scale production, are all important to the design and development a successful delivery system (McClements, 2018).

A series of different delivery systems have been explored and used to deliver bioactive components, such as curcumin nanoparticles (Baek and Cho, 2017), casein micelles (Pan et al., 2014), soy protein complexes (Taha et al., 2018), modified starch (Yuan et al., 2019), liposomes (Cheng et al., 2017), phospholipid complex (Bai et al., 2016), nano emulsions (Artiga-Artigas et al., 2018, Jintapattanakit et al., 2018), and emulsions (Acevedo-Fani et al., 2017, Davidov-Pardo et al., 2016, Kharat et al., 2020). Emulsion-based delivery systems also present a wide range of applications and have been used in the market for decades. The versatility and acceptability of emulsion systems make them a good alternative to the encapsulation of bioactive components. Milk is the commonest and most widespread example of a natural emulsion system.

2.6.1 Emulsion-based delivery systems

Oral lipid delivery systems can be used to increase the bioavailability of poorly water-soluble drugs and functional ingredients. The lipophilic bioactive compound is encapsulated into the oil droplets, allowing for a controlled release. Emulsion-based delivery systems have been increasingly used in the food and pharmaceutical industries for controlled release, encapsulation and protection of bioactive compounds (Porter et al., 2007, Scheuble et al., 2018).

Oil in water emulsions (O/W) and nano-emulsions (NE) are defined as thermodynamically unstable colloidal dispersion systems composed of lipid droplets dispersed within an aqueous medium (Chang et al., 2018, Tadros et al., 2004). O/W and NE can be differentiated from each other by the size of the oil droplets (particles) generated during homogenization: NE have a mean droplet radius <100 nm, while O/W have a mean radius of >100 nm (Ahmed et al., 2012). The method of homogenization and the composition of the system are the main factors involved in the determination of particle size. High-energy emulsification methods (high-shear blending, high-pressure homogenization, and ultrasonic homogenization) as well as low- energy emulsification methods (phase inversion temperature)

can be used. The intense shear flow and turbulence cause dispersion of the oil phase into small oil droplets. To overcome the instability issue, emulsifiers need to be add to stabilize the colloidal system. The surface-active surfactants become adsorbed at the oil–water interface, lowering the surface tension and facilitating further droplet disruption (Dalgleish, 2006). They create a protective layer surrounding the oil droplets.

The small size of NE particles confers better stability to particle aggregation, separation and gravitation (Solans et al., 2005). However, emulsions containing smaller fat globules suffer faster lipolysis than the ones containing larger globules within the same volume of oil, because smaller globules present a larger surface area and thus provide more contact with the enzymes when compared to larger globules (Michalski et al., 2013). A study reported that NE with 79.5 nm droplets was more effective than O/W to increase the anti-inflammatory activity of curcumin (Wang et al., 2008). However, another study reported no major differences in behaviour under gastric conditions between O/W and NE prepared with three different oils for the encapsulation of curcumin (Ahmed et al., 2012). Different types of oil are unlikely to impact particle size significantly, yet it is likely to alter the amount of curcumin encapsulated and rate of digestion. For instance, a study found that among other oils used for curcumin encapsulation, coconut presented the best curcumin solubility (Jintapattanakit et al., 2018).

Emulsifying agents are important constituents in an emulsion system since they act as a surface agent, developing bonds between the two immiscible liquids. Structurally, they are amphiphilic molecules, possessing both hydrophobic and hydrophilic moieties. Their hydrophilic head connects with the water phase and lipophilic tail connects with the oil phase to bring the liquids together. The lipophilic tails point toward the centre of oil droplet and one layer of hydrophilic heads of emulsifying agent surrounds the surface of the oil droplets, avoiding coalescence of oil droplets and stabilizing the emulsion (Singh et al., 2009).

Small molecule surfactants such as Tweens (sorbitan fatty acid esters) and Spans (nonionic surfactant sorbitan fatty acid esters) can create stable emulsions. However, for food products their use has lessened, with the use of natural surfactants instead now increasing due to their market appeal of being label friendly. Those surfactants can be proteins, polysaccharides, or phospholipids, and they are often used as emulsifiers and stabilizers in food emulsions (Bai et al., 2016, Silva et al., 2015). Using sufficient amount of emulsifying agents, emulsions can be made to be more stable over extended time periods (Ramisetty et al., 2015).

Food proteins have high nutritional value and are safe for consumption. Many of them, such as soy protein and the milk proteins whey and casein, have been extensively used as emulsifiers in the food industry because of their amphiphilic nature and ability to form films (Chang et al., 2018, Foegeding and Davis, 2011). They present diverse emulsifying abilities due to variations in their structures, flexibilities, states of aggregation and compositions at the oil-water interface. A range of milk protein ingredients are used to improve the functional properties and nutritional value of food products. Different milk proteins lead to the formation of emulsions with different surface compositions and structures, which consequently interfere in their digestion behaviours (Singh and Ye, 2013). Generally, the emulsions stabilized by proteins are sensitive to temperature, pH, salt and environmental stresses, which result in coalescence, flocculation, creaming and phase separation (Lam and Nickerson, 2013).

Phospholipids are the major lipid components in membranes. In short, phospholipids are lipids that contain phosphorus, a polar portion and a non-polar portion in their structures, being divided into glycerophospholipids (glycerol backbone) and sphingomyelins (sphingosine and glycerol backbones) (Li et al., 2015a). Due to their amphiphilic structure, they tend to form bilayers and lamellar structures, making them an important structural component of cell membranes in plants and animals. Additionally, their properties confer a natural way to promote emulsification of lipid droplets in the storage cells and organelles of plants, animals and microorganisms (Singh et al., 2009). The fact that phospholipids present both polar and nonpolar parts allows them to be adsorb to oil-water interfaces and act as emulsifiers (Pichot et al., 2013). They can create a monolayer around the oil droplets, where the fatty acid tails project into the oil droplets and the hydrophilic head points toward the water, or they can form multiple layers with each layer consisting of two phospholipids lined up head- to-head and tail-to-tail (Li et al., 2015a, Pichot et al., 2013). Phospholipids emulsifiers used in the food industry are typically called lecithin and can be extracted from many sources including soybeans, eggs, milk, rapeseed, canola seed, cottonseed, and sunflower (Klang and Valenta, 2011).

2.7 Emulsion digestion

Lipids are important constituents of the diet, as they provide essential fatty acids, such as linoleic acid and α-linolenic acid, which are not produced by the human body (Simopoulos, 1999). Lipids are also responsible for transporting fat-soluble bioactive molecules, such as hydrophobic polyphenols. Around 20 to 40% of the diet is composed of lipids, which are often ingested in an emulsified format. The digestion of orally ingested lipids directly affects the delivery of lipophilic bioactive compounds. Therefore, understanding the kinetics of lipid

digestion and absorption is paramount for pharmaceutical and food science researchers. The manufacturing of lipid structures for the controlled release of drugs and nutraceuticals allows the formulation of systems to encapsulate and deliver compounds based on understanding their passage through the GI tract (Acevedo-Fani and Singh, 2022, McClements et al., 2009).

A series of *in vitro* digestion models have been used to better understand how lipids are digested in the presence of gastric and pancreatic lipase and bile salts (Bourbon et al., 2018, Cheng et al., 2017, Colle et al., 2012, Gallier et al., 2012, Li et al., 2013, Sarkar et al., 2018, Sek et al., 2002). For instance, (Malaki Nik et al., 2011) used a sequential *in vitro* digestion model to investigate the changes in the physicochemical properties of O/W emulsions prepared using whey protein isolate (WPI) or soy protein isolate (SPI) during gastrointestinal transit. The authors found that the size of the oil droplets significantly changed during the duodenal phase in the presence of bile salts and phospholipids. The particle size is believed to play a critical role in lipid digestion, indicating that the interfacial composition of the original emulsion plays a major role in determining the extent of lipolysis.

It has been reviewed and discussed elsewhere that the fate of emulsions under GIT conditions strongly depends on their original characteristics, such as interfacial structure and composition, droplet size distribution, nature of the lipid phase and continuous phase composition (Acevedo-Fani and Singh, 2022). Emulsified lipids are often surrounded by an interfacial layer of emulsifying molecules, such as proteins, polysaccharides, phospholipids and surfactants. Differences in the oil droplet coatings lead to variations in electrical charge, thickness, permeability, environmental responsiveness, resistance to displacement, and susceptibility to enzymatic digestion. The aggregation state (flocculated or partially coalesced, for example) can also influence the rate of lipid digestion (McClements, 2004). Additionally, emulsified lipids can differ in their physical state and polymorphic form, being liquid, solid, or partially solid at body temperature (Kralova and Sjöblom, 2009).

After ingestion, exposure to salivary, gastric and intestinal fluids and enzymes promotes several complex physical and chemical changes to the emulsified lipids. Those changes directly affect and determine their ability be digested and absorbed. The oral processing of lipids occurs in the mouth, and it is more relevant to solid and semi-solid structures, as those undergo mastication, as opposed to liquid forms that spend less time and experience less effects of the mechanical breakdown of food. In addition to mastication, the salivary fluids promote the lubrication of food into a bolus suitable for swallowing (Acevedo-Fani and Singh, 2022, Sarkar et al., 2009).

In the stomach, the gastric juices and enzymes are mixed with the swallowed bolus through the mechanical action of the peristaltic movements. The stomach's low pH facilitates pepsin's action, breaking down mostly proteins. The presence of surface-active compounds and gastric lipase allows the beginning of lipid digestion in the stomach. It is believed that around 10 – 30% of lipid digestion in adults occurs in the stomach. Research suggests that the human gastric lipase binds to the oil-water interface of emulsion, initiating the breakdown of triacylglycerols (TAG) to diacylglycerol (DAG) and non-esterified fatty acids (NEFA) (Acevedo-Fani and Singh, 2022). Additionally, gastric lipase preferably hydrolyses TAG at the sn-3 position and more efficiently breaks down medium-chain triglycerides than long-chain triglycerides. The partially digested food (chyme) is then emptied from the stomach to the duodenum, where pH changes occur and intestinal digestion starts (Acevedo-Fani and Singh, 2022, McClements and Li, 2010, Pafumi et al., 2002, Rogalska et al., 1990).

The small intestine, composed of the duodenum, jejunum and ileum, is where most lipolysis and lipid absorption occurs. The presence of bile salts, co-lipase and phospholipids facilitate the action of the pancreatic lipase, promoting the further breakdown of TAG into DAG and absorbable monoacylglycerol (MAG) and NEFA. Bile salts are essential constituents in the digestion of lipids, as they are surface-active and can facilitate the emulsification of the lipids by binding to the droplet surface. Phospholipids behave similarly to bile salts, facilitating the absorption of co-lipase to the droplet surface. Co-lipase then anchors the pancreatic lipase to the surface, initiating the lipolysis in the position sn-1 and sn-3 of TAG. In addition, phospholipase A2 also binds to the oil-water interface promoting the hydrolyses of the fatty acyl ester bond at position 2 in phospholipids, releasing NEFA and lysolecithin, such as lyso-phosphatidylcholine. Cholesterol, phospholipids and bile salts facilitate the solubilisation of lipolytic products in the intestinal lumen by forming self-assembled structures called mixed micelles. The jejunum is responsible for most of the uptake and absorption, yet all regions can uptalking TAG digestion products. NEFA comprised of short carbon length (<12) fatty acids are directly absorbed into the portal vein. In contrast, longer chain lengths are re-esterified into TAG, incorporated into chylomicrons and then enter the lymphatic transport pathway. Bioactive lipophilic molecules are believed to be mixed into the mixed micelles and absorbed with FFA digestion products (Carriere et al., 1993, McClements and Li, 2010, D'Aquila et al., 2016, Dennis, 1994, Verger, 1984, Wit et al., 2012, Acevedo-Fani and Singh, 2022).

Each emulsion's structure undergoes a series of rearrangements in its original droplet distribution once it passes through the GIT. Different surface compositions, such as thickness

and the nature of the emulsifier, will therefore influence how these changes occur during digestion. The particle size has also been shown to affect digestion, as smaller particle sizes have a higher surface area. Changes in pH and ionic strength in the stomach can lead to creaming, flocculation or coalescence of oil droplets. In the small intestine, the presence of surface active components further alters the emulsion's structure, leading to the binding of enzymes and structure breakdown, forming mixed micelles. An extensive review by (Acevedo-Fani and Singh, 2022) explored the digestion of emulsions in detail and suggested approaches to tailoring emulsions structures for bioactive delivery.

2.8 Prospects on delivery of bioactive compounds

The use of delivery systems, such as liposomes, is widely employed by the pharmaceutical industry to deliver bioactive components. Such systems can facilitate the crossing of compounds to the bloodstream and their delivery to the desired site of action. Since there is no cure for AD, trials to develop a drug to clear the disease biomarkers and improve cognition are the focus of research groups. Some promising drugs have been developed recently, yet many side effects have been associated with those and the search for alternative treatments continues. That reinforces the fact that prevention continues to be a good approach to the disease prevention and to delay its onset.

Therefore, in this study I aimed to explore the use of bioactive components to create food-based delivery systems aiming to prevent AD. Given the complexity of the disease, advocating for a food supplement to support brain health could provide those affected by dementia with an extra alternative to prevent and delay the disease onset.

Chapter 3 - Materials and equipment

3.1 Materials

The common materials, equipment and methods used across the majority of the experiments are described in this chapter. Those that are specific for individual studies have been included in the related chapters.

3.1.1 Milk Fat Globule Membrane derived material

Milk Fat Globule Membrane derived materials (MFGM) were generously provided by Fonterra Cooperative Ltd., Palmerston North, New Zealand. The fractions varied in phospholipids and protein composition as detailed in Table 3.1 as per manufacturer's specifications. The same materials were used in all experiments.

Table 3.1. MFGM composition

	g/100g sample						
	PE	**PC**	**SM**	**PS**	**PI**	**TPL**	**Protein**
Lipid 700 (MFGM1)	26	33	23	6.3	5.1	41	-
BPC50GU09 (MFGM2)	4.6	3.9	3.3	1.8	1.3	15	50 (skim)
HFWPC70 (MFGM3)	1.5	1.4	1.4	0.7	0.5	5.4	72 (whey)

Phosphatidylethanolamine (PE), Phosphatidylcholine (PC), Sphingomyelin (SM), Phosphatidylserine (PS), Phosphatidylinositol (PI), Total phospholipids (TPL)

3.1.2 Curcumin

Curcumin (turmeric extract) was provided by RMF nutraceuticals, Christchurch, New Zealand and sourced from Shaanxi Guanjie Bio-technology Co., Ltd. China. Curcumin purity was 95.5% tested by HPLC assay, particle size higher than 95% (80 mesh) and 0.54% moisture. The extract complied with all the specifications according to manufacturer's declaration. The same curcumin was used in all experiments.

3.1.3 Coconut oil (CO)/Medium Chain triglyceride oil (MCT)

Virgin coconut oil (CO) brand Essente cold press organic was obtained from Davis Trading Company, Palmerston North, New Zealand. The fatty acid profile was not specified, and gas chromatography was used to determine the composition of fatty acids (Table 3.2) following the protocol described by Zhu and collaborators (Zhu et al., 2011). The CO was used without further purification.

CocoMCT® oil (MCT) was a gift from Chemrez technologies, inc., Quezon City, Philippines. CocoMCT® is purified coconut oil that contains caproic acid, caprylic acid, aapric acid, and lauric acid.

Table 3.2. Fatty acid composition of Essente and CocoMCT® oils used for emulsion preparation

	Carbon chain distribution (%)	
	Essente virgin coconut oil	**CocoMCT®**
Caproic acid (C6:0)	N/D	0.16
Caprylic acid (C8:0)	6.64	42.2
Capric acid (C10:0)	6.12	25.9
Lauric acid (C12:0)	48.3	31.7
Myristic acid (C14:0)	18.2	N/A
Palmitic acid (C16:1)	9.34	N/A
Stearic acid (C18:0)	3.09	N/A
Oleic acid (C18:1)	5.46	N/A
Linolenic acid (C18:2)	1.35	N/A

The composition of commercial Essente oil was determined using gas chromatography. The composition of CocoMCT® was provided by Chemrez certificate of analysis. N/D=peak not detected; N/A= purified and therefore not present or stated in the certificate of analysis.

Initial experiments were conducted using Essente CO oil. CO was replaced with CocoMCT® later in the study; the CO or MCT product used is specified in each relevant chapter.

3.1.4 Fish oil (FO)

Fish oil (FO) was provided by EPAXß®, Ålesund Norway. The total ω-3 fatty acids composition was 82%, with 13% being EPA (C20:5), 54% DHA (C22:6) and 11% DPA (C22:5). The remaining fatty acids were composed of saturated fatty acids (2%) and monosaturated fatty acids (9%). The same FO was used in all experiments.

3.1.5 Phospholipid standard

Fonterra NMR certified dairy ingredient PC700 was used as the standard for LC-MS quantification of phospholipid in samples.

3.1.6 Curcumin Standard

Curcumin, catalogue number 78246, ≥99.5 purity (HPLC), molecular weight 368.38, Diferuloylmethane-1,7-bis(4-Hydroxy-3-methoxyphenyl)-1,6-heptadiene-3,5-dione was

purchased from Sigma Aldrich Chemical Co., St. Louis, MO, USA and used as the standard for the HPLC analysis.

3.1.7 Chemicals

Milli-Q water (purified by filtration with Milli-Q apparatus; Millipore Corp., Bedford, MA, USA) was used as a solvent throughout the experiments. The common chemicals and reagents used throughout the experiments and their respective CAS number are specified below (Table 3.3).

Table 3.3. List of general chemicals used throughout the experiments. Chemicals used for specifically for each individual set of experiments are described in each chapter and were purchased from Sigma Aldrich Chemical Co., St. Louis, MO, USA unless otherwise specified.

Number	Chemical/Reagent	CAS number
1	Hydrochloric acid (HCl)	7647-01-0
2	Sodium hydroxide (NaOH)	1310-73-2
3	Fast green FCF	2353-45-9
4	Lissamine™ rhodamine B sulfonylchloride	62796-29-6
5	Methanol	67-56-1
6	Ethanol	64-17-5
7	Glacial acetic acid	64-19-7
8	Chloroform	67-66-3
9	Potassium chloride	7447-40-7
10	Ammonium acetate	631-61-8
11	Acetonitrile	75-05-8

3.2 Equipment

The common equipment used for most of the experiments is described in this section. Experimental techniques and equipment specific to each experiment have been included in individual chapters.

3.2.1 Water bath

Samples were heated in a “T” shaped water bath tank attached to an open bath heating circulator with a temperature-controlled heating coil (MA-6, Julabo ED, Germany). The temperature was adjusted to solubilise materials into solutions and checked using a hand-held thermometer. A hot plate stirrer (F20500162 ARE, VELP Scientifica, Italy) was fitted under the water bath and used to stir the heated samples; only the stirring function was used as the

heating was provided by the water bath to ensure even and more accurately controlled temperature.

3.2.2 pH meter

A pH meter was used to adjust the pH of solutions and samples throughout the experiments (ECPH51042S-I, Oakton Instruments - Illinois, US). The equipment was calibrated daily before starting the measurements using standard buffer solutions of pH 4 and 7. While not in use the pH meter probe was left in a storage solution of 3M potassium chloride as per the manufacturer's instructions.

3.2.3 High-performance liquid chromatography (HPLC)

A 1200 HPLC system (Agilent Technologies, Santa Clara, CA, USA) controlled by EziChrom software (Agilent Technologies, USA) was used to determine curcumin concentrations in fresh and digested samples. The equipment was equipped with an autosampler and Synergi Hydro-RP 4 μm analytical column (150 × 4.6 mm, 4 μm, Phenomenex, USA).

3.2.4 Centrifuges

Different centrifuges were used throughout the experiments according to different speed and volume requirements. Samples that required less than 5000 x g were centrifuged using a benchtop centrifuge (ST40, Thermo Scientific, Lanenselbold, Germany). For samples that required speeds higher than 5000 x g, a Sorvall WX Ultra Series ultracentrifuge was used (Thermo Fisher Scientific, Asheville, US). Samples prepared or extracted in small volumes (Eppendorf tubes) were centrifuged using an Eppendorf centrifuge 5424 (Eppendorf®, Hamburg, Germany) operating at a maximum speed of 15000 x g.

3.2.5 Handheld homogeniser

An Ultra-Turrax T-25 hand-held homogeniser (Janke & Kunkel, Staufen, Germany) operating at 13,500 rev/min was used to prepare primary emulsions (coarse emulsions).

3.2.6 Homogeniser

A two-stage valve homogeniser (APV 2000, Silkeborg, Denmark) (Figure 3.1), operating at 40000 kilopascals (kPa) bar for the first stage and 50000 kPa for the second stage, was used to prepare the final emulsions. Emulsions were prepared at least in triplicate and passed three times through the homogeniser.

Figure 3.1. Two valve homogenizer APV 2000, Silkeborg, Denmark

3.2.7 Mastersizer

The oil droplets diameter throughout the experiments was determined by laser light scattering using a Mastersizer 2000 E (Malvern Instruments, Malvern, Worcestershire, UK) (Figure 3.2). The Mastersizer measures the angular dependence of the scattered light from the emulsion droplets and fits the scattering data to well-known theoretical models. A monochromatic light beam passes through the measurement cell, where the emulsion droplets scatter it. The intensity of the scattered light is measured as a function of the scattering angle using a range of photosensitive detectors. The scattering angle is usually an inverse function of the droplet size so that the scattering pattern contains information about the droplet size distribution of the emulsion. Therefore, a low-angle scattering is more sensitive to larger droplets, and wide-angle measurements are generally more responsive to smaller droplets. The droplet size distribution is calculated based on the statistical fit between the measurements of intensity vs scattering angles predicted by the Mie theory. The Sauter-average diameter, d_{32} (μm) and volume-mean diameter, d_{43} (μm), were calculated. Samples were analysed at least in

triplicate, and the values of the three readings were used to calculate the mean particle size and plot particle size distribution.

Figure 3.2. Mastersizer 2000 E (Malvern Instruments, Malvern, Worcestershire, UK)

3.2.9 Zetasizer

The zeta potential (mV) values of the emulsions and their respective digested materials were measured by laser doppler velocimetry and phase analysis light scattering technique using a Malvern Zetasizer Nano ZS (ZEN3600, Malvern Instruments Ltd. Malvern, Worcestershire, UK) (Figure 3.3). The system uses micro-electrophoresis in a capillary cell with electrodes at both ends, to which a potential is applied. The droplets within the dispersion move towards the oppositely charged electrode at a certain velocity, which is determined by measuring the frequency shift of the incident laser beam. The velocity is converted to zeta potential following Henry's equation, where known variables such as the dielectric constant of the medium and viscosity are substituted. Samples were measured shortly after 100-fold dilution in continuous phase or appropriate background buffer. The temperature of the electrophoresis cell was kept at 25°C. The zeta-potential measurements were reported as the mean and standard error of at least six readings. All measurements were conducted on at least two freshly prepared emulsions.

Figure 3.3. Zetasizer nano ZS (ZEN3600, Malvern Instruments Ltd. Malvern, Worcestershire, UK)

3.2.10 HPLC-LC/MS

An Agilent 1200 series HPLC system (Santa Clara, CA, USA), interfaced to a SCIEX 6500 QTrap mass spectrometer (AB SCIEX, Framingham, MA, USA) and quantified in positive mode, was used to characterise the phospholipid (PL) composition of emulsions, digesta and plasma samples. The PL separation was archived using an APS-2 hypersil hydrophilic column (150 mm × 2.1 mm, 3 μm, ThermoFisher Scientific, Waltham, MA). Further operational details of the system are described in the individual chapters.

3.2.11 Confocal Laser Scanning Microscopy

Confocal scanning laser microscopy was used to provide high-resolution images of the microstructure of the samples. Confocal scanning laser microscope (SP5 DM6000B, Leica Microsystems, Heidelberg, Germany) had a motorised focus and a 63 X oil immersion objective with an excitation line of 488 nm from an argon laser. A 100 X oil immersion objective with sequential excitation lines of 488nm from argon laser and 633nm from a helium-neon laser was used.

Chapter 4 - Milk fat globule membrane derived material as an emulsifying agent in the preparation of curcumin loaded oil-in-water emulsions

Abstract

The milk fat globule membrane (MFGM) is a complex tri-layer membrane encapsulating fat globules in milk. In addition to its natural emulsifying abilities, the MFGM has gained interest due to its health promoting properties. Curcumin is a potent antioxidant extensively studied over years against a series of diseases, including Alzheimer's disease (AD). However, curcumin presents very low bioavailability, limiting its use as a natural treatment for AD and other conditions. In this study, we evaluated the potential applications of MFGM-derived materials to produce oil in water (O/W) emulsion systems and encapsulate curcumin. Three commercial MFGM derived materials - Lipid700 (MFGM1), BPC50GU09 (MFGM2) and HFWPC70 (MFGM3) - were used to prepare emulsion systems using virgin coconut oil (CO) or a combination of CO and fish oil (FO).

The emulsifying capacity of various MFGM fractions and their ability to encapsulate curcumin were studied. Emulsion particle size decreased significantly with increasing concentration of the emulsifier, reaching a plateau after addition of 3 and 5% (w/w). The mean particle sizes of emulsions prepared using MFGM2 and MFGM3 were significantly lower than those prepared using MFGM1 as an emulsifier. The smallest particle size was obtained using MFGM3 ($d_{3,2}$ 0.25μm), and the largest with MFGM1 ($d_{3,2}$ 0.43μm). All emulsions were stable to particle size changes over 40 days at 4°C and presented negative zeta-potential varying from -50 to -20mV. MFGM1-prepared emulsions had higher curcumin loading efficiency (>80%) compared to MFGM2 and MFGM3 stabilised emulsions (<80%). Phase separation studies indicated that most of the curcumin in the system was entrapped inside the oil droplets, being present at higher than 90% in the cream phase. Phospholipids also preferably adsorbed to the droplets of emulsions stabilised by MFGM2 (>70%) and MFGM3 (>80%), as opposed to only about 50% of phospholipids in MFGM1 being in the cream phase. Differences in the phospholipid and protein composition were responsible for differences observed in size, zeta-potential and position of curcumin in phospholipids in the systems. Overall, all MFGM fractions were efficient to create emulsions with small particle size, that were stable over time and were able to encapsulate curcumin.

4.2 Introduction

Curcumin, the main constituent in the rhizomes of the herb turmeric, is a polyphenol widely studied and used as a nutraceutical. Throughout history, dried turmeric roots have been used for medicinal purposes in traditional Chinese medicine and Ayurvedic Indian medicine to treat skin disease, allergies, hepatic disorders, inflammation, sinusitis and oxidative stress-related conditions (Ammon, 1991). Fresh turmeric roots and dried turmeric powders are composed of a mixture of curcuminoids, with the three predominant ones being curcumin, desmethoxycurcumin (DMC) and bisdemethoxycurcumin (BDMC). While curcuminoid mixtures have shown health benefits (Samanta et al., 2010), curcumin alone is the compound with the most potent antioxidant and anti-inflammatory activities (Subramanian et al., 1994).

Despite *in vitro* and *in vivo* benefits of curcumin against inflammation (Wang et al., 2008, Khayyal et al., 2018), oxidative stress (Wei et al., 2006), cancer (Huang et al., 1994) and AD (Jeyapriya Raja Sundaram, 2017, Lim et al., 2001a), clinical evidence of its benefits are still limited, due mainly to curcumin's low bioavailability and rapid degradation (Strimpakos and Sharma, 2007). Curcumin is soluble in organic solvents and oils but very poorly in water, which is the main constituent of physiological fluids. Once ingested, curcumin is rapidly metabolised by the liver and conjugated into curcumin glucuronide, curcumin sulphate and other metabolites (Ravindranath and Chandrasekhara, 1981, Sharma et al., 2001). To reach the desired site of action, the amount of curcumin that needs to be administrated is often very high, creating barriers to long-term trials and sensory acceptance. In the last decade, researchers have focused on increasing curcumin's oral bioavailability through encapsulation in a variety of delivery systems.

The development of delivery systems to improve the delivery of nutraceuticals, improve palatability and increase bioaccessibility involves manipulating microstructure and physicochemical properties. Understanding the relationship between food properties, digestion and absorption can facilitate developing delivery systems (McClements and Li, 2010). Considering the high hydrophobicity of curcumin and the mainly aqueous base of physiological fluids, a delivery system using a lipid-based strategy to solubilise and encapsulate curcumin has been shown to be a good approach (Araiza-Calahorra et al., 2018).

Emulsion-based delivery systems are widely used as they are a simple, effective, easy to reproduce and scalable systems. An emulsion consists of the dispersion of two immiscible liquids, usually oil and water, stabilised by a surfactant (Sarkar et al., 2018, McClements and

Li, 2010). Small droplets of one liquid are dispersed in the other immiscible liquid, and depending on the proportions and arrangement, they can be classified as oil-in-water (O/W) or water-in-oil (W/O). Emulsions are thermodynamically unstable, and surfactants or emulsifiers need to be used to reduce interfacial tension and prevent destabilisation over time, avoiding creaming, sedimentation, flocculation and coalescence (Singh et al., 2009). Protein ingredients derived from milk and eggs are the most commonly used food emulsifying agents (Dickinson, 1988).

The emulsifiers are simultaneously adsorbed to the oil-water interface during homogenisation, creating a stable layer at the droplet surface. The layer surrounding oil droplets can be composed of different adsorbed materials such as low molecular weight emulsifiers, proteins, phospholipids, monoacylglycerols and fatty acid esters (Singh et al., 2009). Proteins are readily absorbed into the oil-water interface when used as emulsifiers, and they undergo rearrangements to create a stabilising layer (McClements, 2004). Phospholipids derived from milk, egg and soybean can be used to create a monolayer or a multi-lamellar structure around the oil-water interface. The type of structure varies according to the amount of phospholipid added during emulsion formation (Dalgleish, 2006). There has been an increased interest in the use of natural emulsifiers and the attempt to mimic food structures, as they present complex structures with the potential to control the delivery of desired compounds.

Milk is a naturally occurring emulsion, with droplet size varying from 0.1 to 15 μm. A unique characteristic of fat globules in milk is the membrane coating and stabilising the oil droplets, the milk fat globule membrane (MFGM). This unique membrane is produced by the mammalian cells and is a complex tri-layer structure surrounding each lipid droplet in milk. The inner layer comprises a lipid monolayer and an outer lipid bilayer consisting of enzymes, glycoproteins, proteins, neutral lipids, and polar lipids such as phospholipids and glycosphingolipids (Dewettinck et al., 2008).

The emulsifying properties of the MFGM have led to research into its isolation and application as a natural and functional food ingredient to encapsulate several nutraceuticals (Singh, 2006). For instance, Liu and collaborators prepared liposomes loaded with positively charged lactoferrin (LF) using MFGM-derived phospholipids and observed that the liposomes were stable and protected the entrapped LF from pepsin hydrolysis, yet pancreatin disrupted the system promoting release of LF (Liu et al., 2013). O/W emulsions prepared with MFGM protein or polar lipid (phospholipids) concentrates showed that at identical concentrations, MFGM protein concentrate had a better emulsifying ability than phospholipid concentrate,

indicating that MFGM protein from reconstituted buttermilk is a better emulsifier in the preparation of emulsions compared to phospholipids concentrate (Phan et al., 2016). Corredig and Dalgleish used a fraction derived from MFGM isolated from fresh raw cream and found a strong molecular interaction between the adsorbed MFGM (composed of phospholipid and protein) at the oil-water interface. The membrane formed around oil droplets was not affected by the presence of other surfactants, suggesting that this MFGM fraction was a good emulsifier, which promoted a structure with a different behaviour from emulsions stabilized by other milk proteins (Corredig and Dalgleish, 1998). Assessments of MFGM for the delivery of cyclosporine *in vivo* indicated enhanced delivery to blood and lymphatic fluid. Cyclosporine is used as an immunosuppressant medication and was encapsulated in olive oil emulsions with or without the bioactive and administered via intraduodenal route in rats. The authors suggest that MFGM can be used as an intestinal absorption enhancer of cyclosporine (Sato et al., 1994)

In addition to good emulsification properties, MFGM components have received great interest because of their health benefits. Sphingolipids and phospholipids are complex biological lipids that define the structural properties of membranes and lipoproteins. These compounds mediate important transmembrane signalling mechanisms that can regulate cell growth, development and differentiation (Schmelz, 1996, Spitsberg, 2005b, Singh, 2006). The MFGM phospholipids and proteins have been reported to have bioactivities, including anti-cancer, anticholesterolemic and antibacterial effects (Spitsberg, 2005a). For example, sphingomyelin has been shown to possess anti-cancer properties, reducing the number of colon tumours and aberrant crypt foci in a carcinoma mouse model (Schmelz, 1996). Complex lipids are also associated with age-related diseases, stress responses, cellular apoptotic pathways and the development of AD (Bouhours and Bouhours, 1981, Conklin, 2002, Singh, 2006).

The main objective of this chapter was to assess the emulsifying ability of different commercial MFGM materials and their ability to create stable emulsions, while carrying higher amounts of curcumin.

4.3 Materials and Methods

4.3.1 Materials

MFGM-derived materials were provided by Fonterra Co-operative Ltd. and differed in their phospholipid and protein concentrations. MFGM1 had no protein content and a mean total phospholipids (TPL) content of 332.46 mg of per gram of sample. MFGM2 comprised 50%

skim protein and 100.46 mg/g TPL, while MFGM3 had 72% whey protein and only 32.36 mg/g TPL. Virgin coconut oil (CO) and fish oil (FO) were sourced as cited in 3.1.3 and 3.1.4 respectively.

Curcumin (95.5% purity) was provided by RMF nutraceuticals, Christchurch, New Zealand and sourced from Shaanxi Guanjie Bio-technology Co., Ltd., China. Curcumin catalogue number 78246, ≥99.5 purity (HPLC), molecular weight 368.38, Diferuloylmethane-1,7-bis(4-Hydroxy-3-methoxyphenyl)-1,6-heptadiene-3,5-dione was purchased from Sigma Aldrich Chemical Co., St. Louis, MO, USA and used as the standard for the HPLC analysis. Fonterra NMR certified dairy ingredient PC700 was used as the standard for LC-MS quantification of phospholipid in samples.

4.3.2 Methods

4.3.2.1 Preparation of oil phase

Curcumin (turmeric extract, 95.5% purity) was weighed into an Erlenmeyer flask, and CO was added at 2 mg curcumin/g of oil to create the desired curcumin solubility. The selection of curcumin concentration per gram of oil was determined by curcumin solubility in CO (Appendix A4.1), which was in accordance with previous literature (Jintapattanakit et al., 2018). The mixture was stirred for at least 4 hours at 60°C to allow complete curcumin solubilisation in the oil. To avoid oxidation, FO was added to CO (1:1) after the temperature dropped to < 30°C. The final curcumin concentration was 2 mg/g for CO oil and 1 mg/g for CO: FO (1:1) mixture.

4.3.2.2 Preparation of MFGM solutions

Emulsifier solutions (0.5 to 5.0 wt%) were prepared by dissolving an appropriate amount of MFGM materials in milli-Q water and stirring for 2h at 40°C to allow complete dissolution. For MFGM1, the pH was adjusted to 5.0 to allow better solubility. The MFGM preparations were mostly composed of water-soluble components. The pH for all MFGM solutions was adjusted to 7.0 using 1M NaOH or 1M HCl before homogenisation with the oil phase.

4.3.2.3 Preparation of O/W emulsions

The previously prepared oil phase was added to MFGM solutions to form final emulsions composed of 20 wt% oil and 80 wt% aqueous phases (Table 4.1). The oil and aqueous phases were mixed as described in 3.2.5 and 3.2.6. Emulsions were prepared at least in triplicate.

Table 4.1. Emulsions coding and composition. CO = virgin coconut oil; FO = Fish oil

Emulsion code	Oil composition – 20% (w/w)	Emulsifier composition
S1	CO	MFGM1 (Lipid700) – 5% (w/w)
S2	CO:FO (1:1)	MFGM1 (Lipid700) – 5% (w/w)
S3	CO	MFGM2 (BPC50 GU09) – 3% (w/w)
S4	CO:FO (1:1)	MFGM2 (BPC50 GU09) – 3% (w/w)
S5	CO	MFGM3 (HFWPC70) – 3% (w/w)
S6	CO:FO (1:1)	MFGM3 (HFWPC70) – 3% (w/w)

4.3.2.4 Determination of surface composition

The total unabsorbed curcumin and phospholipid concentrations were determined using the method of Ye (2008) with some modifications. Emulsions were centrifuged at 45,000xg for 40 min at 25°C in a temperature-controlled centrifuge (Sorvall RC5C, DuPont Co., Wilmington, DE). The top cream phase was carefully removed using a spatula. The cream layer was dispersed in Mili-Q water and re-centrifuged at 45,000g for 40 min. The cream layer was then extracted for phospholipid and curcumin analysis, as described in sections 4.3.2.5d and 4.3.2.5e. The surface phospholipid concentration (%) was calculated from the difference between the amount of phospholipid or curcumin used to prepare the emulsion and that measured in the cream phase after centrifugation.

4.3.2.5 Characterisation techniques

The analytical techniques used for the physicochemical characterisation of emulsions and emulsions submitted to treatments presented in the following chapters are presented in this section.

a) Particle size

The diameter of the oil droplets was measured by laser light scattering using a Mastersizer 2000 E (Malvern Instruments, Malvern, Worcestershire, UK). The particle size is

widely used to characterise emulsions, and the most common instruments used are Mastersizer and Zetasizer (McClements, 2004). Mastersizer uses static light scattering to measure the angular dependence of the scattered light from the emulsion droplets and fits the scattering intensity data to theoretical models. A laser generates a monochromatic light beam that passes through a measurement cell scattered by the emulsion droplets. The refractive index of the dispersed phase was set at 1.470 (with an absorption index of 0.001), and that of water was at 1.330. Particle diameters were calculated from at least 10 measurements and presented as mean ± SEM.

b) Zeta potential

The zeta potential (mV) was measured shortly after diluting the emulsions (100 fold) in milli-Q water using a Zetasizer Nano ZS (Malvern Instruments Ltd. Malvern, Worcestershire, UK). The technique for measurement uses laser doppler velocimetry and phase analysis light scattering (M3-PALS), where a capillary cell (with electrodes at both ends) is used to attract droplets with opposite charges at a certain velocity that is determined by the frequency shift of the incident beam light measurement. The speed at which the droplets move to the fields is then converted to zeta-potential. The temperature of the cell was maintained at 25°C. The results of zeta-potential were represented as the mean of at least 5 readings.

c) Confocal Laser Scanning Microscopy

Confocal laser scanning microscopy provided high-resolution images of the emulsion's microstructure. The confocal scanning laser microscope (SP5 DM6000B, Leica Microsystems, Heidelberg, Germany) had a motorised focus and a 63 X oil immersion objective with an excitation line of 488 nm from an argon laser. A 100 X oil immersion objective with sequential excitation lines of 488nm from an argon laser and 633nm from a helium-neon laser was used.

d) Curcumin loading efficiency

The mobile phase contained 5% acetic acid and acetonitrile (25:75), was eluted isocratically at 1.0 mL/min, and curcumin was detected at 424 nm (25°C) as described in 3.2.3. The relationship between curcumin and detected concentration was linear between 0.1 and 10 µg/mL curcumin, and the standard curve was generated accordingly (appendix A4.2). Curcumin content in the emulsion was assumed to be the total curcumin concentration, while

the curcumin in the cream phase was considered the loaded curcumin. Unabsorbed curcumin concentration was calculated by the difference between total and absorbed curcumin.

e) Phospholipid concentration

The protocol described by (Norris et al., 2009) was used to extract phospholipids. Briefly, 100 mg of emulsions was weighed into a 2mL Eppendorf tube and dissolved in 2 mL Milli-Q water to dilute the samples. 0.5mL of the diluted samples were then transferred to a 10mL Kimax tube where 2 ml of methanol: chloroform (2:1) was added. Tubes were mixed by vortex, rocked for 20 minutes and centrifuged at 2000g for 30 minutes. The supernatant was then transferred to a clean 15 ml Kimax tube where 0.25 mL of Milli-Q water and 1 mL of methanol:chloroform (2:1) were added into each tube again. The process was followed precisely to allow complete extraction. The supernatants were combined, and 0.65 mL of 0.1M KCl was added. The tubes were mixed well by vortex and centrifuged at 2000g for 30min. The upper phase was discarded, and another 0.375 mL of methanol and 0.25 mL of 0.1M KCl were added to the lower phase. After mixing well by vortex, the tubes were centrifuged at 2000g for 30min again. The upper phase was discarded, and the lower phase was transferred into a 5mL volumetric flask. The volume was adjusted to the 5 mL mark with methanol:chloroform (2:1). Further dilutions were made if needed. The mass of each sample was used for phospholipid concentration calculations.

A calibration curve was prepared using NMR certified PC700. 1 mg/mL solution was made with methanol:chloroform (2:1), and further diluted to reach the concentrations of 500, 250, 125, 62.5, 31.25, 15.625, 7.813, 3.906, 1.953, 0.977 and 0.488 µg/mL (appendix A4.3).

Phospholipids were separated on an Agilent 1200 series HPLC system (Santa Clara, CA, USA) equipped with an APS-2 Hypersil column (150 mmx2.1 mm, 3mm), interfaced to a SCIEX 6500 QTrap mass spectrometer (AB SCIEX, Framingham, MA, USA) and quantified in positive mode as described by (Norris et al., 2009). The flow rate was 0.5mL/min. The column temperature was kept at 60°C, while the sample temperature was 5°C with an injection volume of 5µL. A gradient of mobile phase was used, where phase A was composed of 95% acetonitrile, 5% 50 mM ammonium acetate buffer at pH 5.6, with 0.1% formic acid; and phase B was composed of 50% acetonitrile, 50% 50 mM ammonium acetate buffer at pH 5.6, with 0.1% formic acid. The elution gradient is presented in Table 4.2.

Table 4.2. HPLC elution gradient

	Time (min)	Flow (ml/min)	% A	% B
1	0	0.5	95	5
2	2	0.5	95	5
3	7.5	0.5	60	40
4	9.5	0.5	0	100
5	15	0.5	0	100
6	16	0.5	95	5
7	20	0.5	95	5

Sphingomyelin (SM), phosphatidylcholine (PC) and lyso-PC were monitored using the precursor ion 184 (phosphorylcholine). Phosphatidylethanolamine (PE) and lyso-PE were monitored using the neutral loss of ion 141 (phosphoryl ethanolamine). Phosphatidylserine (PS) was monitored using a neutral loss of ion 185 (phosphoryl serine). Phosphatidylinositol (PI) was monitored using a neutral loss of ion 260 (phosphoryl inositol). The mass spectrometer (MS) scan rate was 1000 Da/s, and the flow of the first 2 min (0-2 min) and the last 8 min (12-20 min) from LC were diverted to waste. The ion source and scanning conditions were set as described in Table 4.3 and Table 4.4.

Table 4.3. Ion source conditions

Curtain gas	20
Collision gas (cad)	Low
Ion spray voltage (is)	5500
Temperature (tem)	500
Ion source gas 1 (gs1)	18
Ion source gas 2 (gs2)	30

Table 4.4. Precursor Ion (PIS) and Neutral loss (NL) scanning conditions

	PIS 184	NL 141	NL 185	NL 260
Decluttering Potential	200	180	200	180
Entrance Potential	10	10	10	10
Collision Energy	28	27	30	25
Collision Cell Exit Potential	12	23	30	24

4.3.2.5 Statistical analysis

Statistical analyses were performed using SAS (SAS/STAT version 9.4). A polynomial regression analysis (up to quintic order) was first conducted on emulsifier, concentration and the interaction between emulsifier and concentration on the particle size ($d_{3,2}$ and $d_{4,3}$). Only significant ($P < 0.05$) terms were kept in the final polynomial model, which was selected by

comparing full models with reduced models (i.e., removing predictors that did not affect the response variable) by using the log-likelihood ratio test.

Once the concentration of the emulsifier was selected, a two-way ANOVA model was used to determine the effect of the emulsifier, oil type, and their interaction on several responses (e.g., particle size, zeta potential, curcumin loading efficiency and phospholipid distribution) using the Proc Mixed procedure. The model diagnostics (e.g., normal distribution) for each response variable were tested using the ODS Graphics procedure and the repeated statement of SAS. When the model assumptions were not fulfilled the raw data was transformed. When the F-value of the model was significant ($P < 0.05$), the mean values of the two-way ANOVA were compared using the adjusted Tukey-Kramer test. Probability values were considered statistically different when $P < 0.05$, and values of $0.051 < P < 0.10$ were considered a trend.

4.4 Results and discussion

i) Selection of emulsions components

CO was selected based on its published health promoting properties, especially those related to ketogenic metabolism and potential effects against dementia (Augustin et al., 2018). MCT, the main components in coconut oil, were selected based on their ability to be easily absorbed and metabolised by the liver, being converted to ketone bodies, an alternative energy source in the brain. Studies suggest that MCT may be beneficial to people developing or already with memory impairment, such as AD (Fernando et al., 2015), thereby justifying their inclusion. In addition to CO, a FO rich in ω-3 long-chain PUFA (EPA and DHA) was added to the emulsions due to increasing evidence of the FO's health promoting properties; PUFA are critical to normal brain development and function later in life, promoting synaptic activity, neurogenesis and dendritic spine density, and protecting against age-related neuronal damage due to oxidative stress and inflammation (Chen et al., 2019).

MFGM derived materials with varying compositions were analysed for their phospholipid concentrations and used to prepare O/W emulsions. CO was used in this assay as an initial assessment to select working emulsifier concentrations for following experiments. MFGM fractions presented decreasing concentration of TPL (MFGM1>MFGM2>MFGM3). MFGM1 had no added protein, contained lactose in its composition, and phosphatidylcholine was the major phospholipid group for this fraction, while for MFGM2 and MFGM3 phosphatidylethanolamine was the major phospholipid group (Table 4.5). Additionally,

MFGM fractions 2 and 3 had 50% and 72% milk protein, respectively, in their composition. The effects of those fractions on emulsion structure, mainly particle size, are presented and discussed below.

Table 4.5. Mean ± SEM (N=3) phospholipid concentrations of MFGM fractions.

	Phospholipid concentration (mg/g)							
	PE	**PC**	**SM**	**PS**	**PI**	**LPE**	**LPC**	**TPL**
MFGM1	74.0 ± 0.62	121 ± 1.12	91.0 ± 1.46	22.9 ± 0.36	14.2 ± 0.52	6.46 ± 0.28	2.95 ± 0.10	332 ± 3.49
MFGM2	31.9 ± 0.39	29.1 ± 0.52	23.1 ± 0.57	9.32 ± 0.23	5.83 ± 0.33	0.84 ± 0.05	0.39 ± 0.02	100 ± 1.91
MFGM3	12.3 ± 0.40	7.27 ± 0.24	7.81 ± 0.31	3.36 ± 0.07	1.40 ± 0.12	0.14 ± 0.02	0.09 ± 0.01	32.4 ± 1.10

PE, phosphatidylethanolamine; PC, phosphatidylcholine; SM, sphingomyelin; PS, phosphatidylserine; PI, phosphatidylinositol; LPE, lyso-phosphatidylethanolamine; LPC, lyso-phosphatidylcholine; TPL, total phospholipids.

ii) Selection of emulsifier concentrations based on particle size and stability over time

The particle sizes of emulsions prepared by applying the same homogenisation pressure were measured. Using the same number of passes while varying the concentrations of the three different MFGM fractions showed an increasingly smaller mean size ($d_{3,2}$) as the emulsifier concentration increased from 0.5 to 5% (Figure 4.1). During homogenisation, the passage of the unstable oil and water mixture through the homogeniser valve and the applied shear force created by pressure disrupted the liquid into smaller droplets that the emulsifying agent then adsorbed into the oil-water interface. The smaller the particle size, the higher the surface area of the droplets, and consequently, the more emulsifier was needed to cover the surface and stabilise the droplets. In addition to the particle size, the oil concentration in the system was found to be a determining factor for the amount of emulsifier needed, with higher oil concentration requiring higher amounts of emulsifier.

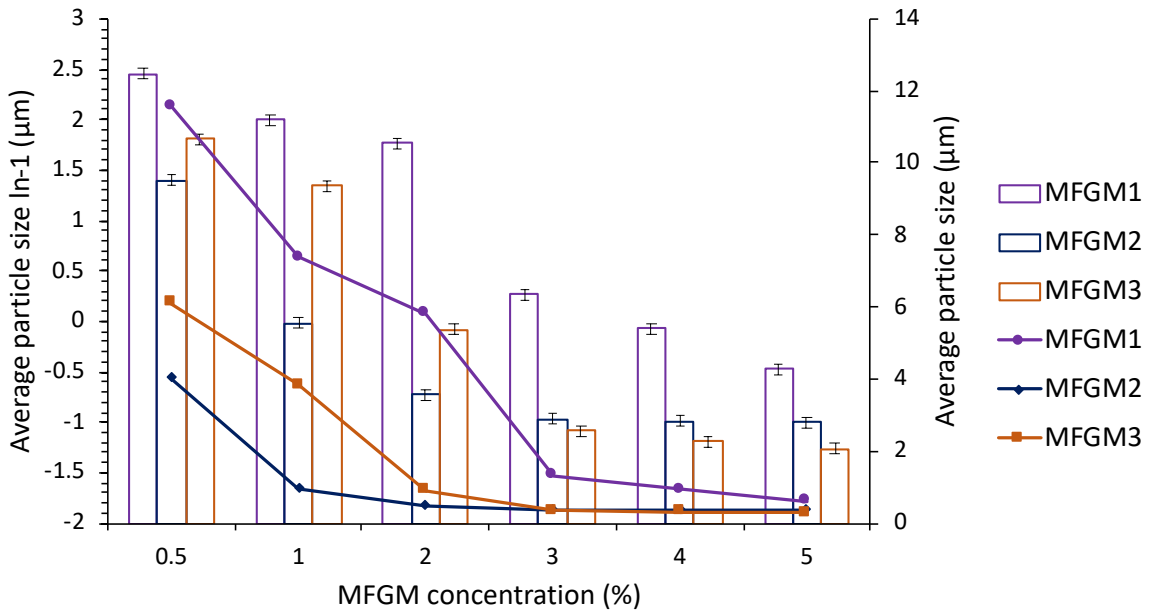

Figure 4.1. Mean particle size ($d_{3,2}$) of emulsions prepared using varying concentrations of three MFGM materials (MFGM1, MFGM2 and MFGM3 with 0.5 to 5.0% w/w MFGM, 20% w/w coconut oil). Lines show the back transformation of log values back to its original scale to allow more meaningful and intuitive data interpretation (N=3 secondary y-axis). Bars show mean ± SEM of natural log-transformed data to fulfil normality and homogeneity of variance (primary y-axis).

In this study, emulsions were passed three times through a homogeniser operating at 40,000/5,000 kPa (maximum pressure supported). The effect of concentration and emulsifier type on the particle size was selected as a determining parameter for choosing the concentration of each emulsifier. The mean particle size ($d_{3,2}$) for MFGM2 and MFGM3 stabilised emulsions reached a plateau after addition of 3% powder to the total emulsion volume. In contrast, the mean size for MFGM1 stabilized emulsions continued to decrease until the concentration of powder reached 5%, although the reduction was negligible after 3% concentration compared to the decrease observed between 0.5 and 3% (Figure 4.1). Since the beneficial health properties of MFGM phospholipids are of interest in this research and the mean particle size of MFGM1 emulsions compared to MFGM2 and MFGM3 was significantly higher at 3%, a concentration of 5% was selected for MFGM1, and a concentration of 3% was chosen for MFGM2 and MFGM3.

At 3% concentration, MFGM2 and MFGM3 fractions were better emulsifying agents in the preparation of emulsions when compared to MFGM1 considering particle size as the response parameter. Although those were able to create emulsions with smaller particle size, MFGM1 presented a sufficiently small particle size at 5% concentration for the purposes of this study. A bimodal distribution with two modes was identified representing different particle populations (Figure 4.2). To calculate the average particle size, a weighted mean approach was

used, considering the relative proportions of each particle populations. The weighted means for both modes were combined to obtain the overall average particle size, providing a representative measure that considers the distinct contributions of each mode. A previous study used MFGM derived material to prepare liposomes with a higher concentration of phospholipids than those used in this study. They found that an increased number of passes and a higher pressure in a microfluidiser led to smaller mean particle size (Thompson and Singh, 2006). Peel (1999) found that, after 5 passes at 130 bar, the mean diameter stabilised at approximately 125 nm using a high-pressure homogeniser, which is lower than those used in our study, indicating that even at lower pressure the number of passes can reduce the size of oil droplets. While the mean particle size for MFGM1 was higher compared to MFGM2 and MFGM3, it presented a monodispersed and narrow distribution from 3% and higher concentrations (Figure 4.2). In addition, the MFGM1 fraction had the highest concentration of sphingomyelin and phosphatidylcholine, both phospholipids associated with health-promoting properties.

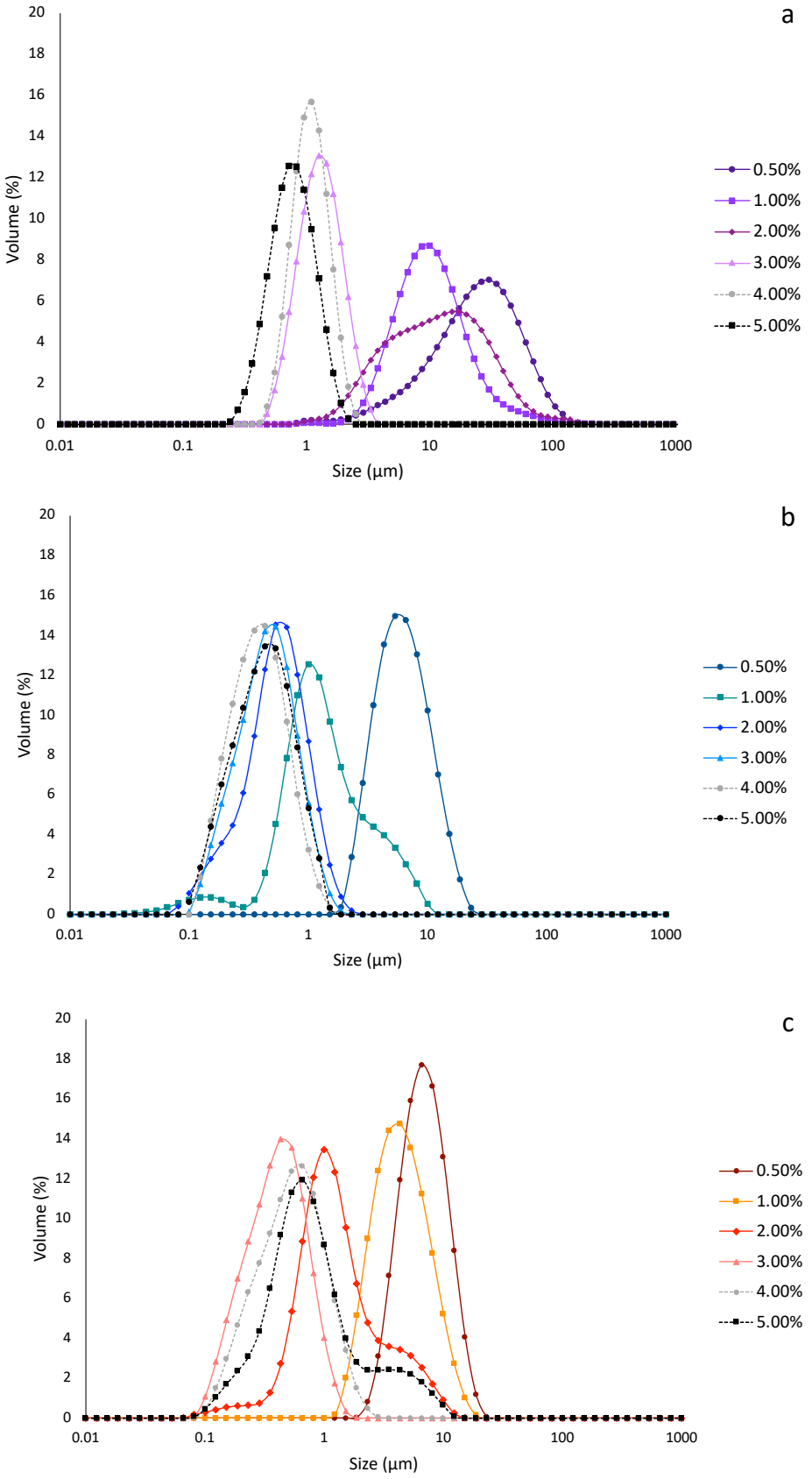

Figure 4.2. Particle size distribution of emulsions prepared using varying concentrations of three MFGM materials (MFGM1, MFGM2 and MFGM3 - 0.5 to 5.0% w/w MFGM, 20% w/w coconut oil).

Lopez et al. (2017) used an ingredient rich in MFGM lipids and proteins to produce emulsions. Lipid droplets were coated with MFGM fragments such that they were adsorbed at the surface and protruding in the aqueous phase. These emulsions did not show coalescence upon 30 days of storage. The authors concluded that the MFGM-rich ingredient had excellent emulsifying properties. Corredig and Dalgleish (1998) also observed that emulsions prepared with MFGM isolates were stable at neutral pH but were destabilised at low pH. They found that 1% (w/w) MFGM was sufficient to produce stable emulsions with a small particle size (0.35 μm) using 10% soybean oil and that a strong molecular interaction between the adsorbed MFGM (phospholipid and protein) occurred at the interface. As the oil concentration and the MFGM composition differed in this study, a higher amount was needed to create stable emulsions.

iii) Characterization of emulsions prepared using selected MFGM concentrations

a) Particle size

Emulsifier concentrations were selected based on particle size changes over time, as described above, and the following experiments were conducted using the same concentration of 5% for MFGM1 and 3% for MFGM2 and MFGM3. It was of interest to determine whether MFGM1, while requiring a higher amount to achieve the same particle size, might result in improved overall results and thereby justify the greater cost to incorporate it into the end product.

Overall, there was no significant interaction between oil and emulsifier type on the mean particle size ($d_{3,2}$) for MFGM emulsions (Pr > F 0.088). Similarly, the effect of oil (CO alone or combined with FO) had no effect on emulsion's mean particle size, indicating that at the same pressure and number of passes, both oils had equal $d_{3,2}$ mean size (Pr > F 0.496). However, the emulsifier type had a significant effect on particle size (Pr > F 0.0003), with emulsions S3 to S6 (prepared using MFGM2 and MFGM3) having significantly smaller mean particle size than S1 and S2, which were prepared using MFGM1 (Table 4.6).

Table 4.6. Mean particle size ($d_{3,2}$) of emulsions prepared using selected emulsifier concentrations

Emulsion code	Oil type 20%	Emulsifier 3 or 5%	$d_{3,2}$ (μm)
S1	CO	MFGM1	0.43 +/- 0.03[a]
S2	CO:FO (1:1)	MFGM1	0.41 +/- 0.03[a]
S3	CO	MFGM2	0.34 +/- 0.03[b]
S4	CO:FO (1:1)	MFGM2	0.30 +/- 0.03[b]
S5	VCO	MFGM3	0.30 +/- 0.03[b]
S6	CO:FO (1:1)	MFGM3	0.25 +/- 0.03b

S1, 5% w/w M1, 20% w/w coconut oil; **S2**, 5% w/w M1, 10% w/w coconut oil, 10% w/w fish oil; **S3**, 3% w/w M2, 20% w/w coconut oil; **S4**, 3% w/w M2, 10% w/w coconut oil, 10% w/w fish oil; **S5**, 3% w/w M3, 20% w/w coconut oil; **S6**, 3% w/w M3, 10% w/w coconut oil, 10% w/w fish oil). Data are shown as mean ± SEM of 6 replicates. Different letters represent significant difference ($p<0.05$) between mean size.

Early reports on the use of MFGM-derived materials indicated that those fractions were able to act as natural emulsifying agents, with the majority using non-purified fractions or looking into the ability of proteins to emulsify fat globules (Corredig and Dalgleish, 1998, KANNO et al., 1991, Sato et al., 1994). Similar to the findings in this experiment, more recent studies assessing the differences between lipid-rich and protein-rich fractions found that proteins adsorb more easily to the oil droplet surface, therefore acting as a better emulsifier when compared to lipid fractions (He et al., 2017, Phan et al., 2016). The fact that S1 and S2 had no protein in their composition as opposed to the other emulsions might be the reason why there were significant differences in particle size, and that protein assisted in the formation of the adsorbed layer for emulsions S3, S4, S5 and S6.

MFGM materials used as emulsifiers effectively created visually stable emulsions to coalescence over time. A broad size distribution can be observed in Figure 4.3, despite average being smaller. Different samples were used; however, average particle size was kept consistent throughout the experiments. Emulsions stored at 4°C for up to 2 months kept their emulsified state without phase separation or creaming. Particle size distribution for the emulsion made with all MFGM fractions remained unchanged compared to day 0 (Figure 4.3), indicating that all MFGM fractions used had an excellent stability and effectively created stable O/W emulsions for the encapsulation of curcumin.

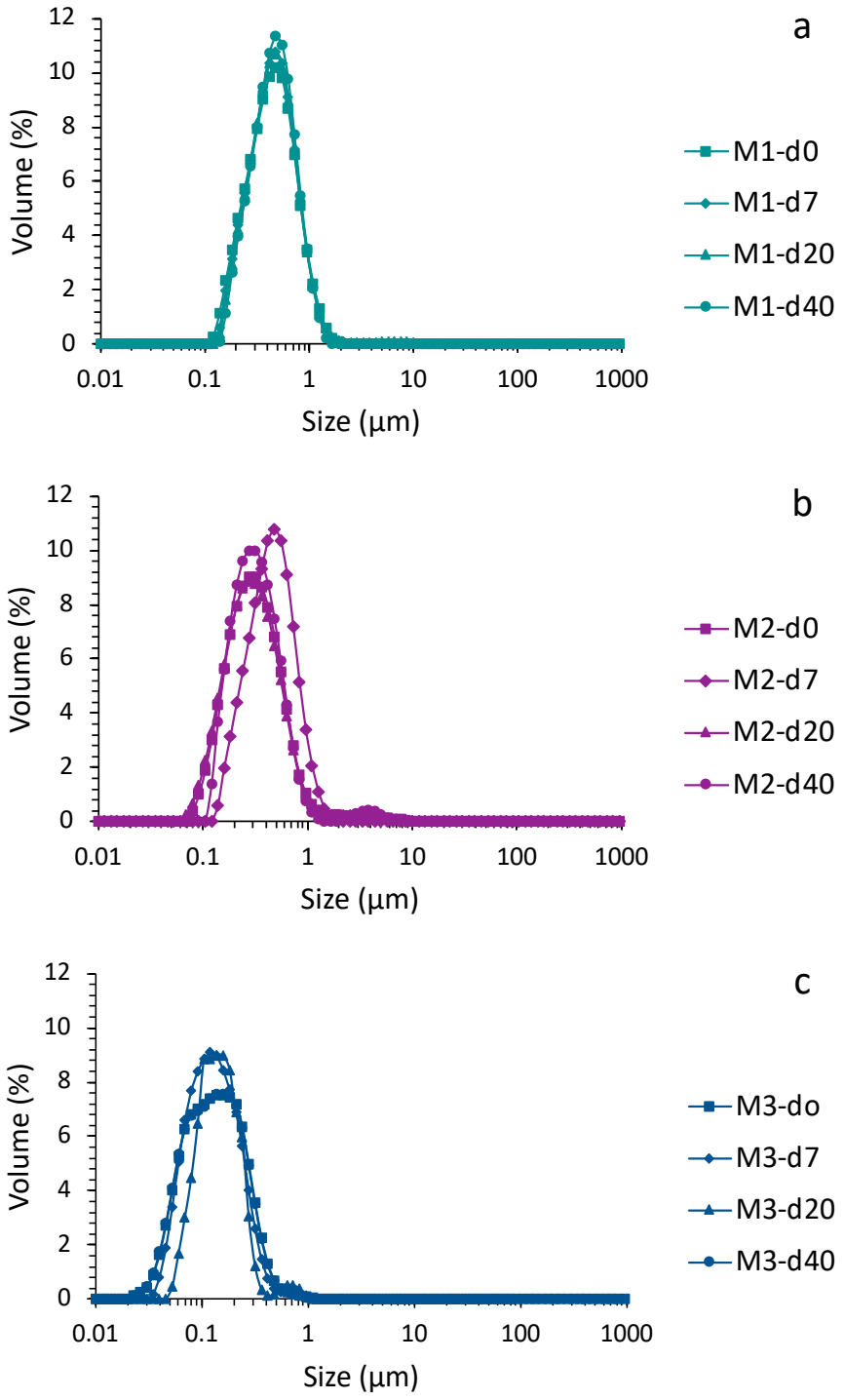

Figure 4.3. Particle size distribution of emulsions at day 0 (square), day 7 (diamond), day 20 (triangle) and day 40 (circle) of storage at 4°C (a=MFGM1, b=M2FGM, c=MFGM3)

The MFGM's original function is to stabilize fat globules in milk, making the materials isolated from buttermilk or cream efficient naturally-occurring surface-active materials with high emulsifying capacity. Similar to the results observed in this study, Cooredig and Dalgleish (1998) also observed that MFGM material isolated from raw cream created stable emulsions at neutral pH. They observed a strong molecular interaction between the adsorbed MFGM,

composed of phospholipid and protein, at the interface of the oil droplets (Corredig and Dalgleish, 1997, Corredig and Dalgleish, 1998). It is important to note that some of the processes applied in the manufacture of buttermilk, such as heat and churning, might cause extensive denaturation of the membrane proteins and the association of β-lactoglobulin with MFGM proteins, leading to fractions with a poor emulsifying ability (KANNO et al., 1991).

A more recent study attempted to mimic the functions of MFGM in milk and used an ingredient rich in MFGM containing polar lipids and proteins as an emulsifier. They observed that the emulsions were susceptible to pH changes, and aggregation occurred at a pH lower than 5.5. The MFGM fragments were not only adsorbed at the surface of fat globules but also protruded into the aqueous phase. Similar to the current study, they observed no coalescence after 30 days of storage of emulsions (Lopez et al., 2017).

b) Zeta-potential

The zeta-potential of the fat globules in milk is approximately −10 mV, which indicates relatively low contributions from electrostatic repulsions. Partial coalescence of fat globules is known to occur upon milk storage at low temperatures because of the formation of fat crystals, which can protrude from the globule surface and damage the MFGM (Singh, 2019, Thompson and Singh, 2006, Walstra, 2005). Emulsions prepared using MFGM-derived materials as emulsifiers had negative charges, higher than those in the naturally occurring milk fat globules. The MFGM1 emulsions, composed of only phospholipids, had the highest negative zeta-potential and stronger electrostatic repulsion (S1 and S2), followed by MFGM3 (S5 and S6) and MFGM2 (S3 and S4), with the lowest (negative) zeta-potential and weaker electrostatic repulsion (Figure 4.4).

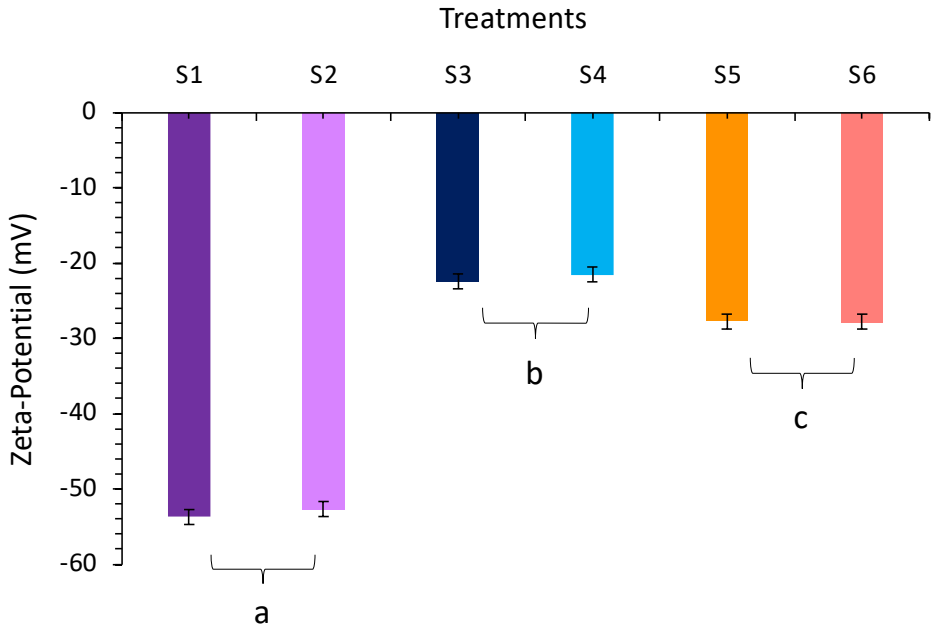

Figure 4.4. Zeta-potential of emulsions prepared using selected emulsifier concentrations (**S1**, 5% w/w MFGM1, 20% w/w coconut oil; **S2**, 5% w/w MFGM1, 10% w/w coconut oil, 10% w/w fish oil; **S3**, 3% w/w MFGM2, 20% w/w coconut oil; **S4**, 3% w/w MFGM2, 10% w/w coconut oil, 10% w/w fish oil; **S5**, 3% w/w MFGM3, 20% w/w coconut oil; **S6**, 3% w/w MFGM3, 10% w/w coconut oil, 10% w/w fish oil). Data are shown as mean ± SEM of N=6 replicates. Different letters represent significant difference ($p<0.05$).

There was no significant interaction between oil type and emulsifier on the zeta potential (Pr > F 0.1052). Different oil compositions led to statistically equal zeta-potential (Pr > F 0.8034), while the emulsifier type did affect the zeta-potential (Pr > F <0.0001), resulting in statistical differences between fractions with increasing electrostatic repulsion from MFGM1>MFGM3>MFGM2. The understanding of electric charge interactions is key in the development of food systems as they determine the type of interactions between particles and the surrounding media, therefore determining food structure and stability. The zeta potential is the most widespread charge measurement related to colloidal stability, with threshold between stable and unstable systems been considered within ± 0 to10, ± 10 to 20, ± 20 to 30, and ± 30 mV as very unstable, relatively stable, moderately stable, and highly stable respectively (Sherman, 1970, Cano-Sarmiento et al., 2018). Surface layers of fat globules in artificial emulsions are formed by milk proteins and the zeta-potential values of these products were found to be −19 mV for homogenized fat globules of a commercial milk emulsion, −22 mV for natural fat globules of a commercial cream, about − 36 mV for fat globules of a recombined milk emulsion, and about −19 mV for fat globules of recombined cream emulsion (Wade and Beattie, 1997). The emulsions prepared using MFGM derived material in this study presented zeta-potential similar to those in surface layer of fat globules, except for MFGM1 which presented higher zeta-potential, potentially due to the lack of serum protein in its composition.

Based on stability threshold, emulsions in this study can be considered moderately stable (S3 to S6) and highly stable (S1 and S2).

c) Confocal laser scanning microscopy

The selected MFGM concentrations led to emulsions with similar particle size distribution (Figure 4.5) and small mean particle size. In a monodispersed colloidal system, the surface weighted mean diameter ($d_{3,2}$) and volume-weighted mean diameter ($d_{4,3}$) are the same, while these will be different in a polydispersed design. The volume-weighted mean diameter ($d_{4,3}$) values were suggested to be more sensitive to coalescence or flocculation as compared to surface weighted mean diameter ($d_{3,2}$) values (McClements, 2015). Statistical analysis indicated no effect of oil on mean particle size, and emulsions prepared using same emulsifier and different oil types showed similar size distribution (Figure 4.5); therefore only CO emulsions were used for structural representation using confocal laser scanning microscopy (CLSM) (Figure 4.6).

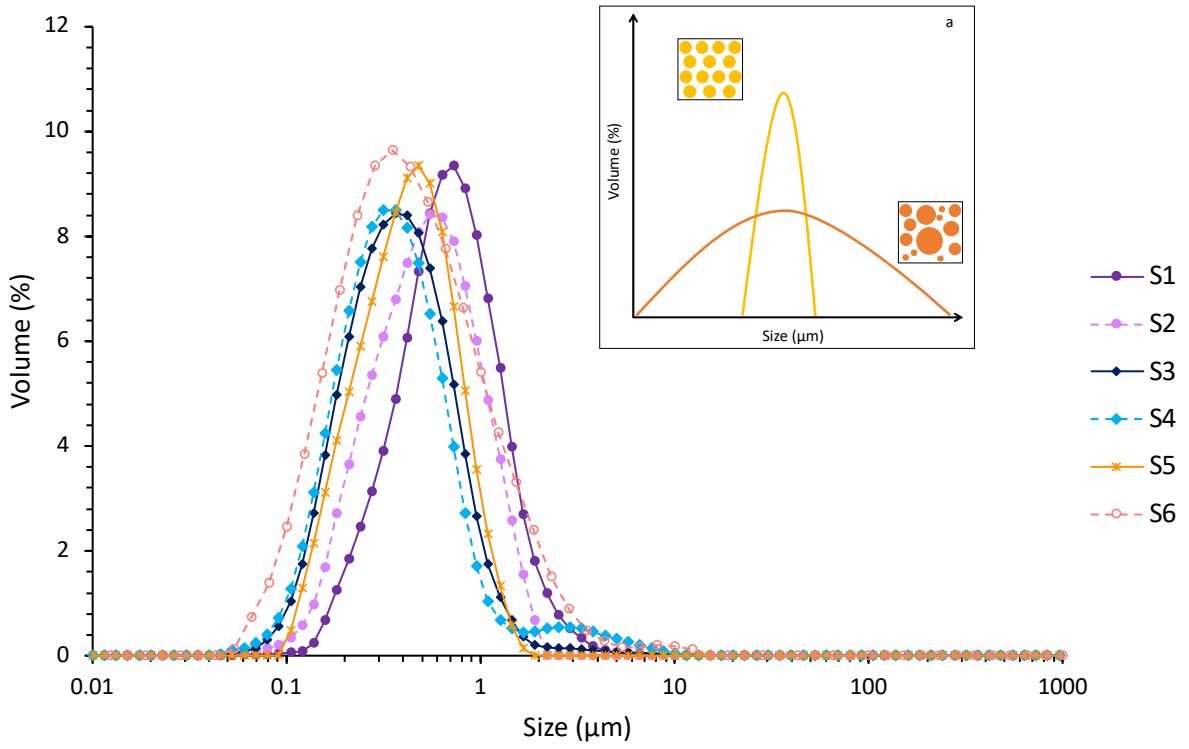

Figure 4.5. Particle size distribution of emulsions prepared using selected emulsifier concentrations (**S1**, 5% w/w MFGM1, 20% w/w coconut oil; **S2**, 5% w/w MFGM1, 10% w/w coconut oil, 10% w/w fish oil; **S3**, 3% w/w MFGM2, 20% w/w coconut oil; **S4**, 3% w/w MFGM2, 10% w/w coconut oil, 10% w/w fish oil; **S5**, 3% w/w MFGM3, 20% w/w coconut oil; **S6**, 3% w/w M3, 10% w/w coconut oil, 10% w/w fish oil). Figure (a) illustrates mono- (yellow) and poly- (orange) dispersed colloidal systems.

The broader the distribution, the lower the homogeneity in particle size. A monomodal distribution with a narrow size range was observed. However, CLSM images indicated the presence of both small and large particles in MFGM-prepared emulsions. Emulsions S3 and S5, prepared using MFGM2 and MFGM3, had milk protein in their compositions, which promoted flocculation of droplets. Those can be observed in Figure 4.6 (b and c) by agglomerates of protein (green-stained) bringing small oil droplets together (red-stained). Purple-coloured images (d to f) illustrate the binding of phospholipids to the droplet surface.

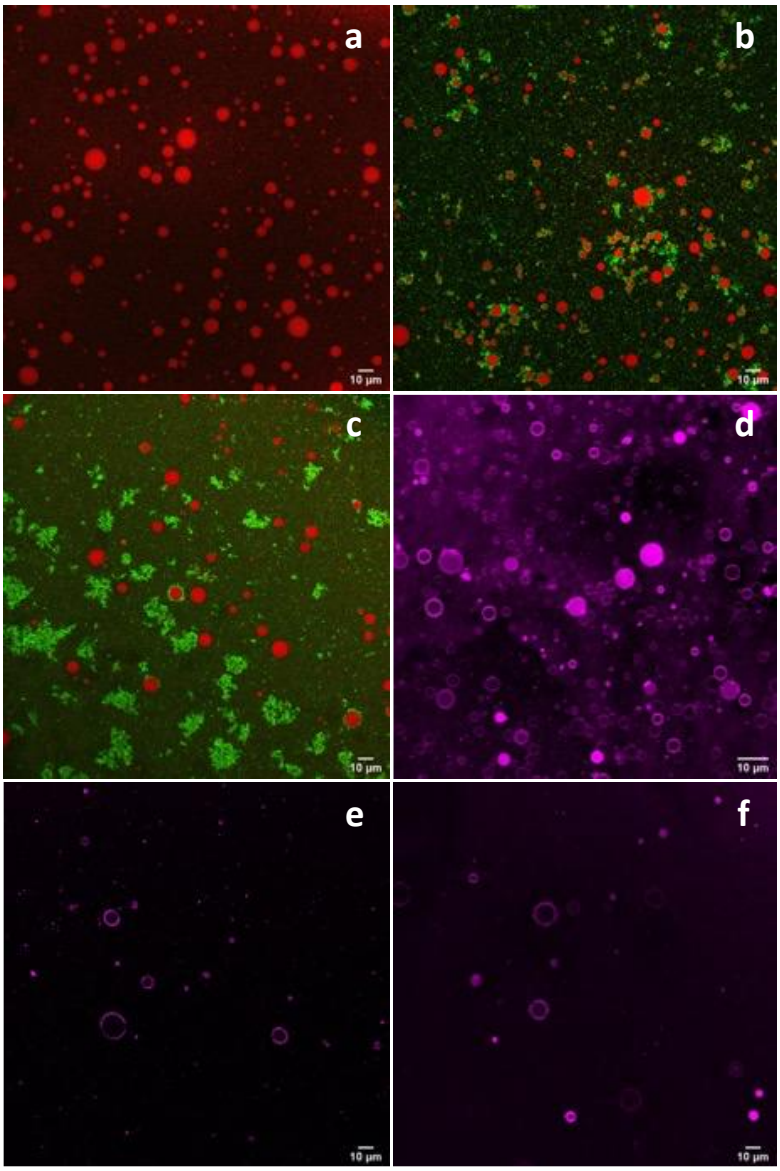

Figure 4.6. CLSM images of emulsions prepared using selected emulsifier concentrations, (**a** and **d** = 5% w/w MFGM1, 20% w/w coconut oil; **b** and **e** = 3% w/w MFGM2, 20% w/w coconut oil; **c** and **f** = 3% w/w MFGM3, 20% w/w coconut oil. A,b,c = oil was stained with Nile Red (color-coded red) and proteins were stained with Fast Green (color-coded green); d,e,f = stained with Rd-DOPE, a fluorescent phospholipid analogue.

d) Curcumin loading efficiency

The term loading efficiency (LE) is used to describe the entrapment capacity of a bioactive in an emulsion system. It can also be described as "yield", "encapsulation efficiency", or "incorporation efficiency", all providing quantitative information as a percentage of the total curcumin added vs the mass of curcumin entrapped into the delivery system (Araiza-Calahorra et al., 2018, McClements et al., 2009).

The emulsions prepared using MFGM fractions showed high LE with significant higher values ($p<0.05$) for those prepared using MFGM1 (S1 and S2), followed by those prepared using MFGM2 (S3 and S4) and MFGM3 (S5 and S6). There was no significant interaction between oil and emulsifier type on LE (Pr > F 0.2811). Although no statistical differences were observed for MFGM2 and MFGM3, emulsions S5 and S6 presented slightly lower LE (Figure 4.7). While emulsifier type affected LE (Pr > F 0.0231), the type of oil did not influence LE (Pr > F 0.5636). A total of 2 mg curcumin per gram of oil was added to prepare CO emulsions (S1, S3 and S5), leading to a total of 1 mg curcumin per gram of oil in CO and FO (1:1) emulsions. Since oil was heated to allow curcumin solubilisation and FO is susceptible to oxidation, no heat was applied to FO, and the CO containing solubilised curcumin was mixed (1:1) with FO.

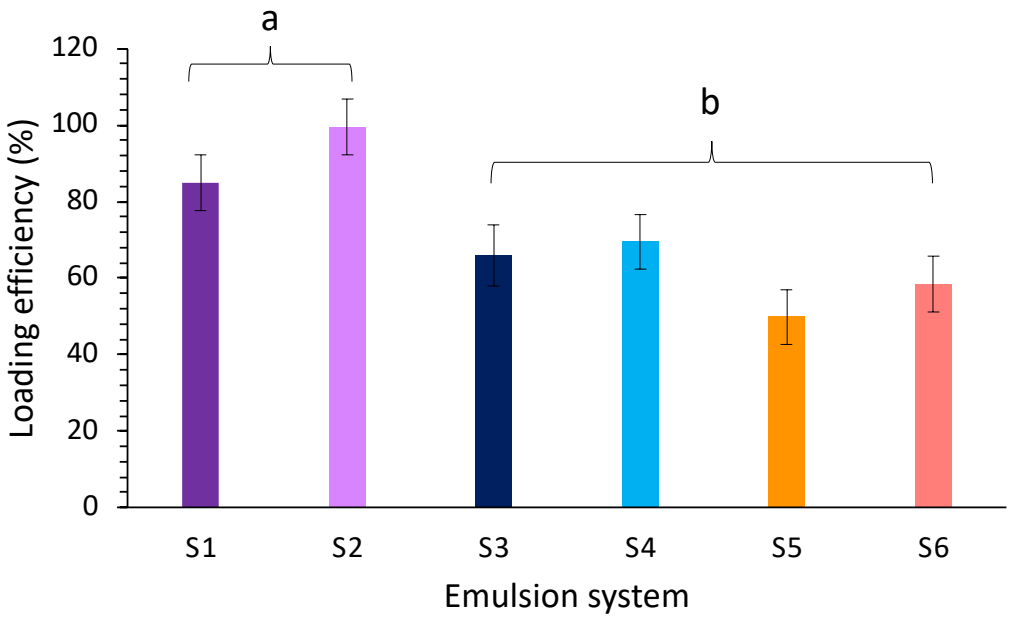

Figure 4.7. Loading efficiency (LE - total emulsion basis) of emulsions prepared using selected emulsifier concentrations (**S1**, 5% w/w MFGM1, 20% w/w coconut oil; **S2**, 5% w/w MFGM1, 10% w/w coconut oil, 10% w/w fish oil; **S3**, 3% w/w MFGM2, 20% w/w coconut oil; **S4**, 3% w/w M2, 10% w/w coconut oil, 10% w/w fish oil; **S5**, 3% w/w MFGM3, 20% w/w coconut oil; **S6**, 3% w/w M3, 10% w/w coconut oil, 10% w/w fish oil). Data are shown as mean ± SEM of N=6 replicates. Different letters represent significant difference ($p<0.05$) between LE.

Considering that high amounts of curcumin are needed for the desired effects, a high LE is ideal. The LE of emulsions is influenced by the type of emulsifier and its structural arrangements at the interface or the curcumin-surfactant interactions. Curcumin molecules consist of mainly hydrophobic and some hydrophilic groups that can interact with surfactant molecules via hydrophobic and electrostatic interactions (Yu and Huang, 2010). Emulsions stabilised by mixed surfactant systems, both hydrophilic and hydrophobic parts, might contribute to the solubilisation of curcumin. In this study, curcumin incorporation was higher for emulsions prepared using MFGM material rich in phospholipids (MFGM1), suggesting that interactions between curcumin and phospholipids might have contributed to LE. A previous study encapsulated 15 mg of curcumin into 30mL nanoemulsions prepared by thin-film hydration method stabilised by optimised mixtures of hydrogenated L-α- phosphatidylcholine (HEPC) (surfactant) and polyoxyethylene hydrogenated castor oil 60 (HCO-60) (co-surfactant) or HEPC and Tween 80. The authors found LE of 100% and ~97% for HEPC/HCO-60 and HEPC/Tween 80, respectively (Anuchapreeda et al., 2012). Jintapattanakit et al (2018) tested the solubility of 10 vegetable oils varying in chain length and found that coconut oil showed the highest solubility for curcumin. The predominance of MCT and the high polar groups per unit mass of coconut oil could be the reason for curcumin's higher solubility through dipole-dipole interactions.

e) Phospholipids

Emulsions prepared using different MFGM fractions presented significant differences in their phospholipid concentration (Table 4.7). There was no interaction between oil and emulsifier type on the phospholipid concentration of emulsions for any PL group ($Pr>F > 0.05$). Similarly, oil composition had no effect on phospholipids concentrations, and only emulsifier type promoted significant changes in the emulsion composition for all phospholipids classes ($Pr>F < 0.05$). Emulsions presented similar concentrations of phospholipids groups to their correspondent MFGM fractions. However, variations were observed between overall absolute composition among individual phospholipids groups for all MFGM fractions and their corresponding emulsions (Figure 4.8).

Table 4.7. Phospholipid class distribution in emulsions prepared using selected emulsifier concentrations

	Phospholipid concentration µg/mg (mg/g)							
Emulsion	**PE**	**PC**	**SM**	**PS**	**PI**	**LPE**	**LPC**	**TPL**
S1	3.84 ± 0.08^{a}	4.52 ± 0.07^{a}	4.73 ± 0.07^{ab}	0.91 ± 0.06^{a}	0.63 ± 0.09^{a}	0.17 ± 0.00^{a}	0.09 ± 0.00^{a}	14.9 ± 0.19^{a}
S2	3.50 ± 0.15^{a}	5.19 ± 0.47^{a}	4.99 ± 0.07^{ab}	0.98 ± 0.08^{a}	0.57 ± 0.09^{ab}	0.23 ± 0.02^{a}	0.14 ± 0.02^{a}	15.6 ± 0.72^{a}
S3	0.68 ± 0.16^{bc}	0.73 ± 0.15^{b}	1.73 ± 0.94^{bc}	0.17 ± 0.06^{b}	0.30 ± 0.13^{ab}	0.04 ± 0.02^{b}	0.02 ± 0.02^{ab}	3.67 ± 1.22^{b}
S4	0.95 ± 0.06^{c}	0.86 ± 0.08^{b}	1.86 ± 0.72^{bc}	0.20 ± 0.04^{b}	0.38 ± 0.12^{ab}	0.04 ± 0.01^{b}	0.02 ± 0.01^{b}	4.31 ± 0.76^{b}
S5	0.31 ± 0.05^{c}	0.23 ± 0.04^{c}	0.83 ± 0.30^{c}	0.07 ± 0.01^{b}	0.15 ± 0.04^{b}	$-^{b}$	$-^{b}$	1.60 ± 0.29^{c}
S6	0.31 ± 0.03^{c}	0.22 ± 0.02^{c}	0.60 ± 0.23^{c}	0.07 ± 0.02^{b}	0.16 ± 0.06^{b}	0.01 ± 0.00^{b}	$-^{b}$	1.37 ± 0.24^{c}

S1, 5% w/w MFGM1, 20% w/w coconut oil; S2, 5% w/w MFGM1, 10% w/w coconut oil, 10% w/w fish oil; S3, 3% w/w MFGM2, 20% w/w coconut oil; S4, 3% w/w MFGM2, 10% w/w coconut oil, 10% w/w fish oil; S5, 3% w/w MFGM3, 20% w/w coconut oil; S6, 3% w/w MFGM3, 10% w/w coconut oil, 10% w/w fish oil) PE=Phosphatidylethanolamine, PC=Phosphatidylcholine, SM=Sphingomyelin, PS=Phosphatidylserine, PI=phosphatidylinositol, LPE- Lyso-Phosphatidylethanolamine, LPC-Lyso-Phosphatidylcholine. Data are shown as mean ± SEM of N=6 replicates. Different letters indicate significant differences between lines in the same column.

Overall, SM was the predominant phospholipid group for all emulsifiers, with exemption of S2 emulsions, prepared using MFGM1, were PC was the predominant phospholipid group. The remaining groups were distributed equally in emulsions compared to MFGM1 and its emulsions, indicating similar phospholipid compositions. More prominent differences were observed for MFGM2 and its corresponded emulsions S3 and S4, with a shift from highest PE concentrations in the MFGM fraction to highest concentration of SM in emulsions. Similar behaviours were observed for MFGM 3 and emulsions S5 and S6, where the highest concentration of SM was observed in emulsions compared to the MFGM fraction used for its preparation. It is likely that the emulsification process promoted interactions between the MFGM fractions and the system, interfering with their arrangements and contributing to differences in the extraction and recovery of those samples from emulsions as compared to MFGM fractions alone. Additionally, working with emulsions instead of powdered fractions can inflict homogeneity problems.

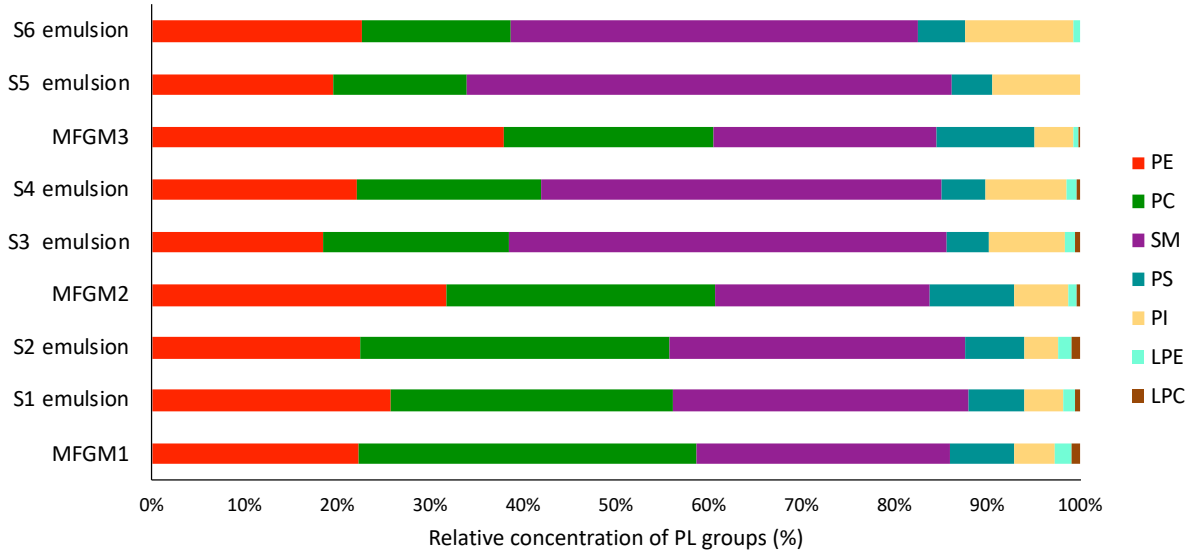

Figure 4.8. Phospholipid class distribution in emulsions prepared using selected emulsifier concentrations (**S1**, 5% w/w MFGM1, 20% w/w coconut oil; **S2**, 5% w/w MFGM1, 10% w/w coconut oil, 10% w/w fish oil; **S3**, 3% w/w MFGM2, 20% w/w coconut oil; **S4**, 3% w/w MFGM2, 10% w/w coconut oil, 10% w/w fish oil; **S5**, 3% w/w MFGM3, 20% w/w coconut oil; **S6**, 3% w/w MFGM3, 10% w/w coconut oil, 10% w/w fish oil) PE=Phosphatidylethanolamine, PC=Phosphatidylcholine, SM=Sphingomyelin, PS=Phosphatidylserine, PI=phosphatidylinositol, LPE- Lyso-Phosphatidylethanolamine, LPC- Lyso-Phosphatidylcholine

While it is easy to obtain a homogenous sample of powdered MFGM fraction, once this fraction is incorporated in an oil phase the recovery and collection of a homogenous sample can present a challenge. Although samples were vigorously mixed before extraction, that could explain the differences observed from raw material to corresponding emulsions in their relative phospholipid group distributions.

iii) Curcumin and phospholipid distribution between the oil and aqueous phase

Studies using MFGM-derived materials as emulsifiers have mostly focused on the protein characterization at the interface, and there are limited data on phospholipids available in the published literature. The study by Corredig and Dalgleish (1998), for example, described mainly the results obtained from observations of the protein fractions of MFGM isolates. The authors isolated the MFGM from fresh raw cream, which contained 40% less protein compared to the freeze-dried material. The authors specified that the MFGM isolate was composed mainly of PE, PC and SM (30, 16 and 10% of total lipid, respectively). A more recent study assessed the formation and stability under *in vitro* gastrointestinal conditions of liposomes formed either by soybean or MFGM phospholipids. The MFGM fraction used was composed of PC (> 23%), polar lipids (>73%), and saturated fatty acids (>37%). The authors analysed changes in structure, such as particle size and zeta potential, the lipolysis and release of calcein

in vitro, where calcein was used as a "model" compound to observe the release behaviour. However, no details on phospholipids composition and changes after simulated gastrointestinal digestion were described (Liu et al., 2012).

The curcumin entrapped inside the oil droplets is considered to be encapsulated. It is therefore critical to understand its distribution between the cream and aqueous phase of emulsions. High speed centrifugation of emulsions allowed for the separation into cream and aqueous phases. The top cream phase was assumed to contain the encapsulated curcumin, the phospholipids and proteins absorbed to the surface of oil droplets, and the aqueous phase was assumed to contain unabsorbed phospholipids, proteins and curcumin. The curcumin extracted from both fractions was measured and the results presented as the percentage in each phase, calculated as [cream or aqueous curcumin × 100] ÷ total curcumin (Figure 4.9).

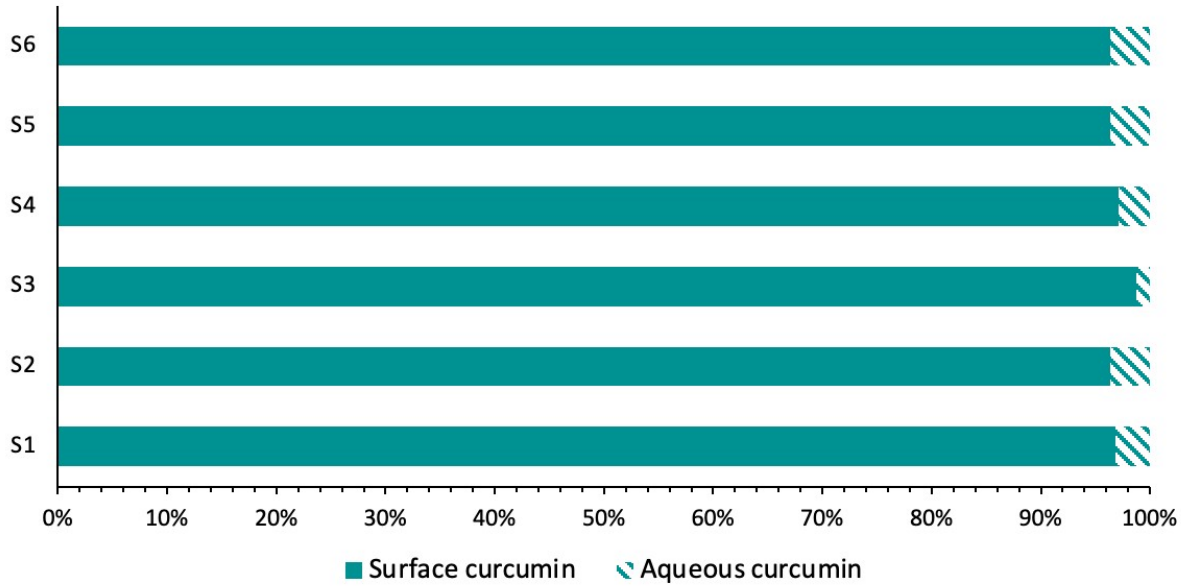

Figure 4.9. Curcumin concentration in cream phase (green) and aqueous phase (pink) of emulsions prepared using selected emulsifier concentrations (**S1**, 5% w/w MFGM1, 20% w/w coconut oil; **S2**, 5% w/w MFGM1, 10% w/w coconut oil, 10% w/w fish oil; **S3**, 3% w/w MFGM2, 20% w/w coconut oil; **S4**, 3% w/w MFGM2, 10% w/w coconut oil, 10% w/w fish oil; **S5**, 3% w/w MFGM3, 20% w/w coconut oil; **S6**, 3% w/w MFGM3, 10% w/w coconut oil, 10% w/w fish oil) after centrifugation.

For all emulsions, independent of oil, most curcumin was found in the cream phase, indicating that curcumin was present in the emulsion's surface and/or present inside the oil droplets. Although no significant differences were observed between the systems, the type of emulsifier had a significant effect (Pr>F 0.0231) on the entrapment of curcumin, with emulsions prepared by MFGM2 (S3 and S4) presenting a slightly higher entrapment than those prepared with MFGM1 and MFGM3. PC was one of the predominant phospholipid groups for all emulsions systems. Some commercially available formulations have used PC to improve

curcumin's bioavailability, suggesting that interactions between curcumin and phospholipids occurred and potentially influenced the loading efficiency for the emulsions in this study.

Curcumin has polar groups that are believed to bond via hydrogen and dipole interactions with the polar head groups of PC, resulting in phospholipid particles carrying curcumin at their surface (Barry et al., 2009, Semalty et al., 2010). Barry et al. (2009) found that curcumin interacts with cell membranes, altering membrane and restricting the movement of the lipid acyl chains through strong binding to phospholipid micelles, positioning the water-labile β-diketone moiety into the lipid bilayer and shielding it from hydrolytic degradation reactions. They concluded that curcumin bound to liposomes is protected from aqueous degradation, consequently enhancing the clinical efficiency of curcumin when administered in a liposomal form.

Several studies have been designed to understand the behaviour of proteins adsorbed at the lipid droplets in O/W emulsions, including those emulsified using MFGM derived materials (Corredig and Dalgleish, 1998, Ye, 2008, Gallier et al., 2015, Young et al., 2018). However, very little has been reported on the behaviour of phospholipids at the interface of oil droplet; hence I tried to understand how the phospholipids behave during the preparation of O/W emulsion by identifying the phospholipid distribution in the cream (adsorbed) phase and aqueous (unabsorbed) phase. The concentration for individual phospholipid groups in both phases can be found in Table 4.8.

Table 4.8. Mean phospholipid concentration of emulsions prepared using selected emulsifier concentrations

	Phospholipid concentration µg/mg (mg/g)							
	PE*	**PC***	**SM**	**PS***	**PI**	**LPE**	**LPC***	**TPL**
S1 emulsion	3.84 ± 0.08	4.52 ± 0.07	4.73 ± 0.07	0.91 ± 0.06	0.63 ± 0.09	0.17 ± 0.00	0.09 ± 0.00	14.9 ± 0.19
S1 cream	1.33 ± 0.03^{a}	1.69 ± 0.02^{a}	1.86 ± 0.03^{a}	0.43 ± 0.03^{a}	0.34 ± 0.05^{a}	0.07 ± 0.00^{a}	0.03 ± 0.00^{a}	5.65 ± 0.07
S1 aqueous	1.81 ± 0.04	1.94 ± 0.03	2.04 ± 0.03	0.33 ± 0.02	0.18 ± 0.03	0.05 ± 0.00	0.03 ± 0.00	6.46 ± 0.08
S2 emulsion	3.50 ± 0.15	5.19 ± 0.47	4.99 ± 0.07	0.98 ± 0.08	0.57 ± 0.09	0.23 ± 0.02	0.14 ± 0.02	15.6 ± 0.72
S2 cream	2.40 ± 0.06^{b}	2.58 ± 0.16^{b}	2.32 ± 0.28^{a}	0.27 ± 0.04^{ab}	0.15 ± 0.02^{a}	0.09 ± 0.01^{a}	0.06 ± 0.00^{b}	7.90 ± 0.45
S2 aqueous	2.40 ± 0.05	2.98 ± 0.18	3.13 ± 0.06	0.39 ± 0.02	0.25 ± 0.02	0.05 ± 0.00	0.09 ± 0.01	9.31 ± 0.29
S3 emulsion	0.68 ± 0.16	0.73 ± 0.15	1.73 ± 0.94	0.17 ± 0.06	0.30 ± 0.13	0.04 ± 0.02	0.02 ± 0.02	3.67 ± 1.22
S3 cream	0.40 ± 0.04^{c}	0.50 ± 0.04^{c}	1.65 ± 0.46^{ab}	0.08 ± 0.02^{bc}	0.32 ± 0.06^{ab}	0.04 ± 0.01^{b}	0.03 ± 0.01^{abc}	3.35 ± 0.31
S3 aqueous	0.08 ± 0.01	0.12 ± 0.01	0.68 ± 0.19	0.02 ± 0.00	0.11 ± 0.02	0.01 ± 0.00	-	1.19 ± 0.11
S4 emulsion	0.95 ± 0.06	0.86 ± 0.08	1.86 ± 0.72	0.20 ± 0.04	0.38 ± 0.12	0.04 ± 0.01	0.02 ± 0.01	4.31 ± 0.76
S4 cream	0.50 ± 0.01^{c}	0.53 ± 0.03^{c}	1.35 ± 0.39^{ab}	0.16 ± 0.02^{cd}	0.37 ± 0.08^{ab}	0.03 ± 0.00^{b}	0.02 ± 0.01^{bc}	3.18 ± 0.35
S4 aqueous	0.13 ± 0.03	0.14 ± 0.01	0.43 ± 0.12	0.02 ± 0.00	0.08 ± 0.02	0.02 ± 0.00	0.01 ± 0.00	0.91 ± 0.11
S5 emulsion	0.31 ± 0.05	0.23 ± 0.04	0.83 ± 0.30	0.07 ± 0.01	0.15 ± 0.04	-	-	1.60 ± 0.29
S5 cream	0.26 ± 0.01^{d}	0.19 ± 0.01^{d}	1.21 ± 0.28^{b}	0.05 ± 0.01^{d}	0.19 ± 0.03^{b}	0.02 ± 0.00c	0.01 ± 0.01 ^{c}	1.94 ± 0.21
S5 aqueous	0.05 ± 0.01	0.03 ± 0.01	0.18 ± 0.09	0.01 ± 0.00	0.02 ± 0.01	-	-	0.31 ± 0.12
S6 emulsion	0.31 ± 0.03	0.22 ± 0.02	0.60 ± 0.23	0.07 ± 0.02	0.16 ± 0.06	0.01 ± 0.00	-	1.37 ± 0.24
S6 cream	0.26 ± 0.01^{d}	0.21 ± 0.01^{d}	0.75 ± 0.21^{b}	0.06 ± 0.01 ^{d}	0.21 ± 0.05^{b}	0.01 ± 0.00^{c}	0.01 ± 0.00^{c}	1.64 ± 0.16
S6 aqueous	0.04 ± 0.00	0.04 ± 0.00	0.11 ± 0.03	0.01 ± 0.00	0.03 ± 0.01	-	-	0.24 ± 0.03

Cream data refers to adsorbed phospholipids, while aqueous refers to unabsorbed phospholipids. **S1**, 5% w/w MFGM1, 20% w/w coconut oil; **S2**, 5% w/w MFGM1, 10% w/w coconut oil, 10% w/w fish oil; **S3**, 3% w/w MFGM2, 20% w/w coconut oil; **S4**, 3% w/w MFGM2, 10% w/w coconut oil, 10% w/w fish oil; **S5**, 3% w/w MFGM3, 20% w/w coconut oil; **S6**, 3% w/w MFGM3, 10% w/w coconut oil, 10% w/w fish oil). PE=Phosphatidylethanolamine, PC=Phosphatidylcholine, SM=Sphingomyelin, PS=Phosphatidylserine, PI=phosphatidylinositol, LPE- Lyso-Phosphatidylethanolamine, LPC- Lyso-Phosphatidylcholine. Asterix (*) indicates significant interactions between oil and emulsifier in the absorbed concentration of phospholipid (cream phase). Different letters indicate significant differences in individual phospholipids groups in each column.

A significant interaction between oil type and the phospholipids adsorbed to the emulsion's surface was observed for the phospholipid groups PE (Pr > F 0.0001), PC (Pr > F 0.001), PS (Pr > F 0.0153) and LPC (Pr > F 0.0035), indicating a higher adsorption of PE, PC, PS and LPC to the surface compared to what was present in the original MFGM sample. Those changes in distribution in the cream phase were dependant on oil and emulsifier type. For PE, higher concentrations were observed for emulsions prepared using a combination of CO and FO and MFGM1. For MFGM 2 and MFGM 3, the type of oil did not influence PE concentration; only emulsifier did so. Similar behaviours can be observed for PC, PS and LPE, with significant differences occurring as indicated in Table 4.8. Conversely, SM, PI and LPC showed no significant interactions between oil and emulsifier. Changes for those phospholipid groups were only dependent on emulsifier type, with no effect of oil. MFGM1 stabilised emulsions had significantly higher concentrations of SM (Pr > F 0.0015) than MFGM3, while no differences were observed between MFGM1 and MFGM2 and MFGM2 and MFGM3 emulsions for SM distribution in cream phase. Similar behaviour was observed for PI (Pr > F 0.0464), while LPE (Pr > F 0.003) concentrations differed among MFGM fractions in the cream phase.

The total phospholipid was considered the sum of individual phospholipid classes. For MFGM1 prepared emulsions, 46.5% of the TPL was found in the cream phase, indicating that a significant amount of the phospholipid emulsifier was not adsorbed to the surface of the lipid droplets. In contrast, for MFGM2 and MFGM3, TPL were present primarily on the surface, with means of 76 and 86.5%, respectively (Figure 4.11).

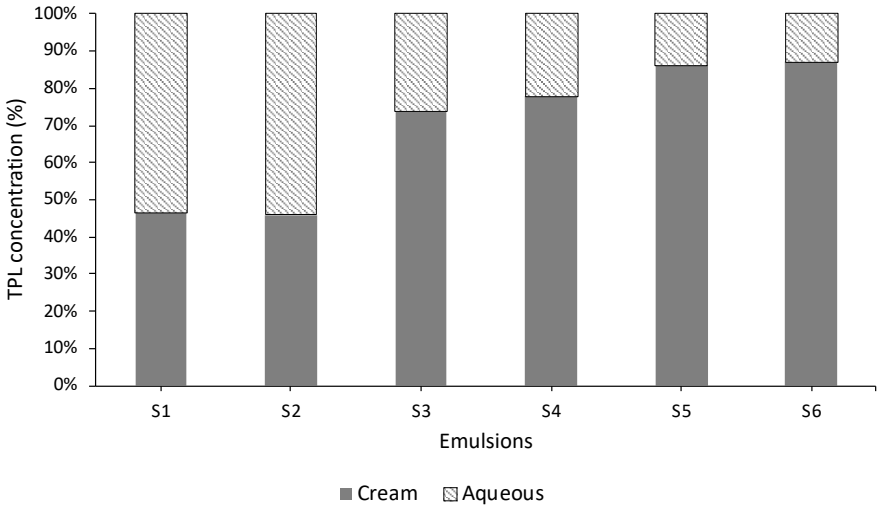

Figure 4.10. Total phospholipid concentration in surface and aqueous phases of emulsions prepared using selected emulsifier concentrations after phase separation by centrifugation. **S1**, 5% w/w MFGM1, 20% w/w coconut oil; **S2**, 5% w/w MFGM1, 10% w/w coconut oil, 10% w/w fish oil; **S3**, 3% w/w MFGM2, 20% w/w coconut oil; S4, 3% w/w MFGM2, 10% w/w coconut oil, 10% w/w fish oil; **S5**, 3% w/w MFGM3, 20% w/w coconut oil; **S6**, 3% w/w MFGM3, 10% w/w coconut oil, 10% w/w fish oil).

Interestingly, the smaller the amount of phospholipids in the fraction, the more they moved to the surface, with the fraction containing the lowest concentration (MFGM3) presenting the highest proportion of phospholipids attached to the surface. A higher concentration of MFGM1 was needed to reach a smaller particle size. However, phospholipid distribution data suggested that extra emulsifier was added to the system, and that a concentration of 2.5% could be sufficient for full droplet coverage. The excess in phospholipids indicated that the oil droplets were already saturated and suggested that formation of phospholipid micelles occurred in the aqueous phase. Those differences can additionally be attributed to the protein composition of fractions. Proteins adsorbed to the oil surface more preferably than phospholipids. MFGM2 and MFGM3 were composed of a mixture of protein and phospholipids, while MFGM1 had only phospholipids present. Nevertheless, MFGM1 emulsions S1 and S2 presented the highest loading efficiency and higher phospholipids than other fractions even at lower percentages in the cream phase.

4.5 Conclusions

In this chapter, it has been demonstrated that the tested MFGM fractions were efficient and effective in creating O/W emulsions with small particle size. MFGM2 and MFGM3 had significantly smaller particle size and had most of the phospholipids adsorbed to the oil surface, yet all emulsions were stable to coalescence over 40 days of storage. The curcumin loading efficiency was above 80% for all emulsions, with curcumin preferably located in the cream

phase of emulsions. Even though MFGM1 prepared emulsions had a larger particle size and only about half of the phospholipids were present in the cream phase, those emulsions were the ones with the highest loading efficiency. The absolute phospholipid concentration in the cream phase of MFGM1 stabilised emulsions was still higher than MFGM2 and MFGM3 stabilised emulsions. A high loading efficiency is desirable for the final goal of this study and Chapters 5 and 6 will further explore the behaviour of those emulsions systems under *in vitro* and *in vivo* gastrointestinal digestion as well as their curcumin bioaccessibility and bioavailability. The successful findings from the first stage of the study, presented in this Chapter, indicate that all MFGM fractions are good candidates to prepare delivery systems for curcumin encapsulation, enabling the formation of a stable phospholipid layer to stabilise the system.

Chapter 5 - Behaviour of curcumin loaded oil-in-water emulsions prepared using milk fat globule membrane material under *in vitro* gastrointestinal conditions

Abstract

Curcumin has very low solubility in physiological fluids, leading to low bioavailability and systemic delivery. Encapsulation in a lipid system was the chosen strategy for this study to encapsulate and protect curcumin from degradation in the gastrointestinal tract (GIT), consequently increasing the chances of improved delivery. The aim of this chapter was to evaluate if oil-in-water emulsions prepared using a number of milk fat globule membrane (MFGM) materials were able to increase curcumin bioaccessibility through protection against *in vitro* gastrointestinal digestion.

Changes in emulsion structure and curcumin bioaccessibility were studied. The particle size of emulsions prepared using MFGM materials increased significantly after gastric digestion; for MFGM3, the $d_{3,2}$ value was 0.46μm before versus 1.25μm after simulated gastric digestion. These changes promoted flocculation and coalescence of oil droplets. Significant differences were observed after simulated intestinal digestion, with pancreatin promoting disruption of emulsion structure, release of free fatty acids (FFA), and formation of mixed micelles.

The maximum release of FFA was 38%, indicating that a portion of the oil remained undigested. Those results confirm the relatively low bioaccessibility observed for MFGM2 and MFGM3 stabilised emulsions (12 to 25%). MFGM1 stabilised emulsions showed higher bioaccessibility (43 and 46%), which can be attributed to a higher concentration of phospholipids and their self-assembly into micelles, even with low FFA release. Individual phospholipid groups were measured and changes observed after *in vitro* intestinal digestion, with an increase in the lyso-, or hydrolysed, forms of PE and PC. Total phospholipids preferably attached to the cream phase of emulsions when present in small concentrations, 76% for MFGM2 and 87% for MFGM3, as opposed to 46% for MFGM1, which contained significantly higher concentration of phospholipids. After submitting to *in vitro* gastric digestion, the concentration of total phospholipids in the cream phase increased to 97%, 95% and 100% for MFGM1, MFGM2 and MFGM3, respectively.

5.1 Introduction

The human gastrointestinal system, also referred to as the gastrointestinal tract (GIT), consists of mouth, oesophagus, stomach, small intestine and large intestine. In addition, adjacent organs are involved in the complex functioning of the tract, including the liver and pancreas. All these play a vital role in breaking down complex food structures into small and readily absorbable compounds, allowing the body to obtain the necessary nutrients to operate healthily and efficiently (Singh and Gallier, 2017). Many health conditions, such as obesity, hypertension and cardiovascular disease, have been strongly associated with food habits. Acquiring relevant knowledge and understanding the mechanisms behind the treatment, transportation and utilisation of the major food components in the digestive system is critical to tackle those issues and help improve overall health (Norton et al., 2006).

Food structure and composition are critical in the digestive process. Understanding food interactions with the gastrointestinal fluids enables manufactures to tailor-made foods with improved nutrition. Lipids are essential dietary nutrients and are present in many food sources that humans ingest daily, being often present in food in the form of an emulsion or part of a complex food structure. Among foods designed for specific needs are those used to encapsulate and improve the delivery of bioactive compounds. Emulsion-based systems are widely used to enhance the delivery of hydrophilic bioactive compounds, such as curcumin, quercetin, ascorbic acid and lycopene (Di Lorenzo et al., 2021, McClements and Xiao, 2017). They can be designed using different oil compositions and concentrations, which can determine the amount of bioactive compound that the system can carry and their functionality. Proteins, phospholipids, and other compounds are often used as emulsifiers due to their amphiphilic nature. These are essential to creating emulsions and forming an adsorbed layer at the oil droplet. The nature of the adsorbed layer determines not only the system's stability under storage, but more importantly its fate and stability throughout the GIT (Farhang et al., 2012, McClements and Xiao, 2017, Singh, 2019).

Milk is a naturally occurring emulsion in which triglycerides are encapsulated by a complex tri-layer membrane of phospholipids and proteins known as the milk fat globule membrane (MFGM) (Singh, 2006). Study designs inspired by the properties of MFGM have attempted to mimic this naturally occurring system. For instance, Livney et al. (2017) created a prototype of a MFGM-resembling lamellar phospholipid structure by preparing double

emulsions coated by lactoferrin and milk-phospholipid concentrate. The emulsions had a zeta potential of -26.1 mV after phospholipid incorporation, which allied with microstructure images that confirmed the coverage of the droplet surface with phospholipids (Livney et al., 2017).

Proteins and phospholipids derived from MFGM have different properties in stabilising emulsions. One study isolated both fractions from reconstituted buttermilk and found that proteins were preferentially adsorbed to the emulsion droplet surface compared with phospholipids (Phan et al., 2016). Another study found superior emulsifying stability for emulsions prepared using phospholipid concentrate compared to those prepared using milk protein concentrate, which indicated that MFGM phospholipids are more suitable as membrane materials to simulate human milk fat globules (Sun et al., 2022). Corredig & Dalgleish (1998) also used a fraction derived from MFGM isolated from fresh cream to stabilise emulsions. The stability of their emulsions was analysed under varying pH and temperature, and the authors found that emulsions prepared with MFGM fractions were more stable at neutral pH. In addition, the droplet surface was not displaced by addition of other surfactants, indicating a strong molecular interaction between the adsorbed MFGM fraction composed by proteins and phospholipids to the oil droplet.

Dietary lipids (triglycerides) are the constituents of fats (solid) and oils (liquid) found in both animal-based and vegetable-based food sources. The esterification and position (sn-1, sn-2, sn-3) of fatty acids, the chain length, and the position and presence of double bonds collectively determine the physicochemical properties of triglycerides and contribute to the degree of lipolysis they undergo in the GIT (Singh et al., 2009). As shown in Figure 5.1, lipids ingested as an emulsion undergo structural changes and rearrangements in their surface structure that eventually enable the action of lipophilic enzymes to break down triglycerides into monoacylglycerol (MAG), diacylglycerol (DAG) and free fatty acids (FFA) (Acevedo-Fani and Singh, 2022). Curcumin has been incorporated into emulsion-based delivery systems in many research studies, yet curcumin's low bioaccessibility remains an issue due to its low solubility in aqueous solutions (< 0.03M in buffer at pH < 7), susceptibility to degradation in aqueous environments, and low bioavailability (Armand, 2007, Price and Buescher, 1997, Tønnesen H.H., 1982, Tønnesen et al., 2002).

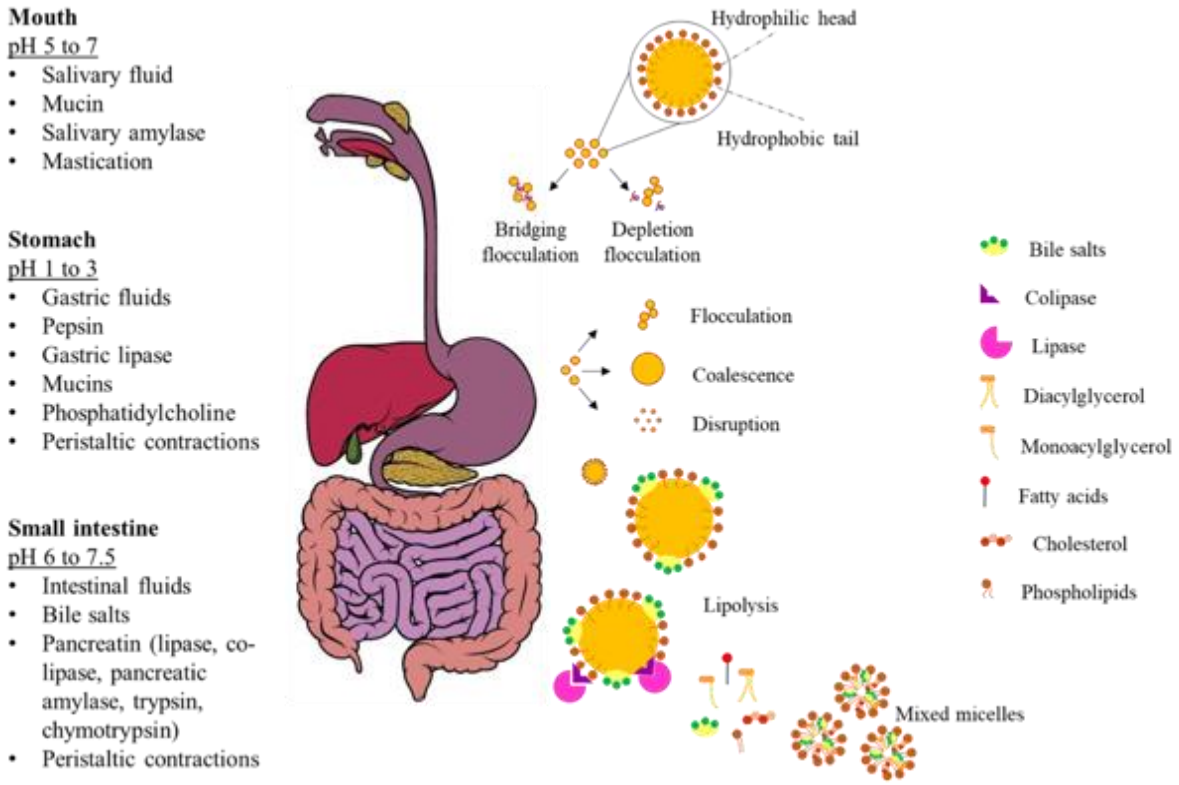

Figure 5.1 Schematic representation of lipid digestion and the possible changes in emulsion structure as it passes through the GIT from mouth to small intestine. Adapted from Singh, Ye & Horne, 2009.

Once ingested, the interaction of an emulsion with salivary enzymes and salts of different ionic strengths, as well as the mechanical effect of shear and peristaltic movements, starts promoting structural changes such as flocculation. The initial effects may be attributed in part to salivary fluids and proteins, mainly mucins. However, the period of time that liquid emulsions stay in the mouth is very short, and the mucin concentration in human saliva is low (0.02%), suggesting that the minor changes occurring during this step might be related to interactions with other components (Singh et al., 2009, Acevedo-Fani and Singh, 2022).

During swallowing, a series of movements promoted by the tongue, throat, oesophagus and stomach move the emulsion from the oral to the gastric cavity. Those movements might affect the emulsion structure, but this mechanism has not been fully explored (Weisbrodt, 2001). In addition to high shear, the gastric environment presents a low pH and a series of enzymes and minerals. The pH and ionic strength vary across individuals, representing differences in the rate of digestion between adults and the elderly, for example. The combination of emulsions with digestive juices promotes structural changes such as flocculation, coalescence and modification of the interfacial layer. Competitive adsorption between surface components and dietary and endogenous surface-active compounds facilitates

emulsification and alters the emulsion's adsorbed layer (Carriere et al., 1993, Armand et al., 1994). The action of pepsin at an optimum pH 2-3 promotes mainly the breakdown of proteins; however, 10-30% of lipolysis may occur in the stomach by the action of gastric lipase. Gastric lipase has its optimum lipolytic activity at pH 5–5.4 and promotes the hydrolysis of triacylglycerol (TAG) at the sn3 position, leading to the formation of sn1,2-DAG (Rogalska et al., 1990).

Peristaltic movements promote gastric emptying with the passage of chyme (or modified emulsions) to the small intestine, where most lipolysis occurs. In the duodenum, emulsions are mixed with bile salts and other surface-active components that promote partial or total displacement of adsorbed material to the lipid droplets. The high pH and ionic strength in the small intestine and the displacement of the surface constituents by bile salts allow colipase to bind to the oil-water interface, anchoring pancreatic lipase at the surface and thus providing an adequate environment for the breakdown of TAG. The extent of binding is related to the physicochemical and compositional structure of the interface. During hydrolysis of the droplet core by lipase, DAG, MAG and FFA are produced and can also act as surface-active compounds (Wickham et al., 1998, Fave et al., 2004, Bezzine et al., 1999). The majority of lipid hydrolysis products are insoluble in water; however, they are solubilised by the liquid luminal contents of the intestine through the formation of micelles or self-assembled structures containing bile salts, fatty acids, MAG, phospholipids and cholesterol. Enterocytes, or polarised epithelial cells, are responsible for the uptake and absorption of most nutrients in the form of mixed micelles containing bioactive compounds, after which the enterocytes transport these nutrients to the blood (D'Aquila et al., 2016).

The bioavailability of curcumin is determined by its bioaccessibility, which is described as the fraction initially ingested that is solubilised within the gastrointestinal fluid in a form that can be absorbed by the epithelial cells (Fernandez-Garcia et al., 2009). Bioaccessibility refers to the portion of a nutrient, compound, or substance present in a given matrix, such as food, that is liberated and accessible for potential absorption in the gastrointestinal tract post-digestion. It assesses the release and solubilization of the substance in relation to its matrix, offering insights into its initial availability for absorption. On the other hand, bioavailability refers to the fraction of a substance that is effectively absorbed, undergoes systemic distribution, and becomes biologically available for utilization by the body. This includes processes such as metabolism and excretion that influence the substance's functionality. Together, these concepts provide a comprehensive understanding of how substances interact

with the body, from initial liberation to physiological utilization (Rutherfurd et al., 2015; Greger, 1998). The bioaccessibility of a nutraceutical is defined as the portion of bioactive that has been incorporated into mixed micelles in the small intestine and is ready for absorption through the intestinal wall. Oral bioaccessibility is a crucial parameter to assess the relationship between food and its health benefits (Ahmed et al., 2012). Therefore, in this chapter the fate of emulsions stabilised by MFGM under *in vitro* gastrointestinal conditions and the bioaccessibility of curcumin were studied. The main objective was to identify the differences between selected emulsifiers and oil composition on curcumin's bioavailability, with the intent to select the optimal system for a subsequent *in vivo* animal trial.

5.2 Materials and Methods

5.2.1 Materials

For detailed information about general materials used for emulsion preparation and characterization, refer to Chapter 3 (Materials and equipment) and Chapter 4 (milk fat globule membrane derived material as an emulsifying agent in the preparation of curcumin loaded oil-in-water emulsions). Chemicals of general use have also been listed in Chapter 3 (3.1.7). Porcine pepsin (CAS 9001-75-6), bovine bile extract (CAS 8008-63-7), porcine pancreatin (CAS 8049-47-6), KCl (CAS 7447-40-7), KH_2PO_4 (CAS 7778-77-0), $NaHCO_3$ (CAS 144-55-8), NaCl (CAS 7647-14-5), $MgCl_2$ (CAS 7786-30-3), $(NH_4)_2CO_3$ (CAS 506-87-6) and Pefabloc® (CAS 30827-99-7) were purchased from Sigma-Aldrich Co. LLC, USA.

5.2.2 Methods

5.2.2.1 Preparation and characterisation of O/W emulsions

Six emulsion systems were prepared using high pressure homogenisation and characterized by particle size distribution, zeta-potential and microscopic structure as described in Chapter 4. Curcumin and phospholipid distribution in the emulsion system was also determined using chromatography. Emulsions were prepared at least in triplicate using medium-chain triglyceride oil (MCT) either alone or in combination with fish oil (FO), combined with one of three MFGM-derived materials (Table 5.1).

Table 5.1. Emulsions coding and composition. MCT = Medium chain triglyceride oil; FO = Fish oil

Emulsion code	Oil composition – 20% (w/w)	Emulsifier composition
S1	MCT	MFGM1 (Lipid700) – 5% (w/w)
S2	MCT:FO (1:1)	MFGM1 (Lipid700) – 5% (w/w)
S3	MCT	MFGM2 (BPC50 GU09) – 3% (w/w)
S4	MCT:FO (1:1)	MFGM2 (BPC50 GU09) – 3% (w/w)
S5	MCT	MFGM3 (HFWPC70) – 3% (w/w)
S6	MCT:FO (1:1)	MFGM3 (HFWPC70) – 3% (w/w)

5.2.2.2 Simulated gastrointestinal digestion

The gastrointestinal digestion was carried out using the static INFOGEST digestion protocol as described by Brodkorb et al., (2019) without the addition of gastric lipase. The oral phase was conducted without the addition of amylase and used for purposes of dilution, as the emulsions contained no starch and liquid forms remain for a short period in the oral cavity (Brodkorb et al., 2019).

a) Oral phase

Simulated salivary fluid (SSF) consisted of 15.1 mM KCl, 3.7 mM KH_2PO_4, 13.6 mM $NaHCO_3$, 0.15 mM $MgCl_2(H2O)_6$ and 0.06 mM $(NH4)_2CO_3$. The pH was adjusted to 7 with the addition of HCl. Freshly prepared emulsions were mixed with SSF at a ratio of 1:1 (w/w) and 0.3M $CaCl_2$ was added to achieve 1.5mM $CaCl_2$ in the final mixture. No mastication simulation was needed for liquid emulsions; however, they were incubated in a water bath at 37°C with magnetic stirring at 350 rpm for 2 min to ensure the formation of a homogeneous oral bolus.

b) Gastric phase

Simulated gastric fluid (SGF) consisted of 6.9 mM KCl, 0.9 mM KH_2PO_4, 25 mM $NaHCO_3$, 47.2 mM NaCl, 0.12 mM $MgCl_2(H2O)_6$ and 0.5 mM $(NH_4)_2CO_3$. The pH was adjusted to 3 with the addition of HCl and $CaCl_2$ (0.3M) was added to achieve 0.15 mM $CaCl_2$ in the final mixture. The emulsion was mixed with SSF at a ratio of 1:1 (w/w) and pepsin was added to achieve 2000 U/mL activity in the final mixture. The samples were then incubated at 37°C for 2 h in a shaking water-bath. Aliquots were collected at 15, 30, 60 and 120min for analysis of particle size, microstructural changes, and bioaccessibility. Enzyme inactivation after simulated gastric digestion was obtained by the addition of NaOH to reach pH 8.

c) Intestinal phase

Simulated intestinal fluid (SIF) consisted of 6.8 mM KCl, 0.8 mM KH_2PO_4, 85 mM $NaHCO_3$, 38.4 mM NaCl and 0.33 mM $MgCl_2(H_2O)_6$. $CaCl_2$ (0.3M) was added to achieve 0.6 mM in the final mixture. Gastric digesta were mixed with SIF and bile salts (10mM in the final mixture). The pH was adjusted to 7 with the addition of NaOH or HCl and pancreatin solution was added. The final ratio of oral digesta and SIF + bile + pancreatin solution was 1:1 (v/v) and the samples were incubated at 37 °C under magnetic stirring at 350 rpm for 2 h. Pancreatin solution was prepared to achieve a lipase activity of 2000 U/mL in the final mixture. Aliquots were collected at 15, 30, 60 and 120min for analysis of particle size, microstructural changes, and bioaccessibility. The hydrolysis reaction was stopped by the addition of 5mM of Pefabloc®/mL of digesta.

d) Kinetics of free fatty acid release

The release of free fatty acids (FFA) during simulated intestinal digestion was quantified over 2 h while maintaining the pH at 7.0 by the addition of 0.05 M NaOH using a pH-stat (TIM 854, Radiometer). The percentage of FFA released was calculated based on the volume of NaOH consumed, assuming that lipase will hydrolyse two FFAs per triglyceride molecule (Li and McClements, 2010):

$$\%FFA = [100 \times (V_{NaOH} \, x \, M_{NaOH} \, x \, M_{W\,lipid})] \div (2 \times W_{lipid}) \quad (1)$$

where V_{NaOH} is the volume (L) of 0.05 M NaOH solution consumed to neutralise the FFAs produced, M_{NaOH} is the molarity (M) of the NaOH solution used, $M_{W\,lipid}$ is the mean molecular mass (g mol^{-1}) of the triglycerides and W_{lipid} is the total mass (g) of lipid present in the sample used for titration.

The kinetic parameters for the initial FFA release were calculated using Equation (2) (Li & McClements, 2010):

$$\Phi_t = \Phi_{max}[1 - (1 + k_1 t)^{-2}] \quad (2)$$

where t is the intestinal digestion time (min), Φmax *i*s the maximum total FFA level (%) and k_1 is the first-order rate constant of FFA release (%FFA min^{-1}), which was calculated using the following equation:

$$k_1 = 3kM_w/2d_0.p_0 \quad (3)$$

where k (mol s^{-1} m^{-2}) is the lipid conversion rate per unit area of the droplet surface, occurring at maximum lipase surface coverage, M_w is the molecular weight of the lipid, d_0 is the initial mean diameter of the emulsion (d_{32}) and p_0 is the density of the lipid.

In this study, Equation (2) was used as the mathematical model that gave the best fit to the experimental data. Non-linear regression analyses were done with R version 3.6.0 (R Core Team, 2019) using RStudio 1.1.447 (RStudio, Boston, MA, USA) and the nls function in the statistics package (version 3.6.0). The lipolysis half time (t1/2, min), i.e. the time required to achieve 50% lipid digestion, was obtained from the experimental FFA curve.

5.2.2.3 Bioaccessibility

After *in vitro* digestion, emulsions were centrifuged (15,000 g) at 25 °C for 30 min. The samples separated into a sediment phase at the bottom, a clear soluble phase in the middle (assumed to be the micellar phase), and sometimes an oil and/or cream phase at the top. Aliquots (0.5mL) of the soluble phase were collected using a pipette, vortexed with 0.5 ml of methanol, and then centrifuged at 15,000g (at room temperature) for 10 min. The top methanol layer was collected and set aside, while the bottom layer was vortexed with another 0.5 ml of methanol, and centrifuged again. The second top layer was added to the previously collected methanol layer, mixed, and analysed by HPLC as described in 3.2.3 and 4.3.2.5d. The bioaccessibility was calculated by dividing the curcumin concentration present in the soluble phase by the total observed curcumin concentration after simulated digestion and multiplying by 100 to obtain percentage values ([curcumin micelle × 100] ÷ total curcumin after digestion).

5.2.2.4 Statistical analysis

A 3-way ANOVA model was used to determine the effect of the emulsifier, oil type, and their interaction on several responses (e.g., particle size, zeta potential, curcumin loading efficiency and phospholipid distribution) using the Proc Mixed procedure. The model diagnostics (e.g., normal distribution) for each response variable were tested using the ODS Graphics procedure and the repeated statement of SAS. When the model assumptions were not fulfilled the raw data were transformed. When the F-value of the model was significant ($P < 0.05$), the mean values of the two-way ANOVA were compared using the adjusted Tukey-

Kramer test. Probability values were considered statistically different when $P < 0.05$, and values of $0.051 \leq P \leq 0.10$ were considered a trend.

5.3 Results and discussion

a) Particle size and zeta-potential during *in vitro* gastrointestinal digestion

A liquid food, even if structured in a complex system such as milk, will have less interaction with salivary fluids, mucins and enzymes present in the mouth than a solid food that requires mastication. Considering that emulsions would experience minimal effects from those conditions, only salivary fluids were added to the oral phase of the *in vitro* gastrointestinal digestion in this experiment for purposes of dilution and electrolyte concentrations.

Food emulsions can present a range of variations in structure, pH, rheology, ionic strength, and temperature. Consequently, the behaviour of different types of emulsions in the mouth can vary. A study by Sarkar et al., (2009) investigated the interaction of salivary fluids and mucins with positively and negatively charged emulsion systems. The negatively charged systems stabilised by β-lactoglobulin showed no structural changes when exposed to artificial saliva without mucin and became unstable only after addition of more than 0.5% mucin. Depletion flocculation was observed at 1% mucin concentration, indicating interaction of mucin with the negatively charged protein layer of emulsions (Sarkar et al., 2009). The incubation time of mucin and emulsion in the study was 30 min, although for the ingestion of an emulsion in the form of a beverage or yogurt, the time in the mouth would be most likely less than 2 minutes. This reinforces the justification for use of fluids only for dilution purposes since interactions are unlikely to destabilise or cause major changes in food structure for the emulsion systems in this study.

Emulsions prepared using various MFGM-derived materials and oil compositions showed mean particle size ($d_{4,3}$), varying from 0.46 μm for the emulsion prepared using MFGM3 to 0.60 μm for the emulsion prepared using MFGM1 (Table 5.2). All freshly prepared emulsions showed monomodal particle size distribution, and confocal microscopy images indicated the presence of both small and larger particles (Figure 5.2). No significant differences were observed between fresh emulsions for mean particle size; however, the interaction of emulsifier, oil type and treatment promoted a significant ($Pr > F$ 0.0003) increase in particle

size after gastric and intestinal simulated digestion (Table 5.2). This indicates that the effect of the digestion treatment on the mean particle size was dependent on oil and emulsifier type.

Table 5.2. Mean particle size (d_{43}) and zeta-potential of fresh emulsions systems stabilized by MFGM and corresponding gastric and intestinal digestion

	Fresh emulsion		Gastric digesta		Intestinal digesta	
Emulsion	**d43 (µm)***	**Zeta-potential (mV) pH 7.0**	**d43 (µm)***	**Zeta-potential (mV) pH 3.0**	**d43 (µm)***	**Zeta-potential (mV) pH 7.0**
S1	-0.58 ± 0.06 [a] (0.56)	-52.20 ± 5.58	0.57 ± 0.14 [b] (1.76)	-27.10 ± 1.72	4.26 ± 0.29 [c] (70.5)	-48.60 ± 3.49
S2	-0.53 ± 0.09 [a] (0.59)	-54.60 ± 0.68	0.78 ± 0.02 [b] (2.17)	-25.30 ± 1.64	4.70 ± 0.25 [c] (110)	-39.10 ± 3.18
S3	-0.68 ± 0.10 [a] (0.51)	-23.30 ± 0.57	0.67 ± 0.07 [b] (1.95)	19.20 ± 3.58	4.60 ± 0.13 [c] (99.0)	-43.10 ± 3.87
S4	-0.73 ± 0.14 [a] (0.48)	-22.00 ± 0.60	0.82 ±0.07 [b] (2.26)	27.00 ± 0.41	4.73 ± 0.16 [c] (113)	-64.00 ±7.02
S5	-0.76 ± 0.20 a (0.47)	-28.40 ± 1.28	0.22 ± 0.26 [ba] (1.25)	15.90 ± 0.35	4.64 ± 0.19 [c] (103) ±	-53.00 ± 1.90
S6	-0.78 ± 0.03 a (0.46)	-27.30 ± 0.82	0.73 ± 0.40 [dba] (2.08)	14.80 ± 1.88	2.39 ± 0.31 [d] (10.9)	-79.10 ± 0.93

S1, 5% w/w MFGM1, 20% w/w MCT; **S2**, 5% w/w MFGM1, 10% w/w MCT oil, 10% w/w fish oil; **S3**, 3% w/w MFGM2, 20% w/w MCT oil; **S4**, 3% w/w MFGM2, 10% w/w MCT oil, 10% w/w fish oil; **S5**, 3% w/w MFGM3, 20% w/w MCT oil; **S6**, 3% w/w MFGM3, 10% w/w MCT oil, 10% w/w fish oil. The values are shown as mean ± SD of N≥3. *Raw data were log transformed to obtain normality of variance for statistical analysis. The values showed in parentheses are the back transformation of log values back to its original scale to allow more meaningful and intuitive data interpretation. Different letters indicate significant difference between samples on average particle size ($p<0.05$).

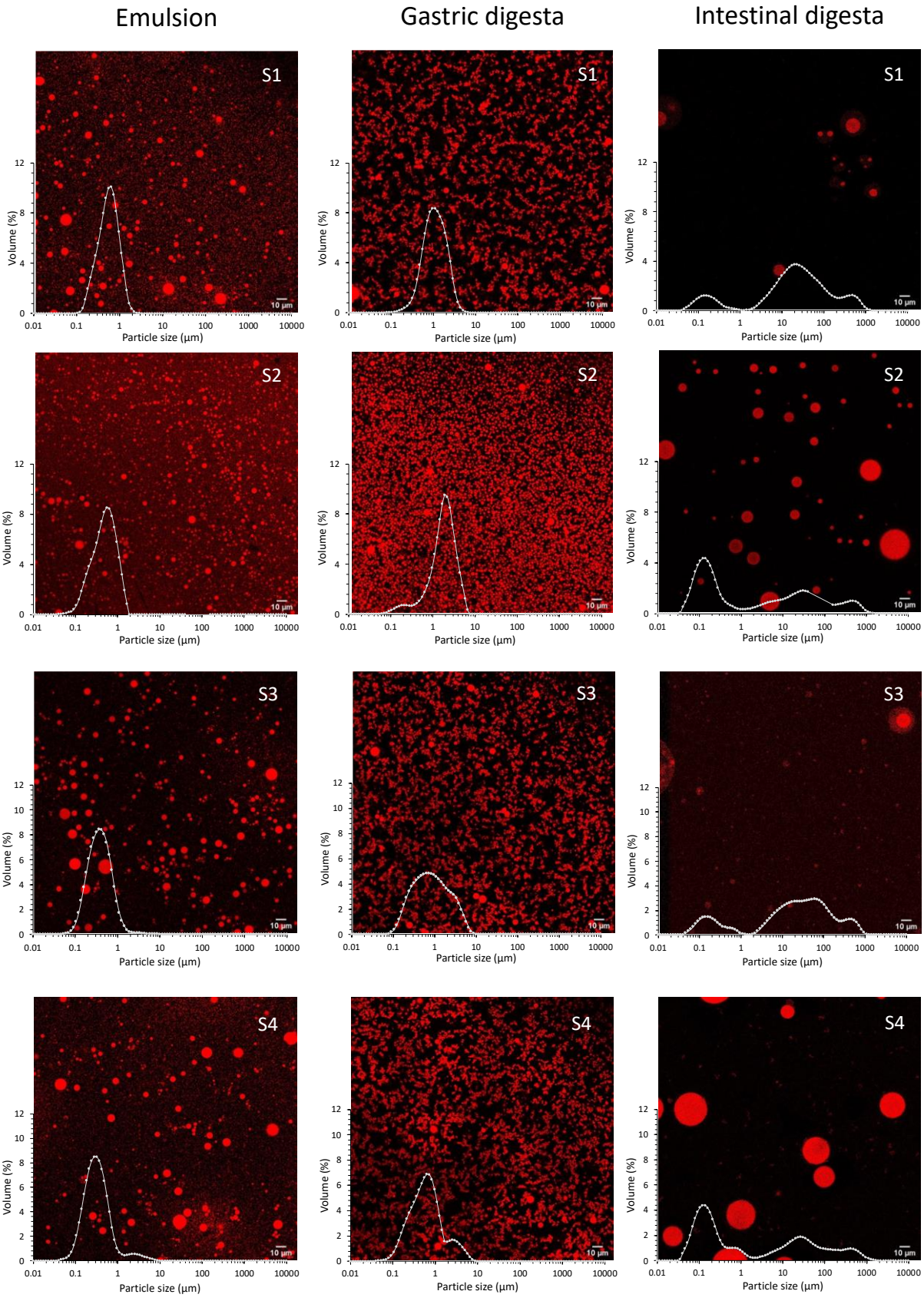
Emulsion
Gastric digesta
Intestinal digesta
S1
S2
S3
S4
Volume (%)
Particle size (µm)
10 µm

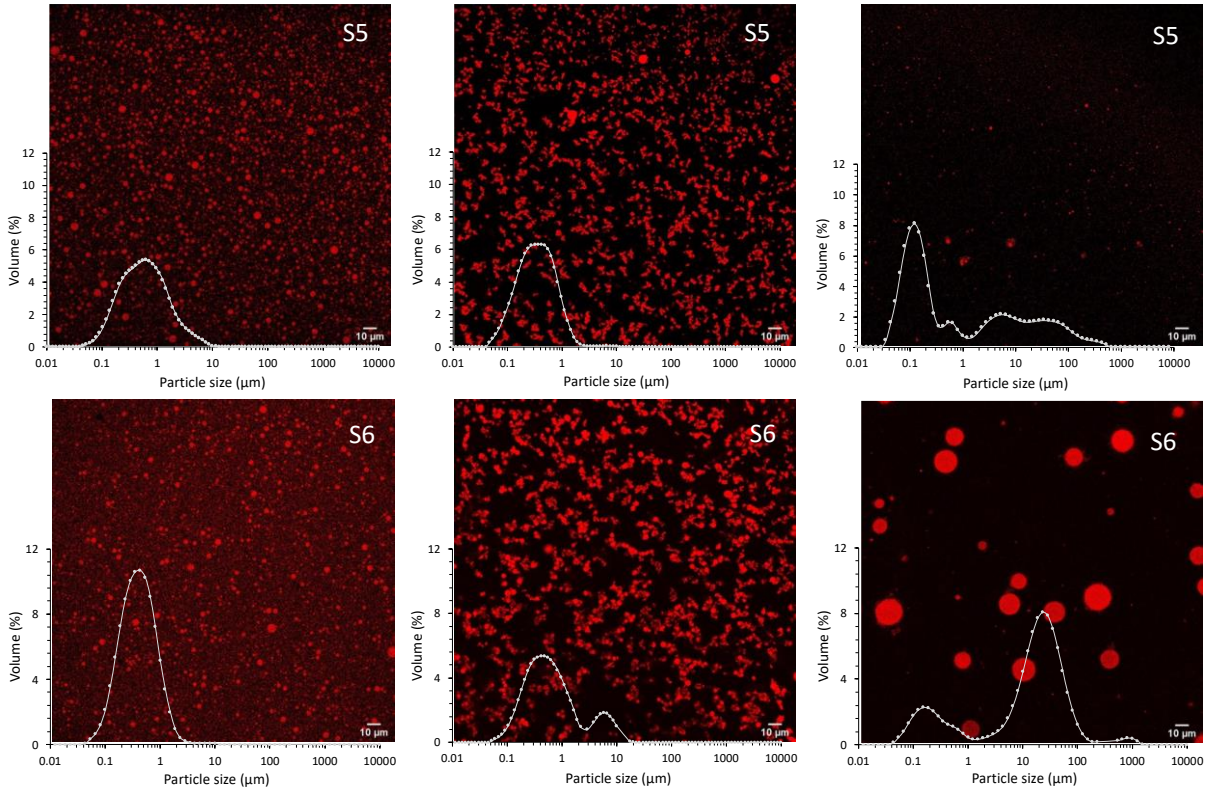

Figure 5.2. Confocal images and particle size distribution of emulsion systems stabilized by MFGM derived materials (**S1**, 5% w/w MFGM1, 20% w/w coconut oil; **S2**, 5% w/w MFGM1, 10% w/w MCT oil, 10% w/w fish oil; **S3**, 3% w/w MFGM2, 20% w/w MCT oil; **S4**, 3% w/w MFGM2, 10% w/w MCT oil, 10% w/w fish oil; **S5**, 3% w/w MFGM3, 20% w/w MCT oil; **S6**, 3% w/w MFGM3, 10% w/w MCT oil, 10.% w/w fish oil) and corresponding gastric and intestinal digesta. The red colour represents the oil phase. No dye was added; instead, curcumin's natural fluorescence was used to capture the images.

The mean particle size ($d_{4,2}$) of emulsions showed a significant increase after simulated gastric digestion. The drop in pH and the change in ionic strength after the addition of simulated digestive fluids promoted rearrangements of droplets that led to flocculation and coalescence, likely to be caused by electrostatic attraction between gastric-digested and non or partially digested globules, contributing to higher average particle size values (Figure 5.2). The mean $d_{4,2}$ size for emulsions prepared using MFGM1 (S1 and S2) increased from 0.58 to 1.97μm after gastric digestion (Table 5.2). Similar changes were observed for MFGM2 (S3 and S4) and MFGM3 (S5 and S6) stabilised emulsions, which increased from 0.5 to 2.11μm and 0.47 to 1.67μm respectively. Emulsion S5, prepared using MCT and MFGM3, had a slightly less marked increase from fresh emulsions to gastric digesta compared to other systems. Despite the increase in particle size, no phase separation was observed after gastric digestion, indicating that the emulsion's structure was able to retain curcumin encapsulated inside the oil droplets. Emulsions prepared using MFGM material can therefore be considered to be resistant to simulated gastric conditions.

However, the addition of pancreatic enzymes and bile salts promoted disruption of the emulsion systems, resulting in hydrolysis of triglycerides and formation of mixed micelles from the released fatty acids. After intestinal digestion, emulsion systems presented a broad droplet distribution, with a significant increase in the mean droplet diameter for all systems to 90.3μm, 106μm and 57μm for MFGM1, MFGM2 and MFGM3 stabilised emulsions, respectively (Figure 5.2). This increase in size can be related to the formation of amorphous structures as a result of protein and lipid degradation by pancreatic enzymes and bile salts, as well as droplet agglomeration (Park et al., 2017). The hydrolysis of protein is believed to generate peptides with low molecular weights that can be observed as amorphous structures, which could have occurred for MFGM2 and MFGM3 stabilised emulsions. Emulsion S6, prepared using MFGM3 as emulsifier and MCT + FO, had a significantly smaller mean $d_{4,2}$ when compared to other systems after being submitted to intestinal conditions. In fact, an approximate ten-fold difference was observed between S6 and the matching preparations made with MFGM1 or MFGM2 at this stage in the digestion process, which could reflect MFGM3 promoting better emulsifying properties (Table 5.2). However, emulsion S5, which was prepared using MFGM3 but a different oil combination, also had nearly ten-fold larger particle size compared to S6, which indicates that the an interaction with the oil phase for this specific emulsifier can be attributed to having significantly affected the digestion behaviour. During

lipid digestion, the products of lipolysis are removed from the emulsion's interface by incorporation into mixed micelles spontaneously formed by the interaction with bile salts (Acevedo-Fani and Singh, 2022).

The zeta-potential was measured to determine the changes in the potential at the surface of shear of MFGM-stabilised emulsions during digestion under simulated GIT conditions. Changes in pH and ionic strength created during *in vitro* gastrointestinal conditions can affect zeta-potential and determine the behaviour of oil droplets. In this study, the interaction of the MFGM fraction, oil type and treatment was significant (Pr>F 0.0004) on emulsion zeta-potential, with changes being observed between MFGM fractions after gastrointestinal treatment for both oil types. Emulsion droplets were negatively charged at pH 7.0, which meant that the overall charge of the components was negative. The pH reduction under gastric conditions caused a shift from negatively charged to positively charged emulsions for MFGM2 and MFGM3 stabilised emulsions; however, the emulsions prepared using MFGM1 remained negative even at low pH (Table 5.2).

The isoelectric point is defined as the pH in which the charges of a solution are neutral, or become zero. Once the pH is above this point, the charges are negative, whilst if below they become positive. The isoelectric point for MFMG-derived materials ranges from 4 to 5 (Corredig and Dalgleish, 1998). Lopez and collaborators assessed the effect of pH on the structure of emulsions prepared using MFGM-rich material and found that the absolute zeta-potential (-61 ± 1 mV at neutral pH) for the emulsions decreased as the pH decreased, with isoelectric point stablished to be at pH 4.3 (Lopez et al., 2017). Below the isoelectric point values, the charge become positive, which indicates that MFGM2 and MFGM3 emulsions behaved in a similar way to ones in previous studies, presenting a positive charge for pH below 4. Interestingly, pH had a less significant effect on the charge for MFGM1 stabilised emulsions. Proteins are more susceptible to changes in zeta-potential than phospholipids. As MFGM1 had no protein in its composition this finding suggests that protein has likely contributed to changes from negative to positively charges under gastric pH conditions for MFGM2 and MFGM3-stabilised emulsions. This matches similar findings elsewhere, in which Liu et al. (2012) found that the zeta-potential of crude liposomes prepared with phospholipids from soybean or MFGM were −13.3±1.2 mV and −1.6±0.6 mV respectively, and did not undergo changes during digestion in gastric conditions for up to 240 min. The ionic properties of phospholipids are also important in their function as emulsifiers. MacGibbon and Fong (2021) described the typical

ionization constants of various phospholipids at normal pH 6.7 to range from a zwitterion with no net charge (phosphatidylcholine, phosphatidylethanolamine), to an acid with a net negative charge (phosphatidylserine, phosphatidylinositol). Additionally, the isoelectric point for some of the phospholipid groups present in the MFGM1 fraction is approximately 2, which is below the pH 3 at which emulsions were submitted to gastric digestion.

A decrease in negative charges for emulsion systems leads to a decrease in the repulsive electrostatic interactions, favouring their aggregation at pH conditions below 5. This was observed for most of the emulsion systems in this study (Figure 5.2) and is in accordance with a previous study that found that pH affected the interfacial properties of the lipid droplets covered by MFGM material, causing phase separation but no coalescence (Corredig and Dalgleish, 1998).

Kinetics of free fatty acid (FFA) release

The lipolysis of MFGM stabilised emulsions under simulated intestinal conditions was quantified by determining the release of free fatty acids (FFA). Emulsions using different oil and MFGM fractions as emulsifiers showed most of the FFA release occurring during the first 15 minutes of digestion (Figure 5.3). There was no significant interaction between oil type and emulsifier on the release of free fatty acids (Pr>F 0.2788); however, the individual factors of oil type and MFGM fraction had a significant effect on the extent of FFA release, indicating differences across both oil type (Pr>F 0.0021) and emulsifier (Pr>F 0.012). Maximum release of FFA showed higher release for emulsions prepared using a combination of MCT and fish oil when compared to those prepared only with MCT, with emulsions S4 and S6 presenting the highest FFA release.

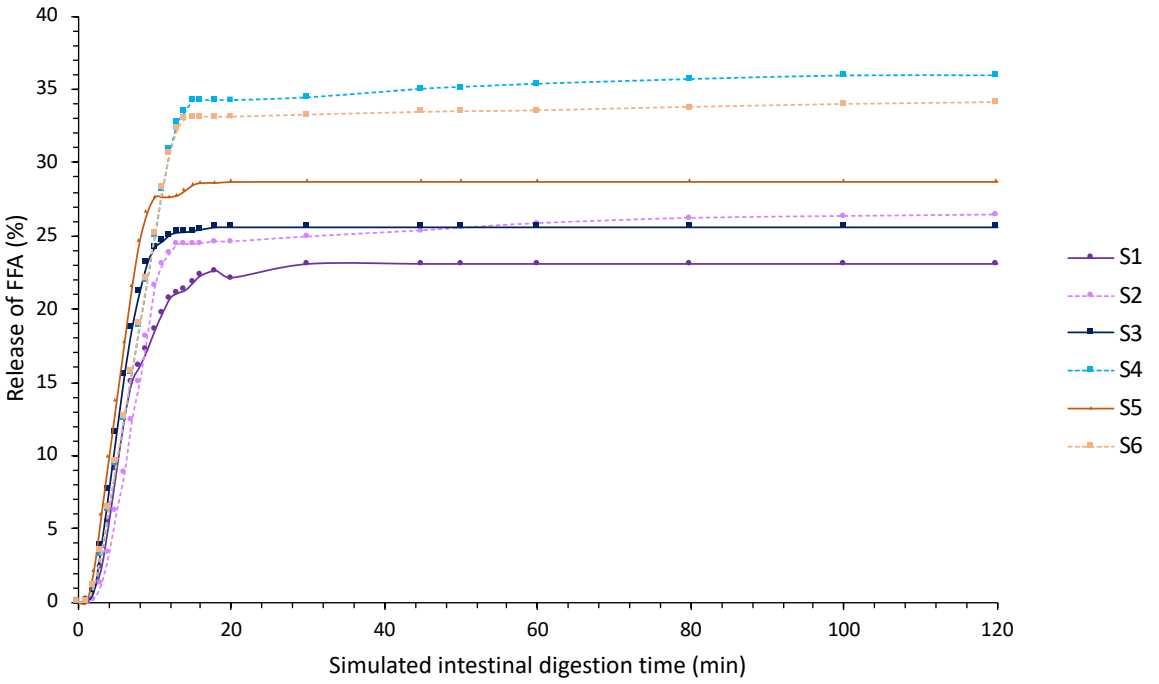

Figure 5.3. Kinetics of Free Fatty Acid (FFA) release from emulsions prepared using MFGM (**S1**, 5% w/w M1, 20.0% w/w coconut oil; **S2**, 5% w/w M1, 10.0% w/w coconut oil, 10.0% w/w fish oil; **S3**, 3% w/w M2, 20.0% w/w coconut oil; **S4**, 3% w/w M2, 10.0% w/w coconut oil, 10.0% w/w fish oil; **S5**, 3% w/w M3, 20.0% w/w coconut oil; **S6**, 3% w/w M3, 10.0% w/w coconut oil, 10.0% w/w fish oil).

A study compared the rate of lipid digestion and FFA release in nanoemulsions prepared using short (SCT), medium (MCT) or long (LCT) chain triglycerides. The authors found that the final amount of FFA produced depended strongly on lipid type, with a release of 68% for LCT, 90% for SCT and LCT:SCT and 113% for MCT (Ahmed et al., 2012). Another study also observed higher lipid digestion rates for MCT as compared to LCT. The lower extent of lipid digestion might be explained by the accumulation of fatty acids to the droplet surface, inhibiting the action of enzymes if enough bile is not present (Deckelbaum et al., 1990). Conversely, medium chain fatty acids are known to be more readily dispersible in the aqueous phase and therefore do not tend to accumulate at droplet surfaces and inhibit lipid digestion (Sek et al., 2002). Based on these observations, it would be expected that emulsions in our study prepared by a combination of MCT and fish oil (LCT) to have lower digestibility; however, the opposite was observed. This may be explained by our findings being similar to those of Ahmed et al (2012), wherein the combination of MCT with LCT from fish oil might have facilitated digestion.

In addition to oil composition, the initial particle size of emulsions is believed to play a role in lipolysis. A study conducted by Liu and collaborators looked into the digestion of emulsions covered by membrane phospholipids and assessed the effect of different particle

sizes on the rate of lipolysis. They found that small particle size emulsions had higher release of FFA than the large particle size emulsions, both were stabilised by phospholipids (Liu et al., 2021a). The initial mean particle size for all emulsions systems in the present study was similar, yet marked differences were observed between samples, suggesting that oil or MFGM composition were responsible for the changes in the lipolysis profile.

With regards to the MFGM fraction, it was observed that MFGM1 promoted significantly lower maximum FFA release than MFGM2 and MFGM3; the latter two were equivalent to each other (Table 5.3). This suggests that the nature of the oil droplet surface contributed to higher digestibility of emulsions. Emulsion S1, prepared with MFGM fraction containing only phospholipids and MCT, presented significantly lower release of free fatty acids (24.2%) compared to all other systems. Emulsions S2, which had the same emulsifier but different oil composition, had significantly higher release (27.5%) than S1, but was equal to S3 (26.7%), which was emulsified by MFGM2. Emulsion S5, emulsified by MFGM3, showed higher release (29.9%) than previously mentioned emulsions, but significantly lower than emulsions S4 and S6 (37.8% and 35.8%) prepared using MFGM2 and MFGM3, respectively.

Emulsions prepared using MFGM fractions containing protein in their composition had a higher hydrolysis rate compared with fractions containing only phospholipids in their composition, with exception of S3. The half-time for FFA release was short and varied from 3.92 min for S5 to 7.19 for S4 (Table 5.3). The behaviour of emulsions did not show clear trends and thus associations between oil or emulsifier type are difficult to identify, indicating that overall for the systems tested less than 50% of the total FFA were released and transformed into mixed micelles. According to a 2006 study, MFGM-derived phospholipid contains a high proportion of saturated fatty acids (Thompson and Singh, 2006). A high degree of acyl chain saturation has been associated with a decrease in the hydrolysis rate of phospholipids in liposome dispersions (Grit and Crommelin, 1993). In line with those findings, Liu et al. (2012) observed a lower rate of hydrolysis in liposomes prepared using MFGM-derived phospholipid than liposomes from soybean-derived phospholipid. These collective findings are in accordance with the FFA profile of emulsions prepared using MFGM phospholipids in this study.

Table 5.3. Lipolysis kinetic data of *in vitro* intestinal digestions of various emulsions prepared using MFGM-derived materials.

Emulsions	K1 (% FFA min^{-1})	φmax	t (1/2) min
S1	2.09 ± 0.43	24.2 ± 0.88^{d}	5.49 ± 0.43^{c}
S2	1.44 ± 0.26	27.5 ± 0.94^{c}	6.61 ± 1.08^{ab}
S3	2.61 ± 0.49	26.7 ± 0.82^{c}	6.08 ± 1.06^{bc}
S4	1.33 ± 0.17	37.8 ± 0.97^{a}	7.19 ± 0.66^{a}
S5	2.75 ± 0.47	29.9 ± 0.81^{b}	3.92 ± 0.93^{a}
S6	1.44 ± 0.20	35.8 ± 0.94^{a}	6.64 ± 0.55^{a}

K1 (first-order rate constant); **φmax** (Maximum release); **t (1/2)** (half-life of the reaction process) **S1**, 5% w/w MFGM1, 20% w/w MCT; **S2**, 5% w/w MFGM1, 10% w/w MCT oil, 10% w/w fish oil; **S3**, 3% w/w MFGM2, 20% w/w MCT oil; **S4**, 3% w/w MFGM2, 10% w/w MCT oil, 10% w/w fish oil; **S5**, 3% w/w MFGM3, 20% w/w MCT oil; **S6**, 3% w/w MFGM3, 10% w/w MCT oil, 10% w/w fish oil. Values are shown as mean ± SD of $N \geq 3$. Samples in the same column with different superscript letters are significantly different ($p<0.05$).

Short-chain fatty acids and medium-chain fatty acids are known to have a high dispersibility in aqueous media and will, therefore, be solubilised easily into mixed bile salt-phospholipid micelles and further transported to the systemic circulation *in vivo*. In contrast, long-chain fatty acids tend to accumulate at the oil-water interface, inhibiting the action of lipases until they are precipitated by calcium ions into insoluble soaps (Singh and Gallier, 2017). Therefore, it would be expected that systems created using MCT (S1, S3 and S5) would have a higher rate of FFA release compared to those containing added LCT (S2, S4 and S6). However, the opposite occurred, and no discernible trends were observed. We hypothesise that this occurred because the emulsions were prepared using a combination of oils of different chain lengths instead of only long-chain fatty acids. An alternative explanation is that the effect was due to the differences in emulsifier composition as discussed previously. Regardless, it is clear that lipid type and concentration have an influence on the structure of the micelle phase formed at the end of the lipid digestion process. As well as forming mixed micelles, the bile salts, phospholipids, and lipid digestion products may assemble into various other types of association colloids during the lipid digestion process, including vesicles and lamellar structures. The concentration and structure of these associated colloids is likely to change throughout the digestion process and will be dependent on the molecular characteristics of the carrier oil, which may affect their ability to incorporate lipophilic bioactive ingredients such as curcumin.

Curcumin bioaccessibility and phospholipid distribution

The bioaccessible curcumin was calculated as the fraction of curcumin still present in the micellar phase after *in vitro* digestion, meaning that the curcumin was retained in the micelles rather than being released into the aqueous medium where it would no longer be bioavailable to gut enterocytes. The micelle fraction was obtained after centrifugation of the gastric and intestinal digesta followed by methanol extraction. The proportion of bioaccessible curcumin was calculated based on the total curcumin in the analysed sample. Emulsions S1 (7.12%) and S2 (12.2%), prepared using MFGM1, showed significantly higher curcumin bioaccessibility after gastric digestion compared to all other emulsions. Emulsions S3 (1.01%) and S4 (0.57%), prepared using MFGM2, greatly reduced curcumin bioaccessibility in the gastric phase; however, these were still significantly higher than emulsions S5 (0.20%) and S6 (0.12%), which were prepared using MFGM3 (Table 5.4).

These findings suggest that MFGM3 was more effective in retaining curcumin inside the oil droplets under gastric conditions, with little release occurring into the aqueous (micellar) phase. MFGM2 and MFGM1 emulsions followed this pattern to a lesser extent. The higher release of curcumin in samples prepared using MFGM1 may be related to its high phospholipid concentration. An excess of MFGM1 was added to prepare emulsions, and approximately 50% of the phospholipids were present in the aqueous phase, as opposed to much lower concentrations for MFGM2 and MFGM3 stabilised emulsions (Figure 5.5). Previous studies have suggested that curcumin's polar groups promote phospholipid complexation via hydrogen bonding and dipole interactions with the polar head groups of phosphatidylcholine (Cuomo et al., 2011). Therefore, it is likely that a complex of curcumin with phospholipids present both in cream and aqueous phases of MFGM1-prepared emulsions led to higher bioaccessibility after gastric phase digestion with the formation of self-assembled micelles.

Table 5.4. Curcumin bioaccessibility after *in vitro* gastric and intestinal digestion of emulsions stabilized by MFGM.

	Bioaccessibility	
Sample	**Gastric digesta**	**Intestinal digesta**
S1	1.96 ± 0.19^{a} (7.12 %)	3.84 ± 0.19^{a} (46.3 %)
S2	2.50 ± 0.03^{a} (12.2 %)	3.76 ± 0.03^{a} (43.0 %)
S3	0.01 ± 0.19^{b} (1.01 %)	2.71 ± 0.19^{bc} (15.0 %)
S4	-0.57 ± 0.03^{b} (0.57 %)	3.20 ± 0.03^{b} (24.5 %)
S5	-1.62 ± 0.19^{c} (0.20 %)	3.22 ± 0.19^{b} (25.0 %)
S6	-2.14 ± 0.03^{c} (0.12 %)	2.50 ± 0.03^{c} (12.2 %)

S1, 5% w/w MFGM1, 20% w/w MCT; **S2**, 5% w/w MFGM1, 10% w/w MCT oil, 10% w/w fish oil; **S3**, 3% w/w MFGM2, 20% w/w MCT oil; **S4**, 3% w/w MFGM2, 10% w/w MCT oil, 10% w/w fish oil; **S5**, 3% w/w MFGM3, 20% w/w MCT oil; **S6**, 3% w/w MFGM3, 10% w/w MCT oil, 10% w/w fish oil. The values are shown as mean $\pm$ SD of $N \geq 3$. *Raw data were log transformed to obtain normality of variance for statistical analysis. The values showed in parentheses are the back transformation of log values back to its original scale to allow more meaningful and intuitive data interpretation in percentage. Samples in the same column with different superscript letters are significantly different ($p<0.05$).

Pancreatic enzymes and bile salts promoted interactions and rearrangements of the surface layer of oil droplets, leading to increase in particle size and digestion of phospholipids and fatty acids by lipolytic enzymes including lipase, phospholipase A2, and cholesterol esterase. Pancreatic lipase is known to catalyse the hydrolysis of sn1-fatty acids of phospholipids, releasing fatty acids and 1-acyl lyso-phospholipids (Haas et al., 1965). As the release of FFA increases, so will the bioaccessibility of the encapsulated bioactive through the solubilisation and formation of mixed micelles in the aqueous phase. However, in the present study, the release of FFA and bioaccessibility of curcumin did not follow the expected trend. The maximum release of FFA observed increased from S1<S3<S2<S5<S6<S4, while the bioaccessibility of curcumin increased from S6<S3<S4<S5<S2<S1 (12%, 25%, 24,5%, 15%, 43% and 47%) (Table 5.4). A significant interaction of oil and MFGM fraction was observed (Pr>F <0.0001), indicating that both oil composition and MFGM fraction had an effect on the differences in bioaccessibility.

While these findings were initially unexpected, they can be explained. It is expected that both the type and amount of lipid carrier and the nature of the emulsifier will impact the amount of curcumin that is released and solubilised in the micellar phase. Ahmed et al (2012) used oils ranging from short- to long-chain triglycerides and found varying bioaccessibilities from 1% to 58%. They attributed low bioaccessibility for SCT to the fact that short-chain fatty acids, such as those produced by digestion of SCT, do not form mixed micelles that are capable

of solubilising highly lipophilic components (Ahmed et al., 2012). The presence of micellar structures formed after lipid digestion by lipase and pancreatin are believed to accommodate curcumin within their core, consequently increasing curcumin's bioaccessibility. A previous study conducted to determine curcumin bioaccessibility found that curcumin solubilised in buffer presented 16% bioaccessibility against 72% of encapsulated curcumin after intestinal digestion (Aditya et al., 2015).

The relatively low bioaccesibility for emulsions with curcumin encapsulated using MFGM fractions can be related to the relatively low release of FFA. The highest release observed for FFA was 38%, suggesting that curcumin release would be as low or potentially lower. This was true for emulsions S3 to S6, for which observed values of bioaccessibility were <25%. However, S1 and S2 prepared using MFGM1 presented significantly higher bioaccessibility. Similar to the observations in samples after gastric digestion, the presence of a higher concentration of phospholipids can be associated with the formation of mixed micelles and complexing with curcumin molecules. However, the oil was not completely digested by pancreatic enzymes, as evidenced by an undigested oil layer observed after both gastric and intestinal simulated digestions (Figure 5.4).

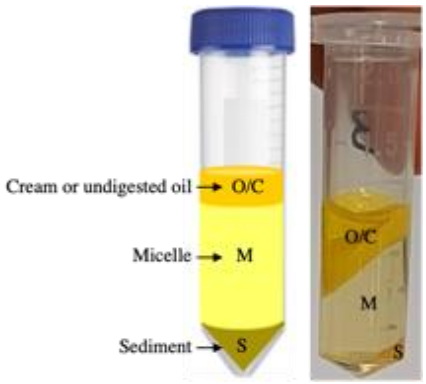

Figure 5.4. Representation of sample phase separation after high speed centrifugation (left) and an emulsion system centrifuged (15000g) after simulated *in vitro* gastric digestion.

There have been a number of studies designed to understand the behaviour of protein stabilised emulsion systems; however, little evidence is available on the understanding of phospholipid distribution after *in vitro* digestion. Therefore, the phospholipid distribution in fresh emulsions and their corresponding gastric digesta in cream and aqueous phases were assessed. The cream phase is accepted to be the phase where the oil droplets are covered by the MFGM fractions, and the proportions in which they were found are shown in Figure 5.5.

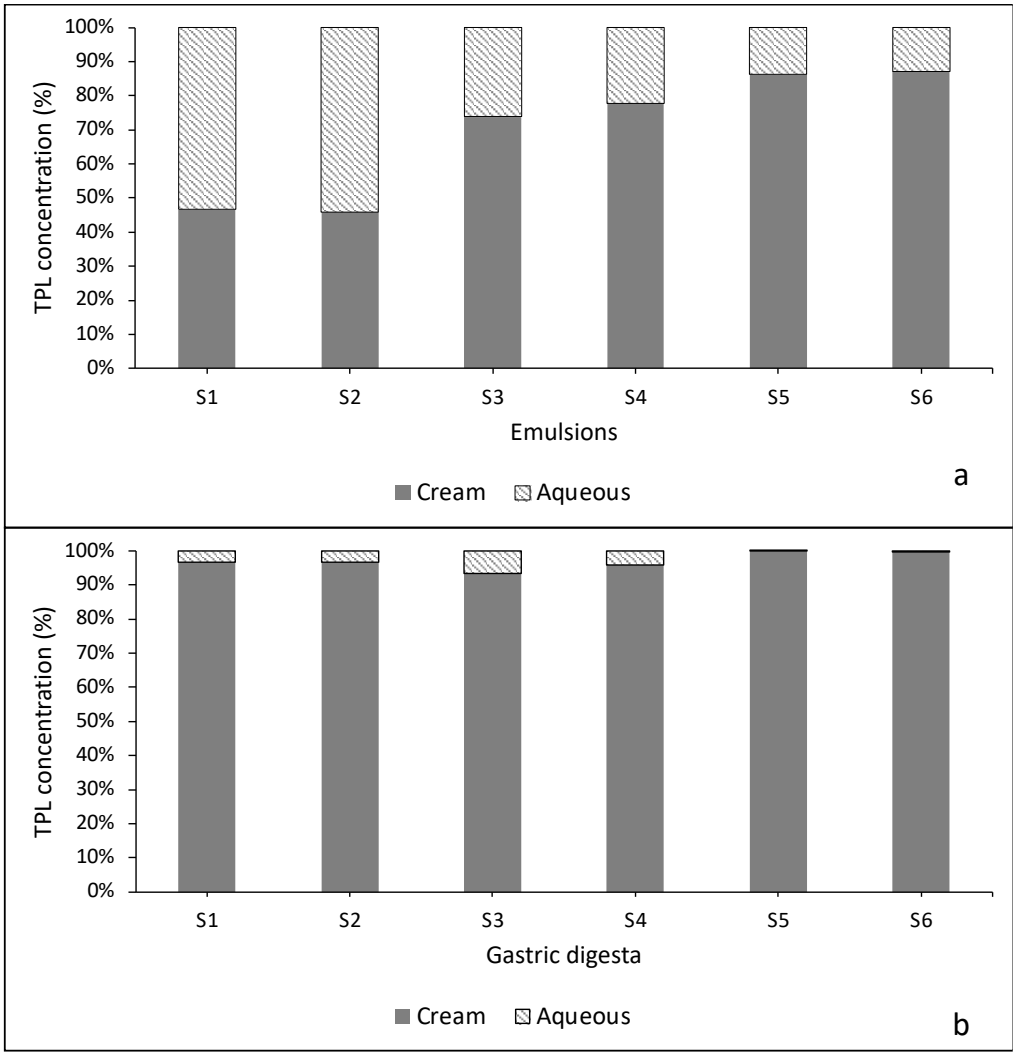

Figure 5.5 Phospholipid distribution in the cream and aqueous phase of emulsions (a) prepared using MFGM (**S1**, 5% w/w MFGM1, 20% w/w MCT oil; **S2**, 5% w/w MFGM1, 10% w/w MCT oil, 10% w/w fish oil; **S3**, 3% w/w MFGM2, 20% w/w MCT oil; **S4**, 3% w/w MFGM2, 10% w/w MCT oil, 10% w/w fish oil; **S5**, 3% w/w MFGM3, 20% w/w MCT oil; **S6**, 3% w/w MFGM3, 10% w/w MCT oil, 10% w/w fish oil) and their respective gastric digesta (b).

S1 and S2 were created using higher concentrations of MFGM1 compared to MFGM2 and MFGM3 for S3, S4, S5 and S6 (5% vs 3%). Although 54% of the total phospholipids were dispersed in the aqueous phase, a concentration of 5% was needed to enable the creation of more stable emulsions using this material. It is likely that less phospholipids were found in the cream phase due to excess MFGM1 added and the fact that this fraction had a much higher phospholipid concentrations than the other fractions. MFGM2 and MFGM3 emulsions had most of the phospholipids present in the cream phase, with only 24% and 13% present in the aqueous phase, respectively (Figure 5.5).

MFGM3 had the highest concentration of phospholipids in the cream phase in fresh emulsions (87%) and gastric digesta (99.8%). This suggests that when present in lower

concentrations, phospholipids adhered preferably to the cream phase. In addition, MFGM3 seemed to have better emulsifying ability, as the low curcumin bioaccessibility of emulsions prepared using MFGM3 after gastric indicate that those emulsions were more efficient in keeping curcumin encapsulated, with little being released to the micellar phase (Table 5.4). MFGM2 presented 76% of total phospholipids in the cream phase for fresh emulsions, and shifted to 95% in the aqueous phase, while MFGM1 shifted from only 46% to 97% in cream, reinforcing the effect of ionic strength in phosphate group of phospholipids. For all the fractions, the addition of simulated salivary and gastric fluids and changes in pH and ionic strength promoted the rearrangement of phospholipids from the aqueous phase to the cream layer. The change in low to high ionic strength is believed to be the main reason for the change in positioning of total phospholipids in the emulsions systems. Calcium ions in simulated fluids bind to phosphate groups and promote the creation of calcium salts. After intestinal digestion, no cream phase was observed, and only an oil layer was observed after centrifugation (Figure 5.4).

The MFGM's lateral phospholipid distribution with the coexistence of a liquid-ordered phase rich in sphingomyelin and cholesterol, and a liquid-disordered phase rich in unsaturated phospholipids, is believed to play a role in the digestion of fat globules in milk. The MFGM exerts an inhibitory effect on hydrolytic action of pancreatic lipase, indicating that incubation with gastric lipase prior would facilitate this process (Gallier et al., 2012, Bauer et al., 2005). In this study, only pancreatic lipase was added and minor changes were observed in the phospholipid composition after simulated gastric digestion, compared to intestinal simulation, where the formation of lyso-phospholipids were observed. Lyso-phospholipids are the product of phospholipid hydrolysis and consist of soluble amphiphiles that will be incorporated onto mixed micelles. Phospholipids are known to enhance the ability of bile salts to form mixed micelles, which are required to promote the passage of non-polar lipids across the unstirred water layer adjacent to the mucosal cells, thereby facilitating absorption (Bauer et al., 2005). Micelle formation occurs when amphiphilic molecules, such as surfactants or lipids, arrange themselves in a specific manner to minimize their exposure to the surrounding solvent. Micelles are formed by the aggregation of these molecules, with their hydrophobic tails facing inward and their hydrophilic heads facing outward towards the solvent. Sphingomyelin possesses both hydrophilic and hydrophobic regions. It has a hydrophilic phosphorylcholine headgroup and a hydrophobic ceramide tail. However, due to the relatively larger size and

complex structure of sphingomyelin compared to typical surfactants or phospholipids, its self-assembly into micelles is less common.

Despite significant differences in the absolute concentrations of phospholipid groups between each individual emulsion and its subsequent gastric digesta due to dilution (Figure 5.6), the relative distributions of the PL were similar for each pairing as shown in Figure 5.7, with minor variations between those two phases being attributed to potential heterogeneous sample collection. All emulsions showed similar behaviour after intestinal digestion, with an observed proportional reduction in PE, PC and PS while SM and PI concentrations were retained at levels similar to fresh emulsions and gastric digesta. At the same time, an increase in LPE and LPC proportions can be observed in the intestinal digesta fraction (Figure 5.6). The poor digestibility in *in vitro* conditions could be due to lack of specific enzymes to cleave SM; however, an *in vivo* study found intact SM in faeces of rats. The authors observed that after administration of 6.6 or 32 μmol SM, significant amounts of intact SM and ceramide were found in intestinal contents, colon, and excreted faeces. In the intestine, SM undergoes cleavage to ceramide and sphingosine through action of sphingomyelinase (Nyberg et al., 1997). The findings above suggest that it is more difficult for enzymes to digest SM than PC *in vivo*. Additionally, the complexation of sphingomyelin and phosphatidylcholine with curcumin in the emulsions in the aqueous and cream phase could be an indication of increase bioaccessibility, potentially leading to higher absorption and bioavailability.

The decrease in concentrations of PE and PC and increase of the LPE and LPC (enzymatic breakdown materials) from fresh emulsions and gastric digesta to intestinal digesta reflect the interaction of bile salts with the components of emulsions in SIF and subsequent hydrolysis of phospholipids promoted by pancreatic enzymes, including phospholipase A2. Pancreatin from porcine pancreas contains lipolytic enzymes, including lipase, phospholipase A2, and cholesterol esterase. Pancreatic lipase has been found to catalyse the hydrolysis of sn1-fatty acids of phospholipids, releasing fatty acids and 1-acyl lyso-phospholipids (Haas et al., 1965). In addition, phospholipase A2 in the pancreatic extracts catalyses the sn-2 ester bond hydrolysis of phospholipids to glycerophosphoric acids and 2-acyl lyso-phospholipids. Moreover, cholesterol esterase promotes the hydrolysis of phospholipids (Howles et al., 1996). It was therefore assumed that phospholipids were either digested and solubilised in the micellar phase or have been not being digested and moved to the pellet after centrifugation rather than

to the cream phase. The oil layer present after intestinal digestion also suggests that the oil has been only partially digested by pancreatin and therefore the release of FFA was low.

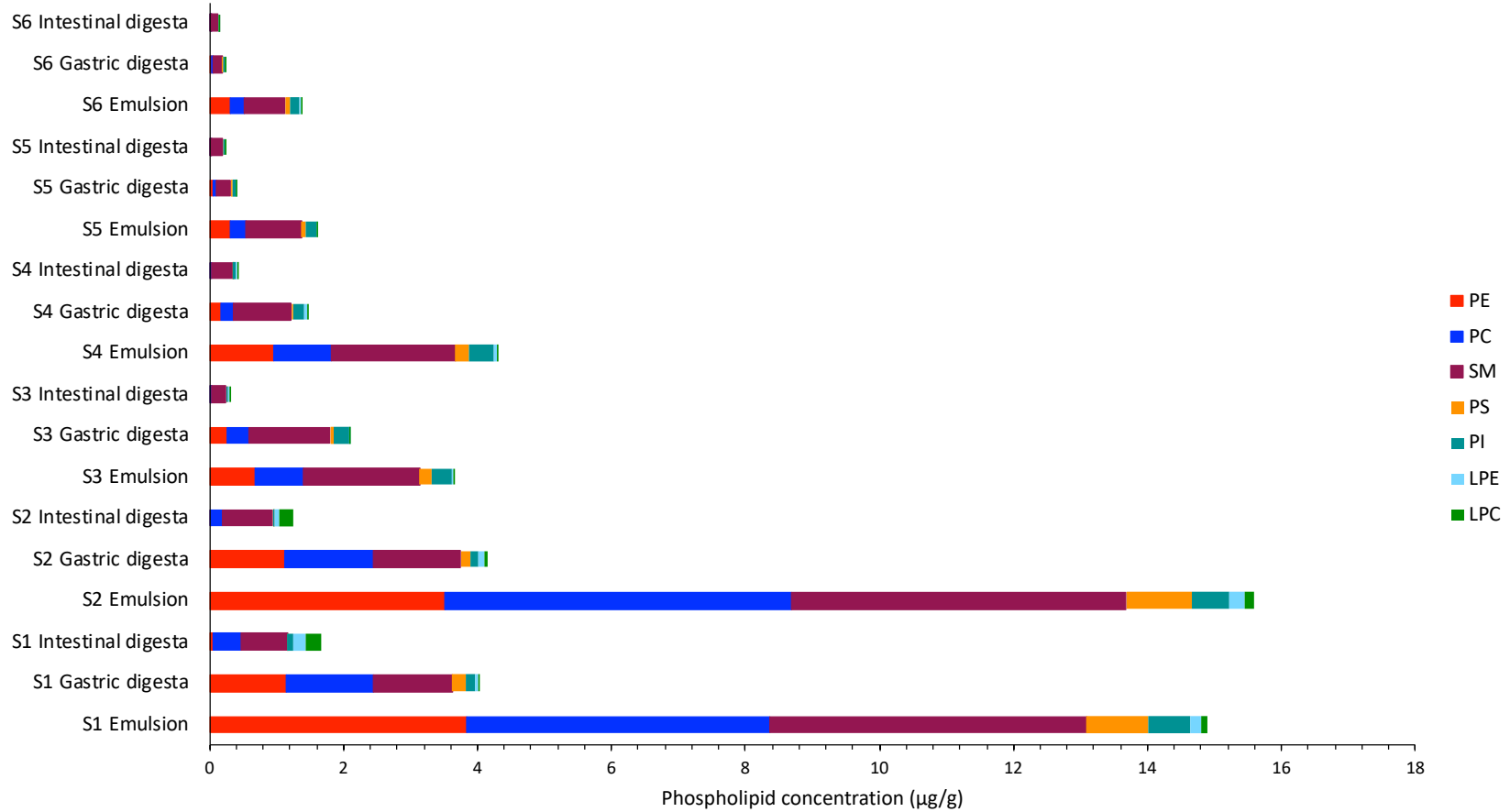

Figure 5.6. Phospholipid concentration and absolute class distribution in emulsion systems prepared using MFGM fractions and their respective gastric and intestinal digesta. **S1**, 5% w/w MFGM1, 20% w/w coconut oil; **S2**, 5% w/w MFGM1, 10% w/w coconut oil, 10% w/w fish oil; **S3**, 3% w/w MFGM2, 20% w/w coconut oil; **S4**, 3% w/w MFGM2, 10% w/w coconut oil, 10% w/w fish oil; **S5**, 3% w/w MFGM3, 20% w/w coconut oil; **S6**, 3% w/w MFGM3, 10% w/w coconut oil, 10% w/w fish oil). PE=Phosphatidylethanolamine, PC=Phosphatidylcholine, SM=Sphingomyelin, PS=Phosphatidylserine, PI=phosphatidylinositol, LPE=Lyso-phosphatidylethanolamine, LPC=Lyso-phosphatidylcholine.

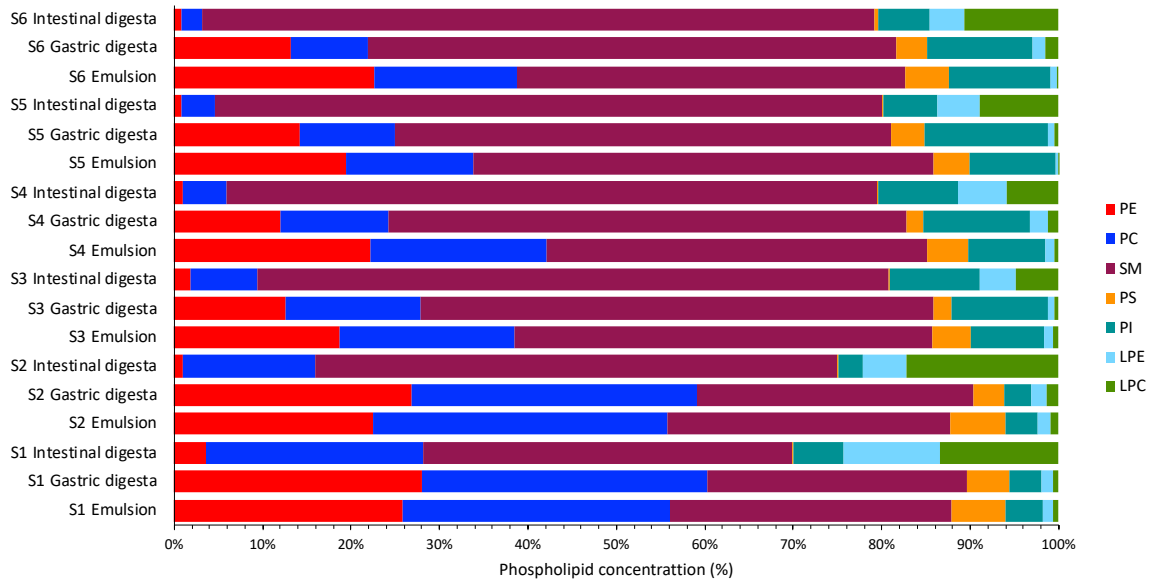

Figure 5.7. Relative phospholipid class distribution in emulsion systems prepared using MFGM fractions and their respective gastric and intestinal digesta. **S1**, 5% w/w MFGM1, 20% w/w coconut oil; **S2**, 5% w/w MFGM1, 10% w/w coconut oil, 10% w/w fish oil; **S3**, 3% w/w MFGM2, 20% w/w coconut oil; **S4**, 3% w/w MFGM2, 10% w/w coconut oil, 10% w/w fish oil; **S5**, 3% w/w MFGM3, 20% w/w coconut oil; **S6**, 3% w/w MFGM3, 10% w/w coconut oil, 10% w/w fish oil). PE=Phosphatidylethanolamine, PC=Phosphatidylcholine, SM=Sphingomyelin, PS=Phosphatidylserine, PI=phosphatidylinositol, LPE=Lyso-phosphatidylethanolamine, LPC=Lyso-phosphatidylcholine.

Details on the distribution of individual phospholipid groups can be found in Table 5.5. To the best of our knowledge the identification of phospholipids in cream and aqueous phases of emulsions and their correspondent digested materials has not been reported elsewhere, and therefore these findings provided new insights on the behaviour of phospholipids as emulsifiers. To obtain an accurate reading of phospholipids, an homogeneous sample is ideal. When working with phospholipid extraction from emulsions, especially the cream phase, such homogeneity can be a challenge.

Ideally, the sum of cream and aqueous fraction should equal the phospholipid in the emulsion, which was not observed for all groups and samples in our study. For instance, while PE concentration in S5 fresh emulsion (0.31 μg/g) is the exact sum of its cream (0.26 μg/g) and aqueous (0.05 μg/g) phases, PE after gastric digestion observed in only cream phase (0.47μg/g) is significantly higher than PE found in the whole gastric digesta for S5 (0.06 μg/g) even after accounting for dilution factors. This difference can be observed for other individual phospholipid classes reflecting in the total phospholipid composition. To the best of our knowledge, the discrepancies between phases can be explained by the difficulty in obtaining homogeneous samples and efficiently extracting phospholipid groups from oily sources. In

addition, the presence of simulated fluids and salts might have interfered with the extraction protocol. We therefore, suggest that additional tests should be performed to standardize this method for emulsions' cream and aqueous extraction and confidently express individual and total phospholipids between phases of both fresh and digested emulsions.

Nevertheless, a three-way ANOVA was conducted to determine the effect of oil, emulsifier and digestion on the phospholipid concentrations in emulsions and their correspondent aqueous and cream phase. Statistical findings on the effects of individual factors and their interactions have been summarize in Table 5.6. Overall, for the majority of phospholipids groups the digestion step, the emulsifier, and their interaction promoted significant differences among samples, with MFGM1 emulsions having higher phospholipids, followed by MFGM2 and MFGM3. While type of oil seemed to present less effect on the differences observed between phospholipid class distribution, both type of MFGM fraction and digestion treatment had marked effects on those changes (Table 5.6). The differences in MFGM fraction's initial concentrations might have influenced the effect of digestion, with MFGM1 requiring a higher amount of pancreatic enzymes to promote its breakdown when compared to MFGM2 and MFGM3, which had less initial phospholipids. The headgroups in different phospholipid classes might also have influenced the extend of enzymatic action as enzymes will present different affinity for different phospholipid groups.

Taken together the results for individual phospholipid groups support the findings described above (Figure 5.5) for total phospholipid distributions in the cream and aqueous phase of emulsions, with MFGM3 presenting the highest concentration of phospholipids in the cream phase for both fresh emulsions and gastric digesta, followed by MFGM2 and MFGM1. However, MFGM1 was the fraction that had the highest concentration for all classes after simulated intestinal digestion, as it was expected due to its higher initial phospholipid composition.

Table 5.5. Phospholipid distribution in emulsions prepared using MFGM and their correspondent cream and aqueous phase and gastric and intestinal digesta.

	Corrected µg/mg (mg/g)							
	PE	**PC**	**SM**	**PS**	**PI**	**LPE**	**LPC**	**TPL**
S1 Emulsion	3.84 ± 0.08	4.52 ± 0.07	4.73 ± 0.07	0.91 ± 0.06	0.63 ± 0.09	0.17 ± 0.00	0.09 ± 0.00	14.9 ± 0.19
S1 Cream	1.33 ± 0.03	1.69 ± 0.02	1.86 ± 0.03	0.43 ± 0.03	0.34 ± 0.05	0.07 ± 0.00	0.03 ± 0.00	5.65 ± 0.07
S1 Aqueous	1.81 ± 0.04	1.94 ± 0.03	2.04 ± 0.03	0.33 ± 0.02	0.18 ± 0.03	0.05 ± 0.00	0.03 ± 0.00	6.46 ± 0.08
S1 Gastric digesta	1.13 ± 0.03	1.30 ± 0.05	1.19 ± 0.02	0.19 ± 0.01	0.15 ± 0.02	0.05 ± 0.00	0.03 ± 0.00	4.04 ± 0.04
S1 GD Cream	1.26 ± 0.03	1.55 ± 0.06	1.19 ± 0.02	0.20 ± 0.01	0.17 ± 0.03	0.06 ± 0.00	0.03 ± 0.00	4.45 ± 0.05
S1 GD Aqueous	0.04 ± 0.00	0.05 ± 0.00	0.05 ± 0.00	0.01 ± 0.00	0.01 ± 0.00	ND	ND	0.16 ± 0.00
S1 Intestinal digesta	0.06 ± 0.01	0.41 ± 0.09	0.69 ± 0.15	ND	0.09 ± 0.03	0.18 ± 0.04	0.22 ± 0.05	1.66 ± 0.34
S1 Micelle	0.06 ± 0.02	0.48 ± 0.16	0.82 ± 0.25	ND	0.07 ± 0.02	0.22 ± 0.07	0.22 ± 0.06	1.86 ± 0.58
S2 Emulsion	3.50 ± 0.15	5.19 ± 0.47	4.99 ± 0.07	0.98 ± 0.08	0.57 ± 0.09	0.23 ± 0.02	0.14 ± 0.02	15.6 ± 0.72
S2 Cream	2.40 ± 0.06	2.58 ± 0.16	2.32 ± 0.28	0.27 ± 0.04	0.15 ± 0.02	0.09 ± 0.01	0.06 ± 0.00	7.90 ± 0.45
S2 Aqueous	2.40 ± 0.05	2.98 ± 0.18	3.13 ± 0.06	0.39 ± 0.02	0.25 ± 0.02	0.05 ± 0.00	0.09 ± 0.01	9.31 ± 0.29
S2 Gastric digesta	1.11 ± 0.03	1.34 ± 0.03	1.30 ± 0.04	0.14 ± 0.01	0.13 ± 0.01	0.07 ± 0.02	0.06 ± 0.00	4.15 ± 0.12
S2 GD Cream	1.24 ± 0.21	1.60 ± 0.09	1.30 ± 0.06	0.15 ± 0.02	0.15 ± 0.02	0.08 ± 0.02	0.06 ± 0.00	4.57 ± 0.29
S2GD Aqueous	0.04 ± 0.01	0.05 ± 0.01	0.05 ± 0.01	0.01 ± 0.00	0.01 ± 0.00	ND	ND	0.16 ± 0.04
S2 Intestinal digesta	0.01 ± 0.00	0.19 ± 0.01	0.74 ± 0.03	ND	0.03 ± 0.00	0.06 ± 0.00	0.22 ± 0.01	1.26 ± 0.04
S2 Micelle	0.02 ± 0.00	0.30 ± 0.04	1.12 ± 0.21	ND	0.06 ± 0.01	0.11 ± 0.02	0.36 ± 0.06	1.96 ± 0.33
S3 Emulsion	0.68 ± 0.16	0.73 ± 0.15	1.73 ± 0.94	0.17 ± 0.06	0.30 ± 0.13	0.04 ± 0.02	0.02 ± 0.02	3.67 ± 1.22
S3 Cream	0.40 ± 0.04	0.50 ± 0.04	1.65 ± 0.46	0.08 ± 0.02	0.32 ± 0.06	0.04 ± 0.01	0.03 ± 0.01	3.35 ± 0.31
S3 Aqueous	0.08 ± 0.01	0.12 ± 0.01	0.68 ± 0.19	0.02 ± 0.00	0.11 ± 0.02	0.01 ± 0.00	-	1.19 ± 0.11
S3 Gastric digesta	0.27 ± 0.01	0.32 ± 0.01	1.22 ± 0.03	0.04 ± 0.00	0.23 ± 0.01	0.02 ± 0.00	0.01 ± 0.00	2.10 ± 0.05
S3 GD Cream	0.62 ± 0.02	0.74 ±0.05	3.4 ± 0.24	0.11 ± 0.02	0.74 ± 0.08	0.08 ± 0.01	0.03 ± 0.01	5.71 ± 0.36
S3 GD Aqueous	0.04 ± 0.00	0.05 ± 0.00	0.21 ± 0.03	0.01 ± 0.00	0.08 ± 0.01	0.01 ± 0.00	-	0.40 ± 0.04
S3 Intestinal digesta	0.01 ± 0.00	0.02 ± 0.00	0.22 ± 0.04	-	0.03 ± 0.01	0.01 ± 0.00	0.01 ± 0.00	0.30 ± 0.06
S3 Micelle	-	0.02 ± 0.01	0.49 ± 0.14	-	0.09 ± 0.03	0.03 ± 0.01	0.04 ± 0.01	0.68 ± 0.19

Table 5.5 (continued)

S4 Emulsion	0.95 ± 0.06	0.86 ± 0.08	1.86 ± 0.72	0.20 ± 0.04	0.38 ± 0.12	0.04 ± 0.01	0.02 ± 0.01	4.31 ± 0.76
S4 Cream	0.50 ± 0.01	0.53 ± 0.03	1.35 ± 0.39	0.16 ± 0.02	0.37 ± 0.08	0.03 ± 0.00	0.02 ± 0.01	3.18 ± 0.35
S4 Aqueous	0.13 ± 0.03	0.14 ± 0.01	0.43 ± 0.12	0.02 ± 0.00	0.08 ± 0.02	0.02 ± 0.00	0.01 ± 0.00	0.91 ± 0.11
S4 Gastric digesta	0.18 ± 0.12	0.18 ± 0.08	0.86 ± 0.33	0.03 ± 0.02	0.18 ± 0.08	0.03 ± 0.01	0.02 ± 0.01	1.47 ± 0.63
S4 GD Cream	0.60 ± 0.06	0.71 ± 0.05	3.15 ± 0.29	0.17 ± 0.06	0.87 ± 0.10	0.09 ± 0.03	0.06 ± 0.02	5.66 ± 0.42
S4 GD Aqueous	0.03 ± 0.01	0.03 ± 0.00	0.14 ± 0.00	0.01 ± 0.00	0.03 ± 0.00	-	-	0.24 ± 0.01
S4 Intestinal digesta	-	0.02 ± 0.00	0.32 ± 0.02	-	0.04 ± 0.00	0.02 ± 0.00	0.03 ± 0.00	0.44 ± 0.03
S4 Micelle	-	0.01 ± 0.00	0.34 ± 0.04	-	0.05 ± 0.00	0.02 ± 0.00	0.03 ± 0.00	0.46 ± 0.05
S5 Emulsion	0.31 ± 0.05	0.23 ± 0.04	0.83 ± 0.30	0.07 ± 0.01	0.15 ± 0.04	-	-	1.60 ± 0.29
S5 Cream	0.26 ± 0.01	0.19 ± 0.01	1.21 ± 0.28	0.05 ± 0.01	0.19 ± 0.03	0.02 ± 0.00	0.01 ± 0.01	1.94 ± 0.21
S5 Aqueous	0.05 ± 0.01	0.03 ± 0.01	0.18 ± 0.09	0.01 ± 0.00	0.02 ± 0.01	-	-	0.31 ± 0.12
S5 Gastric digesta	0.06 ± 0.00	0.04 ± 0.00	0.22 ± 0.01	0.02 ± 0.00	0.06 ± 0.00	-	-	0.40 ± 0.02
S5 GD Cream	0.47 ± 0.01	0.43 ± 0.02	1.94 ± 0.09	0.15 ± 0.01	0.40 ± 0.03	0.02 ± 0.00	0.01 ± 0.00	3.41 ± 0.16
S5 GD Aqueous	-	-	-	-	-	-	-	-
S5 Intestinal digesta	-	0.01 ± 0.00	0.19 ± 0.01	-	0.02 ± 0.00	0.01 ± 0.00	0.02 ± 0.00	0.26 ± 0.02
S5 Micelle	-	-	0.02 ± 0.00	-	-	-	-	0.03 ± 0.00
S6 Emulsion	0.31 ± 0.03	0.22 ± 0.02	0.60 ± 0.23	0.07 ± 0.02	0.16 ± 0.06	0.01 ± 0.00	-	1.37 ± 0.24
S6 Cream	0.26 ± 0.01	0.21 ± 0.01	0.75 ± 0.21	0.06 ± 0.01	0.21 ± 0.05	0.01 ± 0.00	0.01 ± 0.00	1.64 ± 0.16
S6 Aqueous	0.04 ± 0.00	0.04 ± 0.00	0.11 ± 0.03	0.01 ± 0.00	0.03 ± 0.01	-	-	0.24 ± 0.03
S6 Gastric digesta	0.03 ± 0.00	0.02 ± 0.00	0.14 ± 0.01	0.01 ± 0.00	0.03 ± 0.00	-	-	0.23 ± 0.02
S6 GD Cream	0.52 ± 0.08	0.48 ± 0.09	2.40 ± 0.44	0.19 ± 0.05	0.57 ± 0.07	0.03 ± 0.01	0.02 ± 0.00	4.21 ± 0.74
S6 GD Aqueous	-	-	0.01 ± 0.00	-	-	-	-	0.01 ± 0.00
S6 Intestinal digesta	-	-	0.12 ± 0.01	-	0.01 ± 0.00	0.01 ± 0.00	0.02 ± 0.00	0.16 ± 0.02
S6 Micelle	-	-	0.03 ± 0.00	-	-	-	-	0.04 ± 0.00

S1, 5% w/w MFGM1, 20% w/w coconut oil; **S2**, 5% w/w MFGM1, 10% w/w coconut oil, 10% w/w fish oil; **S3**, 3% w/w MFGM2, 20% w/w coconut oil; **S4**, 3% w/w MFGM2, 10% w/w coconut oil, 10% w/w fish oil; **S5**, 3% w/w MFGM3, 20% w/w coconut oil; **S6**, 3% w/w MFGM3, 10% w/w coconut oil, 10% w/w fish oil. PE=Phosphatidylethanolamine, PC=Phosphatidylcholine, SM=Sphingomyelin, PS=Phosphatidylserine, PI=phosphatidylinositol, LPE=Lyso-Phosphatidylethanolamine, LPC=Lyso-Phosphatidylcholine

Table 5.6. Statistical findings based on 3-wayANOVA on the effects of MFGM fraction, oil type and digestion on the distribution of individual phospholipid groups across emulsions and their corresponded cream phase

	Pr > F						
	Fresh emulsions						
	PE	**PC**	**SM**	**PS**	**PI**	**LPE**	**LPC**
Digestion	<.0001	<.0001	<.0001	<.0001	0.0001	0.0003	<.0001
MFGM	<.0001	<.0001	<.0001	<.0001	<.0001	<.0001	<.0001
Digestion*MFGM	<.0001	0.0002	<.0001	<.0001	0.0105	0.0044	<.0001
Oil	0.3829	0.4491	0.9479	0.829	0.5763	0.7958	0.0042
Digestion*Oil	0.8079	0.2219	0.6255	0.0791	0.8152	0.0162	0.2098
MFGM*Oil	0.1322	0.6106	0.1986	0.9331	0.7061	0.2876	0.9657
Digestion*MFGM*Oil	0.2748	0.1928	0.7095	0.143	0.591	0.0933	0.0638
	Cream phase						
	PE	**PC**	**SM**	**PS**	**PI**	**LPE**	**LPC**
Digestion	0.1193	0.3718	0.0002	0.4137	<.0001	0.0391	0.0614
MFGM	<.0001	<.0001	0.0025	<.0001	<.0001	0.0001	<.0001
Digestion*MFGM	0.0006	<.0001	<.0001	<.0001	<.0001	0.079	0.0727
Oil	0.0034	0.0007	0.9839	0.8481	0.4549	0.2227	0.0034
Digestion*Oil	0.0037	0.0021	0.5336	0.2101	0.0546	0.2701	0.0508
MFGM*Oil	0.0111	0.0016	0.2975	0.0024	0.0025	0.4538	0.0005
Digestion*MFGM*Oil	0.0061	0.0027	0.1581	0.409	0.9027	0.9707	0.1954

S1, 5% w/w MFGM1, 20% w/w coconut oil; **S2**, 5% w/w MFGM1, 10% w/w coconut oil, 10% w/w fish oil; **S3**, 3% w/w MFGM2, 20% w/w coconut oil; **S4**, 3% w/w MFGM2, 10% w/w coconut oil, 10% w/w fish oil; **S5**, 3% w/w MFGM3, 20% w/w coconut oil; **S6**, 3% w/w MFGM3, 10% w/w coconut oil, 10% w/w fish oil. PE=Phosphatidylethanolamine, PC=Phosphatidylcholine, SM=Sphingomyelin, PS=Phosphatidylserine, PI=phosphatidylinositol, LPE=Lyso-phosphatidylethanolamine, LPC=Lyso-phosphatidylcholine

5.5 Conclusions

Emulsion systems stabilised by MFGM-derived materials were resistant to pepsin digestion in the simulated stomach phase, yet pancreatin and bile salts promoted destabilisation of the system with release of curcumin and formation of mixed micelles to some extent under intestinal conditions. Changes in ionic strength and pH promoted flocculation of oil droplets in the gastric phase and migration of phospholipids to the cream layer. The encapsulation of curcumin inside MCT and fish oil droplets increased curcumin bioacessibility (S1>S2>S5>S4>S3>S6) when compared to free curcumin. Enhancing absorption and delivery of lipophilic curcumin is the main goal of this study; therefore, the use of MFGM fractions was intended to protect emulsions throughout gastrointestinal digestion. Protection against

enzymatic breakdown and lipid digestion can increase curcumin bioavailability. One valuable observation was the retention of intact, measurable SM throughout the digestive process. This finding suggests that maximising inclusion of SM in emulsion designs could optimise protection and bioaccessibility of curcumin by ensuring its complexation both in aqueous and cream phases. In this study, the low bioaccessibility was related to incomplete digestion of fatty acids, suggesting that the systems were relative resistant to *in vitro* digestion. MFGM1 emulsified systems had the highest bioaccessibility, despite having lowest release of FFA, which can be related to the complexation of curcumin and phospholipid groups, especially PC and the poor digestibility of phospholipid groups, such as SM. This system showed promising outcomes for their use in the development of more complex functional foods, such as a functional beverage or yogurt. Further research is warranted to design *in vitro* experiments with more specific enzymes, shear patterns, oral surfaces and time in mouth cavity, in order to understand the behaviour of different types of emulsions with more precision. Understanding the *in vivo* behaviour of the emulsions systems prepared in this study is key for the development of more complex food structures incorporating these systems. Emulsions prepared using MFGM1 were selected for further investigation and fed to rats for assessment or oral delivery of curcumin to the blood and brain.

Chapter 6 - *In vivo* delivery of curcumin and its metabolites to the brain and plasma of male and female Sprague-Dawley rats

Abstract

In this study a milk fat globule membrane (MFGM)-derived material rich in phospholipids was selected as an emulsifier to create an emulsion delivery system for encapsulation of curcumin. In addition to curcumin as a nutraceutical and MFGM as a novel health-promoting functional material, medium chain triglycerides (MCT) and omega-3(ω-3) polyunsaturated fatty acids (PUFA) were selected based on previously reported benefits against Alzheimer's disease (AD) biomarkers. A rat model was chosen to assess the delivery of curcumin, curcumin glucuronide (CG) and curcumin sulfate (CS) into blood and brain from 4 different formulations: free curcumin (free Curc), a commercial formulation (Meriva®), emulsion 1 and emulsion 2.

The kinetics for the appearance of curcumin and its metabolites in the plasma differed depending on the format in which it was administered. For free Curc, the accumulation of curcumin and its metabolites occurred slowly, with minimal amounts present at 15 to 30 minutes, then rising thereafter. Curcumin and its metabolites from Meriva® were present in significantly higher concentrations at 15 to 30 minutes, suggesting improved bioavailability and absorption. However, the levels changed little between 15 minutes and 60 minutes; as with free Curc, only during the second hour did Meriva® curcumin and its metabolites accumulate in the plasma in significantly higher concentrations. In contrast, curcumin and its metabolites from the emulsions peaked in plasma immediately and were present at significantly higher concentrations than free Curc or Meriva® treatments at 15 and 30 minutes. Moreover, these levels remained high, except for EM2 at 120 minutes, with no significant differences between the time points for either emulsion. Overall, the emulsions and Meriva® improved bioavailability and absorption of the delivered curcumin compared to free Curc, with the emulsions resulting in significantly more curcumin and its metabolites in the plasma than Meriva® over the first hour post-ingestion. Accumulation of curcumin in the brain occurred rapidly, peaking at 30 to 60 minutes for all treatment groups except for Meriva®, which showed a higher peak occurring at 120 minutes, suggesting that curcumin delivery by Meriva® may be superior in improving curcumin accumulation in the brain.

6.1 Introduction

Naturally occurring curcumin presents very low bioavailability and poor delivery to the desired site of action in the body. The protection of curcumin molecules through encapsulation has been studied and tested over the last several years to improve its health-promoting properties (Aditya et al., 2015, Cheng et al., 2017, Huo et al., 2019, Ibrahim et al., 2018, Li et al., 2015b, Lin et al., 2009, Peng et al., 2018, Sorasitthiyanukarn et al., 2018, Tang et al., 2019). Curcumin formulations currently being tested in clinical trials for Alzheimer's disease (AD) are primarily administered as supplements (capsules) rather than in a food format. This can be problematic since many AD patients are elderly and suffer from dysphagia, making swallowing tablets difficult (Takizawa et al., 2016, Seçil et al., 2016). Among those formulations, Meriva® has shown positive outcomes in animal trials and is also being tested in clinical trials for AD. Meriva® consists of a standardised mixture of natural curcuminoids and lecithin in a 1:2 ratio, with two parts of microcrystalline cellulose added to improve the physical state (Cuomo et al., 2011).

Polar lipids (glycerophospholipids and sphingolipids) are essential cell membrane constituents and play a key role in apoptosis and cell signalling. In addition, sphingolipids have been defined as a network of bioactive lipids (Coant et al., 2017). The biosynthesis, chemical structure and function of sphingolipids and glycerophospholipids, such as phosphatidylethanolamine (PE), phosphatidylserine (PS), phosphatidylcholine (PC) and phosphatidylinositol (PI) have been described by Castro-Gomez et al., (2015). Among those functions, the role of PC and PS in brain development and improvements in cognition are highlighted, suggesting their use as a nutraceutical to improve memory (Castro-Gómez et al., 2015). Sphingomyelin plays a crucial role in the central nervous system, as its degradation by sphingomyelinases results in the formation of bioactive signalling ceramide molecules that can cross the blood-brain barrier (Echten-Deckert and Alam, 2018). Thus, there is interest in including bioactive lipids in functional foods designed for people with neurological disorders such as AD. Souvenaid® is an example, sold as a beverage containing a combination of nutraceuticals including ω-3 polyunsaturated fatty acids (DHA and EPA), uridine, choline, phospholipids and other cofactors. This is believed to be the first medical nutrition product, and it has been designed to support synapse formation and function in early AD. Souvenaid® has demonstrated cognitive benefits in patients with mild AD. It was well tolerated and improved episodic memory performance in two randomised, double-blind, controlled trials (12 and 24 weeks) in patients with mild AD (Scheltens et al., 2012). However, this product does

not contain curcumin. Thus, there is an obvious gap in the market: a formulated food that contains both curcumin and bioactive lipids.

Studies on curcumin delivery have used a wide variety of curcumin concentrations, curcumin formats and modes of administration (Table 6.1). The use of high curcumin doses is often recommended but the results show that even at very high doses, concentrations are still low in plasma (Vareed et al., 2008), due to both low bioavailability and rapid metabolism. In addition, some studies have tested low doses of curcumin without presenting delivery data but have reported improvements in tested biomarkers for a condition (Antiga et al., 2015). Even though considerable data prove the benefits of curcumin for cognition in *in vitro* and animal models, these benefits are rarely reflected in conclusive human studies. The most commonly-used justification for the remaining gap in human confirmation of curcumin benefits is the need for more extended prospective studies. The organoleptic traits are also quite relevant in a human trial, and dropouts are usually due to feeling unwell or unpleasantness of ingestion of high doses.

Finally, it is worth noting that most of the published animal trials (Table 6.1) have been conducted in male rats or mice, despite AD occurring in human females at greater than twice the prevalence of males. Sex-related differences in pharmacokinetics have frequently been considered potentially important determinants for the clinical effectiveness of drug therapy. Those differences have also been observed for curcuminoids, with a study showing variations in oral bioavailability between sexes. The authors observed a two-fold greater area under the plasma concentration-time curve for women compared to men. This variation can be attributed to differences in the hepatic drug efflux transporter P-glycoprotein, which is more active in men (Gleiter and Gundert-Remy, 1996, Briskey et al., 2019).

Prevention and delayed onset are still the best approaches against dementia and AD since there is no cure yet. Therefore, more functional science-based food products would be beneficial for the prevention of AD and dementia. In this study, I created a food-based delivery system containing curcumin incorporated in a stable lipid emulsion to improve bioavailability, plus additional components that may have protective effects against AD such as functional oils and milk fat globule membrane (MFGM) phospholipids. The dosage of curcumin incorporated was determined by the maximum amount supported by the emulsion systems. In addition to the encapsulation limit, an extrapolated dose based on body weight that would be realistic for humans to consume daily over the long term was proposed. Based on results from previous chapters, I observed that all three MFGM fractions tested were effective in creating stable

emulsion systems, with MFGM1 presenting the highest bioaccessibility for both oil combinations. I therefore hypothesised that a MFGM1-based emulsion would result in the highest curcumin bioavailability and subsequent circulating plasma levels.

Although the oil type seemed to have less impact on the structure of emulsion systems digested *in vitro*, the well-established effect of ω-3 PUFA on brain health and cell plasticity justified the selection of the two oil combinations for curcumin delivery study *in vivo*. A comprehensive assessment of previously published human and animal trials was undertaken to assess the range of curcumin doses used and the resultant circulating plasma levels, as shown in Table 6.1. Therefore, in this chapter, the oral delivery of curcumin at a low dose (20 mg/kg body weight) and subsequent digestion and transfer of curcumin to the plasma and brain of Sprague-Dawley rats was tested to provide a proof of concept to support the use of lower and more sustainable dose administration of encapsulated curcumin delivered orally. Matching studies were conducted on female and male rats to determine whether sex-dependent differences occurred. A commercially available formulation, Meriva®, was used as a positive control, and the free curcumin powder used to prepare the emulsion systems used as a negative control to compare with emulsion systems using the MFGM fraction rich in phospholipid.

Table 6.1. Pre-clinical and clinical studies using various formats, doses and administration routes for curcumin

Author/year	Type	Target	Dose/Duration	Format	Way of administration
Garcea et al., 2004	Human (4 female and 8 male)	Normal and malignant human liver tissue	450, 1800 or 3600 mg, for 1 week	Purified turmeric extract formulated in capsules	Oral
Marczylo et al., 2007	Male Wistar albino rats	Concentration in plasma, intestinal mucosa and liver	340mg/kg once	Unformulated curcumin and Meriva	Oral gavage
Vareed et al., 2008	Human (5 males and 7 females)	Concentration in plasma	10 g or 12 g after a high-fat breakfast (42% fat) once	Curcumin capsules	Oral
Antiga et al., 2015	Human (32 males and 31 females)	Patients with psoriasis	2g (400mg curcumin) 2x a day for 12 weeks	Meriva	Oral
Mahale et al., 2018	C57 BL/6 J male mice	Concentration in plasma and lung tissue from mice	70mg/kg once	Meriva and unformulated	Oral gavage
Shoba et al., 1998	Wistar rats of both sexes (n for gender not specified)	Bioavailability in rats and in healthy volunteers	2g/kg + 200mg piperine once	Curcumin alone and in combination with piperine	Oral
Yang et al., 2007	Male Sprague-Dawley rats	Bioavailability in rats	500 mg/kg and 10 mg/kg once	Curcuminoid mixture and herbal preparation	Orally and intravenously injection
Sankar et al., 2016	Male Wistar rats	Sodium arsenite-induced renal and neuronal oxidative damage	100mg/kg and 100mg/Kg CUR-NP for 14 days	Free Curcumin and curcumin nanoparticles	Oral gavage
Kakkar and Kaur 2011	Male Laca rats	Aluminium induced toxicity in Alzheimer's and bioavailability	100mg/kg; 50 mg/kg; 1, 12.5, 25, 50 mg/kg; 1.5 mg/kg	Free curcumin, free curcumin in 25% tween, C-SLNs, rivastigmine	Oral
Kundu et al., 2016	Male Balb/c mice	Bioavailability of curcumin	100 mg/kg once	Free curcumin and formulated curcumin	Oral gavage

6.2 Materials and Methods

6.2.1 Materials

Curcumin standard (C≥99.5%) was purchased from Sigma-Aldrich (Sigma, St. Louis, MO). Curcumin β-D-glucuronide (CG >96%), curcumin sulfate tetrabutylammonium (CS >98%), $_2H^6$-curcumin (D6C >98%) and bisphenol A-d6 β-D-glucuronide (BPAG-d6 >95%) were purchased from Toronto Research Chemicals (Toronto, ON, Canada). LC/MS-grade methanol, HPLC-grade water, ACS-grade formic acid and ammonium format were obtained from Sigma-Aldrich (St. Louis, MO, USA). Additional chemical reagents used in this trial are listed in chapter three (materials and equipment).

Meriva® was kindly donated by Indena S.p.A., Milan – Italy. Maltodextrin (M040) was provided by Brenntag New Zealand Ltd, Auckland, New Zealand. Smooth, no-added-salt/sugar peanut butter (Sanitarium™) was purchased from a local supermarket, and raw honey was donated by a local apiary (H5206). MFGM, curcumin and oils used were sourced as cited in 3.1.1, 3.1.2, 3.1.3 and 3.1.4, respectively.

6.2.2 Methods

6.2.2.1 Emulsion preparation

Emulsions were prepared using high-pressure homogenisation as described in 4.3.2.3, and characterised through particle size, zeta-potential and microscopic structure as described in 4.3.2.5. For this trial, the MFGM1, lipid 700 fraction high in phospholipid content [details can be found in 4.4 (Table 4.8)] was used to encapsulate curcumin inside medium chain triglyceride oil (MCT) and fish oil (FO). In the previous chapters, curcumin was solubilised in the oil phase at a saturation point of 2 mg curcumin/g of oil. To increase the dose for *in vivo* delivery, this dose was increased to 5 mg/g of oil, which was achieved by increasing the solubilisation time from at least 4 hours to 24 hours. Some curcumin precipitate was observed in the oil phase; however, in the emulsified format, no precipitation was observed (Figure 6.1). Maltodextrin was added to the emulsion at a concentration of 5% to assist the drying process. Since emulsions contain 70% water and low doses of curcumin, the systems were freeze-dried before incorporation into "rat treats" (Table 6.2). Emulsions were weighed into plastic trays, added to the freeze drier and allowed to dry for two days. The trays with dried material were weighed again and stored at -80 freezer in the dark until treat preparation.

Freeze-drying protocol was as follows: a) Pre-freezing; frozen samples were added to the freeze drier and frozen overnight at -40°C to eliminate the moisture introduced to the sample and freeze-drier chamber during loading. Samples were kept at -40°C overnight since this temperature is below the eutectic point of the sample. b) Primary drying; vacuum of 13.3 Pa = 0.133 mbar was built at -40°C, and the sample was kept to dry overnight, allowing the system to recalibrate. The temperature was then adjusted to -15°C, and sample was dried further until the next morning. c) Secondary drying; the temperature was adjusted to +10°C in order to remove excessive moisture for 4h. After those stages of drying, the vacuum was released and samples were unloaded, immediately into a sealed bag to avoid absorption of moisture. Samples were kept at -30°C freezer until their use.

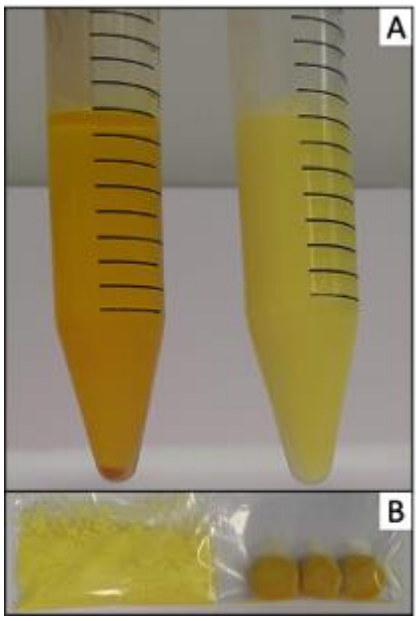

Figure 6.1 Curcumin dissolved in MCT oil (5 mg/ml) on the left and curcumin solubilised in oil in emulsified state after high pressure homogenisation on the right (A); Dried emulsion after freeze-drying on the left, and example of treatment treats on the right (B),

6.2.2.2 *In vivo* assay using Sprague-Dawley rats

An *in vivo* study was undertaken using 102 Sprague-Dawley rats (51♂ + 51♀). Ethics approval was obtained from the Massey University Animal Ethics Committee, Protocol No. 20/60.

Eight-week-old male and female Sprague-Dawley rats (429 ± 13g body weight) were randomised into four test groups, pair-housed by sex in large shoe-box cages with wire lids and trained over one-to-three-week period to eat treats made of peanut butter, honey, and maltodextrin as an inert carrier (Table 6.2).

Rats were offered water *ad libitum.* Commercial chow (Teklad/Fort Richards) was also offered *ad libitum,* except for the 8 hours prior to trial feeding, when the rats were fasted. A single treat (3.4 ± 0.1g) containing the treatment (freeze-dried emulsions, Meriva® or free curcumin) was then fed to the rats (Figure 6.2). Curcumin was included in all test treats at a dose of 20 mg/kg body weight. Rats were weighed the day before trial and treats were tailor-made for each rat based on its individual body weight. Treats were then orally delivered at a dose which equated to the dose humans would be easily able to consume in a yoghurt-type format. A small number of rats did not voluntarily eat the treats, and for these individuals a syringe administration technique was applied, allowing the rat to chew the material placed in its mouth before giving it more of the treatment (Figure 6.3). A group of control rats (N=6) were fed peanut butter treats containing no curcumin to serve as a negative control, and their blood and tissue samples collected only at the 60 min time point.

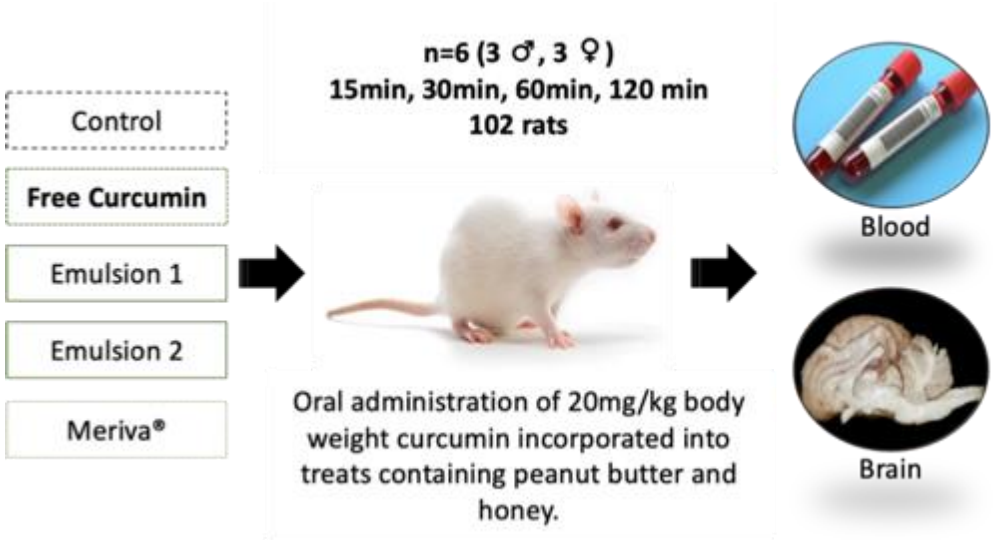

Figure 6.2. Schematic representation of rat trial

At the selected time points, rats were anesthetised with gas anaesthesia following SAPU "Isoflurane anaesthesia in rats and mice" SOP. When rats reached a state of surgical plane of anaesthesia, blood was collected using 18 gauge needle, transferred to vacutainer tubes and immediately placed on ice. Blood was divided into 2 different tubes, BD Vacutainer Serum tubes (silica sprayed, red top), to obtain serum samples for future use in cell treatment; and BD Vacutainer Plasma tubes (Sodium or Lithium Heparin, green top) used to obtain a plasma sample for curcumin analysis. Blood samples were centrifuged at 3000xg for 10 min to obtain plasma and serum samples. Plasma/serum samples were transferred to cryotubes and stored at -80 freezer until analysis. Effective exsanguination was carried out under deep anaesthesia as the initial stage of euthanasia. Subsequently, the chest cavity was opened to induce

pneumothorax. The organs were then collected, weighed, wrapped in foil, placed in a plastic bag, and immediately immersed into dry ice for snap-freezing. Frozen samples were stored at -80 ˚C until analysis.

6.2.2.3 Preparation of rat feed

Treatments were incorporated into treats (Table 6.2) offered to rats for voluntary consumption, with syringe feeding as an alternative for those not accepting the treats (Figure 6.3).

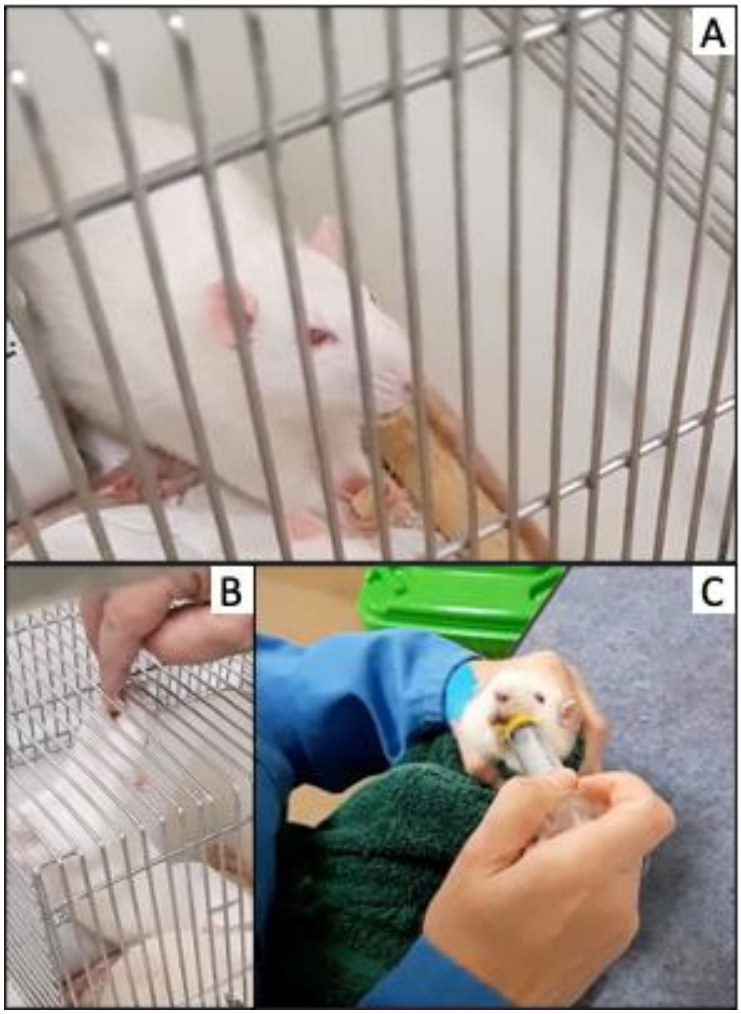

Figure 6.3. A) Rat eating a solid treat; B) Rat voluntarily grabbing treat after training period; C) Syringe administration applied to rats that were not accepting treat eating

Honey was added to make the treats more appealing at a concentration of 20-26%. Peanut butter, in addition to being added as an appealing ingredient to increase palatability, was added to match the fat composition of dry emulsions. Maltodextrin was added to enable the binding of ingredients. Maltodextrin is a food additive (texturiser) composed of hydrolysed starch (glucose) that is easily digested and absorbed.

Table 6.2. Final composition of rat treats used to deliver curcumin

	Rat treat composition (%)			
	Free curcumin	**Meriva**	**Emulsion 1**	**Emulsion 2**
Honey	20.0	24.6	25.9	25.9
Peanut butter	49.9	49.2	N/A	N/A
Maltodextrin	29.9	24.6	3.69	3.69
Meriva®	N/A	1.20	N/A	N/A
MCT	N/A	N/A	66.5	33.3
FO	N/A	N/A	N/A	33.3
MFGM 1	N/A	N/A	3.69	3.69
Curcumin	0.24	0.30	0.25	0.25

MCT= Medium chain trygliceryde oil; FO= Fish oil; MFGM 1 = Milk fat globule membrane fraction one (Lipid 700), a phospholipid rich MFGM fraction. Curcumin denotes the amount of free curcumin added to the treat (first column) or the amount of curcumin pre-incorporated into the test product (Meriva and emulsions)

6.2.2.4 Sample preparation and HPLC-LC/MS analysis

The protocols reported by Kunati and Yoon (Kunati et al., 2018, Yoon et al., 2020) were followed.

a) Preparation of standard solutions:

Stock solutions of C, CG and CS were prepared in methanol (1mg/mL). Curcumin β-D-glucuronide (CG, Toronto Research Chemicals, Toronto, Canada) stock solution at the same concentration was prepared in methanol/H2O (70/30). Working curcuminoid mixture solutions were prepared from the stock solutions by serial dilution in methanol. In addition, 2H6-curcumin (D6C, Toronto Research Chemicals, Toronto, Canada) and 2H6-tetrahydrocurcumin (D6TC, Toronto Research Chemicals, Toronto, Canada) solutions (internal standards, ISs) were prepared in methanol at concentrations of 1mg/mL, respectively. All standard solutions were stored at −80 °C in the dark.

b) Preparation of plasma calibrators and quality controls:

Plasma calibrators (0.125, 0.5, 1.0, 2.5, 5.0, 10, 25 and 50 ng mL^{-1}) and plasma quality controls (7.50, 55.0, and 400 ng mL^{-1}) were prepared by diluting standard solutions in 100 uL of blank rat plasma. After addition of the ISs (25ng mL^{-1} D6C and 100 ng mL^{-1} D6TC in 10 µL of methanol), the standard samples were processed together with biological samples. Calibration curves for plasma and brain can be found in appendix A6.1 and A6.2.

c) Curcumin extraction of rat plasma samples

Plasma samples were prepared in triplicate by transferring aliquots of plasma (100 μL) to 2 mL microcentrifuge tubes. The ISs (25ng mL^{-1} D6C and 100 ng mL^{-1} D6TC in 10 μL of methanol) were added to each sample. The samples were briefly mixed, then treated with cold (4°C) acetic acid in methanol (10 mM, 1 mL). After rigorous mixing, incubation (4 °C, 1 h), and centrifugation (16,000 g at room temperature for 5 min) supernatants were transferred to microcentrifuge tubes and dried in a vacuum centrifuge. The dried samples were tightly capped and stored at −80 °C. The residue was reconstituted in 100 μL of methanol and ammonium formate solution (10.0 mM, pH 3.0) (1:1 v/v), vortex mixed for 30 s and centrifuged at 17000 x g at 4◦C for 10 min. The solution was transferred into an amber glass vial for LC–MS/MS analysis.

d) Phospholipid extraction of rat plasma samples

PL were isolated from plasma samples using solvent extraction. Briefly, 50μL of plasma were diluted in 50uL Mili-Q water in a 1.5mL Eppendorf tube. 400μL of methanol: chloroform (2:1) was added into each tube and mixed well by vortex. The tubes were then centrifuged at 16000xg for 10 min and the supernatant was transferred to a new 1.5mL Eppendorf tube. The extraction was repeated with the addition of 50μL Milli-Q water and 200μL of methanol: chloroform (2:1) into each tube, followed by homogenization by vortex and centrifugation at 16000xg for 10 min. The supernatant was pooled together with previously collected supernatant, to which 130μL of 0.1M KCl was added. Homogenization by vortex and centrifugation at 16000xg for 10min followed. The upper phase was discarded and the extraction was repeated with the addition of 75μL of methanol and 50μL of 0.1M KCl to the lower phase. and mix them well with vortex. After final homogenisation and centrifugation, the upper phase was discarded and the volume was adjusted to 0.5mL in the Eppendorf tube using methanol: chloroform (2:1). Diluted extractions were transferred to dark HPLC vials and used for HPLC-LC/MS.

e) Curcumin extraction of brain tissue

Acetic acid (720 μL, 10 mM), ethyl acetate/methanol (95/5, 3mL), and a solution of ISs (25ng mL^{-1} D6C and 100 ng mL^{-1} D6TC in 10 μL of methanol) were added to pre-weighed freeze-dried brain tissue (1400 mg average) in 15 mL centrifuge tubes containing ceramic beads. The samples were homogenised in a vortex (thrice for 60 s each time at RT). The

homogenate was vigorously mixed (5 min), centrifuged (16,000 g for 5 min at RT), and the supernatant was transferred to microcentrifuge tubes and dried in a vacuum centrifuge. The dried samples were tightly capped and stored at −80 °C. The residue was reconstituted in 100 μL of methanol and ammonium formate solution (10.0 mM, pH 3.0) (1:1 v/v), vortex mixed for 30 s and centrifuged at 17000 x g at 4◦C for 10 min. The solution was transferred into an amber glass vial for LC–MS/MS analysis, which was conducted as described in 4.3.2.5(e).

6.2.2.5 HPLC-LC/MS

The liquid chromatography-tandem mass spectrometry (LC–MS/MS) system used in this work consisted of a Shimadzu (Columbia, MD, USA) Prominence UFLC unit with a controller (CBM-20A), two binary pumps (LC-20AD), an autosampler (SIL- 20AC), and an AB Sciex (Foster City, CA, USA) API 3200 turbo-ion-spray® triple quadrupole tandem mass spectrometer equipped with an electrospray ionisation (ESI) probe. The LC–MS/MS system was controlled by AB Sciex Analyst® (version 1.5.1) software for its operation, data acquisition, and processing. The triple quadrupole mass spectrometer was operated under negative electrospray ionisation mode (ESI^-) and tuned for compound-dependent and source-dependent parameters. The optimised compound-dependent parameters obtained followed protocol by Kunati et al (2018). Curtain gas at 30 psi; collision assisted dissociation gas at 6 psi; ionisation voltage at −4500 V; source temperature at 400 ° C; sheath gas at 50 psi; desolvation gas at 55 psi; and resolution at 0.7 amu. Quantitation of analytes and the IS was done in multiple-reaction-monitoring (MRM) mode and the following mass transitions were used: curcumin at 367 > 149; CG at 543 > 217; CS at 447 > 217; curcumin-d_6 at 373 > 152; and BPAG-d_6 at 409 > 233. The dwell time for each transition was 35 ms. Analytical separation of curcumin, CG, and CS (analytes), and curcumin-d_6 and BPAG-d_6 (internal standards, IS) was carried out at room temperature in gradient mode at a flow rate of 0.250 mL min^{-1} on a Waters (Milford, MA, USA) XTerra® MS C18 column (2.1 mm × 50 mm, 3.5 μm) connected to a Waters XTerra® MS C18 guard column (2.1 mm × 10 mm, 3.5 μm). The gradient elution program conducted using 10.0mM ammonium formate (pH 3.0) (Solvent-A) and methanol (solvent B) at a flow rate of 0.250 mL min^{-1} was as follows: 0–3.0 min (25–90% B), 3.0–7.50 min (90–90% B), 7.50–7.51 min (90–25% B), 7.51–11.0 min (25–25% B). Methanol was used as the wash solvent between injections. For each analysis, 10.0 μL of the sample was injected

into the system by the autosampler set at 4 ° C. The total run time was 11.0 min per sample and eluent of the first 2 min was diverted to waste. Prior to sample analysis, the column was equilibrated with mobile phase for at least 20 column volumes.

6.2.2.6 Statistical analysis

Statistical analysis were performed using SAS (SAS/STAT version 9.4). A two-way ANOVA model was used to determine the effect of treatment, time and their interaction as a fixed factors on curcumin and its metabolites in plasma and brain of rats using the Proc Mixed procedure. The sex of the rats was included in each model as a random effect, but in none of the response variables the effect was significant. Thus, it was removed from the final model.

The model diagnostics (e.g., normal distribution) for each response variable were tested using the ODS Graphics procedure and the repeated statement of SAS. When the model assumptions were not fulfilled the raw data were transformed. When the F-value of the model was significant ($P < 0.05$), the mean values of the two-way ANOVA were compared using the adjusted Tukey-Kramer test. Probability values were considered statistically different at $P \leq 0.05$, and values of $0.051 \leq P \leq 0.10$ were considered a trend.

6.3 Results and discussion

Curcumin has a short half-life and it undergoes rapid metabolic reduction and conjugation, resulting in poor systemic bioavailability after oral administration. To my knowledge there is no evidence that curcumin accumulates in the brain with repeated dosage in healthy rats and humans. Limited data available suggest instead that curcumin is eliminated from the body within a few hours (Ireson et al., 2001, Pan et al., 1999b, Asai and Miyazawa, 2000, Vareed et al., 2008, Liu et al., 2020b, Dibaei M, 2019). Specifically, when incorporated into the rat diet, curcumin concentrations in the brain did not differ between days 1, 4, 12, 25 or 90 (Bansal et al., 2012). For this reason, curcumin and its metabolites were analysed in plasma and brain after a single delivery.

Male and female rats were used in this study (n=3/3), but no differences were observed and this factor was subsequently ignored for statistical analysis, increasing the n to 6 per group when assessing the effects of treatment and time after administration of blood and brain concentrations. However, this observation is important and of interest, since most of rat studies have used only males (Table 6.1) with little to none inter-sex comparisons of curcumin uptake

or distribution in rats published. This finding indicates that in future similar studies, it will be of less importance to use animals of both sexes.

HPLC-LC/MS was used to detect curcumin and its metabolites in plasma and brain, and an internal standard (IS) was added to each sample to calculate concentrations, ensuring more accurate representation of the data. The peak area for a known concentration in the calibration curve was divided by the area of its correspondent internal standard peak and plotted against the known concentration divided by the internal standard concentration (eg. $Area_{Cu}/Area_{Cu\text{-}d6}$ on x axis vs. $Concentration_{Cu}/Concentration_{Cu\text{-}d6}$ on y axis). A linear trendline was then applied and the obtained equation was used to calculated observed concentrations for each sample (Appendix A6.1 and A6.2). Quality controls were used for all the analysed compounds and the mean recovery was used to correct sample calculations (48% ± 0.02 Curc; 69% ± 0.14 CG; 100% ± 0.11 CS). As expected, no curcumin or curcumin metabolites were detected in the plasma or brain of rats fed control treats without curcumin, thus eliminating any possibility of false positives. Examples of detected peaks for standard curve, quality control and samples are shown in Figure 6.4 and Figure 6.5.

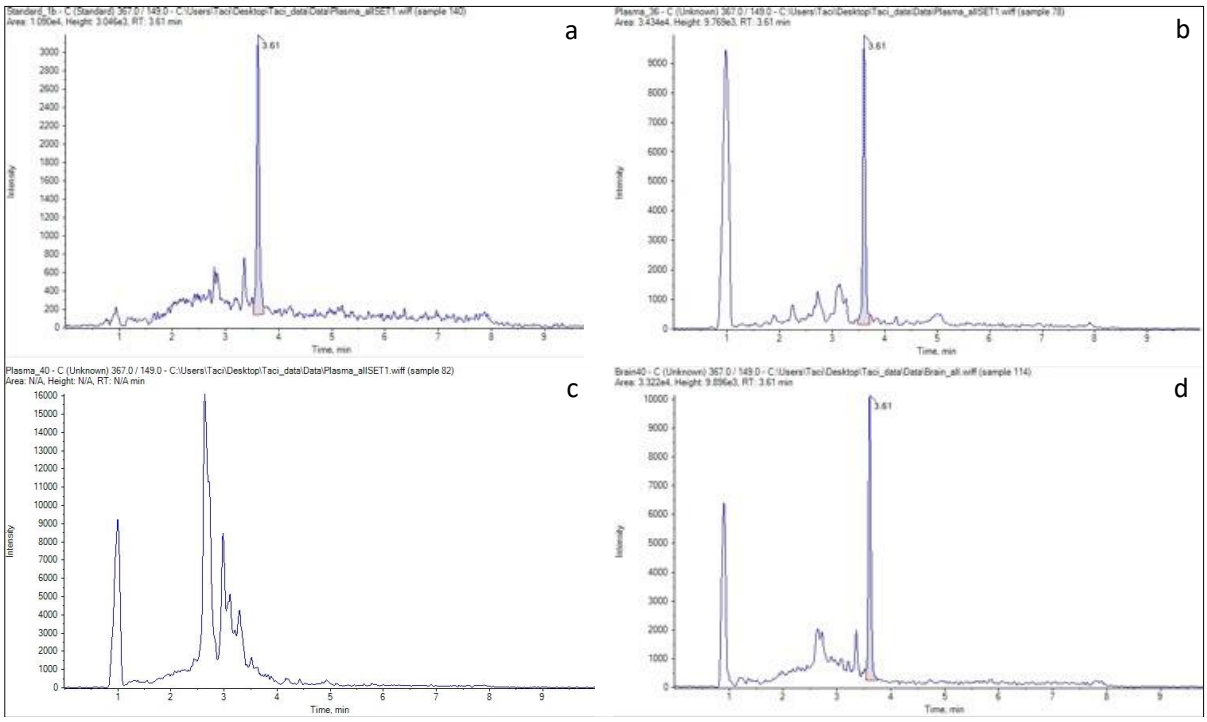

Figure 6.4. Curcumin peaks detected by HPLC-LC/MS. On x axis is the retention time, while y axis contains the intensity of the peak. Generated areas were used for concentration calculations based on standard curve. On the top left centre (a), image of the lowest calibration curve point for curcumin. Top right image (b), shows a detection peak in rat plasma. Bottom left (c) illustrates a peak not identified (control), where there is no clear peak for curcumin retention time (3.61). Bottom right (d) image represents a curcumin peak detected in rat brain.

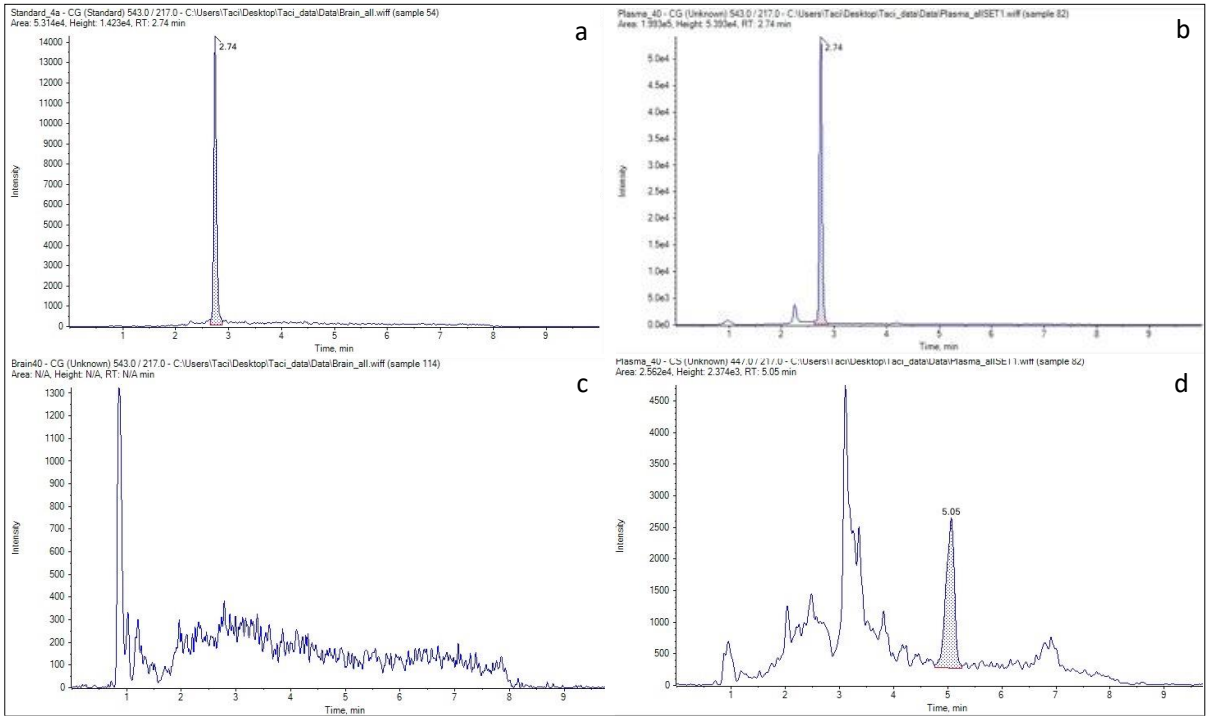

Figure 6.5. Curcumin metabolite peaks detected by HPLC-LC/MS. . On x axis is the retention time, while y axis contains the intensity of the peak. Generated areas were used for concentration calculations based on standard curve. On the top left centre (a), image of a medium range calibration curve point for curcumin glucuronide (CG). Top right image (b), shows a CG detection peak in rat plasma. Bottom left (c) illustrates a peak not identified for CG in brain, where there is no clear peak for CG retention time (2.74) confirming that metabolites do not cross the BBB. Bottom right (d) image represents a curcumin sulphate peak detected in plasma. Similarly to CG, CS could not be detected in brain.

Studies of curcumin bioavailability and delivery to plasma in animals and humans have been presented in varying ways in literature. While the number of studies analysing not only curcumin, but also its metabolised formats (CG and CS) is increasing (Asai and Miyazawa, 2000, Kunati et al., 2018, Marczylo, 2007, Yoon et al., 2020), there is an extensive number of articles that presented data of curcumin after enzymatic reaction to convert metabolites back to curcumin. Many of these studies used the converted or combined concentration of curcumin and its metabolites to report improvements in bioavailability (Kakkar et al., 2010, Briskey et al., 2019, Nasef et al., 2019, Antony et al., 2008, Purpura et al., 2018, Kanai et al., 2012). There are also a number of published reports where this information is missing, leaving it not clear whether enzymatic conversion was performed or not, although the only compound shown was curcumin. In 2019, a study was conducted to compare the results from direct extraction and metabolite analysis vs enzymatic hydrolysis of plasma followed by extraction, and the authors concluded that there is an expressive exaggeration on the amount of curcumin detected after enzymatic hydrolysis. In the above-mentioned study, after oral administration of 400 mg of bioavailable formulation (micellar advanced absorption study product containing 400 mg curcumin, coconut oil, polysorbate-20, and DL-alpha-tocopherol) to adults, curcumin was

found in plasma at a concentration of 0.71ng/mL without hydrolysis against 129.4 mg/mL after enzymatic hydrolysis (Stohs et al., 2019). This suggests that all reported data measuring converted curcumin should be considered unreliable. Therefore, in our study plasma curcumin and its metabolites were measured and reported both separately and additively for better comparison with the published data in the field. As an example of the latter, the data reported as being plasma curcumin in Figure 6.6 consists of the combination of plasma curcumin, plasma CG, and plasma CS.

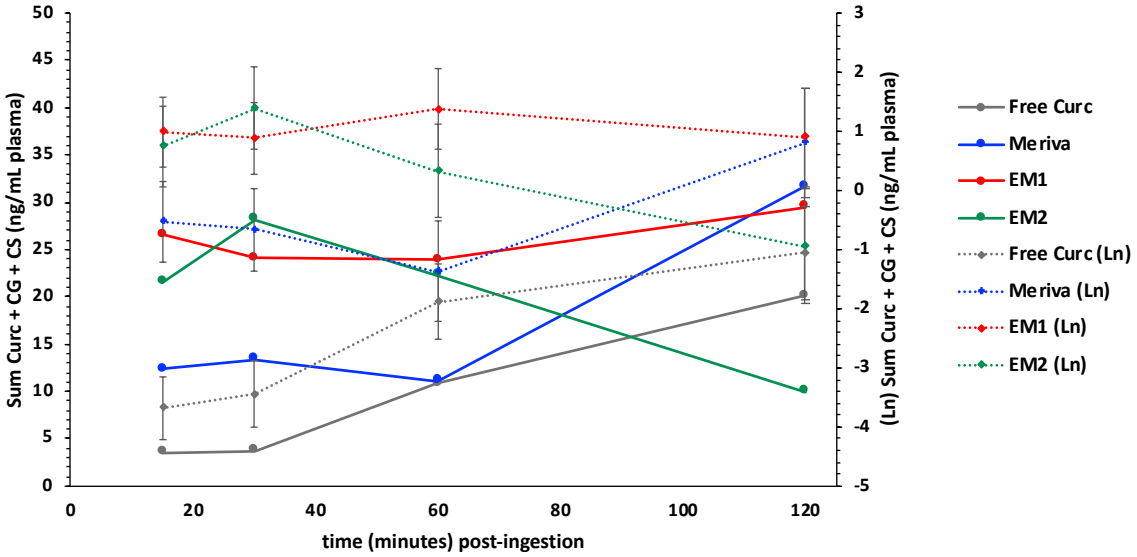

Figure 6.6. Kinetic differences in the appearance of curcumin + metabolites in plasma after oral administration of treats containing free curcumin (free Curc), bioavailable curcumin formulation (Meriva®), emulsion system 1 (EM1) and emulsion system 2 (EM2). Data are shown as the mean ± SEM of 6 animals. *Raw data were log transformed (Ln) to obtain normality of variance for statistical analysis and are presented as the dotted lines in the secondary y axis. The values showed as a solid line (primary y axis) are the back transformation of log values back to its original scale to allow more meaningful and intuitive data interpretation.

The kinetics of appearance of curcumin + metabolites in plasma differed depending on the format in which it was administered. For free Curc, accumulation of curcumin and its metabolites occurred slowly, with minimal amounts present at 15 – 30 minutes, then rising afterwards. Curcumin and its metabolites from Meriva® formulation were present in significantly higher concentrations at 15 – 30 minutes compared to the free Curc treatment, suggesting improved bioavailability and absorption. However, the levels changed little between 15 minutes and 60 minutes; as with free Curc, only during the second hour did Meriva® curcumin and its metabolites accumulate in the plasma in significantly higher concentrations. In contrast, curcumin from the emulsions and its metabolites peaked in plasma immediately, and were present at significantly higher concentrations than either free Curc or Meriva® treatments at 15 and 30 minutes. Moreover, these levels remained high, except for

EM2, with there being no significant differences between any of the time points for either emulsion ($p<0.05$). Emulsions and Meriva® improved overall bioavailability and absorption of the delivered curcumin compared to free Curc, with the emulsions resulting in significantly more curcumin and its metabolites in plasma compared to Meriva® over the first hour post-ingestion. These findings suggest that the emulsion formats were superior to free curcumin and similar to Meriva® with regards to improving rapid and sustained delivery of curcumin + metabolites in plasma.

When compared to published reports, the plasma concentrations for Curc+CG+CS in this study were lower than those reported in a study using the same dose of curcumin. Liu and collaborators (2018), found that free curcumin peaked at 30 min with a maximum concentration (Cmax) of 82 ng/mL, while curcumin-loaded rice bran albumin nanoparticles peaked at 60 min with a Cmax of 256 ng/mL. The authors did not mention the addition of glucuronide or sulfate enzymes to convert metabolites back to curcumin; however, only curcumin is represented at a 8.5 fold higher than concentrations observed in our study. There is also no mention of the method of analysis, but a reference to another study (Shaikh et al., 2009) who used HPLC method as opposed to more sensitive HPLC/LC-MS used in our study. Those differences, taken together with findings by Stohs et al. (2019) that enzymatically converting metabolites back to curcumin instead of analysing them separately can account for the overestimated results, could be explained by authors performing enzymatic conversion without mentioning it in the paper, as opposed to individually analysing it as it was performed in our study. The use of different formulations could justify the argument that they achieved higher bioavailability; however, curcumin values after feeding the same dose were 3 times higher (82 ng/mL) when enzymatically converted (Liu et al., 2018) vs data in this study, analysed separately and pooled together (28 ng/mL).

These data were further refined by assessing the individual components: curcumin, CS, and CG. It is deemed desirable to retain plasma curcumin in its native form for as long as possible *in vivo*, since curcumin but not its metabolites can cross the blood-brain barrier. As shown in Figure 6.7, curcumin concentrations were overall quite low and had wide inter-subject variability. Free Curc resulted in the lowest curcumin concentrations in plasma; Meriva® and the two emulsions resulted in similar, higher curcumin concentrations but appeared to have slightly different kinetics, with Meriva® peaking at 15 minutes, EM1 peaking at 60 minutes, and EM2 peaking at 30 minutes. Curcumin concentrations in general declined over time, indicating that it was metabolised. These data were log transformed to obtain

normality for statistical analysis. An analysis of variance was used and the ratio of the mean square for the model to the mean square for the error (F statistic) was used to test the null hypothesis. For curcumin in plasma, the interaction of factors was not significant (Pr>F 0.8556); however, the individual factors of time (Pr>F 0.0279) and treatment (Pr>F 0.0404) indicated significant differences for those parameters. EM1, EM2 and Meriva® had no statistical differences in curcumin concentrations in plasma between them, but all were significantly higher than those of free Curc. Similarly, curcumin concentration at time points 15, 30 and 60 minutes did not statistically differ between them, but were significantly higher than those at 120 min.

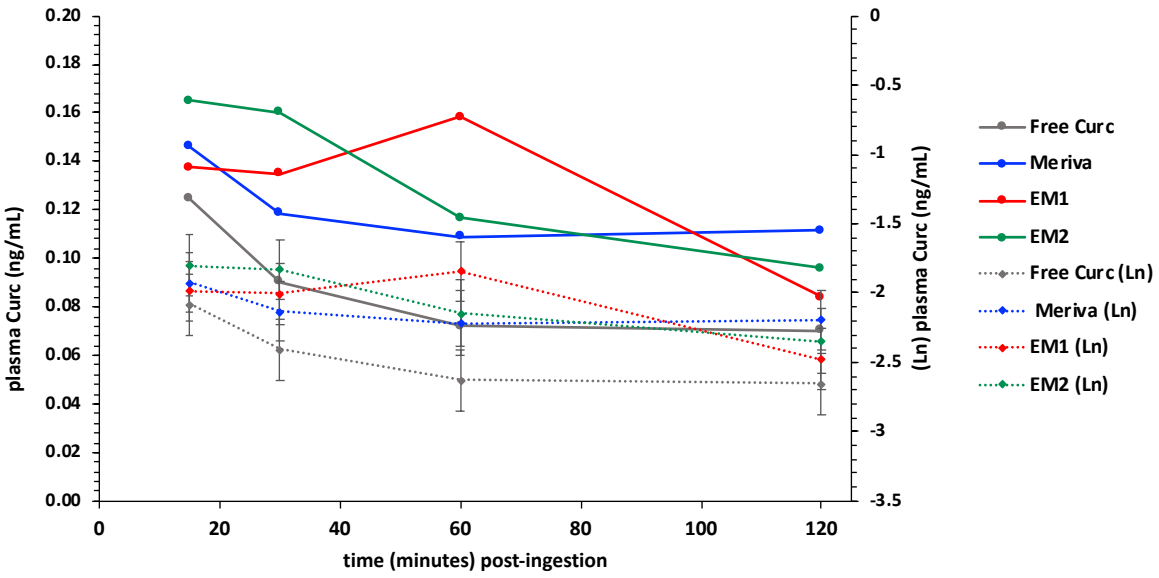

Figure 6.7. Kinetic differences in the appearance of curcumin in plasma after oral administration of treats containing free curcumin (free Curc), bioavailable curcumin formulation (Meriva), emulsion system 1 (EM1) and emulsion system 2 (EM 2). Data are shown as the mean ± SEM of 6 animals . *Raw data were log transformed (Ln) to obtain normality of variance for statistical analysis and are presented as the dotted line in secondary y axis. The values showed as solid lines (primary y axis) are the back transformation of log values back to its original scale to allow more meaningful and intuitive data interpretation.

The two main metabolites generated after curcumin consumption are CG and CS, which are formed when either glucuronide or sulphate molecules bind with curcumin, leading to degradation and subsequent excretion from the body. Those conjugated forms cannot cross the blood-brain barrier (BBB) (Pandey et al., 2020, Dei Cas and Ghidoni, 2019), reinforcing the importance of the correct measurement, analysis and interpretation of curcumin pharmacokinetic studies (Stohs et al., 2019). It is critical that the presence of the metabolites in the plasma be differentiated from curcumin itself for the purposes of identifying the amount of compound present that has the potential to enter the brain and provide protective bioactivity

to this organ. Therefore, in addition to free curcumin, these metabolites were measured in plasma and brain of rats in this study.

CG was found in plasma for Meriva® and emulsion treatments in higher concentrations than the free Curc treatment (Figure 6.8). Overall, CG levels were >10-fold higher than unmetabolized curcumin, indicating that most of the "detectable" curcumin had been transformed into the metabolised form. There was a significant interaction of the factors time and treatment for CG distribution in plasma (Pr>F 0.0014), indicating significant differences for both factors and their interaction.

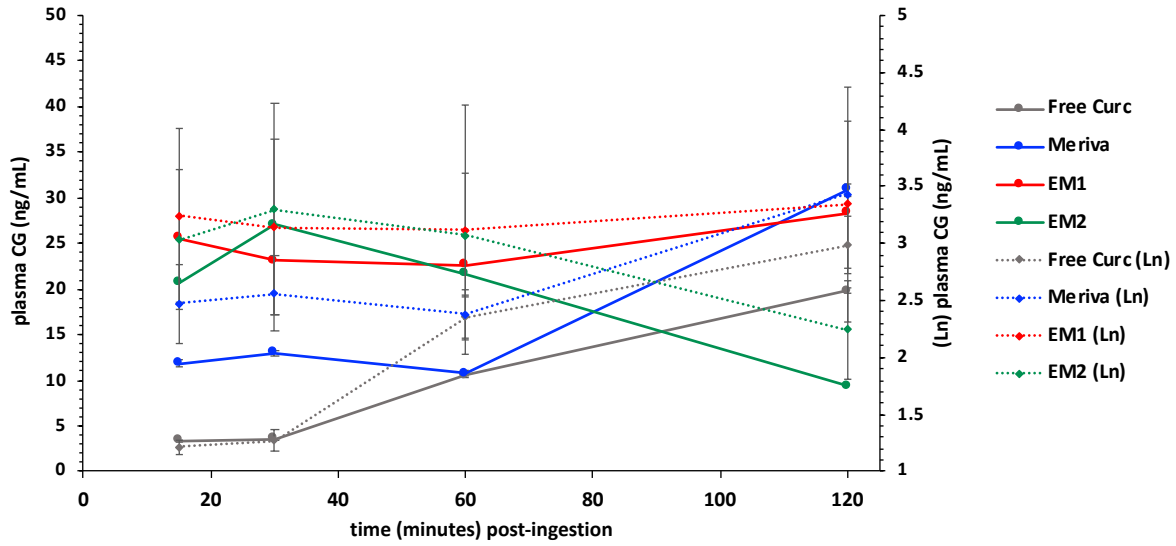

Figure 6.8. Kinetic differences in the appearance of CG in plasma after oral administration of treats containing free curcumin (free Curc), bioavailable curcumin formulation (Meriva), emulsion system 1 (EM1) and emulsion system 2 (EM 2). Data are shown as the mean ± SEM of 6 animals. *Raw data were log transformed to obtain normality of variance for statistical analysis and are presented as the dotted line in secondary y axis. The values showed as solid lines (primary y axis) are the back transformation of log values back to its original scale to allow more meaningful and intuitive data interpretation.

CS was also detected in plasma (Figure 6.7), and a similar significant interaction of the factors time and treatment was observed, indicating that changes between treatments were dependent on time (Pr>F 0.0086). In plasma, the metabolite CG predominated, with levels approximately 40-fold higher than CS and up to 200-fold higher than curcumin.

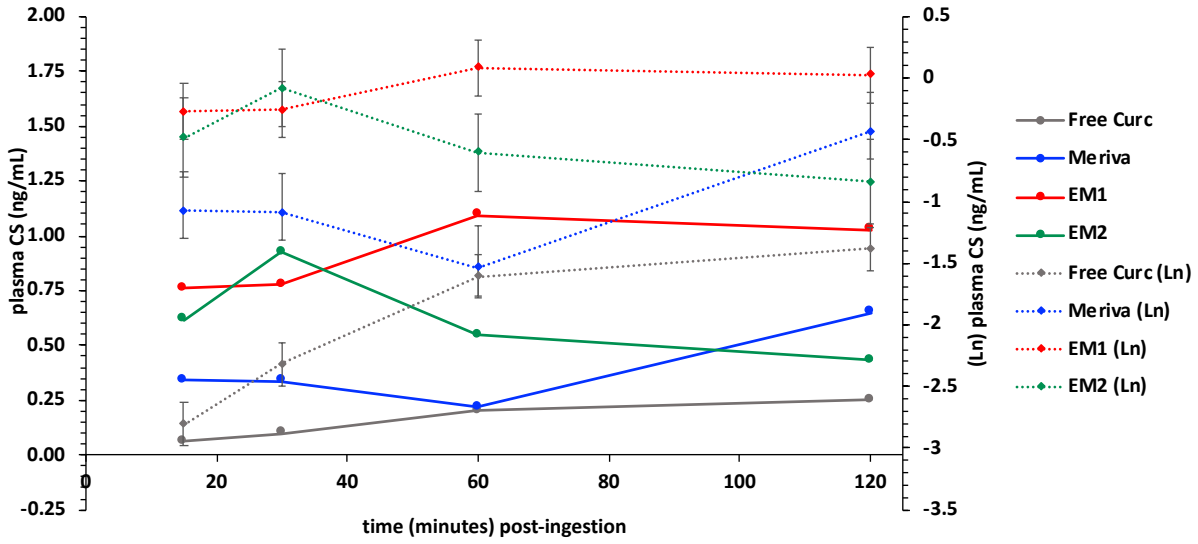

Figure 6.9. Kinetic differences in the appearance of CS in plasma after oral administration of treats containing free curcumin (free Curc), bioavailable curcumin formulation (Meriva), emulsion system 1 (EM1) and emulsion system 2 (EM 2). Data are shown as the mean ±SEM of 6 animals. *Raw data were log transformed to obtain normality of variance for statistical analysis and are presented as the dotted line in secondary y axis. The values showed as solid lines (primary y axis) are the back transformation of log values back to its original scale to allow more meaningful and intuitive data interpretation.

The kinetics differed across the four formats, with the emulsions producing higher concentrations of CG and CS at early time points compared to free Curc and Meriva®. For free Curc and Meriva®, the kinetics for CG and CS were similar. In contrast, the two emulsions had similar kinetics for CG but differed for CS, with EM1 producing a later peak and higher overall concentrations for CS. This mirrored their differences in plasma curcumin, with EM1 producing a more sustained high level of unmetabolized curcumin compared to EM2. The trend of CS distribution in plasma was similar to the one observed for CG, for which it can be assumed that the curcumin was metabolised into CG and CS at similar speed.

It is expected that metabolite concentration will increase in parallel with a decrease in the original compound concentration. For rats that received the free Curc treatment, the plasma concentration of CG followed an increasing trend, which inversely correlated with the decreasing trend observed in the detected doses of curcumin noted previously. The same trend was observed for Meriva®, although this treatment had significantly higher concentrations of CG at 15 and 30 minutes compared to the free Curc control treatment. GC from Meriva® increased to values statistically equal to those of free curcumin at 120 minutes. Both emulsions showed a steady state level of CG for the first hour, with EM1 maintaining that concentration

for the subsequent hour while EM2 decreased in CG between the 60 and 120 minute time points.

It was noticeable that curcumin declined as CG and CS rose, indicating that curcumin was rapidly metabolised. To visualise this more clearly, for each of the four treatments the three compounds were placed on the same graph (Figure 6.10). The value for each compound was normalised to its initial 15 minute time point, which was set to 100%; this is an artificial way of presenting the data but necessary to eliminate the hundred-fold differences in scale between curcumin and CG concentrations. Even so, a different y-axis scale had to be used for the free curcumin format because the differences over time were far greater than observed with Meriva® and the emulsions.

When delivered as free Curc, the concentration of curcumin in plasma decreased slightly over time compared to the 15 minute time point. CS rose dramatically within the first hour and then increased only slightly thereafter, whereas CG continued to rise at the same trajectory from 30 minutes to 2 hours. At 2 hours, the amount of CG in plasma was 8-fold higher than at the 15 minute time point, indicating that curcumin metabolism occurred at a high rate (Figure 6.10a).

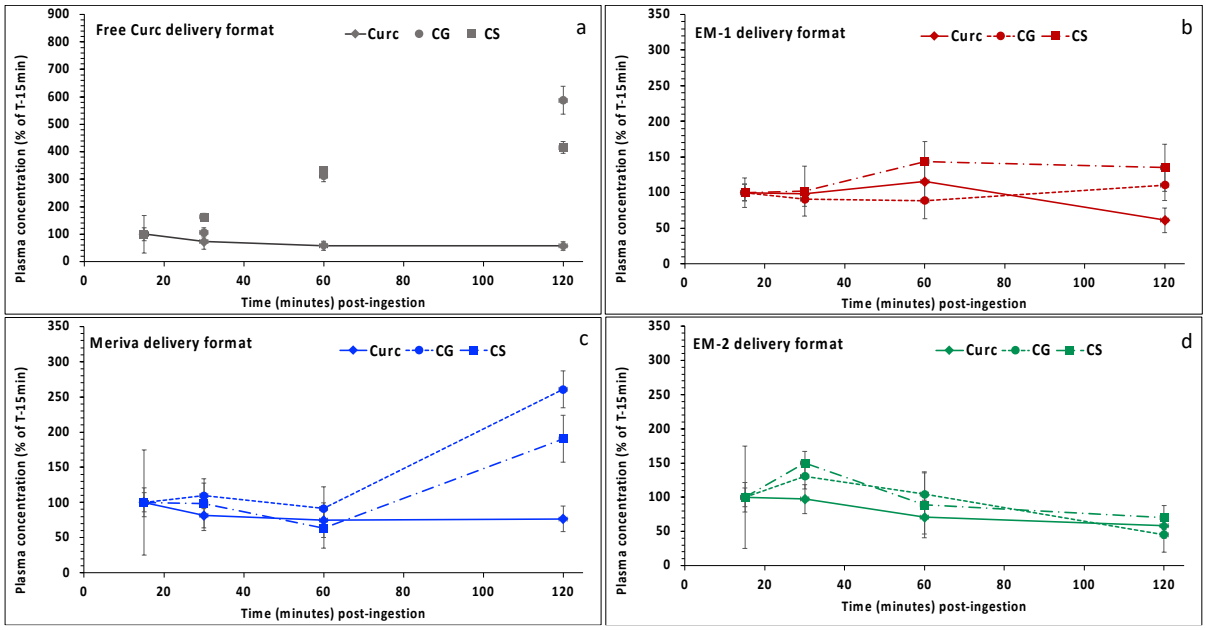

Figure 6.10. Normalised kinetics for Curc, CG and CS in plasma after oral administration of treats containing free curcumin (a), bioavailable curcumin formulation Meriva (b), emulsion system EM1 (c) and emulsion system EM2 (d). Data are shown as the mean ± SEM of 6 animals.

Meriva ® delivery similarly resulted in the slight, gradual decrease of plasma curcumin, but the concentrations of CG and CS did not alter between the 15, 30 and 60 minute time points,

and only rose at 120 minutes to levels approximately 3-fold that of the initial 15 minute concentration (Figure 6.10b). The emulsions behaved markedly differently to free Curc and Meriva®. Curcumin remained steady or rose slightly over the first three time points, then declined slightly at 120 minutes. Interestingly, neither CG nor CS increased over time, with no significant difference across the time points for either metabolite (Figure 6.10c,d). This may indicate slower metabolism of curcumin or faster removal of the metabolites from plasma.

The formulations through which curcumin was administrated in this study affected the way it was metabolised, and the peak time points for concentrations in blood differed between treatments. Meriva® has been used in a series of studies due to its improved bioavailability. It is believed that the lipophilic character of the curcumin–phosphatidylcholine complex in Meriva® may facilitate diffusion of curcumin across biological membranes in the gastro-intestinal tract via formation of a phospholipid monolayer on the mucosal surface, thus supporting the transition of curcumin from the hydrophilic gut content across lipophilic membranes into cells. A study has assessed the delivery of curcumin and its metabolites to plasma at the same time points tested in our study comparing Meriva® with unformulated curcumin, although at a much higher dose (340 mg/kg vs 20mg/kg), and observed marked differences between Meriva® and free curcumin (Marczylo et al., 2007). The authors observed that curcumin and CG peaked at 30 min and CS at 60 when administered as unformulated curcumin, while curcumin peaked at 15 min when administered as Meriva®. Interestingly, the concentrations for curcumin, CG and CS in the Marczylo et al. (2007) study decreased at 120min. However, our study found that as curcumin decreased in concentration over time, with lowest values at 120min, however CG and CS increased, leading to a more stable distribution across time points. The trends observed were contradictory and are likely due to the >15-fold difference in curcumin doses administered between our study and the above-mentioned report.

Curcumin has been shown to peak after oral delivery in the rat at 15 – 30 minutes in blood, which is in accordance with the plasma observations in this study (Kundu et al., 2016, Chen et al., 2012, Marczylo, 2007). However, from the plasma data alone conclusions cannot be drawn as to whether curcumin and its metabolites were excreted from the body, stored intracellularly in the liver or elsewhere, or further metabolised. In particular, it was of interest to determine whether any curcumin entered the brain.

Curcumin is believed to cross the BBB, however, the attachment of glucuronide and sulphate groups precludes this crossing ability. Curcumin may accumulate in the brain of

animals and humans with neurodegenerative disease and provide beneficial health effects as curcumin is capable of binding specifically to Aβ plaques (Maiti et al., 2019, den Haan et al., 2018). Curcumin has been shown to peak in brain after oral delivery in the rat at 60 – 120 minutes (Kundu et al., 2016, Chen et al., 2012, Marczylo, 2007). A single delivery is sufficient and preferable to initially demonstrate bioavailability and BBB-crossing, although daily feeding of curcumin would be needed to demonstrate efficacy against AD.

In this study, curcumin, CG and CS were measured in the rat brains at the selected time points after feeding each of the four test formulations. As expected, no peaks for either CG or CS were detected in the brains of rats fed with free curcumin or the various formulations (Figure 6.5). This verifies the previous reports that neither of these curcumin metabolites is capable of crossing the BBB. Whole brain tissue was also used to measure the transport of curcumin across the BBB and retention of curcumin in the brain. Despite the use of a lower dose than those usually used for rats, curcumin was successfully detected in brain at all time points for all four treatments (Figure 6.11a).

As with plasma curcumin, brain curcumin displayed broad variability between animals. Accumulation of curcumin in the brain occurred rapidly, peaking at 30 – 60 minutes for all treatment groups except for Meriva®, which showed a higher peak occurring at 120 minutes. To eliminate the effect of differences in body weight (which altered the amount of curcumin fed) and brain weight, these data were also normalised to brain curcumin as a proportion of ingested curcumin (Figure 6.11b). The patterns and kinetics remained similar. Statistically, after log transformation, it was observed that the interaction time and treatment was significant, indicating differences between treatments were dependent on time (Pr>F 0.009) with Meriva at 120 min presenting the highest concentrations and EM2 at 15 min the lowest.

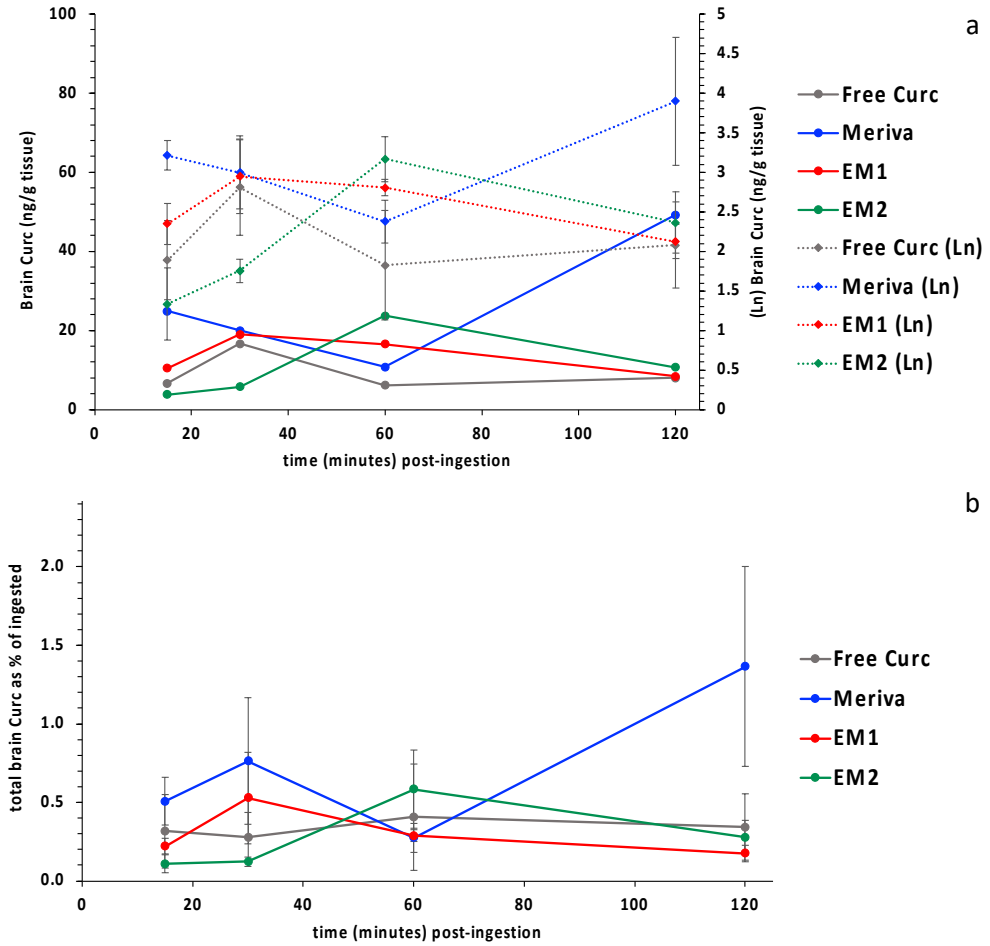

Figure 6.11. Kinetics of Curc in brain of rats after 15, 30, 60 and 120 minutes of oral administration of treats containing free curcumin (free Curc), bioavailable curcumin formulation (Meriva), emulsion system 1 (EM1) and emulsion system 2 (EM 2). Data are shown as the mean of 6 animals plus standard deviation error. *Raw data was log transformed to obtain normality of variance for statistical analysis and are presented as the dotted line in secondary y axis. The values showed as solid lines (primary y axis) are the back transformation of log values back to its original scale to allow more meaningful and intuitive data interpretation (a). Data has also been normalized to percentage of total ingested curcumin (b).

Of the four treatments, Meriva® achieved the highest level of curcumin in the brain sample, with the concentration remaining fairly steady over time but with inter-rat variability increasing at the 2 hour time point. This suggests that curcumin from Meriva® was rapidly transported into the brain and was retained or replaced over two hours of assessment. The delivery of free Curc resulted in less brain curcumin compared with Meriva® after 15 minutes, 1 hour, and 2 hours. Brain curcumin following emulsion feeding was comparatively lower at the 15 minute time point compared to Meriva®, but rose over the next two time points before falling slightly at 2 hours. The slower uptake of curcumin from emulsions compared to Meriva® is likely due to the slower absorption as indicated by the presence of curcumin in the plasma observed earlier, which showed that plasma curcumin from free Curc or Meriva peaked at 15 minutes, whereas for the emulsions it peaked at 30 – 60 minutes. Taken together, these findings

suggest that curcumin delivery by Meriva® may be superior in improving curcumin accumulation in the brain, whereas emulsion delivery changes the rate of curcumin metabolism. However, it is also possible that the emulsion systems may have produced higher brain curcumin at time points later than 2 hours.

The dosage tested in this study extrapolates to a 70 kg human eating 1.6 grams Meriva®; the recommended dose of Meriva in an adult is 1g powder per day. Such doses are in line with human intervention trials feeding adult humans 200 to 500 mg/day of curcumin in native, Meriva®, or other formats (Weir et al., 2018, Cicero et al., 2020), as well as a bioavailability trial feeding 400 milligrams of curcumin (Stohs et al., 2019, Stohs et al., 2018). Similar doses of Meriva® used in a clinical trial for diabetes (equivalent to 180 mg curcumin/day) have shown improvements although no pharmacokinetic analysis were conducted (Thota et al., 2018). If scaled to a rat dose, 180 mg curcumin in human would be equivalent to approximately 29 mg/kg body weight, a dosage similar to the one use in our study. When converting the rat dosage used in our study to a human dose, an equivalent of 3.24 mg/kg body weight would be expected, reflecting a feasible administration dosage of 200 mg curcumin per adult per day (Nair and Jacob, 2016).

Curcumin has been found in measurable levels in the plasma and brain of rodents after a single oral delivery of curcumin at doses of 23 – 50 mg/kg BW (Baek and Cho, 2017, Chen et al., 2012, Khalil et al., 2013). A rat study feeding 40 mg/kg BW resulted in serum curcumin at ~25 ng/mL (~70 nmol/L) (Huang et al., 2019). In humans, a single oral administration of 400 mg curcumin (~0.6 mg/kg BW) resulted in C_{max} of 0.71 ng/mL (0.25 nM) (Stohs et al., 2019). Formulated curcumin, being more bioavailable, has been shown to result in a 5 to 100 fold increase in blood and brain compared to native curcumin (Kundu et al., 2016, Cheng et al., 2017, Im et al., 2015). Curcumin in a submicron crystal solid dispersion (Theracurcumin) was orally administrated to rats at doses of 5mg/kg and 30mg/kg body weight and measurable amount of curcumin was observed in the plasma (764 ng/mL and 1697 ng/mL respectively) with T max of 1 and 2 hours. The same product and dose was administrated to healthy human volunteers and the area under the blood concentration-time curve (AUC) was 27-fold higher than free curcumin (Imaizumi, 2015).

As reported elsewhere, an AIN-93M rodent diet containing curcumin at 0.06% was found to be beneficial in a mouse model of AD (Sharman et al., 2019). In a different neurodegenerative model, positive effects were observed when an optimised curcumin

formulation (Longvida) at 500 ppm (0.05%) was administrated to GFAP-IL6 mice (Ullah et al., 2020a). In a parallel study using this neurodegenerative model, curcumin in the form of Meriva® was effective for most parameters measured when fed at 218 ppm (Ullah et al., 2020b), which equates to approximately 22 mg curcumin/kg BW/day, similar to the dose assessed in rats in our study. Moreover, in a rat model of depression, 20 mg/kg formulated curcumin was superior to the same dose of native curcumin, but was also significantly better than 40 mg/kg for some parameters, indicating that a higher dose is not necessarily more efficacious (Aswar et al., 2020). Native curcumin has also been shown to have efficacy in various rodent models of brain damage when fed at doses equivalent to 5 (Fidelis et al., 2019), 15 (Pyun et al., 2014), 20 (Vasileva et al., 2018) and 30 (Laabbar et al., 2019) mg/kg BW/day. I therefore postulate that feeding 20 mg/kg BW/day in future efficacy studies using a rat or mouse model of brain injury/disease should result in cumulative health benefits and efficacy over time.

Individual phospholipids in plasma were also measured (Figure 6.12). Some differences were observed, particularly for the main phospholipid class phosphatidylcholine (PC), which was significantly higher in the plasma of rats that received Meriva® formulation compared to those who received emulsions. Unfortunately, the incorporation of peanut butter and the prior *ad libitum* feeding of chow, while useful and ethically necessary facets of the study, resulted in the inability to attribute the presence of individual phospholipids in the plasma to Meriva® or the emulsions, since peanut butter and chow also contain phospholipids and thus would have contributed to some of the phospholipids present in the plasma. However, it is interesting to note that, while all test groups received peanut butter treats containing the various curcumin formulations, rats in the control and Meriva groups had significantly more total phospholipids in their plasma at each of the time points compared to those in the emulsion groups and also compared to the control rats receiving peanut butter treats with no curcumin, despite their fat intake having been nearly identical across all groups. For rats in the free-curcumin group, total phospholipids in the plasma peaked at the 120 minute time point, whereas in the other groups the peak occurred at 30 minutes. Interestingly, rats fed emulsions had slightly less PE, PC, and LPC than rats fed treats with no curcumin, despite the emulsion groups ingesting slightly more overall lipid as their treats contained both peanut butter and MFGM.

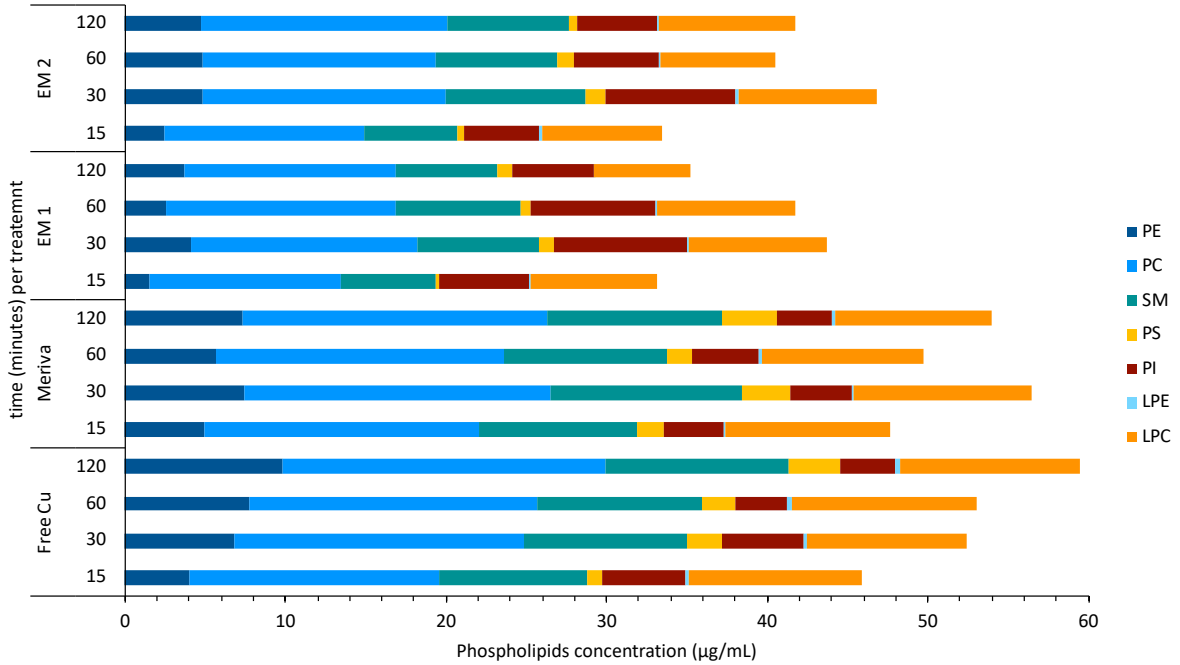

Figure 6.12. Phospholipid distribution in plasma. PE=Phosphatidylethanolamine, PC=Phosphatidylcholine, SM=Sphingomyelin, PS=Phosphatidylserine, PI=phosphatidylinositol, LPE- Lyso-Phosphatidylethanolamine, LPC- Lyso-Phosphatidylcholine

6.4 Conclusions

Taken together, these findings indicate that the delivery format influenced curcumin release and availability in the duodenum due at least in part to differences in the overall digestive process. In addition, the results suggest that the emulsions reduced phospholipid absorption in the gut for two hours post-prandial. It would be of interest to further study how the emulsions specifically affect the kinetics of gastric emptying, lipid digestion, and lipid absorption as well as perceived satiety and unabsorbed lipid excretion.

The components in Meriva® that are believed to increase curcumin bioavailability are attributed to a phospholipid complex derived from sunflower seeds. In contrast, the emulsions used in this study contained phospholipids derived from MFGM. The findings demonstrated that this combination is suitable for improving curcumin bioavailability. They were selected because it has been suggested that these lipids may have brain-protective effects in their own right; it will be of interest in future studies to determine whether this specific lipid-curcumin combination provides additive or synergistic health benefits in neurological disorders such as AD.

Chapter 7 Effect of *in vitro* digested emulsions and *ex vivo* post-prandial serum on neuronal cell viability and protection against amyloid-beta toxicity *in vitro*

7.1 Abstract

Based on evidence from literature on the benefits of curcumin, MCT and ω-3 PUFA against AD biomarkers, and the potential the MFGM has in promoting health, the previously prepared emulsions systems were tested against the toxic Aβ peptide *in vitro*. The human neuroblastoma BE(2)-M17 cell model was used to assess cell viability and cytotoxicity using the 3-[4,5-dimethylthiazol-2-yl]-2,5 diphenyl tetrazolium bromide assay (MTS) assay to evaluate the effect of fresh, *in vitro* and *in vivo* digested emulsions systems containing curcumin. I aimed to assess how different ways to treat cells could affect Aβ protection and observed that fresh emulsions were more efficient as compared to *in vitro* or *in vivo* digested. Fresh emulsions contained all the intact components, while *in vitro* digested samples presented a different structure and had enzymes and salts added to its composition. *In vivo* digested (*ex vivo*) treatments, being the serum collected from rats after they had been fed curcumin in the various formats, were expected to be the closest simulation to what would happen *in vivo*; however, no benefits against Aβ toxicity were observed, although gender differences noted. The use of *ex vivo* treatments in a cell assay such as this could offer an alternative to carrying out simulated digestions; it could also result in the use of animals in non-terminal procedures if only a small serum sample is needed. However, method optimisation would be needed for the results to be considered reliable as the rat serum produced unexpected effects in cell growth. Overall, all three types of treatment offered nutritious media for M17 cells to proliferate over 72 hours of incubation, and even promoted improved survival when compared to standard growth medium containing foetal calf serum.

7.2 Introduction

The two main hallmarks of AD are the extracellular deposition Aβ as senile plaques and the formation of intracellular neurofibrillary tangles, composed of hyper-phosphorylated forms of the microtubule-associated protein tau. Aβ-induced neurotoxicity has been suggested to commence synaptic loss and subsequent neuronal degeneration in AD. It is believed that 90% of the Aβ peptides consist of Aβ1-40 and Aβ1-42, with the latter being the most toxic (Murphy and LeVine, 2010, Selkoe, 2001, Tiwari and Kepp, 2016). In addition to Aβ research,

evidence suggests that oxidative stress plays an early role in AD pathogenesis (Zhu et al., 2004). Once accumulated, peptides and tangles disrupt synapses, creating inflammation, oxidative stress, and consequently loss of memory. Those damages tend to be irreversible and progressive; therefore, early diagnosis and intervention are important.

The recent medication Aducanumab (Aduhelm™), tested in a phase 3 clinical trial, has been shown to clear Aβ from the brain of AD patients and received accelerated FDA approval for the treatment of AD (Budd Haeberlein et al., 2022). However, there is no evidence that the drug can restore cognitive function. In addition, concerns about the drug's safety were raised, with 19% of patients developing microhaemorrhages. The drug is now only available for trials and not commercially available. New approval has been requested, as the manufacturer aims to make it available for those who wish to use it for early AD treatment (Salloway et al., 2022).

Since plaques can start accumulating up to 20 years before symptoms appear, prevention and change in modifiable risk factors have been advocated as the best strategy to delay the disease onset. Diet is a significantly impactful lifestyle for dementia and AD. Obesity and type 2 diabetes are considered risk factors for dementia and are correlated with abdominal fat and eating habits. Dietary interventions, such as the Mediterranean diet, have shown cognitive improvements in clinical trials for dementia. Its benefits are attributed to a high intake of fruits, vegetables and fish, all providing antioxidants and anti-inflammatory compounds. In addition to diets, individual food components with health-promoting properties, also called nutraceuticals, have been tested and gained interest in disease prevention (Cole et al., 2005a, Esposito et al., 2002, Frautschy et al., 2001, Otaegui-Arrazola et al., 2014).

Curcumin has potent antioxidant and anti-inflammatory activities and binds with Aβ peptides generated during the disease progression (Ammon and Wahl, 1991, Barry et al., 2009, Frautschy et al., 2001). Likewise, MCT from coconut oil and ω-3 from fish oil have been studied for their positive effects against AD (Bansal et al., 2019, Marina et al., 2009, Mirzaei et al., 2018, Cole et al., 2005a, Konagai et al., 2013, Shinto et al., 2014). A series of cell models have been used to test those compounds not only against AD biomarkers but also to assess anti-inflammatory and antioxidant properties (Baek and Cho, 2017, Liu et al., 2017, Sadli et al., 2013, Su et al., 2010, Thapa et al., 2013). The human neuroblastoma BE(2)-M17 cell model, for example, has been used to assess chronic oxidative stress caused by tau phosphorylation (Su et al., 2010), mitochondrial dysfunction (Sadli et al., 2013), neurotoxicity associated with hydrogen peroxide production (Taddei et al., 2010), and the effects of nutraceuticals, such as a

synergistic combination of DHA, luteolin and urolithin, against Aβ1–42-induced toxicity (Jayatunga et al., 2021).

Complex biological lipids such as sphingolipids and phospholipids define the structural properties of membranes and lipoproteins. They act as intracellular signalling molecules in biological processes, including development, regulation of cell growth, cross-membrane trafficking and adhesion. Metabolic and age-related diseases, stress responses and apoptosis are also related to complex lipids. They have gained attention due to their demonstrated beneficial effects, being suggested as potential constituents of cancer and AD treatment regimens and as health-favouring ingredients (Spitsberg, 2005a, Singh, 2006, Castro-Gómez et al., 2015, Gallier et al., 2015, García-Serrano et al., 2020, Jiménez-Flores et al., 2009).

As both curcumin and lipids may be bioactive in protecting against AD, it was of interest to determine whether their effects may be additive. Based on their beneficial health-promoting and antioxidative properties, curcumin encapsulated in emulsions prepared using functional oils and stabilized by MFGM phospholipids were tested for potential neuroprotective effects in countering Aβ-induced toxicity in human neuroblastoma BE(2)-M17 cells. The emulsions were tested in three formats: freshly prepared, *in vitro* digested and *in vivo* digested (*ex vivo* serum).

7.3 Materials and methods

7.3.1 Materials

BE(2)-M17 was obtained from ATCC® (CRL-2267™); synthetic amyloid-beta was purchased from the ERI Amyloid Laboratory, Oxford, United States; the 3-[4,5-dimethylthiazol-2-yl]-2,5 diphenyl tetrazolium bromide assay (MTS) CellTiter 96 AQueous One kit was obtained from Promega corporation, USA; 1,1,1,3,3,3-Hexafluoro-2-Propanol, DMSO, Ham's F-12, phenol red-free cell culture media, supplemented with 146 mg/L L-Glutamine, DMEM, F12, 0.25% Trypsin/EDTA, Hanks's balanced salt solution (HBSS) Gibco, Thermo Fisher Scientific - AU.

7.3.2 Methods

a) Cell culture

Human neuroblastoma BE(2)-M17 cells (M17), were maintained in T75 culture flasks containing 15mL of DMEM/F12 (1:1 ratio) media supplemented with 10% (v/v) foetal bovine serum (FBS), 2 mM L-glutamine, 4.5 g/L D-glucose and grown inside a humidified incubator with 5% CO2/95% air at 37°C. Cells were assessed daily during the week for population density. Upon reaching about 80% confluency, the cells were collected as described below and transferred to 96 well plates for viability assays or sub-cultured into fresh cell culture flasks. For all cell culture experiments, the passage number did not exceed 30. Whenever possible, single-use, sterile consumables including plates, flasks, culture medium, and other reagents were used. Other liquid, plastic, and glass materials and items were sterilised by autoclaving. All items were sprayed with 70% ethanol before placing them in the culture hood in order to reduce the chances of contamination. All cell culture procedures were carried out inside a laminar flow cell culture hood after ultraviolet light sterilisation.

The medium was removed from the flask, and previously warmed HBSS was added to wash the remaining DMEM/F12 media, always avoiding disrupting the cell film or touching the cells with the pipette. After a gentle "rinse", HBSS was removed from the flask, and 1 mL of 0.25% trypsin solution was added. The flask was then gently tilted to coat the cells on the growing surface and placed into an incubator for about 3 minutes to allow trypsin to dislodge the cells. After dislodgement, cells were washed off with about 4 mL of growth medium directly onto the cell growing surface; the serum in the growth medium neutralised the trypsin and prevented further enzymatic activity. The medium containing the cell suspension was mixed to break up large cell clusters while avoiding the formation of bubbles. Cells were then counted using a ViCell or haemocytometer.

The cell suspension was adjusted as needed to achieve the desired concentration of cells/mL and was then transferred to 96 well plates. Cells were plated at a density of 10,000 cells/well and allowed to attach for 24 hours before treatment. The remaining cells from the stock solution were added to a new culture flask and allowed to grow until reaching about 80% confluence.

b) Preparation of oligomeric amyloid-beta (Aβ) peptide

Oligomeric $A\beta_{1-42}$ was prepared according to the method of Stine et al. (2011) with some modifications. Briefly, a 1 mM Aβ solution was prepared by adding 1,1,1,3,3,3 hexafluoro 2 propanol (HFIP) directly to a vial containing lyophilized Aβ42 powder. 2.217 mL

HFIP was added to 10 mg peptide. After complete dissolution, the Aβ – HFIP solution was incubated at room temperature for at least 30 min. After incubation, the solution was transferred to 1.5 mL microcentrifuge tubes using a positive-displacement repeated pipetter in 100 µL aliquots (0.45 mg of Aβ42). The tubes were kept open, and HFIP was allowed to evaporate inside a fume hood overnight. The dried tubes were then transferred to a SpeedVac and dried for 1 h without heating to remove any remaining traces of HFIP and moisture. Dried peptide films were stored over desiccant in glass jars at −20°C until their use.

Peptide film was removed from the −20°C freezer and allowed to reach room temperature before use. A 5 mM Aβ DMSO stock was prepared by adding 20 µL DMSO to 0.45 mg Aβ42 peptide (2 µL to 0.045 mg Aβ42). Cold phenol-free F-12 cell culture medium was added to the freshly resuspended 5 mM Aβ42 in DMSO, diluting to a final concentration of 100 µM Aβ (0.25% DMSO). After adding F-12 medium, the solution was kept on ice, and prolonged exposure to light was avoided. Samples were incubated at 4°C for 24 h before being added to cells.

c) *In vitro* digestion and cell treatment

Emulsions were prepared according to the protocol described in 4.3.2.3, and their composition details are described in Table 7.1. Emulsions (5g) were digested *in vitro* following the *Infogest* protocol described in detail in 5.2.2.2. Gastric digestion was stopped by adjusting the pH to 8 to inactivate pepsin. Intestinal digestion was stopped by the addition of Pefabloc® to inactivate intestinal enzymes.

Table 7.1. Composition of emulsions systems

Code	Oil (20%)	MFGM fraction and concentration	Curcumin concentration
S1	MCT	MFGM1 - 5%	0.04%
S2	MCT:FO (1:1)	MFGM1 - 5%	0.02%
S3	MCT	MFGM2 - 3%	0.04%
S4	MCT:FO (1:1)	MFGM2 - 3%	0.02%
S5	MCT	MFGM3 - 3%	0.04%
S6	MCT:FO (1:1)	MFGM3 - 3%	0.02%

MFGM1 - Lipid700, MFGM2 - BPC50 GU09, MFGM3 - HFWPC70 (fractions with varying concentrations of MFGM PL MFGM1>MFGM2>MFGM3); curcumin (95.5% purity); MCT (Medium chain triglyceride oil - CocoMCT); FO (Fish oil).

Digested samples were diluted 10-fold in DMEM/F12 medium to help neutralizing bile salt toxicity through dilution before cell culture. Diluted samples were then filter-sterilised (0.2µm syringe filters) and added to DMEM/F12 media at varying concentrations.

Concentrations of 0.5% and 1% of the diluted digesta were selected based on toxicity tests and previous reports (Brodkorb et al., 2019, Gebhardt et al., 2019). Blood samples from rats orally fed with emulsions, control, free curcumin or Meriva were centrifuged, and serum was kept at -80ºC. Serum was then added to DMEM media at 1% concentration, filter-sterilised and used as a treatment for cells. The compositions of the cell treatments are shown in Table 7.2.

Table 7.2. Composition of cell treatment media

Treatments	Composition
Control	DMEM/F12 + 1% FBS
Fresh emulsions	DMEM/F12 + 0.5% OR 1% S1, S2, S3, S4, S5, S6
Digesta	DMEM/F12 + 0.5% OR 1% S1 digesta, S2 digesta, S3 digesta, S4 digesta, S5 digesta, S6 digesta
Rat serum	DMEM/F12 + 1% untreated group serum, Meriva group serum, EM 1 group serum, EM 2 group serum, Free curcumin group serum (all at 15, 30, 60 and 120min)

S1 (5% w/w MFGM1, 20% w/w MCT oil); S2 (5% w/w MFGM , 10% w/w MCT oil, 10% w/w fish oil); S3 (3% w/w MFGM2, 20% w/w MCT oil); S4 (3% w/w MFGM2, 10% w/w MCT oil, 10% w/w fish oil); S5 (3% w/w MFGM3, 20% w/w MCT oil); S6 (3% w/w MFGM3, 10% w/w MCT oil, 10% w/w fish oil); EM 1 (S1); EM 2 (S2); untreated (peanut butter, honey and maltodextrin). MFGM1 (Lipid700), MFGM2 (BPC50 GU09), MFGM3 (HFWPC70); curcumin (95.5% purity); MCT (Medium chain trygliceryde oil - CocoMCT); FO (Fish oil); Meriva® (Indena S.p.A.).

FBS was not added to the treatment media; 1% FBS in DMEM/F12 was used as control. After 24 hours, seeded plates with adherent cells were transferred to the cell culture hood and the DMEM/F12 + 10% FBS was carefully removed and replaced by 1% FBS media (control) or treatments (DMEM/F12 + 0.5%/1% emulsions and digesta, or DMEM/F12 + 1% rat serum). Each treatment was repeated at least in quadruplicate experimental replicates on the plates in addition to the biological replicates for emulsion preparation, digestion and rat treatments. Synthetic Aβ was added to treated and control cells and incubated for 72 hours. The viability of controls and treated cells, and controls and treated cells + Aβ, was then assessed.

The MTS CellTiter 96 AQueous One kit (Promega) was used to determine cell viability. A stock CellTiter 96 reagent was added (20 μL) to each treatment well and mixed by gently tilting the plate. The plate was then wrapped in foil and placed in the incubator for 4 hours per manufacturer instructions. The soluble formazan salt was quantified by reading the plate in a Perkin-Elmer plate reader with the 450 nm absorbance filter at room temperature. The average cell viability (%) was calculated by dividing the treatment absorbance values by the untreated absorbance values of each group and obtaining the mean, where the untreated value was considered 100%.

7.4 Results and discussion

7.4.1 Effect of non-digested and digested emulsions on cell proliferation

The amyloid precursor protein (APP) is a key factor in the pathogenesis of AD, and therapeutic approaches targeting Aβ are believed to end or reverse AD progression through inhibition of Aβ production, Aβ clearance, or neutralisation of its neurotoxicity (Taddei et al., 2010). In this study, I assessed whether the emulsion systems (fresh, *in vitro* or *in vivo* digested) improved cell proliferation and protected against Aβ-induced neuronal toxicity as assessed by the MTS assay. The MTS assay is an improved version of the MTT assay, a simple colorimetric test of cell proliferation and survival used to determine relative numbers of viable or metabolically active cells (Mosmann, 1983). In the MTS assay, the mitochondrial reduction of salt by dehydrogenase enzyme generates a coloured formazan product that can be read directly at 495 nm (O'Toole et al., 2003), with the absorbance generally corresponding to metabolic cellular activity present in a linear fashion.

A one-way ANOVA was conducted to assess whether the emulsions and the control differed in their effect on M17 proliferation *in vitro* (Figure 7.1). Both fresh and digested emulsions differed from the control for at least one treatment ($p<0.001$). Based on individual *t-tests* for comparison of means, fresh emulsions S5 and S6 were significantly higher than control for both 0.5 and 1% concentrations ($p=0.006$; 0.028; 0.000, 0.000), while S4 was significantly higher only at concentration of 0.5% ($p=0.01$) and S3 at 1% ($p=0.001$). Additionally, S6 was significantly higher than all other emulsions for both concentrations; in fact, viability for this treatment was doubled. Considering that S5, which used the same emulsifier as S6, presented results similar to other treatments, it is difficult to conclude that the improved effect of S6 fresh emulsion can be attributed to the MFGM3. Likewise, other emulsions using combined MCT and FO showed significantly lower viability, and it is unlikely that the oil contributed to the marked improvement in S6 system. However, it cannot be ruled out that accelerated proliferation or metabolic activity occurred due to synergy between micronutrients in the combination of MFGM3 and fish oil that were present in the fresh preparation but lost to the digestion process, as this was the unique factor of S6. It is less likely that the unique combination of factors and processing resulted in the production of a compound that artificially inflated the colourimetric measurement of those wells.

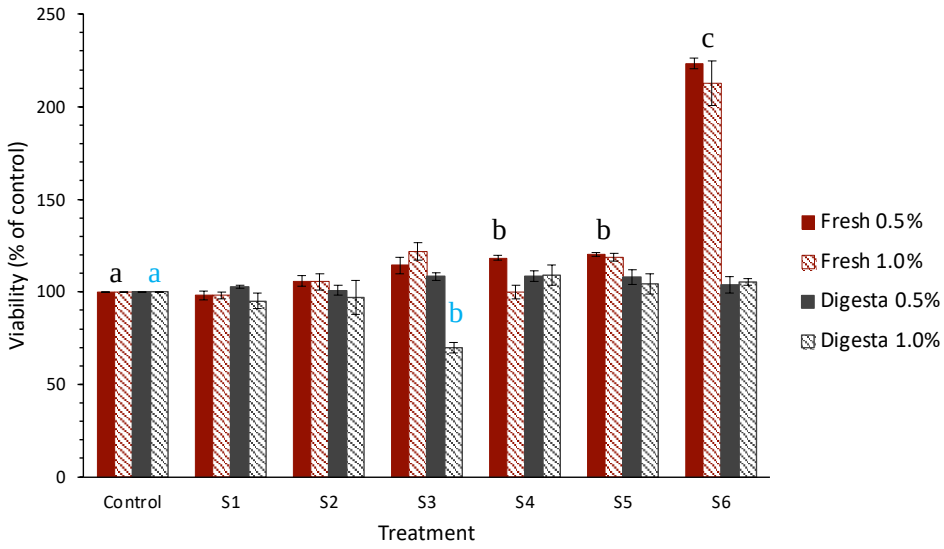

Figure 7.1. Effect of emulsion systems on M17 cell viability after 72 hours incubation at 0.5 and 1% concentration in DMEM/F12 as a replacement for FBS. Viability was calculated as the percentage of control (FBS) using MTS. Different black letters represent differences between control and treatments at 0.5% concentration, while different blue letter represent differences between samples treated at 1% concentration. Unmarked treatments did not differ from control. S1 (5% w/w M1, 20% w/w coconut oil); S2 (5% w/w M1, 10% w/w coconut oil, 10% w/w fish oil); S3 (3% w/w M2, 20% w/w coconut oil); S4 (3% w/w M2, 10% w/w coconut oil, 10% w/w fish oil); S5 (3% w/w M3, 20% w/w coconut oil); S6 (3% w/w M3, 10% w/w coconut oil, 10% w/w fish oil).

As opposed to fresh emulsions, digested emulsions did not improve overall cell viability, with S3 treatment at 1% presenting significant lower viability compared to control ($p=0.000$). All the other emulsions were statistically equal to control cells treated with FBS (Figure 7.1). More nutritional components could explain the differences in viability in the cells in the fresh emulsions treatment. The *in vitro* digestion protocol includes the addition of enzymes that alter the structure of emulsions, such as the disruption of the thin emulsifier layer created around the oil droplets in fresh emulsions. The digesta has been submitted to high-speed centrifugation before the dilution in cell media to remove any undigested solids and oil, resulting in a clear micellar phase containing the soluble digested materials, including micelles containing curcumin.

There are few studies which have used digested materials on cell models, and these are limited mainly to use with human intestinal cells (Caco-2) for determination of transmembrane crossing and delivery of compounds to the blood stream. For instance, a study used vegetable protein isolate to stabilise emulsions and encapsulate conjugated linolenic acid. The researchers treated Caco-2 cells with the micelle obtained from *in vitro* gastrointestinal digestion of emulsions and found that encapsulation improved the delivery of conjugated linolenic acid across Caco-2 cells when compared to free conjugated linolenic acid. Before addition to the cells, the emulsions were diluted (1:40 v/v), which represents a total of 2.5% of the digested

material in the treatment media (Fernandez-Avila et al., 2016). Another study used *in vitro* digested material to assess the influence of the solubilisation of curcuminoids in a liquid formulation containing a high content of phosphatidylcholine on the transport of the curcuminoids across a Caco-2 cells. The authors found that the solubilisation in the phospholipid concentrate significantly increased curcuminoids transport across the Caco-2 cells. For our study, digesta concentrations of 0.5 and 1% were used for cell treatment based on preliminary tests and the results observed by the authors mentioned above (Gebhardt et al., 2019).

To better understand the effect of the different components in the emulsions systems, a 4-way ANOVA was conducted to assess the effect of oil, emulsifier, concentration and treatment plus their interactions on cell viability. All factors significantly affected cell viability ($Pr>F <0.001$), indicating that at least one sample was significantly different from the others for all factors (Figure 7.2). The interaction of oil, emulsifier, concentration and treatment was significant, indicating that the observed differences for one factor were dependent on the combination of other factors. The interactions of concentration and treatment ($Pr>F$ 0.0931) and emulsifier, concentration and treatment ($Pr>F$ 0.1500) were not significant, indicating that concentration was not as significant in influencing the changes in cell viability when compared to treatment, oil and emulsifier. Furthermore, a significant interaction of oil and emulsifier was also observed, indicating that differences in emulsion compositions were responsible for differences in cell viability (Figure 7.2).

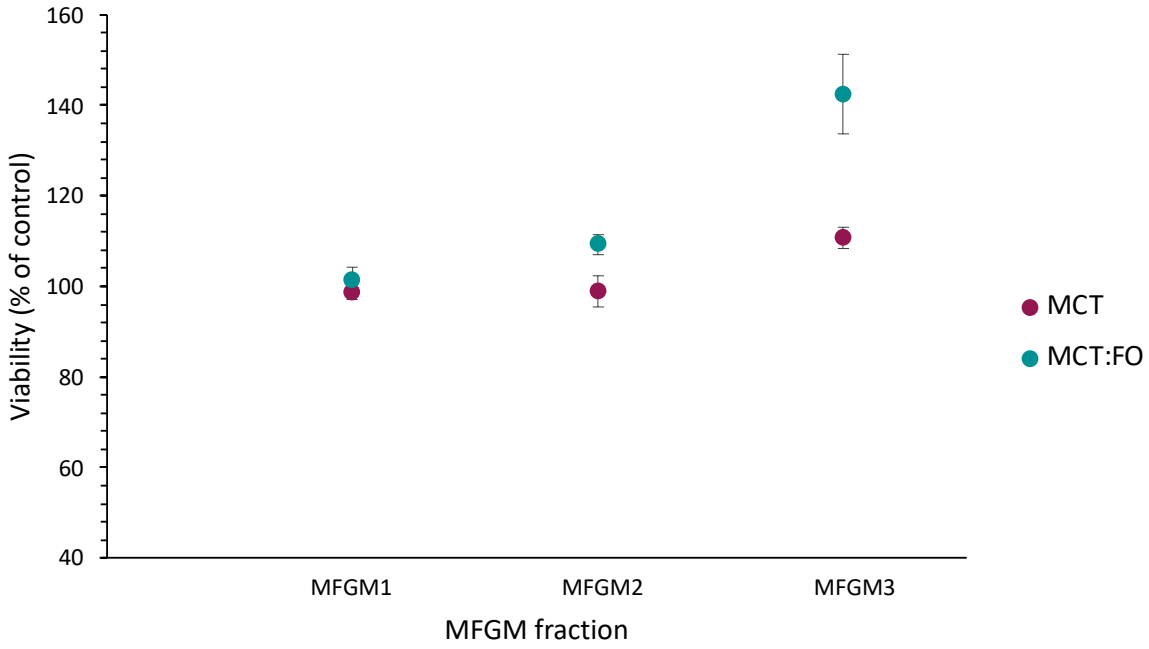

Figure 7.2. Effect of oil and emulsifier on M17 cell viability after 72 hours incubation in DMEM/F12 as a replacement for FBS. Viability was calculated as the percentage of control (FBS) using MTS. S1 (5% w/w M1, 20% w/w coconut oil); S2 (5% w/w M1, 10% w/w coconut oil, 10% w/w fish oil); S3 (3% w/w M2, 20% w/w coconut oil); S4 (3% w/w M2, 10% w/w coconut oil, 10% w/w fish oil); S5 (3% w/w M3, 20% w/w coconut oil); S6 (3% w/w M3, 10% w/w coconut oil, 10% w/w fish oil).

As shown in Figure 7.2, the cell viability for combined MCT and FO was significantly higher than MCT alone ($p<0.000$), suggesting improved cell proliferation, metabolic activity, and/or survival under nutrient-insufficient conditions, any of which could be potentially associated with the beneficial properties of ω-3 fatty acids for cell plasticity. MFGM3 was significantly higher ($p<0.000$) than MFGM1 and MFGM2, which were not statistically different between them ($p=0.1883$). Viability for non-digested samples and 1% concentration were also significantly higher than digests at 0.5% ($p<0.000$). Those differences can be attributed to the strong effect of S6 on cell viability for non-digested emulsions. Fresh emulsions did not present any detrimental effect in cell viability, while their corresponding digested materials did. Using higher concentrations of digesta could lead to improved viability; however, dilutions are paramount to neutralising the potential harm from enzymes, bile salts and other salts. Furthermore, high concentrations of curcumin have been observed to be cytotoxic and to induce apoptosis. Huang and collaborators for instance evaluated the effect of curcumin in adrenocortical carcinoma cells (SW-13) and found that even at 10μM curcumin caused reduction of cell viability. At 50μM curcumin promoted a reduction of 50% in cell viability (IC50). The authors also showed that curcumin induced apoptosis in a concentration dependent manner (Huang et al., 2021).

The M17 human neuroblastoma cell line has been used in several reported studies as a model to study neurotoxicity (Andres et al., 2013) and represents within the published literature a relevant *in vitro* tool for screening new therapeutic agents targeting APP metabolism. However, there is no evidence for the use of digested materials in this neuronal cell model to the best of our knowledge. Therefore, in this study, I aimed to assess if the soluble digested components would improve cell proliferation and assist in Aβ toxicity protection, and if this method could potentially be used as a screening tool for the efficacy of delivery systems against biomarkers.

7.4.2 Effect of non-digested and digested emulsions against Aβ-induced toxicity

Aβ is the toxic peptide formed due to the improper cleavage of APP, and it is present in the brains of people with AD. This peptide is toxic and cannot be eliminated by the body. It also has the property of being sticky, so it accumulates in the form of plaques outside the neurons. Aβ interacts with a wide range of neuronal receptors. The interactions between Aβ and receptors activate cascades that culminate in neuroinflammation, oxidative stress and disruption of signalling pathways (Ferreira et al., 2014). An extensive review on the use of Aβ oligomers in cellular models of AD conducted by Fontana and collaborators provides more details on the effect of endogenous and synthetic Aβ *in vitro*, including in the M17 cell line (Fontana et al., 2020).

A concentration of 20uM Aβ is standard in the protocol followed (Stine et al., 2010) and was used for fresh emulsion systems and digesta assays. Aβ significantly reduced cell viability, and batches were retained and used after they were demonstrated to cause at least 40% toxicity (

Figure **7.3**). The concentration of 25 µM was significantly more toxic to cells.

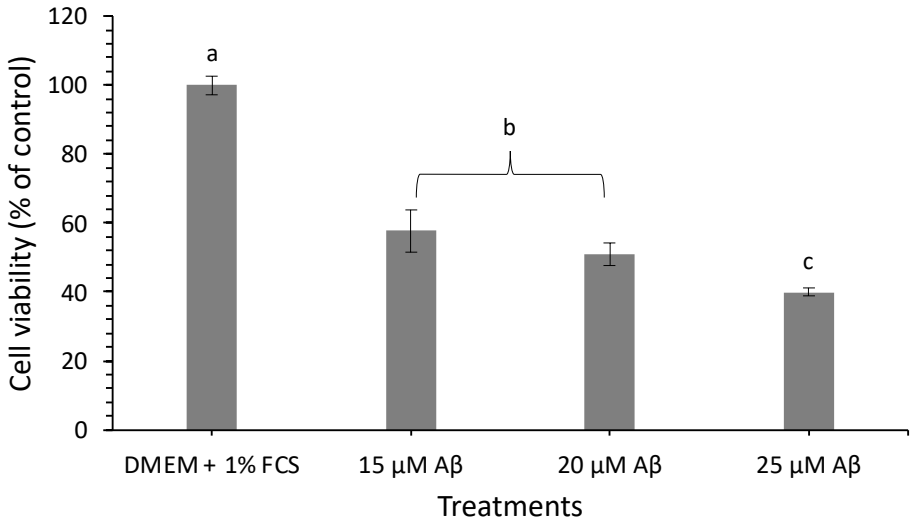

Figure 7.3. Cell viability for *M17* cells treated with Aβ at different concentrations (15, 20, 25uM) over 72 hours incubation. Viable cells expressed in percentage of control. Control: DMEM/F12 media + 1% FBS. Different letter represent significant differences between samples ($p<0.05$).

While higher concentrations of Aβ would likely be more cytotoxic, using such a dose would reduce the chance for a test treatment to provide protection and allow cells to overcome Aβ-induced toxicity. Conversely, a lower concentration of 10 µM has been reported to induce mitochondrial dysfunction but to not alter cell viability (Sadli et al., 2013). Therefore, a concentration of 20 µM was selected, which significantly affected toxicity, yet should also allow the treatments to reverse or alleviate the effects of Aβ. In addition, since the emulsion systems studied are intended as a potential preventative intervention, the amount of Aβ to be cleared from the brain would still be lower than what is found in more severe cases of the disease.

Synthetic Aβ is used to provide toxicity to cells, allowing *in vitro* assessment of drugs' and compounds' potential benefits against AD. The Aβ used in this study is a highly static lyophilised powder which is soluble in polar solvents that exhibit strong hydrogen bonding, such as HFIP. The weighing of precise amounts of the powder is challenging, and inconsistencies between aliquots were often observed. Aβ should ideally promote around 50% reduction in viability for FBS-treated cells; however, I found many challenges in obtaining such toxicity in this study. Each batch of Aβ produced was tested, kept in -30°C inside air tight container and used within four weeks. Even when a batch was toxic to control (FBS) treated wells in the toxicity test, they did not necessarily cause the same toxicity in subsequent treatment plates, with many plates and/or wells showing no toxicity to Aβ (Figure 7.4).

There are no reports in the literature of this assay being so poorly reproducible, so it cannot be determined whether this is an unreported but oft-observed aspect of this assay or whether the Aβ used in this project was particularly problematic. However, for example, (Barr et al., 2016) stated in their methods section that both MTS and Lactate Dehydrogenase (LDH) release were used to determine viability and cell function; the LDH data are shown but the MTS data are not. In this report it is simply stated in the results that "the neuroprotection of the candidate peptides was confirmed using MTS". The variable results in the current study may also be influenced by retinoic acid, which is present in MFGM and has been shown to significantly alter M17 cell differentiation, morphology and function (Andres et al., 2013). It has also been suggested that the temperature and incubation time for preparing Aβ solutions prior to use in culture can impact peptide aggregation and availability (Sadli et al., 2013). Finally, the concentration of Aβ used to induce cytotoxicity ranges from 1 µM (Gu et al., 2022) to 5 µm (Wang et al., 2017) to 10 µm (Sadli et al., 2013) to 20 µM (Dong et al., 2019). Further controversy can be seen in the conflicting claims that one group found 10 µM Aβ treatment did not reduce cell viability (Sadli et al., 2013), while another group showed that 5 µM reduced viability by ~40% (Berry et al., 2018). Taken together, these facts demonstrate that this assay may be inadequately standardised and requires further study and optimisation, although at this time there is no better option available.

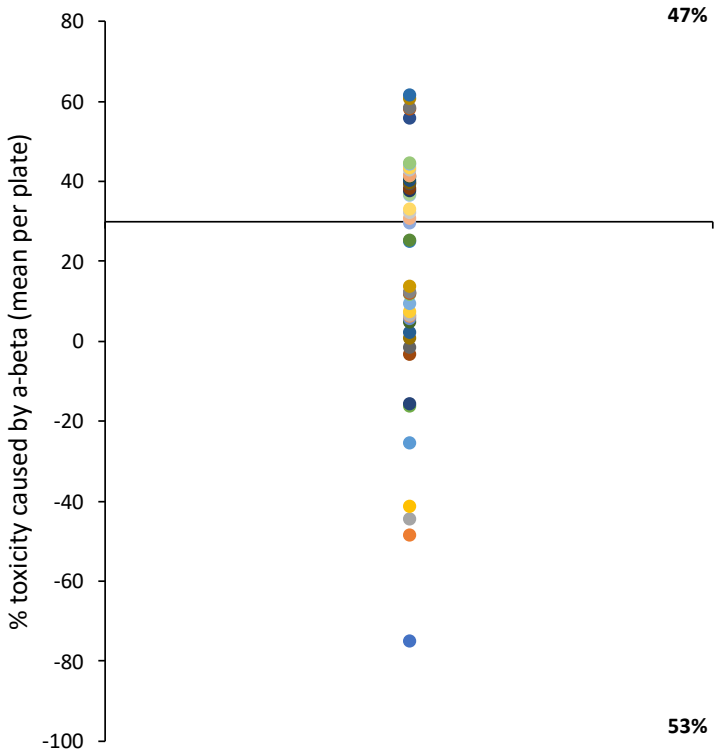

Figure 7.4. Graphical representation of data above and under toxicity threshold. Data from plates above line have been kept for the final analysis, while those below have been excluded. Different coloured "dot" represents a plates used for toxicity calculation. Viability of FBS treated well was assumed to be 100%, therefore, toxicity was calculated as 100 (FBS) – viability of a-beta treated wells.

The average Aβ toxicity for fresh and *in vitro* digested emulsions was 20% (± 2.12). Ideally, higher toxicity should be obtained, and data where significant toxicity was not achieved was excluded. Due to limitations of sample and time, those assays could not be repeated, and data were kept for initial assessment and screening of treatments against Aβ-induced toxicity. Even with low toxicity, significantly higher cell proliferation was observed for most treatments.

Individual t-tests were conducted for both non-digested and digested emulsions and their effect on cell viability after exposure to Aβ (Figure 7.5). Non-digested systems showed higher viability than those submitted to *in vitro* digestion before cell treatment. For non-digested systems, S1 at both 0.5 and 1% ($p=1.000$ and 0.999) and S4 at 1% concentration ($p=1.000$) were equivalent to the control. S4 at 0.5% had significantly lower viability as compared to control. All the other systems showed significantly higher viability than the control, with S2 at both concentrations being higher than all the other treatments. This suggests that these components both blocked the cytotoxic activity of Aβ and provided additional nutrients to support cell proliferation.

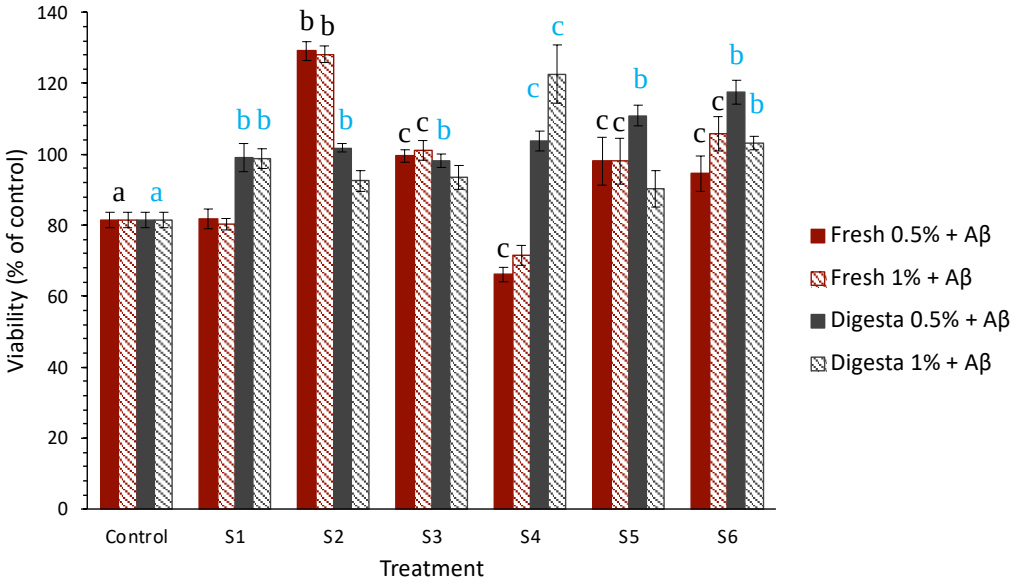

Figure 7.5. Effect of emulsion systems on cell viability after Aβ-induced toxicity over 72 hours incubation at 0.5 and 1% concentration in DMEM/F12 as a replacement for FBS. Viability was calculated as the percentage of control (FBS) using MTS. Different black letters represent differences between control and treatments at 0.5% concentration, while different blue letters represent differences between samples treated at 1% concentration. Unmarked treatments did not differ from control. S1 (5% w/w M1, 20% w/w coconut oil); S2 (5% w/w M1, 10% w/w coconut oil, 10% w/w fish oil); S3 (3% w/w M2, 20% w/w coconut oil); S4 (3% w/w M2, 10% w/w coconut oil, 10% w/w fish oil); S5 (3% w/w M3, 20% w/w coconut oil); S6 (3% w/w M3, 10% w/w coconut oil, 10% w/w fish oil).

Interestingly, once emulsions were digested, S4 at 1%, which had no effect on viability when applied freshly to cells, showed the greatest improvement against Aβ-induced toxicity and S2 at 1% showed no improvements against Aβ after *in vitro* digestion when compared to control (p=0.650). S3 and S5 at 1% were also equal to the control for digested emulsions. All the other treatments significantly improved cell survival after exposure to Aβ. To further understand the effect of factor on Aβ-induced toxicity, a 4-way ANOVA was conducted and it was observed that the concentration factor, of either 0.5 or 1% (Pr>F 0.2186), was the only factor with no significant effect on cell viability. The interactions of oil and treatment (Pr>F 0.7465), concentration and treatment (0.1784), oil, concentration and treatment (Pr>F 0.4358) and the interaction of all factors (Pr>F 0.204) also had no effect on cell viability for Aβ treated cells. However, there was a significant interaction between emulsifier and concentration (Pr>F 0.000), indicating that the composition of emulsions was significant in the differences observed among treatments (Figure 7.6). Overall, non-digested samples promoted higher viability (p=0.002). Digested emulsions composed of MCT and FO presented higher viability than those containing only MCT. MFGM3 was statistically higher than MFGM2 (p=0.004) yet showed no differences from MFGM1 (p=0.118). MFGM1 and MFGM2 also presented no significant differences among them.

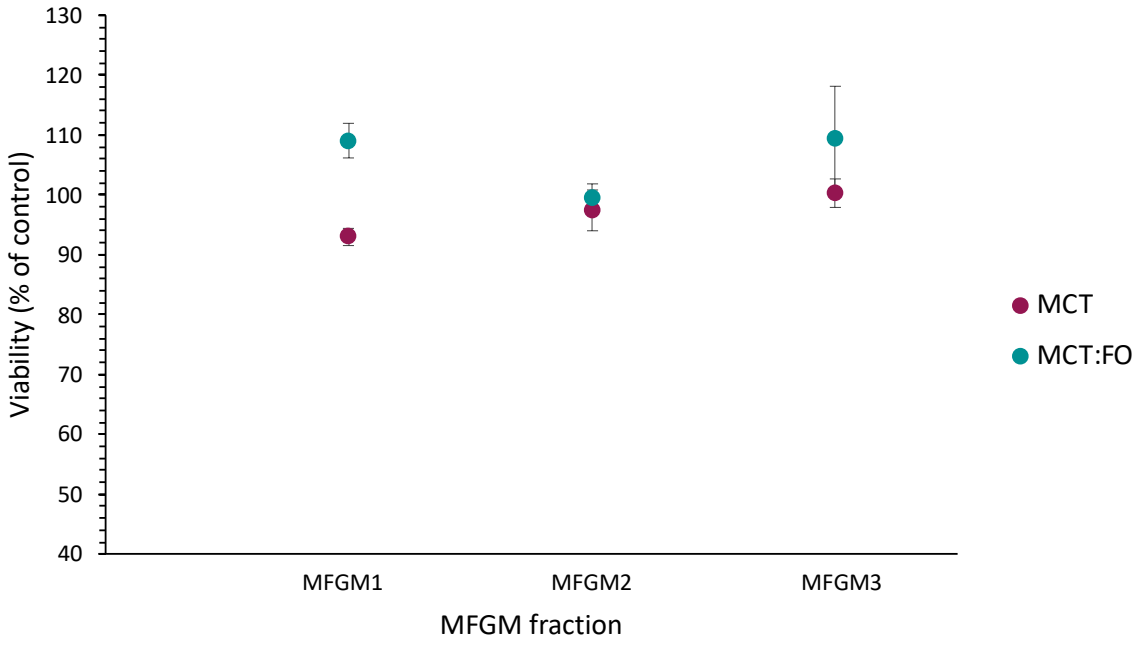

Figure 7.6. Effect of oil and emulsifier on cell viability after Aβ-induced toxicity over 72 hours incubation in DMEM/F12 as a replacement for FBS. Viability was calculated as the percentage of control (FBS) using MTS. S1 (5% w/w M1, 20.0% w/w coconut oil); S2 (5% w/w M1, 10.0% w/w coconut oil, 10.0% w/w fish oil); S3 (3% w/w M2, 20.0% w/w coconut oil); S4 (3% w/w M2, 10.0% w/w coconut oil, 10.0% w/w fish oil); S5 (3% w/w M3, 20.0% w/w coconut oil); S6 (3% w/w M3, 10.0% w/w coconut oil, 10.0% w/w fish oil).

These findings demonstrated that different MFGM preparations resulted in highly different outcomes, suggesting that emulsion and other preparations incorporating MFGM must be carefully selected and assessed. I further observed that the treatment of *in vitro* digestion significantly impacted the effect of treatments on Aβ-induced toxicity, suggesting that the use of digesta on the assessment of biomarkers *in vitro* does not reflect its activity in its natural initial format. Overall, emulsions prepared using fish oil rich in the ω-3 fatty acids DHA and EPA showed improved protection compared to MCT alone.

ω-3 fatty acids have been previously associated with improvements in AD. For instance, a study conducted to identify the effects of ω-3 in patients with MCI used a supplement which contained 1000 mg of DHA and 1000 mg of EPA and found that ω-3 increased Aβ phagocytosis by macrophages. The authors also conducted *in vitro* assays using emulsions prepared with the same fish oil on macrophage cells collected from consecutive patient visits. Overall, the results obtained from the study suggest that fish-derived ω-3s may induce innate immune system pathways that increase Aβ phagocytosis and protect against apoptosis, thus repairing the clearance of Aβ in the AD brain (Olivera-Perez et al., 2017).

In addition to being selected for their anticipated protective effects against AD-induced neurotoxicity, the emulsions in this research were developed to assist membrane crossing, specifically the blood-brain barrier (BBB), for improved delivery of curcumin to the brain. Increasing evidence suggests that phospholipids from MFGM are key for the brain development in infants. Studies found that MFGM-supplemented diets supported brain development in piglets (Fil et al., 2019), and that the combination of commercial concentrated milk phospholipids and coffee polyphenols reduced mortality and preserved long-term memory in SAMP8 mice (Unno et al., 2022). Unno et al. stated that the mechanisms of MFGM phospholipids assisted in the aging process of the brain, yet they somehow improved the effect of polyphenols. Therefore, in this study, emulsions prepared using the more purified MFGM material containing no proteins and high concentrations of phospholipids was selected, with the intention to support membrane crossing and boost not only delivery of curcumin encapsulated in functional oils, but also the effects of MFGM in brain health. Emulsion systems 1 and 2 contained 5% of this MFGM fractions and showed improved curcumin bioaccessibility as reported in Chapter 5. Emulsion 2, which contained FO combined with MCT, also showed promising bioactivity against Aβ-induced toxicity in M17 cells.

7.4.3 Effect of serum of rats fed formulations on cell proliferation

Although *in vitro* gastrointestinal digestion provides the breakdown of macromolecules, there is no metabolite formation. For instance, while enzymes used during *in vitro* digestion promote the breakdown of protein and fat, they do not convert curcumin into its metabolites. Since most orally ingested curcumin is transformed into CG and CS, and it is these metabolites in the circulation that would interact with cells in the body, I proposed using *in vivo* digested samples to assess the potential effect of curcumin on cell survival. Rats were fed either free curcumin or curcumin encapsulated inside MCT and fish oil stabilised by high phospholipid MFGM fraction as emulsifier (previously selected emulsion systems S1 and S2). I hypothesised that higher concentrations of phospholipids, such as phosphatidylcholine and sphingomyelin, could improve the delivery of curcumin through the blood-brain barrier (BBB) and boost protective effects against AD. The selected emulsions, a commercial bioavailable formulation and free curcumin were fed to Sprague-Dawley rats, and data on curcumin absorption, retention, and distribution were presented in Chapter 6.

Serum was collected from the rats at the time of cull (15, 30, 60 and 120 minutes post-prandial), and these serum samples were added to cell culture medium for assessment in the

Aβ-challenged M17 cell assay. To the best of our knowledge, the use of serum from rats or other animals fed with formulations of interest have not been used in any cell assays. There are limited reports of studies which used human cells rather than serum for similar purposes; for example, *ex vivo* assays were conducted on macrophage cells collected from patients diagnosed with mild cognitive impairment and tested for Aβ phagocytosis after treating the cells with emulsions prepared using ω-3 rich oil and resveratrol (Olivera-Perez et al., 2017). Similarly Mizwicki and collaborators tested the immune modulators 1α,25(OH)2-vitamin D3 (1,25D3) and resolvin D1 (RvD1) in peripheral blood mononuclear cells (PBMCs) of AD patients compared to normal controls (Mizwicki et al., 2013). This group concluded that 1,25D3 and RvD1 *in vitro* rebalanced inflammation to promote Aβ phagocytosis, and suggest that low vitamin D3 and DHA intake could contribute to AD onset. However, our approach to identify if the serum of rats fed with formulations would provide protection against cytotoxicity in M17 cells was completely novel and thus neither the outcome nor the optimal assay conditions could be predicted.

Serum from a control rat fed a treat with no curcumin, serum from a treatment-fed rat (EM2 at 60 min), and standard FBS were assessed at a series of concentrations to determine the optimal concentration to use. Cells were incubated for 72 hours with the treatments. After the incubation period, optical density was measured using the MTS assay to determine whether rat serum affected cell proliferation or viability. Although higher serum concentrations provided higher optical density, there were no significant differences between the lowest and higher concentrations (1 and 10%) for FBS and control serum treatments ($p = 0.1389$ and 0.1631), as shown in Figure 7.7. On the other hand, cells treated with serum from the emulsion-fed rat had higher optical density, even when present at 1%, compared to FBS and serum from control rats ($p = 0.00396$ and 7.81E-06, respectively).

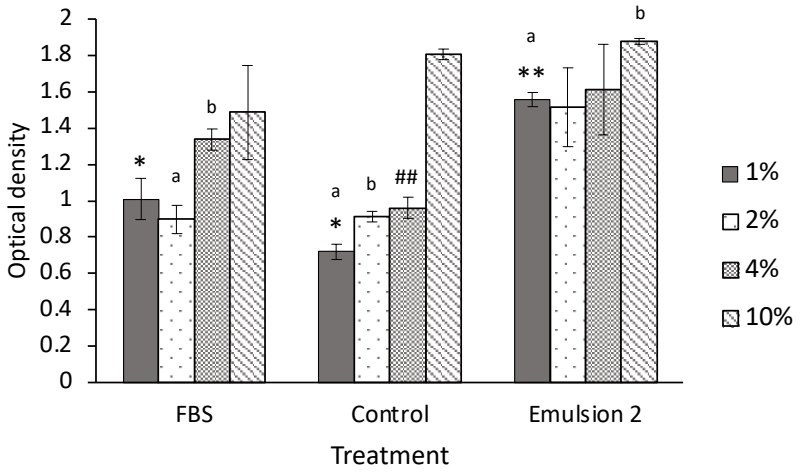

Figure 7.7. The optical density, equating to cell viability, after FBS or serum treatment with control and emulsion 2 treatment rat serum samples, was assessed to determine optimal working concentrations in M17 cells. Different letters indicate differences in concentration within a treatment, while symbols represent differences between treatments at the same concentration after ANOVA and Bonferroni corrected t-test.

In this assay, 10^4 cells are plated per well to ensure that, after the expected cytotoxicity caused by Aβ treatment, there are enough metabolically active cells to obtain a measurable and valid optical density reading. However, in the absence of Aβ treatment, limiting cell proliferation over the 3-day incubation period is necessary. This cell line has a doubling time of 20 to 24 hours (American Type Culture Collection [ATCC], 2022); thus, over 3 days in a nutritionally-replete medium, the number of cells would be expected to reach >8 x 10^4. According to manufacturer, the wells of a 96-well plate have a surface area of 0.32 cm^2 and are unlikely to be able to accommodate >4 x 10^4 adherent cells. It is likely that the use of serum at 4% and 10% might result in rapid proliferation, causing nutrient depletion, consequently insufficient surface area to support the cell numbers, and finally, induction of apoptosis. For this reason, and to limit the apparent proliferative effect of the emulsion-fed serum treatment, and to match the assay conditions used to test the fresh and post-simulated-digested emulsion preparations described earlier in the chapter, a concentration of 1% for all serum samples was utilised for subsequent assays.

The optical density of FBS-treated cells was set to be 100%, and treatments' viabilities were normalised as a percentage of FBS control. The factors of sex, post-prandial time and curcumin treatment were analysed using a 3-way ANOVA. There was no effect of time on cell viability. However, the results indicated a surprising significant interaction between sex and treatment (Pr>F <0.0001; Figure 7.8), so data from female versus male rats were considered separately. The gender differences may be attributable to hormonal differences between sexes that could interact or interfere with cell proliferation or the assay; alternatively, there may be

sex-related differences in how males versus females digest, absorb, and metabolise curcumin or other dietary compounds that ultimately present macro- and micro-nutrients in the serum to the cultured cells. The influence of sex on liver metabolism has been reviewed elsewhere; according to findings it seems like female metabolism significantly differs from males given the role of liver function in the control of metabolism. The authors suggested that female mammals hepatic cells were able to modify, or evolve, their metabolism in relation to the host's reproductive status, with oestrogen playing a role. On the other hand male mammals were not subjected this hormonal and evolutionary pressure, thus, leading to significant divergence between female and male liver functions (Maggi and Della Torre, 2018). These hypotheses could not be verified as the premise was beyond the scope of the thesis, but it would be of interest to explore further and should be considered in future study designs.

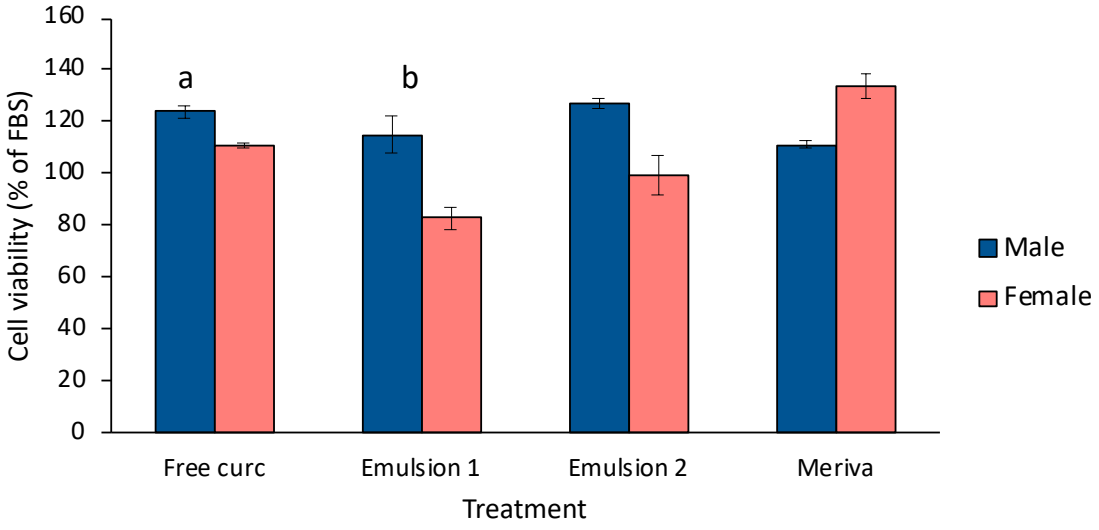

Figure 7.8. Effect of treatment and gender on the viability of M17 cells treated with serum from rats fed free or encapsulated curcumin. Data from time points within a treatment were pooled and are shown as mean ± SEM. Different letters show statistical differences between treatments ($p<0.05$).

Cells treated with serum from free Curc and Meriva®-treated rats showed improved cell viability compared to FBS-treated cells for both male and female rats (Figure 7.9). In contrast, emulsions showed such improvement only for cells treated with male rat serum, except for EM2 at 60 min showing improved viability for female treated cells. Post-hoc comparisons of the main effect indicated that the cell viability of Meriva® and free Curc were higher than control. At the same time, no differences were observed between emulsions 1 and 2 and the control. However, EM2 was higher than EM2 and did not differ from Meriva® and free Curc. Those results suggest that free curcumin and Meriva® provided a more desirable growth environment for M17 cells at 1% concentration. Emulsions differed from free Curc and

Meriva® treatments in their oil composition. While oil is believed to increase the delivery of curcumin, its presence in the serum of rats might have created a less desirable medium for cells to proliferate. Overall, serum from males provided significantly higher mean cell viability compared to female serum treated (<0.0001). However, for Meriva® treated cells at 60 min, female rat serum showed higher viability, hence the association between treatment and sex (Figure 7.9).

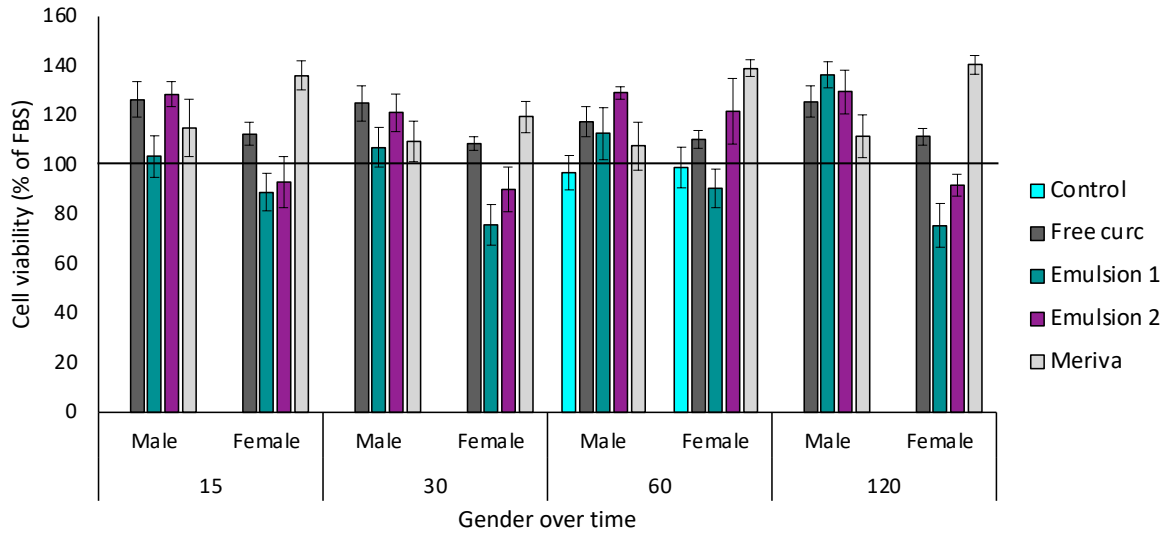

Figure 7.9. Cell viability normalised to FBS treated control wells, which were set at 100% (black horizontal line), for test wells with rat serum samples collected 15 – 120 minutes after ingestion of different curcumin treatments. Serum were added at 1% concentration to DMEM/F12 cell culture medium. Errors bars represent SEM and ANOVA results are described in the text.

7.4.4 Effect of serum from rats fed formulations against AB-induced toxicity

In addition to the effect of rat serum on cell proliferation as a supplement to the culture medium, their effect against the toxic Aβ peptide was also assessed. I faced challenges to reach Aβ toxicity *in vitro* as only half of the plates presented toxicity of at least 30%, as discussed earlier and shown in Figure 7.4. In the assays testing freshly prepared emulsions and *in vitro* digested emulsions all data were retained due to number of repetitions and limitations of sample and time. For the *in vivo* digested *ex vivo* serum samples on the other hand, the higher number of repetitions allowed for a selection of plates where Aβ cause toxicity of at least 30%. Therefore, data on the effect of fresh emulsions vs *in vitro* digest vs *in vivo* digested could not be reliably compared. However, the conclusions and outcomes from *in vivo* digested treated assays explore their potential effects and use as a screening method.

The average toxicity among all FBS wells for all treatments, including both below and above the selected threshold, was 20 +/- 2%. This indicates that, on average, the addition of

Aβ did not cause toxicity at the level expected and desired, making it difficult to determine if the treatments had an effect on cell survival under conditions of stress. After excluding data from wells where no toxicity was achieved, the viability and toxicity were calculated for each well, using the FBS mean for the specific treatment rather than the overall FBS mean. It is important to note that even for plates where FBS control wells did not show enough toxicity, treatment wells on the same plates often did. Similarly, plates where FBS was toxic seemed not to have caused toxicity for treated cells. The most expected and desirable conclusion would be that the treatments protected cells in plates where FBS-treated wells presented toxicity, but treated ones did not. However, since I also observed that even though Aβ did not cause toxicity for FBS, it did for treated wells, this conclusion cannot be drawn. Rather, it must be accepted that this assay is poorly reproducible across wells within a single plate, as discussed earlier.

Treatment (Pr>F 0.0001), time (Pr>F 0.0129), and gender (Pr>F 0.0045) had significant effects on the loss in viability induced by Aβ toxicity (Figure 7.10). An interaction between treatment and time (Pr>F 0.0042) was also observed, indicating that the efficacy of Aβ toxicity in the presence of rat serum is dependent on the time post-feeding and post-digestion that the serum sample was collected. Due to data under the threshold being excluded, some parameters had a small n, and to overcome this some data were pooled together for additional analysis.

Viability for cells in FBS-containing medium challenged with Aβ peptide was 60% on average, indicating that Aβ promoted 40% cytotoxicity. None of the treatments were efficient in promoting extra protection to cells exposed to Aβ, with no differences observed between treatments and control. However, the viability of free Curc-treated wells was significantly higher than serum samples from rats fed Meriva® and emulsion treatments. Interestingly, as opposed to the viability of treatments without Aβ, cells exposed to Aβ and treated with serum from female rats showed higher viability, indicating they induced less toxicity than male rats' serum (Figure 7.10). Sera from 60 min presented significantly higher viability than sera from 15 min, but no other differences were observed across other time points. Interaction of treatment and time indicates that improved viability for free Curc-treated cells was dependent on time, showing a significant increase at 60 and 120 min.

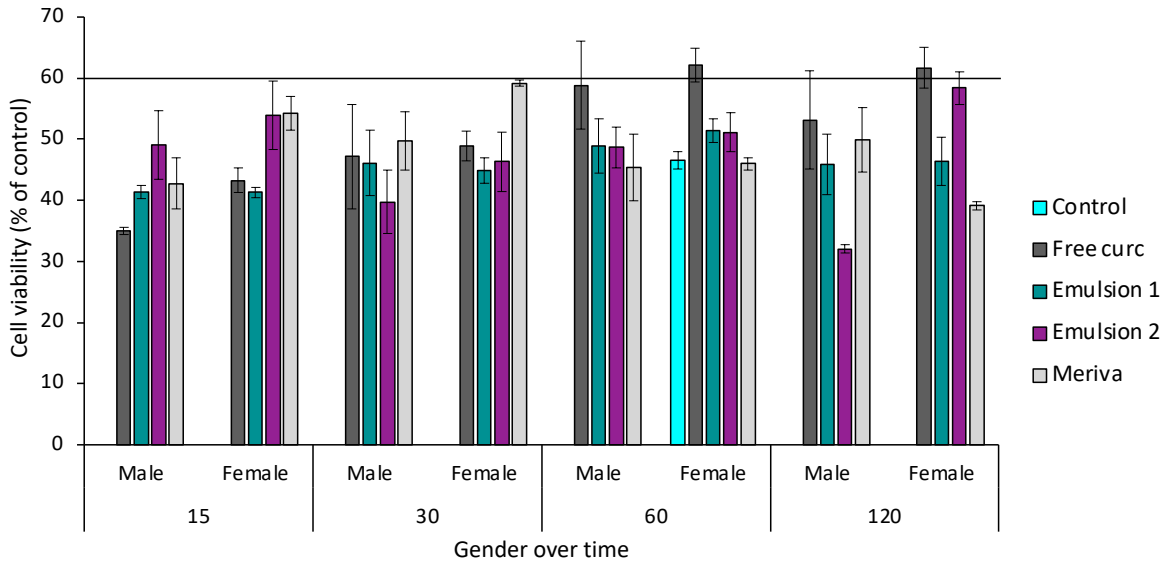

Figure 7.10. Cell viability as a percentage of FBS treated cells over time for different treatments added at 1% concentration to DMEM/F12 cell culture media. Line represents average toxicity for FBS treated cells exposed to Aβ. Errors bars represent SEM and ANOVA results described in the text.

Since time and treatment had a significant interaction by ANOVA analysis, to increase statistical power gender was excluded from the factors, and both males and females were combined to assess the effects of time and treatment, and the data were graphed (Figure 7.11-a). In addition, since gender seemed to have imposed significant differences, another analysis was run to identify the effect of treatment and gender (Figure 7.11-b).

Both treatment (Pr>F 0.0002), time (Pr>F 0.0165) and their interaction (Pr>0.0069) were significant. Free Curc significantly differed from the other treatments, offering more protection against Aβ-induced toxicity depending on time, suggesting that better protection by curcumin occurred at the latter two post-prandial time points (Figure 7.11-a).

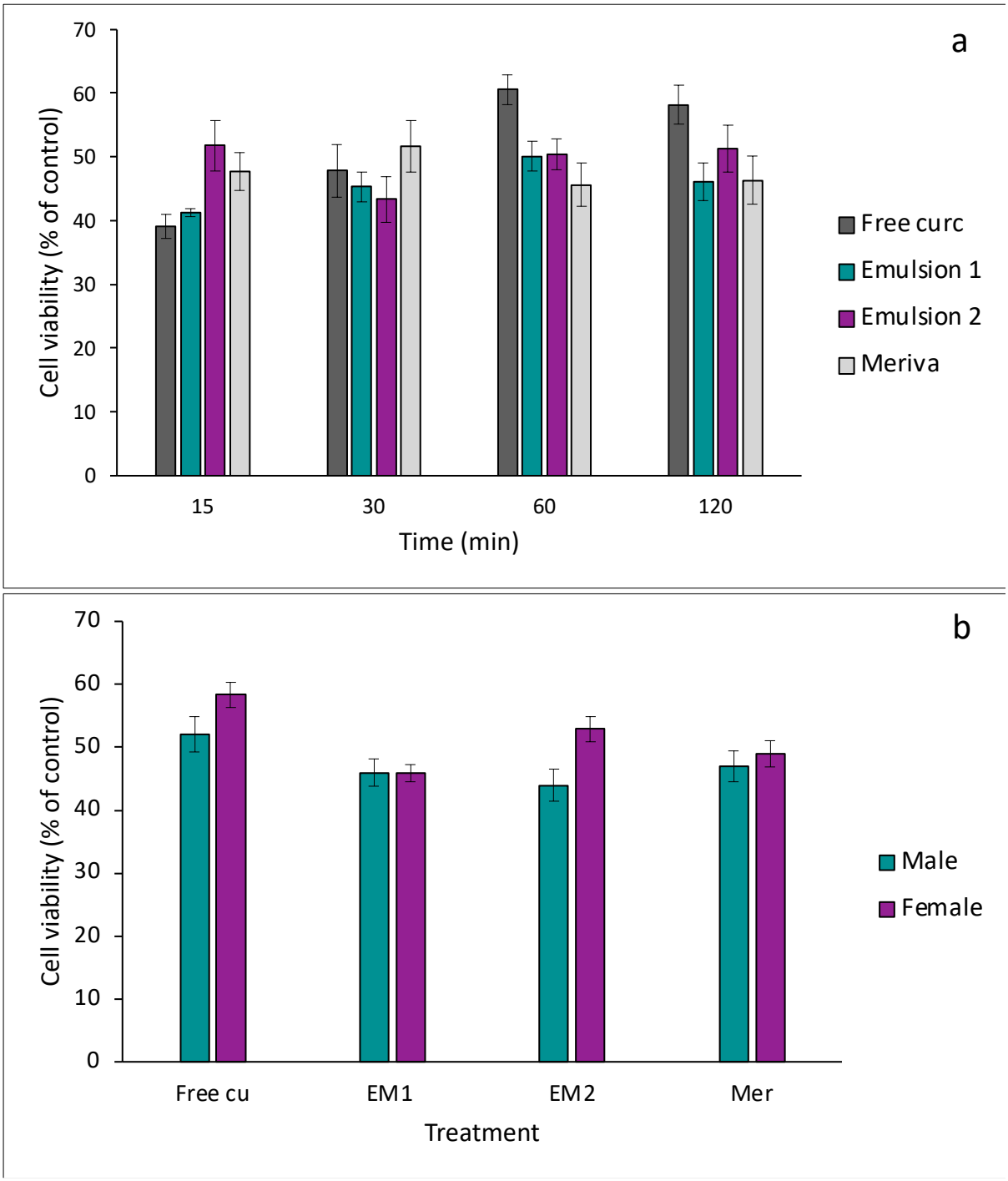

Figure 7.11. Loss in viability induced by Aβ. a) Effect of treatment and time on cell viability. b) Effect of gender and treatment on cell viability.

Serum from female rats provided significantly better protection against Aβ toxicity than serum from male rats (Pr>F 0.0003), and free Curc-treated rats had higher viability than other treatments (Figure 7.11-b). There was no interaction between gender and treatment, indicating that the differences in one factor were not affected by the other.

Unexpectedly, none of the rat serum samples fed test treats provided significantly more protection than serum from rats fed control treats containing no curcumin in any form. In

addition, all of the serum samples provided less or equal protection than 1% FBS. The Aβ treatment resulted in a 37±4% loss in viability in wells with 1% FBS present compared to a 59±6% loss in viability in wells with 1% rat serum present. It is unlikely that this was due to a lack of sufficient nutrients in serum for BE(2)-M17 cell maintenance, as in wells not treated with Aβ, the presence of rat serum appeared beneficial. The optical density, correlating with the number of metabolically active cells, was 0.471+0.044 in the wells containing 1% fetal bovine serum compared to 0.734+0.099 in the wells containing 1% rat serum ($p<0.0001$).

These findings suggest that FBS, but not rat serum, contains a compound that reduces Aβ activity or that rat serum, but not FBS, contains a compound that exacerbates Aβ incorporation into cells and/or subsequent cytotoxic activity. This may be due to the difference in species, or it may be due to the difference in age/maturation of the sources. For example, while adult bovine serum can be used to culture some cell lines with similar success compared to foetal bovine serum, FBS contains far less sex hormones, protein, albumin, complement, gamma-globulin, glucose, cholesterol, sodium, and chloride compared to adult bovine serum, while containing much higher levels of growth factors than adult bovine serum (Gstraunthaler et al., 2013). In addition, adult bovine serum has been shown to differ in the proportions of some components based on the sex of the donor animal (Yu et al., 2013). It is also possible that the rat serum samples contained bilirubin, which can be released but not visible in very mildly haemolysed samples and which can be cytotoxic, compared to FBS which undergoes more stringent collection and processing procedures. For similar reasons, the rat serum may have contained low but physiological concentrations of endotoxin contaminant.

There is a single publication from several decades ago in which rat serum and FBS were compared in assays for serum effects on the cytolytic activity of leukocytes against syngeneic tumour cells; in this study, cytolytic activity was lower with rat serum compared to FBS (Reisser et al., 1989). It is difficult to speculate further on this topic because there are no other reports in the literature of rat serum being used to culture the M17 neuroblastoma cell line or any other. However, overall our findings indicate that rat serum and FBS cannot be used interchangeably in cell culture systems and any culture system using serum from experimental animals such as rats will need to be tested and optimised.

The studies in this chapter were originally designed to compare freshly prepared *in vitro* samples, digested *in vitro* samples, and post-digestion *in vivo* samples. The sample types compared in this study were: (a) freshly prepared emulsions, (b) *in vitro* digested emulsions, (c) serum from rats fed selected emulsions that contained the post-digestion metabolites of

curcumin preparations delivered in peanut butter and honey treats. One of the goals of this aspect of the study, if equal efficacy could be demonstrated, was to determine whether *in vitro* preparations to be used in future, obviating the need for *in vivo* studies and thus fulfilling the "reduce, replace, refine" mandate in animal ethics. As noted above, the curcumin preparations fed to the rats did not significantly differ with regard to protective effects of post-feeding serum samples. Much further work is needed before *in vitro* digested emulsions can be guaranteed to be representative of serum from the circulation post *in-vivo* digestion of the same emulsions, although this remains an important and worthwhile goal.

Curcumin has been shown to bind with Aβ, and as a result has been suggested as a promising agent for early detection of plaque deposition in the brain (Patil et al., 2015) and as an anti-amyloidogenic and anti-tau agent (Serafini et al., 2017). This thesis adds to the body of work that shows that even at low concentrations, curcumin can cross the blood-brain barrier, bind to Aβ and act against AD biomarkers. The mechanisms by which the systems' components improved cell proliferation are out of the scope of this research and need to be further investigated in detail, but previous literature suggests that curcumin can inhibit Aβ aggregation, downregulate BACE1 expression and enhance Aβ phagocytosis by microglia (Serafini et al., 2017).

7.5 Conclusions

Research focusing on Aβ aggregation and reduction of its toxic effects using delivery systems to human neurons *in vitro* may significantly advance the development of novel therapeutics to treat AD. This study shows that fresh and *in vitro* digested emulsions were effective on reducing Aβ cytotoxicity in the M17 cell assay. It is envisioned that this could support parallel *in vivo* work. In a completely novel approach, I tested the use of serum taken from rats post-digestion to treat cells exposed to Aβ, as this can be expected to more closely represent the effects of orally delivered bioactive compounds compared to *in vitro* digestion products. Unfortunately, at the tested concentrations, no beneficial effects could be observed from *in vivo* digested treatments. However, the theory remains relevant and should be further pursued.

Overall, the results described in this chapter highlight several inadequacies and limitations in current methodologies. Undigested compounds tested in *in vitro* cell assays do not reflect the physiological conditions that various cells and organ systems in the body are

exposed to from circulating metabolites post-digestion. The use of a simulated gastric digestive system may result in samples that produce cytotoxic conditions in *in vitro* cell assays, whether due to alterations in pH or osmolarity or due to the presence of non-inactivated enzymes. Serum from animals post-feeding, while theoretically valid as being representative of the exposure of organ systems to post-digestive metabolites, may not be feasible for use in *in vitro* assays that can only support exposure to nutritionally incomplete serum concentrations. Serum from adult rats differs sufficiently to serum from fetal calves so that the two resulted in significant differences even in simple cell growth assays; this was an unfortunate but also valuable and unique finding, since such an approach has never been reported in the literature. Finally, the assay that utilises the human neuroblastoma BE(2)-M17 cell line with the oligomeric $A\beta_{1\text{-}42}$ challenge to recapitulate the cytotoxic effects of plaque formation in the brain of AD is poorly reliable and poorly reproducible, thus requiring excessive numbers of replicate assays and highly selective interpretation of results.

Further assessment of these technical challenges was beyond the scope of the thesis, so it cannot be determined whether this is reproducible, whether the effect is limited to this particular cell line, or whether this is unique to curcumin as an ingredient. However, this would be of great interest to explore in future, as it may have significant ramifications for the use of the simulated gastric digestion system as a comparison with and eventual replacement for *in vivo* models.

Chapter 8 Discussion and future research prospects

8.1 General discussion

Dementia is a public health priority, with AD being the most common form among the elderly. The increase in life expectancy and ageing of the population, aligned with poor health habits, are contributing to an increase in dementia cases that ultimately will culminate in a burden on the health and wealth of societies. According to Livingston et al. (2020) in an article published in the *Lancet*, a cost of approximately US$1 trillion will be needed to support a burden of the expected 152 million worldwide AD cases by 2050. In the absence of a cure and with poor efficacy of current treatments, an approach focused on prevention has been suggested as the best strategy to tackle this devastating disease (Barnett et al., 2013, Livingston et al., 2020).

While age is the main risk factor for dementia, genetics and environmental factors play a significant role. Factors such as age and genetics cannot be changed, yet adjustments in lifestyle can surely contribute to better health and reduce disease risk. In fact, it is believed that around 40% of dementia cases can be prevented. The link between cardiovascular disease and dementia is widely accepted and understood; however, there are a series of other risk factors that can be modified in order to increase overall health and prevent dementia onset. To date, there are twelve recognised modifiable risk factors: (1) excessive alcohol consumption, (2) head injury, (3) air pollution, (4) level of education, (5) hypertension, (6) hearing impairment, (7) smoking, (8) obesity, (9) depression, (10) physical inactivity, (11) diabetes and (12) infrequent social contact (Livingston et al., 2020). From those, at least three are directly correlated to diet, yet more can be indirectly correlated as diet adjustments can contribute to mood and boosted motivation for a more active life.

Considering the relevance in delaying dementia onset and reducing its burden on society plus the major role that food plays in prevention, I proposed the use of a polyphenol, curcumin, as an additive to the diet to help attenuate or reduce the risk of AD. Due to their abundance in foods derived from plants and their potential antioxidant activity, polyphenols have been considerably studied in the past years as compounds with properties that help in attenuating the risk factors for diseases such as cardiovascular, diabetes, cancer, and cognitive disorders (Di Lorenzo et al., 2021, Esposito et al., 2002, Wang et al., 2008). However, polyphenols are poorly bioavailable because of factors such as the interaction with food matrix

and metabolic processes mediated by the liver, intestine and microbiota. Additionally, they can be conjugated with sugars, organic acids or alcohols (Di Lorenzo et al., 2021).

Curcumin specifically presents very low water solubility and therefore undergoes rapid metabolism and excretion by the liver after oral ingestion, as human physiology is largely aqueous-based (Ammon, 1991) (Chattopadhyay et al., 2003). At the same time, extensive research has shown that curcumin acts as a strong antioxidant and anti-inflammatory compound aiding against cancer (Cheng et al., 2001, Heger et al., 2014), arthritis (Khayyal et al., 2018), neurodegenerative disease (Barbara et al., 2017, Gao et al., 2020) and inflammation (Wang et al., 2008). Sadly, despite a series of benefits *in vitro* and in animal studies, the positive outcomes obtained by curcumin are poorly reproducible in human trials. The addition of curcumin in a food-based delivery system for improved bioavailability, but also for potential synergistic effects and easy long-term consumption, are of interest. Therefore, curcumin was combined with functional oils (MCT and FO) and MFGM derived materials to prepare emulsions systems. The MFGM fraction is obtained industrially from the processing of cream. The milk fat globules are disrupted during the churning and the membrane on the lipid surface is removed from the lipid matrix and recovered as buttermilk. Due to their health promoting properties, the use of MFGM PL in the development of new products is increasing (Jiménez-Flores et al., 2009). (Nieuwenhuizen et al., 2006) studied sphingolipids in the reduction of plasma cholesterol and triacylglycerol levels.

As described in details in Chapters 4 and 5, I was able to create emulsions systems with small particle size (Figure 4.1) that were stable over time (Figure 4.3) and increased curcumin bioaccessibility (Table 5.4) and protection through the gastrointestinal tract *in vitro* (Figure 5.2). Those findings are in accordance with a number of recent published studies (Aditya et al., 2015, Cheng et al., 2017, Peng et al., 2018, Silva et al., 2018, Zou et al., 2016). For instance, a recent study (Verma et al., 2021) used milk cream to encapsulate curcumin in an emulsion that was microfluidized at different pressures and passes. Similar to our findings, the authors found high encapsulation efficiency (97.88%), small particle size and homogeneous size distribution. Additionally, the authors found that *in vitro* digestion (oral, gastric and intestinal phases) remarkably increased bioaccessibility and concluded that the use of microfluidization of milk cream would be an inexpensive, potential vehicle for stable and bio-accessible nano-curcumin emulsion. As opposed to the above-mentioned study, in our study, the goal was to focus on one isolated fraction from milk cream. I ultimately determine that all tested MFGM derived

fractions were suitable and effective to create delivery systems for our goal and conclude they can be used as good vehicles for curcumin encapsulation.

Food structure is of extreme importance on the fate of a food delivered orally, and since curcumin is a highly lipophilic molecule, an emulsion-based system was believed to be the best approach. In addition to curcumin, the concentrations of individual phospholipid groups across the fresh and digested emulsions' structures were analysed, and it has been observed that phospholipids were not only able to protect curcumin, but also contributed to the formation of mixed micelles, as discussed in details in Chapter 5. Little change was observed in the phospholipid profile after gastric digestion, with more preeminent changes being noted after simulated intestinal digestion, where phospholipases promoted breakdown of phospholipid groups. I hypothesised that phospholipids from MFGM could not only assist in health-promoting properties, but also contribute to membrane crossing, especially through the blood-brain barrier (BBB).

To confirm that hypothesis, I further analysed the delivery of curcumin *in vivo*, using a rat model as described in Chapter 6. Comparing a commercially bioavailable formulation with the selected emulsions, it was observed that the encapsulation inside MCT and fish oil droplets improved blood and brain delivery of curcumin when compared to free, non-encapsulated, curcumin (Figure 6.7, Figure 6.11). Furthermore, I explored and analysed the profile of metabolite distribution and identified and confirmed that most ingested curcumin was immediately converted into curcumin glucuronide and curcumin sulphate (Figure 6.10). Only plasma and blood were analysed; however, it is expected that curcumin can be found, in perhaps high concentrations, in the liver and even the gastrointestinal tract. The analysis of curcumin in other organs would provide additional insights on the distribution profile and metabolism. Due to time and resource limitations, the analysis of those organs was not possible to be conducted.

I also observed and confirmed that once curcumin has been conjugated with glucuronide or sulphate groups, it becomes unable to cross the BBB, as no metabolites were found in the brains of rats for any of the treatments tested in our study (Figure 6.5). Even though curcumin delivery was improved by its encapsulation, very low concentrations were found in blood, as the initial administration dose was low (20mg/kg/body weight). Nevertheless, the tested dose was able to provide an initial overview on the profile delivery for MFGM delivery

systems and provide insights for more detailed and long-term studies. Here, I attempted to observe the delivery of curcumin, rather than assess curcumin accumulation effects over time.

It is also relevant to mention that the current literature data available on curcumin are highly heterogenous due to the use different formulations, modes of administration and at times lack of specification on the exact product being used. For instance, I used an extract containing 95% curcumin; however, many studies have used turmeric which contained higher concentrations of desmethoxycurcumin and bisdemethoxycurcumin. The interaction and effects of different fractions can have a huge impact on the research outcomes. In animal studies for curcumin bioavailability, enzymatic conversion of curcumin metabolites back to curcumin often resulted in an overestimated bioavailability. Therefore, conclusions in published reports using this methodology should be analysed carefully, as once it is converted to conjugated forms, the curcumin in the body is actually eliminated (Stohs et al., 2019).

In Chapter 7 a cell line model (human neuroblastoma BE(2)-M17) was used to assess the effect of fresh emulsions, *in vitro* digested emulsions and *in vivo* digested emulsions on cell proliferation and cell survival after exposure to oligomeric Aβ1–42. The results obtained from this study were not strong enough to support the use of the emulsions as preventative systems for AD as only the MTS assay was used to determine cell viability, and the Aβ cell assay itself proved to be unreliable. Nevertheless, this study showed that fresh and *in vitro* digested emulsions were effective in reducing Aβ-induced cytotoxicity in the M17 cell assay (Figure 7.5). I projected that this could support parallel *in vivo* work. In a completely novel approach, I tested the use of serum taken from rats post-digestion to treat cells exposed to Aβ, as this can be expected to more closely represent the effects of orally delivered bioactive compounds compared to *in vitro* digestion products. Unfortunately, at the tested concentrations, no beneficial effects could be observed from *in vivo* digested treatments (Figure 7.10), as rat serum produced unexpected and gender-specific effects on cell viability. However, the theory remains relevant and should be further pursued.

8.2 Future research prospects

The promising findings from this study and others suggest that if administered in a consistent manner and in combination with the right carrier, curcumin has the potential to support overall health in the context of neurodegenerative conditions. Phospholipids have been shown to promote liver protection and enhance memory. A study by (Crook, 1992) tested a

specific phospholipid, phosphatidylserine, in patients with AD and found that those who received the formulation for twelve weeks showed improved cognition compared to those receiving placebo treatment. I therefore strongly recommend further investigation on the use of curcumin-MFGM phospholipid conjugation in neurodegenerative disorders.

For future studies I suggest the creation of a more complex surface structure, with the addition of protein or a solid particle in to the phospholipid formed layer. That would further protect the systems through gastrointestinal digestion and potentially improve bioaccessibility and curcumin delivery to the brain. It would also be of interest to increase the amount of curcumin carried in the system. This is limited by the amount of carrier oil in the system; however, higher phospholipid concentrations could help carry more curcumin. I believe that the addition or transformation of this system to a more complex food structure would be of interest for future tests. Future assessments should initially look into the delivery of not only curcumin, but also phospholipids, ketones and fatty acids to the blood, for which a human trial would be more suitable than a rat trial for ethical and physiological reasons.

Once a better bioavailability profile is obtained in a longer term test, rather than on administration, the food systems could be screened in a more reliable cell assay and the most promising candidates then further assessed in an animal model. I understand that more tests need to be conducted in cell assays to confidently affirm that the systems are able to act against AD biomarkers. An animal trial in which behavioural tests can be administered would seem to be a more reliable way to further assess the effects of those systems. Ultimately, after optimising some of the conditions mentioned above, a long-term human clinical trial where the systems are administered orally as part of a complex food systems consistently over time for cognition assessments would be ideal.

References

ACEVEDO-FANI, A. & SINGH, H. 2022. Biophysical insights into modulating lipid digestion in food emulsions. *Progress in Lipid Research,* 85**,** 101129. Available: https://doi.org/10.1016/j.plipres.2021.101129

ACEVEDO-FANI, A., SOLIVA-FORTUNY, R. & MARTÍN-BELLOSO, O. 2017. Nanostructured emulsions and nanolaminates for delivery of active ingredients: Improving food safety and functionality. *Trends in Food Science & Technology,* 60**,** 12-22. Available: https://doi.org/10.1016/j.tifs.2016.10.027

ADITYA, N. P., ADITYA, S., YANG, H., KIM, H. W., PARK, S. O. & KO, S. 2015. Co-delivery of hydrophobic curcumin and hydrophilic catechin by a water-in-oil-in-water double emulsion. *Food Chemistry,* 173**,** 7-13. Available: https://doi.org/10.1016/j.foodchem.2014.09.131

AHMED, K., LI, Y., MCCLEMENTS, D. J. & XIAO, H. 2012. Nanoemulsion- and emulsion-based delivery systems for curcumin: Encapsulation and release properties. *Food Chemistry,* 132**,** 799-807. Available: https://doi.org/10.1016/j.foodchem.2011.11.039

AHMED, T. & GILANI, A.-H. 2009. Inhibitory effect of curcuminoids on acetylcholinesterase activity and attenuation of scopolamine-induced amnesia may explain medicinal use of turmeric in Alzheimer's disease. *Pharmacology Biochemistry and Behavior,* 91**,** 554-559. Available: https://doi.org/10.1016/j.pbb.2008.09.010

AMMON, H. A. W., M. A. 1991. Pharmacology of Curcuma longa. *Planta Med.,* 57**,** 1-7.

AMMON, H. P. & WAHL, M. A. 1991. Pharmacology of Curcuma longa. *Planta Med,* 57**,** 1-7. Available: 10.1055/s-2006-960004

AMORETTI, M., AMSLER, C., BONOMI, G., BOUCHTA, A., BOWE, P., CARRARO, C., CESAR, C. L., CHARLTON, M., COLLIER, M. J. T., DOSER, M., FILIPPINI, V., FINE, K. S., FONTANA, A., FUJIWARA, M. C., FUNAKOSHI, R., GENOVA, P., HANGST, J. S., HAYANO, R. S., HOLZSCHEITER, M. H., JØRGENSEN, L. V., LAGOMARSINO, V., LANDUA, R., LINDELÖF, D., RIZZINI, E. L., MACRÌ, M., MADSEN, N., MANUZIO, G., MARCHESOTTI, M., MONTAGNA, P., PRUYS, H., REGENFUS, C., RIEDLER, P., ROCHET, J., ROTONDI, A., ROULEAU, G., TESTERA, G., VARIOLA, A., WATSON, T. L. & VAN DER WERF, D. P. 2002. Production and detection of cold antihydrogen atoms. *Nature,* 419**,** 456-459. Available: 10.1038/nature01096

ANAND, P., KUNNUMAKKARA, A. B., NEWMAN, R. A. & AGGARWAL, B. B. 2007. Bioavailability of curcumin: problems and promises. *Molecular pharmaceutics,* 4**,** 807-818.

ANDRES, D., KEYSER, B. M., PETRALI, J., BENTON, B., HUBBARD, K. S., MCNUTT, P. M. & RAY, R. 2013. Morphological and functional differentiation in BE (2)-M17 human neuroblastoma cells by treatment with Trans-retinoic acid. *BMC neuroscience,* 14**,** 1-12.

ANTIGA, E., BONCIOLINI, V., VOLPI, W., DEL BIANCO, E. & CAPRONI, M. 2015. Oral Curcumin (Meriva) Is Effective as an Adjuvant Treatment and Is Able to Reduce IL-22 Serum Levels in Patients with Psoriasis Vulgaris. *BioMed Research International,* 2015**,** 283634. Available: 10.1155/2015/283634

ANTONY, B., MERINA, B., IYER, V. S., JUDY, N., LENNERTZ, K. & JOYAL, S. 2008. A Pilot Cross-Over Study to Evaluate Human Oral Bioavailability of BCM-95CG (Biocurcumax), A Novel Bioenhanced Preparation of Curcumin. *Indian J Pharm Sci,* 70**,** 445-9. Available: 10.4103/0250-474x.44591
ANUCHAPREEDA, S., FUKUMORI, Y., OKONOGI, S. & ICHIKAWA, H. 2012. Preparation of lipid nanoemulsions incorporating curcumin for cancer therapy. *Journal of nanotechnology,* 2012.
ARAIZA-CALAHORRA, A., AKHTAR, M. & SARKAR, A. 2018. Recent advances in emulsion-based delivery approaches for curcumin: From encapsulation to bioaccessibility. *Trends in Food Science & Technology,* 71**,** 155-169. Available: https://doi.org/10.1016/j.tifs.2017.11.009
ARMAND, M. 2007. Lipases and lipolysis in the human digestive tract: where do we stand? *Curr Opin Clin Nutr Metab Care,* 10**,** 156-64. Available: 10.1097/MCO.0b013e3280177687
ARMAND, M., BOREL, P., DUBOIS, C., SENFT, M., PEYROT, J., SALDUCCI, J., LAFONT, H. & LAIRON, D. 1994. Characterization of emulsions and lipolysis of dietary lipids in the human stomach. *American Journal of Physiology-Gastrointestinal and Liver Physiology,* 266**,** G372-G381. Available: 10.1152/ajpgi.1994.266.3.G372
ARTIGA-ARTIGAS, M., LANJARI-PÉREZ, Y. & MARTÍN-BELLOSO, O. 2018. Curcumin-loaded nanoemulsions stability as affected by the nature and concentration of surfactant. *Food Chemistry,* 266**,** 466-474. Available: https://doi.org/10.1016/j.foodchem.2018.06.043
ASAI, A. & MIYAZAWA, T. 2000. Occurrence of orally administered curcuminoid as glucuronide and glucuronide/sulfate conjugates in rat plasma. *Life Sciences,* 67**,** 2785-2793. Available: https://doi.org/10.1016/S0024-3205(00)00868-7
ASWAR, M., BHALEKAR, M., TRIMUKHE, A. & ASWAR, U. 2020. Self-microemulsifying drug delivery system (SMEDDS) of curcumin attenuates depression in olfactory bulbectomized rats. *Heliyon,* 6**,** e04482. Available: 10.1016/j.heliyon.2020.e04482
ATWOOD, C. S., OBRENOVICH, M. E., LIU, T., CHAN, H., PERRY, G., SMITH, M. A. & MARTINS, R. N. 2003a. Amyloid-beta: a chameleon walking in two worlds: a review of the trophic and toxic properties of amyloid-beta. *Brain Res Brain Res Rev,* 43**,** 1-16. Available: 10.1016/s0165-0173(03)00174-7
ATWOOD, C. S., OBRENOVICH, M. E., LIU, T., CHAN, H., PERRY, G., SMITH, M. A. & MARTINS, R. N. 2003b. Amyloid-β: a chameleon walking in two worlds: a review of the trophic and toxic properties of amyloid-β. *Brain Research Reviews,* 43**,** 1-16.
AUGUSTIN, K., KHABBUSH, A., WILLIAMS, S., EATON, S., ORFORD, M., CROSS, J. H., HEALES, S. J. R., WALKER, M. C. & WILLIAMS, R. S. B. 2018. Mechanisms of action for the medium-chain triglyceride ketogenic diet in neurological and metabolic disorders. *Lancet Neurol,* 17**,** 84-93. Available: 10.1016/s1474-4422(17)30408-8
BAEK, J. S. & CHO, C. W. 2017. Surface modification of solid lipid nanoparticles for oral delivery of curcumin: Improvement of bioavailability through enhanced cellular uptake, and lymphatic uptake. *Eur J Pharm Biopharm,* 117**,** 132-140. Available: 10.1016/j.ejpb.2017.04.013
BAI, L., HUAN, S., GU, J. & MCCLEMENTS, D. J. 2016. Fabrication of oil-in-water nanoemulsions by dual-channel microfluidization using natural emulsifiers: Saponins, phospholipids, proteins, and polysaccharides. *Food Hydrocolloids,* 61**,** 703-711. Available: https://doi.org/10.1016/j.foodhyd.2016.06.035

BALASUBRAMANIAN, K. 2006. Molecular orbital basis for yellow curry spice curcumin's prevention of Alzheimer's disease. *Journal of Agricultural and Food Chemistry,* 54**,** 3512-3520. Available: 10.1021/jf0603533
BANDYOPADHYAY, D. 2014. Farmer to pharmacist: curcumin as an anti-invasive and antimetastatic agent for the treatment of cancer1. *Frontiers in Chemistry,* 2. Available: 10.3389/fchem.2014.00113
BANSAL, A., KIRSCHNER, M., ZU, L., CAI, D. & ZHANG, L. 2019. Coconut oil decreases expression of amyloid precursor protein (APP) and secretion of amyloid peptides through inhibition of ADP-ribosylation factor 1 (ARF1). *Brain Research,* 1704**,** 78-84. Available: https://doi.org/10.1016/j.brainres.2018.10.001
BANSAL, S. S., KAUSAR, H., VADHANAM, M. V., RAVOORI, S. & GUPTA, R. C. 2012. Controlled systemic delivery by polymeric implants enhances tissue and plasma curcumin levels compared with oral administration. *Eur J Pharm Biopharm,* 80**,** 571-7. Available: 10.1016/j.ejpb.2011.12.009
BARBARA, R., BELLETTI, D., PEDERZOLI, F., MASONI, M., KELLER, J., BALLESTRAZZI, A., VANDELLI, M. A., TOSI, G. & GRABRUCKER, A. M. 2017. Novel Curcumin loaded nanoparticles engineered for Blood-Brain Barrier crossing and able to disrupt Abeta aggregates. *International Journal of Pharmaceutics,* 526**,** 413-424. Available: https://doi.org/10.1016/j.ijpharm.2017.05.015
BARBERGER-GATEAU, P., RAFFAITIN, C., LETENNEUR, L., BERR, C., TZOURIO, C., DARTIGUES, J. F. & ALPÉROVITCH, A. 2007. Dietary patterns and risk of dementia. *Neurology,* 69**,** 1921. Available: 10.1212/01.wnl.0000278116.37320.52
BARNETT, J. H., HACHINSKI, V. & BLACKWELL, A. D. 2013. Cognitive health begins at conception: addressing dementia as a lifelong and preventable condition. *BMC medicine,* 11**,** 1-6.
BARR, R. K., VERDILE, G., WIJAYA, L. K., MORICI, M., TADDEI, K., GUPTA, V. B., PEDRINI, S., JIN, L., NICOLAZZO, J. A. & KNOCK, E. 2016. Validation and characterization of a novel peptide that binds monomeric and aggregated β-amyloid and inhibits the formation of neurotoxic oligomers. *Journal of Biological Chemistry,* 291**,** 547-559.
BARRY, J., FRITZ, M., BRENDER, J. R., SMITH, P. E., LEE, D.-K. & RAMAMOORTHY, A. 2009. Determining the effects of lipophilic drugs on membrane structure by solid-state NMR spectroscopy: the case of the antioxidant curcumin. *Journal of the American Chemical Society,* 131**,** 4490-4498.
BATEMAN, R. J., XIONG, C., BENZINGER, T. L., FAGAN, A. M., GOATE, A., FOX, N. C., MARCUS, D. S., CAIRNS, N. J., XIE, X. & BLAZEY, T. M. 2012. Clinical and biomarker changes in dominantly inherited Alzheimer's disease. *N Engl J Med,* 367**,** 795-804.
BAUER, E., JAKOB, S. & MOSENTHIN, R. 2005. Principles of physiology of lipid digestion. *Asian-Australasian Journal of Animal Sciences,* 18**,** 282-295.
BAUMGART, M., SNYDER, H. M., CARRILLO, M. C., FAZIO, S., KIM, H. & JOHNS, H. 2015. Summary of the evidence on modifiable risk factors for cognitive decline and dementia: a population-based perspective. *Alzheimer's & Dementia,* 11**,** 718-726.
BAZINET, R. P. & LAYÉ, S. 2014. Polyunsaturated fatty acids and their metabolites in brain function and disease. *Nature Reviews Neuroscience,* 15**,** 771-785.
BEHL, C. 1999. Alzheimer's disease and oxidative stress: Implications for novel therapeutic approaches. *Progress in Neurobiology,* 57**,** 301-323. Available: 10.1016/S0301-0082(98)00055-0

BELKOUCH, M., HACHEM, M., ELGOT, A., VAN, A. L., PICQ, M., GUICHARDANT, M., LAGARDE, M. & BERNOUD-HUBAC, N. 2016. The pleiotropic effects of omega-3 docosahexaenoic acid on the hallmarks of Alzheimer's disease. *The Journal of nutritional biochemistry,* 38**,** 1-11.
BENGMARK, S. 2006. Curcumin, an atoxic antioxidant and natural NFκB, cyclooxygenase-2, lipooxygenase, and inducible nitric oxide synthase inhibitor: a shield against acute and chronic diseases. *Journal of Parenteral and Enteral Nutrition,* 30**,** 45-51.
BERRY, B. J., SMITH, A. S. T., LONG, C. J., MARTIN, C. C. & HICKMAN, J. J. 2018. Physiological Aβ Concentrations Produce a More Biomimetic Representation of the Alzheimer's Disease Phenotype in iPSC Derived Human Neurons. *ACS Chemical Neuroscience,* 9**,** 1693-1701. Available: 10.1021/acschemneuro.8b00067
BEZZINE, S., FERRATO, F., IVANOVA, M. G., LOPEZ, V., VERGER, R. & CARRIÈRE, F. 1999. Human Pancreatic Lipase: Colipase Dependence and Interfacial Binding of Lid Domain Mutants. *Biochemistry,* 38**,** 5499-5510. Available: 10.1021/bi982601x
BIESSELS, G. J., STRACHAN, M. W. J., VISSEREN, F. L. J., KAPPELLE, L. J. & WHITMER, R. A. 2014. Dementia and cognitive decline in type 2 diabetes and prediabetic stages: towards targeted interventions. *The Lancet Diabetes & Endocrinology,* 2**,** 246-255. Available: https://doi.org/10.1016/S2213-8587(13)70088-3
BOUDRAULT, C., BAZINET, R. P. & MA, D. W. 2009. Experimental models and mechanisms underlying the protective effects of n-3 polyunsaturated fatty acids in Alzheimer's disease. *The Journal of nutritional biochemistry,* 20**,** 1-10.
BOUHOURS, J.-F. & BOUHOURS, D. 1981. Ceramide structure of sphingomyelin from human milk fat globule membrane. *Lipids,* 16**,** 726-731.
BOURBON, A. I., PINHEIRO, A. C., CERQUEIRA, M. A. & VICENTE, A. A. 2018. In vitro digestion of lactoferrin-glycomacropeptide nanohydrogels incorporating bioactive compounds: Effect of a chitosan coating. *Food Hydrocolloids,* 84**,** 267-275. Available: https://doi.org/10.1016/j.foodhyd.2018.06.015
BOURRE, J.-M. 2007. Dietary omega-3 fatty acids for women. *Biomedicine & pharmacotherapy,* 61**,** 105-112.
BRISKEY, D., SAX, A., MALLARD, A. R. & RAO, A. 2019. Increased bioavailability of curcumin using a novel dispersion technology system (LipiSperse®). *European Journal of Nutrition,* 58**,** 2087-2097. Available: 10.1007/s00394-018-1766-2
BRODKORB, A., EGGER, L., ALMINGER, M., ALVITO, P., ASSUNCAO, R., BALLANCE, S., BOHN, T., BOURLIEU-LACANAL, C., BOUTROU, R., CARRIERE, F., CLEMENTE, A., CORREDIG, M., DUPONT, D., DUFOUR, C., EDWARDS, C., GOLDING, M., KARAKAYA, S., KIRKHUS, B., LE FEUNTEUN, S., LESMES, U., MACIERZANKA, A., MACKIE, A. R., MARTINS, C., MARZE, S., MCCLEMENTS, D. J., MENARD, O., MINEKUS, M., PORTMANN, R., SANTOS, C. N., SOUCHON, I., SINGH, R. P., VEGARUD, G. E., WICKHAM, M. S. J., WEITSCHIES, W. & RECIO, I. 2019. INFOGEST static in vitro simulation of gastrointestinal food digestion. *Nat Protoc,* 14**,** 991-1014. Available: 10.1038/s41596-018-0119-1
BROUET, I. & OHSHIMA, H. 1995. Curcumin, an anti-tumor promoter and anti-inflammatory agent, inhibits induction of nitric oxide synthase in activated macrophages. *Biochemical and biophysical research communications,* 206**,** 533-540.
BUDD HAEBERLEIN, S., AISEN, P. S., BARKHOF, F., CHALKIAS, S., CHEN, T., COHEN, S., DENT, G., HANSSON, O., HARRISON, K., VON HEHN, C.,

IWATSUBO, T., MALLINCKRODT, C., MUMMERY, C. J., MURALIDHARAN, K. K., NESTOROV, I., NISENBAUM, L., RAJAGOVINDAN, R., SKORDOS, L., TIAN, Y., VAN DYCK, C. H., VELLAS, B., WU, S., ZHU, Y. & SANDROCK, A. 2022. Two Randomized Phase 3 Studies of Aducanumab in Early Alzheimer's Disease. *The Journal of Prevention of Alzheimer's Disease,* 9**,** 197-210. Available: 10.14283/jpad.2022.30

CANO-SARMIENTO, C., TÉLLEZ-MEDINA, D. I., VIVEROS-CONTRERAS, R., CORNEJO-MAZÓN, M., FIGUEROA-HERNÁNDEZ, C. Y., GARCÍA-ARMENTA, E., ALAMILLA-BELTRÁN, L., GARCÍA, H. S. & GUTIÉRREZ-LÓPEZ, G. F. 2018. Zeta Potential of Food Matrices. *Food Engineering Reviews,* 10**,** 113-138. Available: 10.1007/s12393-018-9176-z

CARRIERE, F., BARROWMAN, J. A., VERGER, R. & RENÉ, L. 1993. Secretion and contribution to lipolysis of gastric and pancreatic lipases during a test meal in humans. *Gastroenterology,* 105**,** 876-888. Available: https://doi.org/10.1016/0016-5085(93)90908-U

CASTRO-GÓMEZ, P., GARCIA-SERRANO, A., VISIOLI, F. & FONTECHA, J. 2015. Relevance of dietary glycerophospholipids and sphingolipids to human health. *Prostaglandins, Leukotrienes and Essential Fatty Acids,* 101**,** 41-51. Available: https://doi.org/10.1016/j.plefa.2015.07.004

CHAINANI-WU, N. 2003. Safety and anti-inflammatory activity of curcumin: A component of tumeric (Curcuma longa). *Journal of Alternative and Complementary Medicine,* 9**,** 161-168.

CHALLA HJ, A. M., UPPALURI KR 2021. DASH Diet To Stop Hypertension. *StatPearls [Internet]*.

CHANG, H. W., TAN, T. B., TAN, P. Y., ABAS, F., LAI, O. M., WANG, Y., WANG, Y., NEHDI, I. A. & TAN, C. P. 2018. Physical properties and stability evaluation of fish oil-in-water emulsions stabilized using thiol-modified β-lactoglobulin fibrils-chitosan complex. *Food Research International,* 105**,** 482-491. Available: https://doi.org/10.1016/j.foodres.2017.11.034

CHANG, W.-C., KUO, P.-L., CHEN, C.-W., WU, J. S.-B. & SHEN, S.-C. 2015. Caffeic acid improves memory impairment and brain glucose metabolism via ameliorating cerebral insulin and leptin signaling pathways in high-fat diet-induced hyperinsulinemic rats. *Food Research International,* 77**,** 24-33. Available: https://doi.org/10.1016/j.foodres.2015.04.010

CHATTOPADHYAY, I., BISWAS, K., BANDYOPADHYAY, U. & BANERJEE, R. 2003. Turmeric and Curcumin: Biological actions and medicinal applications. *Curr Sci,* 87.

CHEN, A. L., HSU, C. H., LIN, J. K., HSU, M. M., HO, Y. F., SHE, T. S., KO, J. Y., LIN, J. T., LIN, B. R., WU, M. S., YU, H. S., JEE, S. H., CHEN, G. S., CHEN, T. M., CHEN, C. A., LAI, M. K., PU, Y. S., PAN, M. H., WANG, Y. J., TSAI, C. C. & HSIEH, C. Y. 2001. Phase I clinical trial of curcumin, a chemopreventive agent, in patients with high-risk or pre-malignant lesions. *Anticancer Research,* 21**,** 2895-2900.

CHEN, H., WU, J., SUN, M., GUO, C., YU, A., CAO, F., ZHAO, L., TAN, Q. & ZHAI, G. 2012. N-trimethyl chitosan chloride-coated liposomes for the oral delivery of curcumin. *J Liposome Res,* 22**,** 100-9. Available: 10.3109/08982104.2011.621127

CHEN, S. T., VOLLE, D., JALIL, J., WU, P. & SMALL, G. W. 2019. Health-promoting strategies for the aging brain. *The American Journal of Geriatric Psychiatry,* 27**,** 213-236.

CHENG, A. L., HSU, C. H., LIN, J. K., HSU, M. M., HO, Y. F., SHEN, T. S., KO, J. Y., LIN, J. T., LIN, B. R., MING-SHIANG, W., YU, H. S., JEE, S. H., CHEN, G. S.,

CHEN, T. M., CHEN, C. A., LAI, M. K., PU, Y. S., PAN, M. H., WANG, Y. J., TSAI, C. C. & HSIEH, C. Y. 2001. Phase I clinical trial of curcumin, a chemopreventive agent, in patients with high-risk or pre-malignant lesions. *Anticancer Res,* 21.
CHENG, C., PENG, S., LI, Z., ZOU, L., LIU, W. & LIU, C. 2017. Improved bioavailability of curcumin in liposomes prepared using a pH-driven, organic solvent-free, easily scalable process. *RSC Advances,* 7**,** 25978-25986. Available: 10.1039/C7RA02861J
CHERIAN, L., WANG, Y., FAKUDA, K., LEURGANS, S., AGGARWAL, N. & MORRIS, M. 2019. Mediterranean-Dash Intervention for Neurodegenerative Delay (MIND) Diet Slows Cognitive Decline After Stroke. *The Journal of Prevention of Alzheimer's Disease,* 6**,** 267-273. Available: 10.14283/jpad.2019.28
CICERO, A. F. G., SAHEBKAR, A., FOGACCI, F., BOVE, M., GIOVANNINI, M. & BORGHI, C. 2020. Effects of phytosomal curcumin on anthropometric parameters, insulin resistance, cortisolemia and non-alcoholic fatty liver disease indices: a double-blind, placebo-controlled clinical trial. *European Journal of Nutrition,* 59**,** 477-483. Available: 10.1007/s00394-019-01916-7
CLANDININ, M., JUMPSEN, J. & SUH, M. 1994. Relationship between fatty acid accretion, membrane composition, and biologic functions. *The Journal of pediatrics,* 125**,** S25-S32.
COANT, N., SAKAMOTO, W., MAO, C. & HANNUN, Y. A. 2017. Ceramidases, roles in sphingolipid metabolism and in health and disease. *Advances in Biological Regulation,* 63**,** 122-131. Available: https://doi.org/10.1016/j.jbior.2016.10.002
COLE, G. M., LIM, G. P., YANG, F., TETER, B., BEGUM, A., MA, Q., HARRIS-WHITE, M. E. & FRAUTSCHY, S. A. 2005a. Prevention of Alzheimer's disease: Omega-3 fatty acid and phenolic anti-oxidant interventions. *Neurobiology of Aging,* 26**,** 133-136. Available: https://doi.org/10.1016/j.neurobiolaging.2005.09.005
COLE, G. M., LIM, G. P., YANG, F., TETER, B., BEGUM, A., MA, Q., HARRIS-WHITE, M. E. & FRAUTSCHY, S. A. 2005b. Prevention of Alzheimer's disease: Omega-3 fatty acid and phenolic anti-oxidant interventions. *Neurobiology of Aging,* 26**,** S133-S136. Available: 10.1016/j.neurobiolaging.2005.09.005
COLE, G. M., TETER, B. & FRAUTSCHY, S. A. 2007. Neuroprotective effects of curcumin. *Advances in experimental medicine and biology,* 595**,** 197-212.
COLE, S. L. & VASSAR, R. 2007. The Alzheimer's disease beta-secretase enzyme, BACE1. *Molecular neurodegeneration,* 2**,** 22-22. Available: 10.1186/1750-1326-2-22
COLLE, I. J. P., VAN BUGGENHOUT, S., LEMMENS, L., VAN LOEY, A. M. & HENDRICKX, M. E. 2012. The type and quantity of lipids present during digestion influence the in vitro bioaccessibility of lycopene from raw tomato pulp. *Food Research International,* 45**,** 250-255. Available: https://doi.org/10.1016/j.foodres.2011.10.041
CONKLIN, K. A. 2002. Dietary polyunsaturated fatty acids: impact on cancer chemotherapy and radiation. *Alternative medicine review,* 7**,** 4-21.
CONQUER, J. A., TIERNEY, M. C., ZECEVIC, J., BETTGER, W. J. & FISHER, R. H. 2000. Fatty acid analysis of blood plasma of patients with Alzheimer's disease, other types of dementia, and cognitive impairment. *Lipids,* 35**,** 1305-1312.
CORREDIG, M. & DALGLEISH, D. G. 1997. Isolates from industrial buttermilk: Emulsifying properties of materials derived from the milk fat globule membrane. *Journal of Agricultural and Food Chemistry,* 45**,** 4595-4600.
CORREDIG, M. & DALGLEISH, D. G. 1998. Characterization of the interface of an oil-in-water emulsion stabilized by milk fat globule membrane material. *Journal of Dairy Research,* 65**,** 465-477. Available: undefined

CROOK, T. H., PETRIE, W., WELLS, C., & MASSARI, D. C. 1992. Effects of phosphatidylserine in Alzheimer's disease. . *Psychopharmacology Bulletin*, 28 61–66.
CUOMO, J., APPENDINO, G., DERN, A. S., SCHNEIDER, E., MCKINNON, T. P., BROWN, M. J., TOGNI, S. & DIXON, B. M. 2011. Comparative absorption of a standardized curcuminoid mixture and its lecithin formulation. *Journal of Natural Products*, 74**,** 664-669. Available: 10.1021/np1007262
D'AQUILA, T., HUNG, Y.-H., CARREIRO, A. & BUHMAN, K. K. 2016. Recent discoveries on absorption of dietary fat: Presence, synthesis, and metabolism of cytoplasmic lipid droplets within enterocytes. *Biochimica et Biophysica Acta (BBA) - Molecular and Cell Biology of Lipids*, 1861**,** 730-747. Available: https://doi.org/10.1016/j.bbalip.2016.04.012
DALGLEISH, D. G. 2006. Food emulsions—their structures and structure-forming properties. *Food Hydrocolloids*, 20**,** 415-422. Available: https://doi.org/10.1016/j.foodhyd.2005.10.009
DAVIDOV-PARDO, G., GUMUS, C. E. & MCCLEMENTS, D. J. 2016. Lutein-enriched emulsion-based delivery systems: Influence of pH and temperature on physical and chemical stability. *Food Chemistry*, 196**,** 821-827. Available: https://doi.org/10.1016/j.foodchem.2015.10.018
DAVIS, C., BRYAN, J., HODGSON, J. & MURPHY, K. 2015. Definition of the Mediterranean Diet; a Literature Review. *Nutrients*, 7**,** 9139-9153. Available: 10.3390/nu7115459
DE WILLE, J. W. & FARMER, S. J. 1992. Postnatal dietary fat influences mRNAs involved in myelination. *Developmental Neuroscience*, 14**,** 61-68. Available: 10.1159/000111648
DECKELBAUM, R. J., HAMILTON, J. A., MOSER, A., BENGTSSON-OLIVECRONA, G., BUTBUL, E., CARPENTIER, Y. A., GUTMAN, A. & OLIVECRONA, T. 1990. Medium-chain versus long-chain triacylglycerol emulsion hydrolysis by lipoprotein lipase and hepatic lipase: implications for the mechanisms of lipase action. *Biochemistry*, 29**,** 1136-42. Available: 10.1021/bi00457a006
DEI CAS, M. & GHIDONI, R. 2019. Dietary Curcumin: Correlation between Bioavailability and Health Potential. *Nutrients*, 11. Available: 10.3390/nu11092147
DEN HAAN, J., MORREMA, T. H. J., ROZEMULLER, A. J., BOUWMAN, F. H. & HOOZEMANS, J. J. M. 2018. Different curcumin forms selectively bind fibrillar amyloid beta in post mortem Alzheimer's disease brains: Implications for in-vivo diagnostics. *Acta Neuropathol Commun*, 6**,** 75. Available: 10.1186/s40478-018-0577-2
DENNIS, E. A. 1994. Diversity of group types, regulation, and function of phospholipase A2. *Journal of Biological Chemistry*, 269**,** 13057-13060. Available: https://doi.org/10.1016/S0021-9258(17)36794-7
DEWETTINCK, K., ROMBAUT, R., THIENPONT, N., LE, T. T., MESSENS, K. & VAN CAMP, J. 2008. Nutritional and technological aspects of milk fat globule membrane material. *International Dairy Journal*, 18**,** 436-457. Available: https://doi.org/10.1016/j.idairyj.2007.10.014
DI LORENZO, C., COLOMBO, F., BIELLA, S., STOCKLEY, C. & RESTANI, P. 2021. Polyphenols and human health: The role of bioavailability. *Nutrients*, 13**,** 273.
DIBAEI M, R. M., SHEIKHOLESLAMI B, GHOLAMI M, DINARVAND R. 2019. The effect of surface treatment on the brain delivery of curcumin nanosuspension: in vitro and in vivo studies. *Int J Nanomedicine*, 14**,** 5477-5490. Available: https://doi.org/10.2147/IJN.S199624

DICKINSON, E. 1988. *In:* BLANSHARD, J. M. V. & MITCHELL, J. R. (eds.) *Food Structure - Its Creation and Evaluation.* Woodhead Publishing. Available: https://doi.org/10.1533/9781845698348.41
DONG, K., FERNANDO, W., DURHAM, R., STOCKMANN, R., JAYATUNGA, D. P. W. & JAYASENA, V. 2019. P2-051: IN VITRO ASSAY TO ASSESS THE POTENTIAL OF SEA BUCKTHORN AND GOJI BERRY AS THERAPEUTIC AGENTS FOR ALZHEIMER'S DISEASE. *Alzheimer's & Dementia,* 15**,** P592-P592. Available: https://doi.org/10.1016/j.jalz.2019.06.2458
DRUKARCH, B. & VAN MUISWINKEL, F. L. 2001. Neuroprotection for Parkinson's disease: a new approach for a new millennium. *Expert opinion on investigational drugs,* 10**,** 1855-1868.
DUBOIS, B. & ALBERT, M. L. 2004. Amnestic MCI or prodromal Alzheimer's disease? *The Lancet Neurology,* 3**,** 246-248. Available: https://doi.org/10.1016/S1474-4422(04)00710-0
ECHTEN-DECKERT, G. V. & ALAM, S. 2018. Sphingolipid metabolism – an ambiguous regulator of autophagy in the brain. *Biological Chemistry,* 399**,** 837-850. Available: doi:10.1515/hsz-2018-0237
ESPOSITO, E., ROTILIO, D., DI MATTEO, V., DI GIULIO, C., CACCHIO, M. & ALGERI, S. 2002. A review of specific dietary antioxidants and the effects on biochemical mechanisms related to neurodegenerative processes. *Neurobiology of Aging,* 23**,** 719-735. Available: https://doi.org/10.1016/S0197-4580(02)00078-7
FARHANG, B., KAKUDA, Y. & CORREDIG, M. 2012. Encapsulation of ascorbic acid in liposomes prepared with milk fat globule membrane-derived phospholipids. *Dairy Science & Technology,* 92**,** 353-366. Available: 10.1007/s13594-012-0072-7
FARKAS, E., DE WILDE, M. C., KILIAAN, A. J., MEIJER, J., KEIJSER, J. N. & LUITEN, P. G. 2002. Dietary long chain PUFAs differentially affect hippocampal muscarinic 1 and serotonergic 1A receptors in experimental cerebral hypoperfusion. *Brain research,* 954**,** 32-41.
FAVE, G., COSTE, T. & ARMAND, M. 2004. Physicochemical properties of lipids: new strategies to manage fatty acid bioavailability. *Cellular and molecular biology,* 50**,** 815-832.
FERNANDEZ-AVILA, C., ARRANZ, E., GURI, A., TRUJILLO, A. J. & CORREDIG, M. 2016. Vegetable protein isolate-stabilized emulsions for enhanced delivery of conjugated linoleic acid in Caco-2 cells. *Food Hydrocolloids,* 55**,** 144-154. Available: https://doi.org/10.1016/j.foodhyd.2015.10.015
FERNANDEZ-GARCIA, E., CARVAJAL-LERIDA, I. & PEREZ-GALVEZ, A. 2009. In vitro bioaccessibility assessment as a prediction tool of nutritional efficiency. *Nutr Res,* 29**,** 751-60. Available: 10.1016/j.nutres.2009.09.016
FERNANDO, W. M. A. D. B., MARTINS, I. J., GOOZEE, K., BRENNAN, C. S., JAYASENA, V. & MARTINS, R. N. 2015. The role of dietary coconut for the prevention and treatment of Alzheimer's disease: potential mechanisms of action. *British Journal of Nutrition,* 114**,** 1-14.
FERRARI, C. 2001. Oxidative stress pathophysiology: searching for an effective antioxidant protection. *INTERNATIONAL MEDICAL JOURNAL-TOKYO-,* 8**,** 175-184.
FERRARI, C. K. B. 2007. Functional foods and physical activities in health promotion of aging people. *Maturitas,* 58**,** 327-339. Available: 10.1016/j.maturitas.2007.09.011
FERREIRA, S. T., CLARKE, J. R., BOMFIM, T. R. & DE FELICE, F. G. 2014. Inflammation, defective insulin signaling, and neuronal dysfunction in Alzheimer's disease. *Alzheimer's & Dementia,* 10**,** S76-S83. Available: https://doi.org/10.1016/j.jalz.2013.12.010

FIDELIS, E. M., SAVALL, A. S. P., DA LUZ ABREU, E., CARVALHO, F., TEIXEIRA, F. E. G., HAAS, S. E., BAZANELLA SAMPAIO, T. & PINTON, S. 2019. Curcumin-Loaded Nanocapsules Reverses the Depressant-Like Behavior and Oxidative Stress Induced by β-Amyloid in Mice. *Neuroscience,* 423**,** 122-130. Available: 10.1016/j.neuroscience.2019.09.032
FIFRE, A., SPONNE, I., KOZIEL, V., KRIEM, B., YEN POTIN, F. T., BIHAIN, B. E., OLIVIER, J. L., OSTER, T. & PILLOT, T. 2006. Microtubule-associated protein MAP1A, MAP1B, and MAP2 proteolysis during soluble amyloid β-peptide-induced neuronal apoptosis: Synergistic involvement of calpain and caspase-3. *Journal of Biological Chemistry,* 281**,** 229-240. Available: 10.1074/jbc.M507378200
FIL, J. E., FLEMING, S. A., CHICHLOWSKI, M., GROSS, G., BERG, B. M. & DILGER, R. N. 2019. Evaluation of dietary bovine milk fat globule membrane supplementation on growth, serum cholesterol and lipoproteins, and neurodevelopment in the young pig. *Frontiers in pediatrics,* 7**,** 417.
FLORENT-BÉCHARD, S., DESBÈNE, C., GARCIA, P., ALLOUCHE, A., YOUSSEF, I., ESCANYÉ, M. C., KOZIEL, V., HANSE, M., MALAPLATE-ARMAND, C., STENGER, C., KRIEM, B., YEN-POTIN, F. T., OLIVIER, J. L., PILLOT, T. & OSTER, T. 2009. The essential role of lipids in Alzheimer's disease. *Biochimie,* 91**,** 804-809. Available: 10.1016/j.biochi.2009.03.004
FLORENT-BÉCHARD, S., MALAPLATE-ARMAND, C., KOZIEL, V., KRIEM, B., OLIVIER, J. L., PILLOT, T. & OSTER, T. 2007. Towards a nutritional approach for prevention of Alzheimer's disease: Biochemical and cellular aspects. *Journal of the Neurological Sciences,* 262**,** 27-36. Available: 10.1016/j.jns.2007.06.046
FOEGEDING, E. A. & DAVIS, J. P. 2011. Food protein functionality: A comprehensive approach. *Food Hydrocolloids,* 25**,** 1853-1864. Available: https://doi.org/10.1016/j.foodhyd.2011.05.008
FONTANA, I. C., ZIMMER, A. R., ROCHA, A. S., GOSMANN, G., SOUZA, D. O., LOURENCO, M. V., FERREIRA, S. T. & ZIMMER, E. R. 2020. Amyloid-β oligomers in cellular models of Alzheimer's disease. *Journal of Neurochemistry,* 155**,** 348-369. Available: https://doi.org/10.1111/jnc.15030
FOTUHI, M., MOHASSEL, P. & YAFFE, K. 2009. Fish consumption, long-chain omega-3 fatty acids and risk of cognitive decline or Alzheimer disease: a complex association. *Nat Clin Pract Neurol,* 5**,** 140-52. Available: 10.1038/ncpneuro1044
FRAUTSCHY, S. A., HU, W., KIM, P., MILLER, S. A., CHU, T., HARRIS-WHITE, M. E. & COLE, G. M. 2001. Phenolic anti-inflammatory antioxidant reversal of Aβ-induced cognitive deficits and neuropathology. *Neurobiology of Aging,* 22**,** 993-1005. Available: https://doi.org/10.1016/S0197-4580(01)00300-1
FREEMANTLE, E., VANDAL, M., TREMBLAY-MERCIER, J., TREMBLAY, S., BLACHÈRE, J.-C., BÉGIN, M. E., BRENNA, J. T., WINDUST, A. & CUNNANE, S. C. 2006. Omega-3 fatty acids, energy substrates, and brain function during aging. *Prostaglandins, leukotrienes and essential fatty acids,* 75**,** 213-220.
GALLIER, S., VOCKING, K., POST, J. A., VAN DE HEIJNING, B., ACTON, D., VAN DER BEEK, E. M. & VAN BAALEN, T. 2015. A novel infant milk formula concept: Mimicking the human milk fat globule structure. *Colloids and Surfaces B: Biointerfaces,* 136**,** 329-339. Available: https://doi.org/10.1016/j.colsurfb.2015.09.024
GALLIER, S., YE, A. & SINGH, H. 2012. Structural changes of bovine milk fat globules during in vitro digestion. *Journal of Dairy Science,* 95**,** 3579-3592. Available: https://doi.org/10.3168/jds.2011-5223
GAMES, D., ADAMS, D., ALESSANDRINI, R., BARBOUR, R., BERTHELETTE, P., BLACKWELL, C., CARR, T., CLEMENS, J., DONALDSON, T., GILLESPIE, F.

& ET AL. 1995. Alzheimer-type neuropathology in transgenic mice overexpressing V717F beta-amyloid precursor protein. *Nature,* 373**,** 523-7. Available: 10.1038/373523a0
GANGULI, M., CHANDRA, V., KAMBOH, M. I., JOHNSTON, J. M., DODGE, H. H., THELMA, B., JUYAL, R. C., PANDAV, R., BELLE, S. H. & DEKOSKY, S. T. 2000. Apolipoprotein E polymorphism and Alzheimer disease: the Indo-US cross-national dementia study. *Archives of Neurology,* 57**,** 824-830.
GAO, C., CHU, X., GONG, W., ZHENG, J., XIE, X., WANG, Y., YANG, M., LI, Z., GAO, C. & YANG, Y. 2020. Neuron tau-targeting biomimetic nanoparticles for curcumin delivery to delay progression of Alzheimer's disease. *Journal of nanobiotechnology,* 18**,** 71-71. Available: 10.1186/s12951-020-00626-1
GARCÍA-SERRANO, A., TOMÉ-CARNEIRO, J., CARMEN CRESPO, M., VISITACIÓN CALVO, M., PEREDA-PÉREZ, I., BALIYAN, S., BURGOS-RAMOS, E., MONTERO, O., DÁVALOS, A., VENERO, C., VISIOLI, F. & FONTECHA, J. 2020. Concentrates of buttermilk and krill oil improve cognition in aged rats. *Prostaglandins Leukot Essent Fatty Acids,* 155**,** 102077. Available: 10.1016/j.plefa.2020.102077
GEBHARDT, P., HOOGEVEST, P. V. & ENGELHART-JENTZSCH, K. 2019. A liquid phospholipid formulation of a curcumin extract with high concentration of phosphatidylcholine (Phosal® curcumin) improves the transport of curcuminoids across Caco-2 intestinal epithelial cells. *Agro Food Industry Hi-Tech,* 30**,** 56-59.
GERLACH, M., DOUBLE, K. L., BEN-SHACHAR, D., ZECCA, L., YOUDIM, M. B. H. & RIEDERER, P. 2003. Neuromelanin and its interaction with iron as a potential risk factor for dopaminergic neurodegeneration underlying Parkinson's disease. *Neurotoxicity Research,* 5**,** 35-43. Available: 10.1007/bf03033371
GERSTENECKER, A. & MAST, B. 2015. Mild cognitive impairment: a history and the state of current diagnostic criteria. *International Psychogeriatrics,* 27**,** 199-211. Available: 10.1017/S1041610214002270
GLEITER, C. H. & GUNDERT-REMY, U. 1996. Gender differences in pharmacokinetics. *European Journal of Drug Metabolism and Pharmacokinetics,* 21**,** 123-128. Available: 10.1007/BF03190260
GÖTZ, J., STREFFER, J. R., DAVID, D., SCHILD, A., HOERNDLI, F., PENNANEN, L., KUROSINSKI, P. & CHEN, F. 2004. Transgenic animal models of Alzheimer's disease and related disorders: histopathology, behavior and therapy. *Mol Psychiatry,* 9**,** 664-83. Available: 10.1038/sj.mp.4001508
GRANATO, D., NUNES, D. S. & BARBA, F. J. 2017. An integrated strategy between food chemistry, biology, nutrition, pharmacology, and statistics in the development of functional foods: A proposal. *Trends in Food Science & Technology,* 62**,** 13-22. Available: https://doi.org/10.1016/j.tifs.2016.12.010
GRANT, W. B. 1997. Dietary Links to Alzheimer's Disease. *Alzheimer's Disease Review* 2**,** 42-55.
GREEN, K. N., MARTINEZ-CORIA, H., KHASHWJI, H., HALL, E. B., YURKO-MAURO, K. A., ELLIS, L. & LAFERLA, F. M. 2007. Dietary docosahexaenoic acid and docosapentaenoic acid ameliorate amyloid-β and tau pathology via a mechanism involving presenilin 1 levels. *The Journal of neuroscience,* 27**,** 4385-4395.
GRIT, M. & CROMMELIN, D. J. 1993. Chemical stability of liposomes: implications for their physical stability. *Chemistry and physics of lipids,* 64**,** 3-18.
GROENEVELD, O., REIJMER, Y., HEINEN, R., KUIJF, H., KOEKKOEK, P., JANSSEN, J., RUTTEN, G., KAPPELLE, L. & BIESSELS, G. 2018. Brain imaging correlates of mild cognitive impairment and early dementia in patients with type 2

diabetes mellitus. *Nutrition, Metabolism and Cardiovascular Diseases,* 28**,** 1253-1260. Available: https://doi.org/10.1016/j.numecd.2018.07.008
GSTRAUNTHALER, G., LINDL, T. & VAN DER VALK, J. 2013. A plea to reduce or replace fetal bovine serum in cell culture media. *Cytotechnology,* 65**,** 791-793. Available: 10.1007/s10616-013-9633-8
GU, X., ZHANG, G., QIN, Z., YIN, M., CHEN, W., ZHANG, Y. & LIU, X. 2022. Safinamide protects against amyloid β (Aβ)-induced oxidative stress and cellular senescence in M17 neuronal cells. *Bioengineered,* 13**,** 1921-1930. Available: 10.1080/21655979.2021.2022262
HAAS, G. H. D., SARDA, L. & ROGER, J. 1965. Positional specific hydrolysis of phospholipids by pancreatic lipase. *Biochimica et Biophysica Acta (BBA)-Lipids and Lipid Metabolism,* 106**,** 638-640.
HAMAGUCHI, T., ONO, K. & YAMADA, M. 2006. Anti-amyloidogenic therapies: strategies for prevention and treatment of Alzheimer's disease. *Cellular and Molecular Life Sciences CMLS,* 63**,** 1538-1552.
HAMAGUCHI, T., ONO, K. & YAMADA, M. 2010. REVIEW: Curcumin and Alzheimer's Disease. *CNS Neuroscience & Therapeutics,* 16**,** 285-297. Available: doi:10.1111/j.1755-5949.2010.00147.x
HARDY, J. & SELKOE, D. J. 2002. The amyloid hypothesis of Alzheimer's disease: progress and problems on the road to therapeutics. *Science,* 297**,** 353-6. Available: 10.1126/science.1072994
HASHIMOTO, M., HOSSAIN, S., AGDUL, H. & SHIDO, O. 2005a. Docosahexaenoic acid-induced amelioration on impairment of memory learning in amyloid β-infused rats relates to the decreases of amyloid β and cholesterol levels in detergent-insoluble membrane fractions. *Biochimica et Biophysica Acta (BBA)-Molecular and Cell Biology of Lipids,* 1738**,** 91-98.
HASHIMOTO, M., HOSSAIN, S., SHIMADA, T., SUGIOKA, K., YAMASAKI, H., FUJII, Y., ISHIBASHI, Y., OKA, J. I. & SHIDO, O. 2002. Docosahexaenoic acid provides protection from impairment of learning ability in Alzheimer's disease model rats. *Journal of neurochemistry,* 81**,** 1084-1091.
HASHIMOTO, M., TANABE, Y., FUJII, Y., KIKUTA, T., SHIBATA, H. & SHIDO, O. 2005b. Chronic administration of docosahexaenoic acid ameliorates the impairment of spatial cognition learning ability in amyloid β–infused rats. *The Journal of nutrition,* 135**,** 549-555.
HE, S., TANG, H., YI, H., XU, W., MA, Y. & WANG, R. 2017. Properties of emulsions from milk fat globule membrane and its components. *International Journal of Food Properties,* 20**,** 1342-1353. Available: 10.1080/10942912.2017.1343348
HEGER, M., VAN GOLEN, R. F., BROEKGAARDEN, M. & MICHEL, M. C. 2014. The Molecular Basis for the Pharmacokinetics and Pharmacodynamics of Curcumin and Its Metabolites in Relation to Cancer. *Pharmacological Reviews,* 66**,** 222-307. Available: 10.1124/pr.110.004044
HEINRICH, M. & PRIETO, J. M. 2008. Diet and healthy ageing 2100: Will we globalise local knowledge systems? *Ageing Research Reviews,* 7**,** 249-274. Available: http://dx.doi.org/10.1016/j.arr.2007.08.002
HENDERSON, S. T. 2004. High carbohydrate diets and Alzheimer's disease. *Medical Hypotheses,* 62**,** 689-700. Available: 10.1016/j.mehy.2003.11.028
HENEKA, M. T., CARSON, M. J., EL KHOURY, J., LANDRETH, G. E., BROSSERON, F., FEINSTEIN, D. L., JACOBS, A. H., WYSS-CORAY, T., VITORICA, J., RANSOHOFF, R. M., HERRUP, K., FRAUTSCHY, S. A., FINSEN, B., BROWN, G. C., VERKHRATSKY, A., YAMANAKA, K., KOISTINAHO, J.,

LATZ, E., HALLE, A., PETZOLD, G. C., TOWN, T., MORGAN, D., SHINOHARA, M. L., PERRY, V. H., HOLMES, C., BAZAN, N. G., BROOKS, D. J., HUNOT, S., JOSEPH, B., DEIGENDESCH, N., GARASCHUK, O., BODDEKE, E., DINARELLO, C. A., BREITNER, J. C., COLE, G. M., GOLENBOCK, D. T. & KUMMER, M. P. 2015. Neuroinflammation in Alzheimer's disease. *Lancet Neurol,* 14**,** 388-405. Available: 10.1016/s1474-4422(15)70016-5

HERNÁNDEZ-LEDESMA, B., HSIEH, C.-C. & MARTÍNEZ-VILLALUENGA, C. 2017. Food bioactive compounds against diseases of the 21st century 2016. Hindawi.

HERON, D. S., SHINITZKY, M., HERSHKOWITZ, M. & SAMUEL, D. 1980. Lipid fluidity markedly modulates the binding of serotonin to mouse brain membranes. *Proceedings of the National Academy of Sciences,* 77**,** 7463-7467.

HEWLINGS, S. J. & KALMAN, D. S. 2017. Curcumin: A Review of Its Effects on Human Health. *Foods,* 6**,** 92.

HOFMAN, A., BRETELER, M. M. B., VAN DUIJN, C. M., KRESTIN, G. P., POLS, H. A., STRICKER, B. H. C., TIEMEIER, H., UITTERLINDEN, A. G., VINGERLING, J. R. & WITTEMAN, J. C. M. 2007. The Rotterdam Study: objectives and design update. *European Journal of Epidemiology,* 22**,** 819-829. Available: 10.1007/s10654-007-9199-x

HONIG, L. S. 2000. Inflammation in neurodegenerative disease: good, bad, or irrelevant? *Archives of neurology,* 57**,** 786-788.

HOOIJMANS, C. R. & KILIAAN, A. J. 2008. Fatty acids, lipid metabolism and Alzheimer pathology. *European Journal of Pharmacology,* 585**,** 176-196. Available: 10.1016/j.ejphar.2007.11.081

HOOPER, C., DE SOUTO BARRETO, P., PAYOUX, P., SALABERT, A. S., GUYONNET, S., ANDRIEU, S., SOURDET, S., DELRIEU, J., VELLAS, B. & GROUP, M. D. S. 2017. Association of cortical β-amyloid with erythrocyte membrane monounsaturated and saturated fatty acids in older adults at risk of dementia. *The journal of nutrition, health & aging,* 21**,** 1170-1175. Available: 10.1007/s12603-017-0975-3

HU YANG, I., DE LA RUBIA ORTÍ, J. E., SELVI SABATER, P., SANCHO CASTILLO, S., ROCHINA, M. J., MANRESA RAMÓN, N. & MONTOYA-CASTILLA, I. 2015. [COCONUT OIL: NON-ALTERNATIVE DRUG TREATMENT AGAINST ALZHEIMER´S DISEASE]. *Nutr Hosp,* 32**,** 2822-7. Available: 10.3305/nh.2015.32.6.9707

HUANG, M. T., LOU, Y. R., MA, W., NEWMARK, H. L., REUHL, K. R. & CONNEY, A. H. 1994. Inhibitory effects of dietary curcumin on forestomach, duodenal, and colon carcinogenesis in mice. *Cancer Res,* 54.

HUANG, X., LIANG, C., YANG, H., LI, X., DENG, X., LIANG, X., LI, L., HUANG, Z., LU, D. & MA, Y. 2021. Curcumin induces apoptosis and inhibits the growth of adrenocortical carcinoma: Identification of potential candidate genes and pathways by transcriptome analysis. *Oncology Letters,* 21**,** 1-11.

HUANG, Y., DENG, S., LUO, X., LIU, Y., XU, W., PAN, J., WANG, M. & XIA, Z. 2019. Evaluation of Intestinal Absorption Mechanism and Pharmacokinetics of Curcumin-Loaded Galactosylated Albumin Nanoparticles. *International journal of nanomedicine,* 14**,** 9721-9730. Available: 10.2147/IJN.S229992

HUO, X., ZHANG, Y., JIN, X., LI, Y. & ZHANG, L. 2019. A novel synthesis of selenium nanoparticles encapsulated PLGA nanospheres with curcumin molecules for the inhibition of amyloid β aggregation in Alzheimer's disease. *Journal of Photochemistry and Photobiology B: Biology,* 190**,** 98-102. Available: https://doi.org/10.1016/j.jphotobiol.2018.11.008

IBRAHIM, S., TAGAMI, T., KISHI, T. & OZEKI, T. 2018. Curcumin marinosomes as promising nano-drug delivery system for lung cancer. *International Journal of Pharmaceutics,* 540**,** 40-49. Available: https://doi.org/10.1016/j.ijpharm.2018.01.051
IKRAM, M. A., BRUSSELLE, G., GHANBARI, M., GOEDEGEBURE, A., IKRAM, M. K., KAVOUSI, M., KIEBOOM, B. C. T., KLAVER, C. C. W., DE KNEGT, R. J., LUIK, A. I., NIJSTEN, T. E. C., PEETERS, R. P., VAN ROOIJ, F. J. A., STRICKER, B. H., UITTERLINDEN, A. G., VERNOOIJ, M. W. & VOORTMAN, T. 2020a. Objectives, design and main findings until 2020 from the Rotterdam Study. *Eur J Epidemiol,* 35**,** 483-517. Available: 10.1007/s10654-020-00640-5
IKRAM, M. A., BRUSSELLE, G., GHANBARI, M., GOEDEGEBURE, A., IKRAM, M. K., KAVOUSI, M., KIEBOOM, B. C. T., KLAVER, C. C. W., DE KNEGT, R. J., LUIK, A. I., NIJSTEN, T. E. C., PEETERS, R. P., VAN ROOIJ, F. J. A., STRICKER, B. H., UITTERLINDEN, A. G., VERNOOIJ, M. W. & VOORTMAN, T. 2020b. Objectives, design and main findings until 2020 from the Rotterdam Study. *European Journal of Epidemiology,* 35**,** 483-517. Available: 10.1007/s10654-020-00640-5
IM, K., MALIAKEL, A., G, G., KUMAR, D., MALIAKEL, B. & KUTTAN, R. 2015. Improved blood–brain-barrier permeability and tissue distribution following the oral administration of a food-grade formulation of curcumin with fenugreek fibre. *Journal of Functional Foods,* 14**,** 215-225. Available: https://doi.org/10.1016/j.jff.2015.01.049
IMAIZUMI, A. 2015. Highly bioavailable curcumin (Theracurmin): its development and clinical application. *PharmaNutrition,* 3**,** 123-130. Available: https://doi.org/10.1016/j.phanu.2015.08.002
IRESON, C., ORR, S., JONES, D. J., VERSCHOYLE, R., LIM, C. K., LUO, J. L., HOWELLS, L., PLUMMER, S., JUKES, R., WILLIAMS, M., STEWARD, W. P. & GESCHER, A. 2001. Characterization of metabolites of the chemopreventive agent curcumin in human and rat hepatocytes and in the rat in vivo, and evaluation of their ability to inhibit phorbol ester-induced prostaglandin E2 production. *Cancer Res,* 61.
IRESON, C. R., JONES, D. J. L., ORR, S., COUGHTRIE, M. W. H., BOOCOCK, D. J., WILLIAMS, M. L., FARMER, P. B., STEWARD, W. P. & GESCHER, A. J. 2002. Metabolism of the cancer chemopreventive agent curcumin in human and rat intestine. *Cancer Epidemiology Biomarkers and Prevention,* 11**,** 105-111.
JÄGER, R., LOWERY, R. P., CALVANESE, A. V., JOY, J. M., PURPURA, M. & WILSON, J. M. 2014. Comparative absorption of curcumin formulations. *Nutrition Journal,* 13. Available: 10.1186/1475-2891-13-11
JAYATUNGA, D. P. W., HONE, E., FERNANDO, W., GARG, M. L., VERDILE, G. & MARTINS, R. N. 2021. Mitoprotective Effects of a Synergistic Nutraceutical Combination: Basis for a Prevention Strategy Against Alzheimer's Disease. *Front Aging Neurosci,* 13**,** 781468. Available: 10.3389/fnagi.2021.781468
JEYAPRIYA RAJA SUNDARAM, A., B,1 CHARLENE PRISCILLA POORE,A,C NOOR HAZIM BIN SULAIMEE,A,B TEJ PAREEK,E WEI FUN CHEONG,A,C MARKUS R. WENK,A,C HARISH C. PANT,F SALLY A. FRAUTSCHY,G,H CHIAN-MING LOW,A,B,D AND SASHI KESAVAPANYA,C,* 2017. Curcumin Ameliorates Neuroinflammation, Neurodegeneration, and Memory Deficits in p25 Transgenic Mouse Model that Bears Hallmarks of Alzheimer's Disease. *J Alzheimers Dis.* , 60**,** 1429–1442. Available: 10.3233/JAD-170093
JIMÉNEZ-FLORES, R., HIGUERA-CIAPARA, I. & POULIOT, Y. 2009. 11 - Beverages based on milk fat globule membrane (MFGM) and other novel concepts for dairy-based functional beverages. *In:* PAQUIN, P. (ed.) *Functional and Speciality Beverage Technology*. Woodhead Publishing. Available: https://doi.org/10.1533/9781845695569.2.281

JINTAPATTANAKIT, A., HASAN, H. M. & JUNYAPRASERT, V. B. 2018. Vegetable oil-based nanoemulsions containing curcuminoids: Formation optimization by phase inversion temperature method. *Journal of Drug Delivery Science and Technology,* 44**,** 289-297. Available: https://doi.org/10.1016/j.jddst.2017.12.018
JOVANOVIC, S. V., STEENKEN, S., BOONE, C. W. & SIMIC, M. G. 1999. H-Atom Transfer Is A Preferred Antioxidant Mechanism of Curcumin. *Journal of the American Chemical Society,* 121**,** 9677-9681. Available: 10.1021/ja991446m
KAKAR, S. S. & ROY, D. 1994. Curcumin inhibits TPA induced expression of c-fos, c-jun and c-myc proto-oncogenes messenger RNAs in mouse skin. *Cancer letters,* 87**,** 85-89.
KAKKAR, V., SINGH, S., SINGLA, D., SAHWNEY, S., CHAUHAN, A. S., SINGH, G. & KAUR, I. P. 2010. Pharmacokinetic applicability of a validated liquid chromatography tandem mass spectroscopy method for orally administered curcumin loaded solid lipid nanoparticles to rats. *Journal of Chromatography B,* 878**,** 3427-3431. Available: https://doi.org/10.1016/j.jchromb.2010.10.017
KALMIJN, S., LAUNER, L. J., OTT, A., WITTEMAN, J. C. M., HOFMAN, A. & BRETELER, M. M. B. 1997. Dietary fat intake and the risk of incident dementia in the Rotterdam study. *Annals of Neurology,* 42**,** 776-782. Available: https://doi.org/10.1002/ana.410420514
KANAI, M., IMAIZUMI, A., OTSUKA, Y., SASAKI, H., HASHIGUCHI, M., TSUJIKO, K., MATSUMOTO, S., ISHIGURO, H. & CHIBA, T. 2012. Dose-escalation and pharmacokinetic study of nanoparticle curcumin, a potential anticancer agent with improved bioavailability, in healthy human volunteers. *Cancer Chemother Pharmacol,* 69**,** 65-70. Available: 10.1007/s00280-011-1673-1
KANNO, C., SHIMOMURA, Y. & TAKANO, E. 1991. Physicochemical properties of milk fat emulsions stabilized with bovine milk fat globule membrane. *Journal of Food Science,* 56**,** 1219-1223.
KELLOFF, G. J., CROWELL, J. A., HAWK, E. T., STEELE, V. E., LUBET, R. A., BOONE, C. W., COVEY, J. M., DOODY, L. A., OMENN, G. S. & GREENWALD, P. 1996. Strategy and planning for chemopreventive drug development: clinical development plans II. *Journal of Cellular Biochemistry,* 63**,** 54-71.
KEYS, A. 1995. Mediterranean diet and public health: personal reflections. *The American Journal of Clinical Nutrition,* 61**,** 1321S-1323S. Available: 10.1093/ajcn/61.6.1321S
KHALIL, N. M., DO NASCIMENTO, T. C., CASA, D. M., DALMOLIN, L. F., DE MATTOS, A. C., HOSS, I., ROMANO, M. A. & MAINARDES, R. M. 2013. Pharmacokinetics of curcumin-loaded PLGA and PLGA-PEG blend nanoparticles after oral administration in rats. *Colloids Surf B Biointerfaces,* 101**,** 353-60. Available: 10.1016/j.colsurfb.2012.06.024
KHARAT, M., SKRZYNSKI, M., DECKER, E. A. & MCCLEMENTS, D. J. 2020. Enhancement of chemical stability of curcumin-enriched oil-in-water emulsions: Impact of antioxidant type and concentration. *Food Chemistry,* 320**,** 126653. Available: https://doi.org/10.1016/j.foodchem.2020.126653
KHAYYAL, M. T., EL-HAZEK, R. M., EL-SABBAGH, W. A., FRANK, J., BEHNAM, D. & ABDEL-TAWAB, M. 2018. Micellar solubilisation enhances the antiinflammatory activities of curcumin and boswellic acids in rats with adjuvant-induced arthritis. *Nutrition,* 54**,** 189-196. Available: https://doi.org/10.1016/j.nut.2018.03.055

KIM, C.-S., PARK, S. & KIM, J. 2017. The role of glycation in the pathogenesis of aging and its prevention through herbal products and physical exercise. *Journal of exercise nutrition & biochemistry,* 21**,** 55-61. Available: 10.20463/jenb.2017.0027
KIM, D. S., PARK, S.-Y. & KIM, J.-Y. 2001. Curcuminoids from Curcuma longa L.(Zingiberaceae) that protect PC12 rat pheochromocytoma and normal human umbilical vein endothelial cells from βA (1–42) insult. *Neuroscience Letters,* 303**,** 57-61.
KLANG, V. & VALENTA, C. 2011. Lecithin-based nanoemulsions. *Journal of Drug Delivery Science and Technology,* 21**,** 55-76. Available: https://doi.org/10.1016/S1773-2247(11)50006-1
KOEKKOEK, P. S., KAPPELLE, L. J., VAN DEN BERG, E., RUTTEN, G. E. H. M. & BIESSELS, G. J. 2015. Cognitive function in patients with diabetes mellitus: guidance for daily care. *The Lancet Neurology,* 14**,** 329-340. Available: https://doi.org/10.1016/S1474-4422(14)70249-2
KOLEV, T. M., VELCHEVA, E. A., STAMBOLIYSKA, B. A. & SPITELLER, M. 2005. DFT and experimental studies of the structure and vibrational spectra of curcumin. *International Journal of Quantum Chemistry,* 102**,** 1069-1079. Available: https://doi.org/10.1002/qua.20469
KONAGAI, C., YANAGIMOTO, K., HAYAMIZU, K., HAN, L., TSUJI, T. & KOGA, Y. 2013. Effects of krill oil containing n-3 polyunsaturated fatty acids in phospholipid form on human brain function: a randomized controlled trial in healthy elderly volunteers. *Clinical interventions in aging,* 8**,** 1247-1257. Available: 10.2147/CIA.S50349
KRALOVA, I. & SJÖBLOM, J. 2009. Surfactants Used in Food Industry: A Review. *Journal of Dispersion Science and Technology,* 30**,** 1363-1383. Available: 10.1080/01932690902735561
KRIKORIAN, R., SHIDLER, M. D., NASH, T. A., KALT, W., VINQVIST-TYMCHUK, M. R., SHUKITT-HALE, B. & JOSEPH, J. A. 2010. Blueberry Supplementation Improves Memory in Older Adults. *Journal of Agricultural and Food Chemistry,* 58**,** 3996-4000. Available: 10.1021/jf9029332
KRIS-ETHERTON, P. M., HARRIS, W. S. & APPEL, L. J. 2003. Omega-3 Fatty Acids and Cardiovascular Disease. *Arteriosclerosis, Thrombosis, and Vascular Biology,* 23**,** 151-152. Available: doi:10.1161/01.ATV.0000057393.97337.AE
KUMAR, A., SINGH, A. & EKAVALI 2015. A review on Alzheimer's disease pathophysiology and its management: an update. *Pharmacol Rep,* 67**,** 195-203. Available: 10.1016/j.pharep.2014.09.004
KUNATI, S. R., YANG, S., WILLIAM, B. M. & XU, Y. 2018. An LC-MS/MS method for simultaneous determination of curcumin, curcumin glucuronide and curcumin sulfate in a phase II clinical trial. *J Pharm Biomed Anal,* 156**,** 189-198. Available: 10.1016/j.jpba.2018.04.034
KUNDU, P., DAS, M., TRIPATHY, K. & SAHOO, S. K. 2016. Delivery of Dual Drug Loaded Lipid Based Nanoparticles across the Blood-Brain Barrier Impart Enhanced Neuroprotection in a Rotenone Induced Mouse Model of Parkinson's Disease. *ACS Chem Neurosci,* 7**,** 1658-1670. Available: 10.1021/acschemneuro.6b00207
LAABBAR, W., ELGOT, A., ELHIBA, O. & GAMRANI, H. 2019. Curcumin prevents the midbrain dopaminergic innervations and locomotor performance deficiencies resulting from chronic aluminum exposure in rat. *J Chem Neuroanat,* 100**,** 101654. Available: 10.1016/j.jchemneu.2019.101654
LAITINEN, M. H., NGANDU, T., ROVIO, S., HELKALA, E. L., UUSITALO, U., VIITANEN, M., NISSINEN, A., TUOMILEHTO, J., SOININEN, H. & KIVIPELTO,

M. 2006. Fat Intake at Midlife and Risk of Dementia and Alzheimer's Disease: A Population-Based Study. *Dementia and Geriatric Cognitive Disorders,* 22**,** 99-107.
LAM, R. S. H. & NICKERSON, M. T. 2013. Food proteins: A review on their emulsifying properties using a structure–function approach. *Food Chemistry,* 141**,** 975-984. Available: https://doi.org/10.1016/j.foodchem.2013.04.038
LAO, C. D., RUFFIN, M. T. T., NORMOLLE, D., HEATH, D. D., MURRAY, S. I., BAILEY, J. M., BOGGS, M. E., CROWELL, J., ROCK, C. L. & BRENNER, D. E. 2006. Dose escalation of a curcuminoid formulation. *BMC Complement Altern Med,* 6**,** 10. Available: 10.1186/1472-6882-6-10
LAURITZEN, L., HANSEN, H. S., JORGENSEN, M. H. & MICHAELSEN, K. F. 2001. The essentiality of long chain n-3 fatty acids in relation to development and function of the brain and retina. *Progress in Lipid Research,* 40**,** 1-94. Available: 10.1016/S0163-7827(00)00017-5
LI, J., WANG, X., ZHANG, T., WANG, C., HUANG, Z., LUO, X. & DENG, Y. 2015a. A review on phospholipids and their main applications in drug delivery systems. *Asian Journal of Pharmaceutical Sciences,* 10**,** 81-98. Available: https://doi.org/10.1016/j.ajps.2014.09.004
LI, J., YE, A., LEE, S. J. & SINGH, H. 2013. Physicochemical behaviour of WPI-stabilized emulsions in in vitro gastric and intestinal conditions. *Colloids and Surfaces B: Biointerfaces,* 111**,** 80-87. Available: https://doi.org/10.1016/j.colsurfb.2013.05.034
LI, Q., ZHAI, W., JIANG, Q., HUANG, R., LIU, L., DAI, J., GONG, W., DU, S. & WU, Q. 2015b. Curcumin–piperine mixtures in self-microemulsifying drug delivery system for ulcerative colitis therapy. *International Journal of Pharmaceutics,* 490**,** 22-31. Available: https://doi.org/10.1016/j.ijpharm.2015.05.008
LI, Y., DING, R., REN, X., WEN, G., DONG, Z., YAO, H., TAN, Y., YU, H., WANG, X., ZHAN, X., YAO, J., LU, Y., ZHANG, G. & WU, X. 2019. Long-term ketamine administration causes Tau protein phosphorylation and Tau protein-dependent AMPA receptor reduction in the hippocampus of mice. *Toxicol Lett,* 315**,** 107-115. Available: 10.1016/j.toxlet.2019.08.023
LI, Y. & MCCLEMENTS, D. J. 2010. New Mathematical Model for Interpreting pH-Stat Digestion Profiles: Impact of Lipid Droplet Characteristics on in Vitro Digestibility. *Journal of Agricultural and Food Chemistry,* 58**,** 8085-8092. Available: 10.1021/jf101325m
LIANG, K. Y., MINTUN, M. A., FAGAN, A. M., GOATE, A. M., BUGG, J. M., HOLTZMAN, D. M., MORRIS, J. C. & HEAD, D. 2010. Exercise and Alzheimer's disease biomarkers in cognitively normal older adults. *Annals of Neurology,* 68**,** 311-318. Available: https://doi.org/10.1002/ana.22096
LIAU, K. M., LEE, Y. Y., CHEN, C. K. & RASOOL, A. H. 2011. An open-label pilot study to assess the efficacy and safety of virgin coconut oil in reducing visceral adiposity. *ISRN Pharmacol,* 2011**,** 949686. Available: 10.5402/2011/949686
LICHER, S., DARWEESH, S. K. L., WOLTERS, F. J., FANI, L., HESHMATOLLAH, A., MUTLU, U., KOUDSTAAL, P. J., HEERINGA, J., LEENING, M. J. G., IKRAM, M. K. & IKRAM, M. A. 2019. Lifetime risk of common neurological diseases in the elderly population. *Journal of Neurology, Neurosurgery & Psychiatry,* 90**,** 148. Available: 10.1136/jnnp-2018-318650
LIM, G. P., CALON, F., MORIHARA, T., YANG, F., TETER, B., UBEDA, O., SALEM, N., FRAUTSCHY, S. A. & COLE, G. M. 2005. A diet enriched with the omega-3 fatty acid docosahexaenoic acid reduces amyloid burden in an aged Alzheimer mouse model. *The Journal of Neuroscience,* 25**,** 3032-3040.

LIM, G. P., CHU, T., YANG, F., BEECH, W., FRAUTSCHY, S. A. & COLE, G. M. 2001a. The curry spice curcumin reduces oxidative damage and amyloid pathology in an Alzheimer transgenic mouse. *J Neurosci,* 21**,** 8370-7. Available: 10.1523/jneurosci.21-21-08370.2001
LIM, G. P., CHU, T., YANG, F., BEECH, W., FRAUTSCHY, S. A. & COLE, G. M. 2001b. The curry spice curcumin reduces oxidative damage and amyloid pathology in an Alzheimer transgenic mouse. *The Journal of Neuroscience,* 21**,** 8370-8377.
LIN, C.-C., LIN, H.-Y., CHEN, H.-C., YU, M.-W. & LEE, M.-H. 2009. Stability and characterisation of phospholipid-based curcumin-encapsulated microemulsions. *Food Chemistry,* 116**,** 923-928. Available: https://doi.org/10.1016/j.foodchem.2009.03.052
LIN, M. T. & BEAL, M. F. 2006. Mitochondrial dysfunction and oxidative stress in neurodegenerative diseases. *Nature,* 443**,** 787-795. Available: 10.1038/nature05292
LIU, A., LOU, H., ZHAO, L. & FAN, P. 2006. Validated LC/MS/MS assay for curcumin and tetrahydrocurcumin in rat plasma and application to pharmacokinetic study of phospholipid complex of curcumin. *Journal of pharmaceutical and biomedical analysis,* 40**,** 720-727.
LIU, C., YANG, X., WU, W., LONG, Z., XIAO, H., LUO, F., SHEN, Y. & LIN, Q. 2018. Elaboration of curcumin-loaded rice bran albumin nanoparticles formulation with increased in vitro bioactivity and in vivo bioavailability. *Food Hydrocolloids,* 77**,** 834-842. Available: https://doi.org/10.1016/j.foodhyd.2017.11.027
LIU, L., PAN, Y., ZHANG, X., ZHANG, Y. & LI, X. 2021a. Effect of Particle Size and Interface Composition on the Lipid Digestion of Droplets Covered with Membrane Phospholipids. *Journal of Agricultural and Food Chemistry,* 69**,** 159-169. Available: 10.1021/acs.jafc.0c04945
LIU, R. H. 2003. Health benefits of fruit and vegetables are from additive and synergistic combinations of phytochemicals. *American Journal of Clinical Nutrition,* 78**,** 517S-520S.
LIU, S., GAO, J., ZHU, M., LIU, K. & ZHANG, H.-L. 2020a. Gut Microbiota and Dysbiosis in Alzheimer's Disease: Implications for Pathogenesis and Treatment. *Molecular Neurobiology,* 57**,** 5026-5043. Available: 10.1007/s12035-020-02073-3
LIU, T., ZHANG, L., JOO, D. & SUN, S.-C. 2017. NF-κB signaling in inflammation. *Signal Transduction and Targeted Therapy,* 2**,** 17023. Available: 10.1038/sigtrans.2017.23
LIU, W., YE, A., LIU, C., LIU, W. & SINGH, H. 2012. Structure and integrity of liposomes prepared from milk- or soybean-derived phospholipids during in vitro digestion. *Food Research International,* 48**,** 499-506. Available: https://doi.org/10.1016/j.foodres.2012.04.017
LIU, W., YE, A., LIU, W., LIU, C. & SINGH, H. 2013. Stability during in vitro digestion of lactoferrin-loaded liposomes prepared from milk fat globule membrane-derived phospholipids. *Journal of Dairy Science,* 96**,** 2061-2070. Available: https://doi.org/10.3168/jds.2012-6072
LIU, X., HUNTER, D. J., EYLES, J., MCLACHLAN, A. J., ADIWIDJAJA, J., EAGLES, S. K. & WANG, X. 2020b. Pharmacokinetic assessment of constituents of Boswellia serrata, pine bark extracts, curcumin in combination including methylsulfonylmethane in healthy volunteers. *Journal of Pharmacy and Pharmacology,* 72**,** 121-131. Available: 10.1111/jphp.13184
LIU, X., MORRIS, M. C., DHANA, K., VENTRELLE, J., JOHNSON, K., BISHOP, L., HOLLINGS, C. S., BOULIN, A., LARANJO, N., STUBBS, B. J., REILLY, X., CAREY, V. J., WANG, Y., FURTADO, J. D., MARCOVINA, S. M., TANGNEY, C., AGGARWAL, N. T., ARFANAKIS, K., SACKS, F. M. & BARNES, L. L. 2021b.

Mediterranean-DASH Intervention for Neurodegenerative Delay (MIND) study: Rationale, design and baseline characteristics of a randomized control trial of the MIND diet on cognitive decline. *Contemporary Clinical Trials,* 102**,** 106270. Available: https://doi.org/10.1016/j.cct.2021.106270
LIVINGSTON, G., HUNTLEY, J., SOMMERLAD, A., AMES, D., BALLARD, C., BANERJEE, S., BRAYNE, C., BURNS, A., COHEN-MANSFIELD, J. & COOPER, C. 2020. Dementia prevention, intervention, and care: 2020 report of the Lancet Commission. *The Lancet,* 396**,** 413-446.
LIVNEY, Y. D., RUIMY, E., YE, A. M., ZHU, X. & SINGH, H. 2017. A milkfat globule membrane-inspired approach for encapsulation of emulsion oil droplets. *Food Hydrocolloids,* 65**,** 121-129. Available: https://doi.org/10.1016/j.foodhyd.2016.11.017
LOEBER, C. C., AND BUECHNER, A.E. 1748. "Dissertatio inauguralis medica de curcuma officinarum ejusque genuinis virtutibus," *Diss Inaug Halae, eds Praes A. E. Bunchnero (Halle: Halae Magdeburgicae),* 28.
LOPEZ, C., CAUTY, C., ROUSSEAU, F., BLOT, M., MARGOLIS, A. & FAMELART, M.-H. 2017. Lipid droplets coated with milk fat globule membrane fragments: Microstructure and functional properties as a function of pH. *Food Research International,* 91**,** 26-37. Available: https://doi.org/10.1016/j.foodres.2016.11.025
LUCHSINGER, J. A., TANG, M., SHEA, S. & MAYEUX, R. 2002. CAloric intake and the risk of alzheimer disease. *Archives of Neurology,* 59**,** 1258-1263. Available: 10.1001/archneur.59.8.1258
LUKIW, W. J., CUI, J.-G., MARCHESELLI, V. L., BODKER, M., BOTKJAER, A., GOTLINGER, K., SERHAN, C. N. & BAZAN, N. G. 2005. A role for docosahexaenoic acid–derived neuroprotectin D1 in neural cell survival and Alzheimer disease. *The Journal of clinical investigation,* 115**,** 2774-2783.
M.A. HAMID, M. R. S., T.H. MOKHTAR, W.R.W. SULAIMAN AND R.A. AZIZ 2011. Innovative Integrated Wet Process for Virgin Coconut Oil Production. *Journal of Applied Sciences,* 11**,** 2467-2469. Available: 10.3923/jas.2011.2467.2469
MAGGI, A. & DELLA TORRE, S. 2018. Sex, metabolism and health. *Molecular Metabolism,* 15**,** 3-7. Available: https://doi.org/10.1016/j.molmet.2018.02.012
MAITI, P., PLEMMONS, A., BOWERS, Z., WEAVER, C. & DUNBAR, G. 2019. Labeling and Imaging of Amyloid Plaques in Brain Tissue Using the Natural Polyphenol Curcumin. *J Vis Exp*. Available: 10.3791/60377
MAJEED, M., BADMAEV, V., SHIVAKUMAR, U. & RAJENDRAN, R. 1995. Curcuminoids: antioxidant phytonutrients. *Sabinsa Corporation, NJ, USA.*
MALAKI NIK, A., WRIGHT, A. J. & CORREDIG, M. 2011. Impact of interfacial composition on emulsion digestion and rate of lipid hydrolysis using different in vitro digestion models. *Colloids and Surfaces B: Biointerfaces,* 83**,** 321-330. Available: https://doi.org/10.1016/j.colsurfb.2010.12.001
MARCZYLO, T. H., VERSCHOYLE, R. D., COOKE, D. N., MORAZZONI, P., STEWARD, W. P. & GESCHER, A. J. 2007. Comparison of systemic availability of curcumin with that of curcumin formulated with phosphatidylcholine. *Cancer chemotherapy and pharmacology,* 60**,** 171-177.
MARCZYLO, T. H. V., R. D.; COOKE, D. N.; MORAZZONI, P; STEWARD, W. P.; GESCHER, A. J 2007. Comparison of systemic availability of curcumin with that of curcumin formulated with phosphatidylcholine. *Cancer Chemother. Pharmacol,* 60**,** 171-177.
MARINA, A. M., CHE MAN, Y. B. & AMIN, I. 2009. Virgin coconut oil: emerging functional food oil. *Trends in Food Science & Technology,* 20**,** 481-487. Available: https://doi.org/10.1016/j.tifs.2009.06.003

MARSZALEK, J. R., KITIDIS, C., DIRUSSO, C. C. & LODISH, H. F. 2005. Long-chain acyl-CoA synthetase 6 preferentially promotes DHA metabolism. *Journal of Biological Chemistry,* 280**,** 10817-10826. Available: 10.1074/jbc.M411750200
MASSOULIÉ, J. 2002. The origin of the molecular diversity and functional anchoring of cholinesterases. *Neurosignals,* 11**,** 130-43. Available: 10.1159/000065054
MCCLEMENTS 2015. Food Emulsions: Principles, Practices, and Techniques. *CRC Press,* Third Edition (3rd ed.). Available: https://doi.org/10.1201/b18868
MCCLEMENTS, D. J. 2004. Protein-stabilized emulsions. *Current Opinion in Colloid & Interface Science,* 9**,** 305-313. Available: https://doi.org/10.1016/j.cocis.2004.09.003
MCCLEMENTS, D. J. 2018. Advances in nanoparticle and microparticle delivery systems for increasing the dispersibility, stability, and bioactivity of phytochemicals. *Biotechnology Advances*. Available: https://doi.org/10.1016/j.biotechadv.2018.08.004
MCCLEMENTS, D. J., DECKER, E. A., PARK, Y. & WEISS, J. 2009. Structural design principles for delivery of bioactive components in nutraceuticals and functional foods. *Critical reviews in food science and nutrition,* 49**,** 577-606.
MCCLEMENTS, D. J. & LI, Y. 2010. Structured emulsion-based delivery systems: controlling the digestion and release of lipophilic food components. *Adv Colloid Interface Sci,* 159**,** 213-28. Available: 10.1016/j.cis.2010.06.010
MCCLEMENTS, D. J. & XIAO, H. 2017. Designing food structure and composition to enhance nutraceutical bioactivity to support cancer inhibition. *Seminars in Cancer Biology,* 46**,** 215-226. Available: https://doi.org/10.1016/j.semcancer.2017.06.003
MICHALSKI, M. C., GENOT, C., GAYET, C., LOPEZ, C., FINE, F., JOFFRE, F., VENDEUVRE, J. L., BOUVIER, J., CHARDIGNY, J. M. & RAYNAL-LJUTOVAC, K. 2013. Multiscale structures of lipids in foods as parameters affecting fatty acid bioavailability and lipid metabolism. *Prog Lipid Res,* 52**,** 354-73. Available: 10.1016/j.plipres.2013.04.004
MIRZAEI, F., KHAZAEI, M., KOMAKI, A., AMIRI, I. & JALILI, C. 2018. Virgin coconut oil (VCO) by normalizing NLRP3 inflammasome showed potential neuroprotective effects in Amyloid-β induced toxicity and high-fat diet fed rat. *Food and Chemical Toxicology,* 118**,** 68-83. Available: https://doi.org/10.1016/j.fct.2018.04.064
MIZWICKI, M. T., LIU, G., FIALA, M., MAGPANTAY, L., SAYRE, J., SIANI, A., MAHANIAN, M., WEITZMAN, R., HAYDEN, E. Y. & ROSENTHAL, M. J. 2013. 1α, 25-dihydroxyvitamin D 3 and resolvin D1 retune the balance between amyloid-β phagocytosis and inflammation in Alzheimer's disease patients. *Journal of Alzheimer's Disease,* 34**,** 155-170.
MORIGUCHI, T., GREINER, R. S. & SALEM, N. 2000. Behavioral deficits associated with dietary induction of decreased brain docosahexaenoic acid concentration. *Journal of neurochemistry,* 75**,** 2563-2573.
MORRIS, M. C., EVANS, D. A., BIENIAS, J. L., TANGNEY, C. C. & WILSON, R. S. 2004. Dietary fat intake and 6-year cognitive change in an older biracial community population. *Neurology,* 62**,** 1573-1579. Available: 10.1212/01.wnl.0000123250.82849.b6
MORRIS, M. C., TANGNEY, C. C., WANG, Y., SACKS, F. M., BARNES, L. L., BENNETT, D. A. & AGGARWAL, N. T. 2015. MIND diet slows cognitive decline with aging. *Alzheimers Dement,* 11**,** 1015-22. Available: 10.1016/j.jalz.2015.04.011
MORZELLE, M. C., SALGADO, J. M., TELLES, M., MOURELLE, D., BACHIEGA, P., BUCK, H. S. & VIEL, T. A. 2016. Neuroprotective Effects of Pomegranate Peel

Extract after Chronic Infusion with Amyloid-β Peptide in Mice. *PLOS ONE,* 11**,** e0166123. Available: 10.1371/journal.pone.0166123
MOSMANN, T. 1983. Rapid colorimetric assay for cellular growth and survival: application to proliferation and cytotoxicity assays. *Journal of immunological methods,* 65**,** 55-63.
MURPHY, M. & LEVINE, H. 2010. III Alzheimer's disease and the amyloid-beta peptide. *J Alzheimers Dis,* 19**,** 311-323.
NAFAR, F. M., KAREN M.; * 2014. Coconut Oil Attenuates the Effects of Amyloid-β on Cortical Neurons in vitro. *ournal of Alzheimer's Disease,* 39**,** 233-237.
NAIR, A. B. & JACOB, S. 2016. A simple practice guide for dose conversion between animals and human. *Journal of basic and clinical pharmacy,* 7**,** 27-31. Available: 10.4103/0976-0105.177703
NAKSURIYA, O., OKONOGI, S., SCHIFFELERS, R. M. & HENNINK, W. E. 2014. Curcumin nanoformulations: A review of pharmaceutical properties and preclinical studies and clinical data related to cancer treatment. *Biomaterials,* 35**,** 3365-3383. Available: https://doi.org/10.1016/j.biomaterials.2013.12.090
NASEF, N. A., LOVEDAY, S. M., GOLDING, M., MARTINS, R. N., SHAH, T. M., CLARKE, M., COAD, J., MOUGHAN, P. J., GARG, M. L. & SINGH, H. 2019. Food matrix and co-presence of turmeric compounds influence bioavailability of curcumin in healthy humans. *Food & function,* 10**,** 4584-4592.
NEDDENS, J., TEMMEL, M., FLUNKERT, S., KERSCHBAUMER, B., HOELLER, C., LOEFFLER, T., NIEDERKOFLER, V., DAUM, G., ATTEMS, J. & HUTTER-PAIER, B. 2018. Phosphorylation of different tau sites during progression of Alzheimer's disease. *Acta Neuropathologica Communications,* 6**,** 52. Available: 10.1186/s40478-018-0557-6
NEVIN, K. G. & RAJAMOHAN, T. 2004. Beneficial effects of virgin coconut oil on lipid parameters and in vitro LDL oxidation. *Clin Biochem,* 37**,** 830-5. Available: 10.1016/j.clinbiochem.2004.04.010
NICOLLS, M. R. 2004. The clinical and biological relationship between Type II diabetes mellitus and Alzheimer's disease. *Current Alzheimer Research,* 1**,** 47-54.
NIEUWENHUIZEN, N., LOPATA, A. L., JEEBHAY, M. F., DE'BROSKI, R. H., ROBINS, T. G. & BROMBACHER, F. 2006. Exposure to the fish parasite Anisakis causes allergic airway hyperreactivity and dermatitis. *Journal of Allergy and Clinical Immunology,* 117**,** 1098-1105.
NORRIS, C., FONG, B., MACGIBBON, A. & MCJARROW, P. 2009. Analysis of phospholipids in rat brain using liquid chromatography-mass spectrometry. *Lipids,* 44**,** 1047-54. Available: 10.1007/s11745-009-3357-8
NORTON, I., FRYER, P. & MOORE, S. 2006. Product/process integration in food manufacture: engineering sustained health. *AIChE Journal,* 52**,** 1632-1640.
NOVAK, P., SCHMIDT, R., KONTSEKOVA, E., KOVACECH, B., SMOLEK, T., KATINA, S., FIALOVA, L., PRCINA, M., PARRAK, V., DAL-BIANCO, P., BRUNNER, M., STAFFEN, W., RAINER, M., ONDRUS, M., ROPELE, S., SMISEK, M., SIVAK, R., ZILKA, N., WINBLAD, B. & NOVAK, M. 2018. FUNDAMANT: an interventional 72-week phase 1 follow-up study of AADvac1, an active immunotherapy against tau protein pathology in Alzheimer's disease. *Alzheimers Res Ther,* 10**,** 108. Available: 10.1186/s13195-018-0436-1
NYBERG, L., NILSSON, Å., LUNDGREN, P. & DUAN, R.-D. 1997. Localization and capacity of sphingomyelin digestion in the rat intestinal tract. *The Journal of Nutritional Biochemistry,* 8**,** 112-118. Available: https://doi.org/10.1016/S0955-2863(97)00010-7

O'TOOLE, S. A., SHEPPARD, B. L., MCGUINNESS, E. P., GLEESON, N. C., YONEDA, M. & BONNAR, J. 2003. The MTS assay as an indicator of chemosensitivity/resistance in malignant gynaecological tumours. *Cancer Detect Prev,* 27**,** 47-54. Available: 10.1016/s0361-090x(02)00171-x
OEPPEN, J. & VAUPEL, J. W. 2002. Broken Limits to Life Expectancy. *Science,* 296**,** 1029. Available: 10.1126/science.1069675
OKSMAN, M., IIVONEN, H., HOGYES, E., AMTUL, Z., PENKE, B., LEENDERS, I., BROERSEN, L., LÜTJOHANN, D., HARTMANN, T. & TANILA, H. 2006. Impact of different saturated fatty acid, polyunsaturated fatty acid and cholesterol containing diets on beta-amyloid accumulation in APP/PS1 transgenic mice. *Neurobiology of Disease,* 23**,** 563-572. Available: https://doi.org/10.1016/j.nbd.2006.04.013
OLIVERA-PEREZ, H. M., LAM, L., DANG, J., JIANG, W., RODRIGUEZ, F., RIGALI, E., WEITZMAN, S., PORTER, V., RUBBI, L. & MORSELLI, M. 2017. Omega-3 fatty acids increase the unfolded protein response and improve amyloid-β phagocytosis by macrophages of patients with mild cognitive impairment. *The FASEB Journal,* 31**,** 4359.
ONO, K., HASEGAWA, K., NAIKI, H. & YAMADA, M. 2004. Curcumin has potent anti-amyloidogenic effects for Alzheimer's β-amyloid fibrils in vitro. *Journal of neuroscience research,* 75**,** 742-750.
OPPENHEIMER, A. 1937. TURMERIC (CURCUMIN) IN BILIARY DISEASES. *The Lancet,* 229**,** 619-621. Available: https://doi.org/10.1016/S0140-6736(00)98193-5
OTAEGUI-ARRAZOLA, A., AMIANO, P., ELBUSTO, A., URDANETA, E. & MARTÍNEZ-LAGE, P. 2014. Diet, cognition, and Alzheimer's disease: Food for thought. *European Journal of Nutrition,* 53**,** 1-23. Available: 10.1007/s00394-013-0561-3
OTT, A., STOLK, R. P., VAN HARSKAMP, F., POLS, H. A. P., HOFMAN, A. & BRETELER, M. M. B. 1999. Diabetes mellitus and the risk of dementia: The Rotterdam Study. *Neurology,* 53**,** 1937. Available: 10.1212/wnl.53.9.1937
PAFUMI, Y., LAIRON, D., DE LA PORTE, P. L., JUHEL, C., STORCH, J., HAMOSH, M. & ARMAND, M. 2002. Mechanisms of inhibition of triacylglycerol hydrolysis by human gastric lipase. *Journal of Biological Chemistry,* 277**,** 28070-28079.
PAN, K., LUO, Y., GAN, Y., BAEK, S. J. & ZHONG, Q. 2014. pH-driven encapsulation of curcumin in self-assembled casein nanoparticles for enhanced dispersibility and bioactivity. *Soft Matter,* 10**,** 6820-30. Available: 10.1039/c4sm00239c
PAN, M.-H., HUANG, T.-M. & LIN, J.-K. 1999a. Biotransformation of curcumin through reduction and glucuronidation in mice. *Drug metabolism and disposition,* 27**,** 486-494.
PAN, M. H., HUANG, T. M. & LIN, J. K. 1999b. Biotransformation of curcumin through reduction and glucuronidation in mice. *Drug Metab Dispos,* 27.
PANDEY, A., CHATURVEDI, M., MISHRA, S., KUMAR, P., SOMVANSHI, P. & CHATURVEDI, R. 2020. Reductive metabolites of curcumin and their therapeutic effects. *Heliyon,* 6**,** e05469. Available: https://doi.org/10.1016/j.heliyon.2020.e05469
PARK, S.-Y. & KIM, D. S. H. L. 2002. Discovery of Natural Products from Curcuma longa that Protect Cells from Beta-Amyloid Insult: A Drug Discovery Effort against Alzheimer's Disease. *Journal of Natural Products,* 65**,** 1227-1231. Available: 10.1021/np010039x

PARK, S. J., GARCIA, C. V., SHIN, G. H. & KIM, J. T. 2017. Development of nanostructured lipid carriers for the encapsulation and controlled release of vitamin D3. *Food Chemistry,* 225**,** 213-219.
PATIL, R., GANGALUM, P. R., WAGNER, S., PORTILLA-ARIAS, J., DING, H., REKECHENETSKIY, A., KONDA, B., INOUE, S., BLACK, K. L. & LJUBIMOVA, J. Y. 2015. Curcumin targeted, polymalic acid-based MRI contrast agent for the detection of Aβ plaques in Alzheimer's disease. *Macromolecular bioscience,* 15**,** 1212-1217.
PATIL, S. P., TRAN, N., GEEKIYANAGE, H., LIU, L. & CHAN, C. 2013. Curcumin-induced upregulation of the anti-tau cochaperone BAG2 in primary rat cortical neurons. *Neuroscience Letters,* 554**,** 121-125. Available: https://doi.org/10.1016/j.neulet.2013.09.008
PAYTON, F., SANDUSKY, P. & ALWORTH, W. L. 2007. NMR Study of the Solution Structure of Curcumin. *Journal of Natural Products,* 70**,** 143-146. Available: 10.1021/np060263s
PENG, S., LI, Z., ZOU, L., LIU, W., LIU, C. & MCCLEMENTS, D. J. 2018. Improving curcumin solubility and bioavailability by encapsulation in saponin-coated curcumin nanoparticles prepared using a simple pH-driven loading method. *Food Funct,* 9**,** 1829-1839. Available: 10.1039/c7fo01814b
PEPE, S., TSUCHIYA, N., LAKATTA, E. G. & HANSFORD, R. G. 1999. PUFA and aging modulate cardiac mitochondrial membrane lipid composition and Ca2+ activation of PDH. *American Journal of Physiology-Heart and Circulatory Physiology,* 276**,** H149-H158.
PHAN, T. T. Q., LE, T. T., VAN DE WALLE, D., VAN DER MEEREN, P. & DEWETTINCK, K. 2016. Combined effects of milk fat globule membrane polar lipids and protein concentrate on the stability of oil-in-water emulsions. *International Dairy Journal,* 52**,** 42-49. Available: https://doi.org/10.1016/j.idairyj.2015.08.003
PICHOT, R., WATSON, R. L. & NORTON, I. T. 2013. Phospholipids at the interface: current trends and challenges. *Int J Mol Sci,* 14**,** 11767-94. Available: 10.3390/ijms140611767
POLING, J. S., VICINI, S., ROGAWSKI, M. A. & SALEM JR, N. 1996. Docosahexaenoic acid block of neuronal voltage-gated K+ channels: Subunit selective antagonism by zinc. *Neuropharmacology,* 35**,** 969-982. Available: 10.1016/0028-3908(96)00127-X
PORTER, C. J., TREVASKIS, N. L. & CHARMAN, W. N. 2007. Lipids and lipid-based formulations: optimizing the oral delivery of lipophilic drugs. *Nat Rev Drug Discov,* 6**,** 231-48. Available: 10.1038/nrd2197
PRASAD, K. N., COLE, W. C., HOVLAND, A. R., PRASAD, K. C., NAHREINI, P., KUMAR, B., EDWARDS-PRASAD, J. & ANDREATTA, C. P. 1999. Multiple antioxidants in the prevention and treatment of neurodegenerative disease: Analysis of biologic rationale. *Current Opinion in Neurology,* 12**,** 761-770. Available: 10.1097/00019052-199912000-00017
PRICE, L. C. & BUESCHER, R. 1997. Kinetics of alkaline degradation of the food pigments curcumin and curcuminoids. *Journal of food science,* 62**,** 267-269.
PUBCHEM. 2004. *National Center for Biotechnology Information. PubChem Database. Curcumin, CID=969516,* [Online]. [Accessed https://pubchem.ncbi.nlm.nih.gov/compound/Curcumin (accessed on Mar. 27, 2020)].
PURPURA, M., LOWERY, R. P., WILSON, J. M., MANNAN, H., MÜNCH, G. & RAZMOVSKI-NAUMOVSKI, V. 2018. Analysis of different innovative formulations

of curcumin for improved relative oral bioavailability in human subjects. *Eur J Nutr,* 57**,** 929-938. Available: 10.1007/s00394-016-1376-9
PYUN, C. W., KIM, J. H., HAN, K. H., HONG, G. E. & LEE, C. H. 2014. In vivo protective effects of dietary curcumin and capsaicin against alcohol-induced oxidative stress. *Biofactors,* 40**,** 494-500. Available: 10.1002/biof.1172
QIU, C., SIGURDSSON, S., ZHANG, Q., JONSDOTTIR, M. K., KJARTANSSON, O., EIRIKSDOTTIR, G., GARCIA, M. E., HARRIS, T. B., VAN BUCHEM, M. A., GUDNASON, V. & LAUNER, L. J. 2014. Diabetes, markers of brain pathology and cognitive function. *Annals of Neurology,* 75**,** 138-146. Available: https://doi.org/10.1002/ana.24063
QUINN, J. F., RAMAN, R., THOMAS, R. G., YURKO-MAURO, K., NELSON, E. B., VAN DYCK, C., GALVIN, J. E., EMOND, J., JACK, C. R., JR., WEINER, M., SHINTO, L. & AISEN, P. S. 2010. Docosahexaenoic acid supplementation and cognitive decline in Alzheimer disease: a randomized trial. *Jama,* 304**,** 1903-11. Available: 10.1001/jama.2010.1510
RAI, S. K., FUNG, T. T., LU, N., KELLER, S. F., CURHAN, G. C. & CHOI, H. K. 2017. The Dietary Approaches to Stop Hypertension (DASH) diet, Western diet, and risk of gout in men: prospective cohort study. *BMJ,* 357**,** j1794. Available: 10.1136/bmj.j1794
RAINEY-SMITH, S. R., GU, Y., GARDENER, S. L., DOECKE, J. D., VILLEMAGNE, V. L., BROWN, B. M., TADDEI, K., LAWS, S. M., SOHRABI, H. R., WEINBORN, M., AMES, D., FOWLER, C., MACAULAY, S. L., MARUFF, P., MASTERS, C. L., SALVADO, O., ROWE, C. C., SCARMEAS, N. & MARTINS, R. N. 2018. Mediterranean diet adherence and rate of cerebral Aβ-amyloid accumulation: Data from the Australian Imaging, Biomarkers and Lifestyle Study of Ageing. *Transl Psychiatry,* 8**,** 238. Available: 10.1038/s41398-018-0293-5
RAMISETTY, K. A., PANDIT, A. B. & GOGATE, P. R. 2015. Ultrasound assisted preparation of emulsion of coconut oil in water: Understanding the effect of operating parameters and comparison of reactor designs. *Chemical Engineering and Processing: Process Intensification,* 88**,** 70-77. Available: https://doi.org/10.1016/j.cep.2014.12.006
RANSOHOFF, R. M. 2016. How neuroinflammation contributes to neurodegeneration. *Science,* 353**,** 777-83. Available: 10.1126/science.aag2590
RAO, C. V. 2007. Regulation of COX and LOX by curcumin. *The Molecular Targets and Therapeutic Uses of Curcumin in Health and Disease.* Springer.
RAVINDRANATH, V. & CHANDRASEKHARA, N. 1981. Metabolism of curcumin--studies with [3H]curcumin. *Toxicology,* 22. Available: 10.1016/0300-483x(81)90027-5
RAVINDRANATH, V. & CHANDRASEKHARA, N. 1982. Metabolism of curcumn-studies with [3 H] curcumin. *Toxicology,* 22**,** 337-344.
REISSER, D., FADY, C., PELLETIER, H., LAGADEC, P., JEANNIN, J. F. & OLSSON, N. O. 1989. Comparative effect of rat and fetal calf serum on measurement of the natural tumoricidal activity of rat lymphocytes, macrophages and polymorphonuclear cells. *Cancer Immunol Immunother,* 28**,** 34-6. Available: 10.1007/bf00205798
RIEDIGER, N. D., OTHMAN, R. A., SUH, M. & MOGHADASIAN, M. H. 2009. A Systemic Review of the Roles of n-3 Fatty Acids in Health and Disease. *Journal of the American Dietetic Association,* 109**,** 668-679. Available: 10.1016/j.jada.2008.12.022
ROGALSKA, E., RANSAC, S. & VERGER, R. 1990. Stereoselectivity of lipases. II. Stereoselective hydrolysis of triglycerides by gastric and pancreatic lipases. *Journal of*

Biological Chemistry, 265**,** 20271-20276. Available: https://doi.org/10.1016/S0021-9258(17)30500-8
RUAN, Y., TANG, J., GUO, X., LI, K. & LI, D. 2018. Dietary Fat Intake and Risk of Alzheimer's Disease and Dementia: A Meta-Analysis of Cohort Studies. *Current Alzheimer Research,* 15**,** 869-876. Available: 10.2174/1567205015666180427142350
SADLI, N., BARROW, C. J., MCGEE, S. & SUPHIOGLU, C. 2013. Effect of DHA and CoenzymeQ10 Against Aβ- and Zinc-Induced Mitochondrial Dysfunction in Human Neuronal Cells. *Cellular Physiology and Biochemistry,* 32**,** 243-252. Available: 10.1159/000354433
SAHLIN, C., PETTERSSON, F. E., NILSSON, L. N. G., LANNFELT, L. & JOHANSSON, A. S. 2007. Docosahexaenoic acid stimulates non-amyloidogenic APP processing resulting in reduced Aβ levels in cellular models of Alzheimer's disease. *European Journal of Neuroscience,* 26**,** 882-889. Available: 10.1111/j.1460-9568.2007.05719.x
SAHNI, J. K., DOGGUI, S., ALI, J., BABOOTA, S., DAO, L. & RAMASSAMY, C. 2011. Neurotherapeutic applications of nanoparticles in Alzheimer's disease. *Journal of Controlled Release,* 152**,** 208-231. Available: https://doi.org/10.1016/j.jconrel.2010.11.033
SALLOWAY, S., CHALKIAS, S., BARKHOF, F., BURKETT, P., BARAKOS, J., PURCELL, D., SUHY, J., FORRESTAL, F., TIAN, Y., UMANS, K., WANG, G., SINGHAL, P., BUDD HAEBERLEIN, S. & SMIRNAKIS, K. 2022. Amyloid-Related Imaging Abnormalities in 2 Phase 3 Studies Evaluating Aducanumab in Patients With Early Alzheimer Disease. *JAMA Neurol,* 79**,** 13-21. Available: 10.1001/jamaneurol.2021.4161
SAMANTA, L., PANIGRAHI, J., BHANJA, S. & CHAINY, G. B. N. 2010. Effect of turmeric and its active principle curcumin on t(3)-induced oxidative stress and hyperplasia in rat kidney: a comparison. *Indian journal of clinical biochemistry : IJCB,* 25**,** 393-397. Available: 10.1007/s12291-010-0046-6
SANDUR, S. K., ICHIKAWA, H., PANDEY, M. K., KUNNUMAKKARA, A. B., SUNG, B., SETHI, G. & AGGARWAL, B. B. 2007. Role of pro-oxidants and antioxidants in the anti-inflammatory and apoptotic effects of curcumin (diferuloylmethane). *Free radical biology and medicine,* 43**,** 568-580.
SARKAR, A., GOH, K. K. T. & SINGH, H. 2009. Colloidal stability and interactions of milk-protein-stabilized emulsions in an artificial saliva. *Food Hydrocolloids,* 23**,** 1270-1278. Available: https://doi.org/10.1016/j.foodhyd.2008.09.008
SARKAR, A., LI, H., CRAY, D. & BOXALL, S. 2018. Composite whey protein–cellulose nanocrystals at oil-water interface: Towards delaying lipid digestion. *Food Hydrocolloids,* 77**,** 436-444. Available: https://doi.org/10.1016/j.foodhyd.2017.10.020
SASTRE, M., KLOCKGETHER, T. & HENEKA, M. T. 2006. Contribution of inflammatory processes to Alzheimer's disease: Molecular mechanisms. *International Journal of Developmental Neuroscience,* 24**,** 167-176. Available: 10.1016/j.ijdevneu.2005.11.014
SATO, H., LIU, H., ADACHI, I., UENO, M., LEMAIRE, M. & HORIKOSHI, I. 1994. ENHANCEMENT OF THE INTESTINAL ABSORPTION OF A CYCLOSPORINE DERIVATIVE BY MILK FAT GLOBULE MEMBRANE. *Biological & Pharmaceutical Bulletin,* 17**,** 1526-1528. Available: 10.1248/bpb.17.1526
SCHAEFER, E. J., BONGARD, V., BEISER, A. S., LAMON-FAVA, S., ROBINS, S. J., AU, R., TUCKER, K. L., KYLE, D. J., WILSON, P. W. & WOLF, P. A. 2006. Plasma phosphatidylcholine docosahexaenoic acid content and risk of dementia and

Alzheimer disease: the Framingham Heart Study. *Archives of neurology,* 63**,** 1545-1550.
SCHELTENS, P., TWISK, J. W. R., BLESA, R., SCARPINI, E., VON ARNIM, C. A. F., BONGERS, A., HARRISON, J., SWINKELS, S. H. N., STAM, C. J., DE WAAL, H., WURTMAN, R. J., WIEGGERS, R. L., VELLAS, B. & KAMPHUIS, P. J. G. H. 2012. Efficacy of Souvenaid in Mild Alzheimer's Disease: Results from a Randomized, Controlled Trial. *Journal of Alzheimer's Disease,* 31**,** 225-236. Available: 10.3233/JAD-2012-121189
SCHEUBLE, N., SCHAFFNER, J., SCHUMACHER, M., WINDHAB, E. J., LIU, D., PARKER, H., STEINGOETTER, A. & FISCHER, P. 2018. Tailoring Emulsions for Controlled Lipid Release: Establishing in vitro–in Vivo Correlation for Digestion of Lipids. *ACS Applied Materials & Interfaces,* 10**,** 17571-17581. Available: 10.1021/acsami.8b02637
SCHMELZ, E. M., DILLEHAY, D. L., WEBB, S. K., REITER, A., ADAMS, J., & MERRILL, A. H. 1996. Sphingomyelin consumption suppresses aberrant colonic crypt foci and increases the proportion of adenomas versus adenocarcinomas in CF1 mice treated with 1, 2-dimethylhydrazine: implications for dietary sphingolipids and colon carcinogenesis. *Cancer research,* 56**,** 4936-4941.
SEÇIL, Y., ARICI, Ş., İNCESU, T. K., GÜRGÖR, N., BECKMANN, Y. & ERTEKIN, C. 2016. Dysphagia in Alzheimer's disease. *Neurophysiologie Clinique/Clinical Neurophysiology,* 46**,** 171-178. Available: https://doi.org/10.1016/j.neucli.2015.12.007
SEK, L., PORTER, C. J., KAUKONEN, A. M. & CHARMAN, W. N. 2002. Evaluation of the in-vitro digestion profiles of long and medium chain glycerides and the phase behaviour of their lipolytic products. *Journal of pharmacy and pharmacology,* 54**,** 29-41.
SELKOE, D. J. 2001. Alzheimer's disease: genes, proteins, and therapy. *Physiological reviews*.
SEMALTY, A., SEMALTY, M., RAWAT, M. S. M. & FRANCESCHI, F. 2010. Supramolecular phospholipids–polyphenolics interactions: The PHYTOSOME® strategy to improve the bioavailability of phytochemicals. *Fitoterapia,* 81**,** 306-314.
SENEFF, S., WAINWRIGHT, G. & MASCITELLI, L. 2011a. Is the metabolic syndrome caused by a high fructose, and relatively low fat, low cholesterol diet. *Arch Med Sci,* 7**,** 8-20.
SENEFF, S., WAINWRIGHT, G. & MASCITELLI, L. 2011b. Is the metabolic syndrome caused by a high fructose, and relatively low fat, low cholesterol diet? *Archives of medical science : AMS,* 7**,** 8-20. Available: 10.5114/aoms.2011.20598
SENNVIK, K., FASTBOM, J., BLOMBERG, M., WAHLUND, L.-O., WINBLAD, B. & BENEDIKZ, E. 2000. Levels of α-and β-secretase cleaved amyloid precursor protein in the cerebrospinal fluid of Alzheimer's disease patients. *Neuroscience letters,* 278**,** 169-172.
SERAFINI, M. M., CATANZARO, M., ROSINI, M., RACCHI, M. & LANNI, C. 2017. Curcumin in Alzheimer's disease: Can we think to new strategies and perspectives for this molecule? *Pharmacol Res,* 124**,** 146-155. Available: 10.1016/j.phrs.2017.08.004
SHAIKH, J., ANKOLA, D., BENIWAL, V., SINGH, D. & KUMAR, M. R. 2009. Nanoparticle encapsulation improves oral bioavailability of curcumin by at least 9-fold when compared to curcumin administered with piperine as absorption enhancer. *European journal of pharmaceutical sciences,* 37**,** 223-230.

SHARMA, R. A., GESCHER, A. J. & STEWARD, W. P. 2005. Curcumin: The story so far. *European Journal of Cancer,* 41**,** 1955-1968. Available: https://doi.org/10.1016/j.ejca.2005.05.009
SHARMA, R. A., MCLELLAND, H. R., HILL, K. A., IRESON, C. R., EUDEN, S. A., MANSON, M. M., PIRMOHAMED, M., MARNETT, L. J., GESCHER, A. J. & STEWARD, W. P. 2001. Pharmacodynamic and pharmacokinetic study of oral Curcuma extract in patients with colorectal cancer. *Clin Cancer Res,* 7.
SHARMA, R. A., STEWARD, W. P. & GESCHER, A. J. 2007. Pharmacokinetics and pharmacodynamics of curcumin. *The molecular targets and therapeutic uses of curcumin in health and disease.* Springer.
SHARMAN, M. J., GYENGESI, E., LIANG, H., CHATTERJEE, P., KARL, T., LI, Q. X., WENK, M. R., HALLIWELL, B., MARTINS, R. N. & MÜNCH, G. 2019. Assessment of diets containing curcumin, epigallocatechin-3-gallate, docosahexaenoic acid and α-lipoic acid on amyloid load and inflammation in a male transgenic mouse model of Alzheimer's disease: Are combinations more effective? *Neurobiol Dis,* 124**,** 505-519. Available: 10.1016/j.nbd.2018.11.026
SHERMAN, P. 1970. Industrial rheology with particular reference to foods, pharmaceuticals, and cosmetics. *Industrial rheology with particular reference to foods, pharmaceuticals, and cosmetics.*
SHINTO, L., QUINN, J., MONTINE, T., DODGE, H. H., WOODWARD, W., BALDAUF-WAGNER, S., WAICHUNAS, D., BUMGARNER, L., BOURDETTE, D., SILBERT, L. & KAYE, J. 2014. A randomized placebo-controlled pilot trial of omega-3 fatty acids and alpha lipoic acid in Alzheimer's disease. *J Alzheimers Dis,* 38**,** 111-20. Available: 10.3233/jad-130722
SHOBA, G., JOY, D., JOSEPH, T., MAJEED, M., RAJENDRAN, R. & SRINIVAS, P. 1998. Influence of piperine on the pharmacokinetics of curcumin in animals and human volunteers. *Planta medica,* 64**,** 353-356.
SILVA, H. D., CERQUEIRA, M. A. & VICENTE, A. A. 2015. Influence of surfactant and processing conditions in the stability of oil-in-water nanoemulsions. *Journal of Food Engineering,* 167**,** 89-98. Available: https://doi.org/10.1016/j.jfoodeng.2015.07.037
SILVA, H. D., POEJO, J., PINHEIRO, A. C., DONSÌ, F., SERRA, A. T., DUARTE, C. M. M., FERRARI, G., CERQUEIRA, M. A. & VICENTE, A. A. 2018. Evaluating the behaviour of curcumin nanoemulsions and multilayer nanoemulsions during dynamic in vitro digestion. *Journal of Functional Foods,* 48**,** 605-613. Available: https://doi.org/10.1016/j.jff.2018.08.002
SIMOPOULOS, A. P. 1999. Essential fatty acids in health and chronic disease. *The American Journal of Clinical Nutrition,* 70**,** 560s-569s. Available: 10.1093/ajcn/70.3.560s
SINGH, H. 2006. The milk fat globule membrane—A biophysical system for food applications. *Current Opinion in Colloid & Interface Science,* 11**,** 154-163. Available: https://doi.org/10.1016/j.cocis.2005.11.002
SINGH, H. 2019. Symposium review: Fat globules in milk and their structural modifications during gastrointestinal digestion. *Journal of Dairy Science,* 102**,** 2749-2759. Available: https://doi.org/10.3168/jds.2018-15507
SINGH, H. & GALLIER, S. 2017. Nature's complex emulsion: The fat globules of milk. *Food Hydrocolloids,* 68**,** 81-89. Available: https://doi.org/10.1016/j.foodhyd.2016.10.011

SINGH, H. & YE, A. 2013. Structural and biochemical factors affecting the digestion of protein-stabilized emulsions. *Current Opinion in Colloid & Interface Science,* 18**,** 360-370. Available: https://doi.org/10.1016/j.cocis.2013.04.006
SINGH, H., YE, A. & HORNE, D. 2009. Structuring food emulsions in the gastrointestinal tract to modify lipid digestion. *Progress in Lipid Research,* 48**,** 92-100. Available: https://doi.org/10.1016/j.plipres.2008.12.001
SINHA, S. & HAQUE, M. 2022. Obesity, Diabetes Mellitus, and Vascular Impediment as Consequences of Excess Processed Food Consumption. *Cureus,* 14.
SOLANS, C., IZQUIERDO, P., NOLLA, J., AZEMAR, N. & GARCIA-CELMA, M. J. 2005. Nano-emulsions. *Current Opinion in Colloid & Interface Science,* 10**,** 102-110. Available: https://doi.org/10.1016/j.cocis.2005.06.004
SORASITTHIYANUKARN, F. N., MUANGNOI, C., RATNATILAKA NA BHUKET, P., ROJSITTHISAK, P. & ROJSITTHISAK, P. 2018. Chitosan/alginate nanoparticles as a promising approach for oral delivery of curcumin diglutaric acid for cancer treatment. *Materials Science and Engineering: C,* 93**,** 178-190. Available: https://doi.org/10.1016/j.msec.2018.07.069
SOREQ, H. & SEIDMAN, S. 2001. Acetylcholinesterase--new roles for an old actor. *Nat Rev Neurosci,* 2**,** 294-302. Available: 10.1038/35067589
SPITSBERG, V. L. 2005a. Invited Review: Bovine Milk Fat Globule Membrane as a Potential Nutraceutical. *Journal of Dairy Science,* 88**,** 2289-2294. Available: https://doi.org/10.3168/jds.S0022-0302(05)72906-4
SPITSBERG, V. L. 2005b. Invited review: Bovine milk fat globule membrane as a potential nutraceutical. *J Dairy Sci,* 88**,** 2289-94. Available: 10.3168/jds.S0022-0302(05)72906-4
SRIVASTAVA, Y., SEMWAL, A. D., SAJEEVKUMAR, V. A. & SHARMA, G. K. 2017. Melting, crystallization and storage stability of virgin coconut oil and its blends by differential scanning calorimetry (DSC) and Fourier transform infrared spectroscopy (FTIR). *J Food Sci Technol,* 54**,** 45-54. Available: 10.1007/s13197-016-2427-1
STEELE, M., STUCHBURY, G. & MÜNCH, G. 2007. The molecular basis of the prevention of Alzheimer's disease through healthy nutrition. *Experimental Gerontology,* 42**,** 28-36. Available: 10.1016/j.exger.2006.06.002
STINE, W. B., JUNGBAUER, L., YU, C. & LADU, M. J. 2010. Preparing synthetic Aβ in different aggregation states. *Alzheimer's Disease and Frontotemporal Dementia.* Springer.
STOHS, S. J., CHEN, C. Y. O., PREUSS, H. G., RAY, S. D., BUCCI, L. R., JI, J. & RUFF, K. J. 2019. The fallacy of enzymatic hydrolysis for the determination of bioactive curcumin in plasma samples as an indication of bioavailability: a comparative study. *BMC Complementary and Alternative Medicine,* 19**,** 293. Available: 10.1186/s12906-019-2699-x
STOHS, S. J., JI, J., BUCCI, L. R. & PREUSS, H. G. 2018. A Comparative Pharmacokinetic Assessment of a Novel Highly Bioavailable Curcumin Formulation with 95% Curcumin: A Randomized, Double-Blind, Crossover Study. *J Am Coll Nutr,* 37**,** 51-59. Available: 10.1080/07315724.2017.1358118
STRIMPAKOS, A. S. & SHARMA, R. A. 2007. Curcumin: Preventive and Therapeutic Properties in Laboratory Studies and Clinical Trials. *Antioxidants & Redox Signaling,* 10**,** 511-546. Available: 10.1089/ars.2007.1769
SU, B., WANG, X., LEE, H.-G., TABATON, M., PERRY, G., SMITH, M. A. & ZHU, X. 2010. Chronic oxidative stress causes increased tau phosphorylation in M17 neuroblastoma cells. *Neuroscience Letters,* 468**,** 267-271. Available: https://doi.org/10.1016/j.neulet.2009.11.010

SUBRAMANIAN, M., SREEJAYAN, DEVASAGAYAM, T. P. A. & SINGH, B. B. 1994. Diminution of singlet oxygen-induced DNA damage by curcmin and related antioxidants. *Mutation Research/Fundamental and Molecular Mechanisms of Mutagenesis,* 311**,** 249-255. Available: https://doi.org/10.1016/0027-5107(94)90183-X
SUN, Y., YU, X., HUSSAIN, M., LI, X., LIU, L., LIU, Y., MA, S., KOUAME, K. J. E.-P., LI, C., LENG, Y. & JIANG, S. 2022. Influence of milk fat globule membrane and milk protein concentrate treated by ultrasound on the structural and emulsifying stability of mimicking human fat emulsions. *Ultrasonics Sonochemistry,* 82**,** 105881. Available: https://doi.org/10.1016/j.ultsonch.2021.105881
TADDEI, K., LAWS, S. M., VERDILE, G., MUNNS, S., D'COSTA, K., HARVEY, A. R., MARTINS, I. J., HILL, F., LEVY, E., SHAW, J. E. & MARTINS, R. N. 2010. Novel phage peptides attenuate beta amyloid-42 catalysed hydrogen peroxide production and associated neurotoxicity. *Neurobiology of Aging,* 31**,** 203-214. Available: https://doi.org/10.1016/j.neurobiolaging.2008.03.023
TADROS, T., IZQUIERDO, P., ESQUENA, J. & SOLANS, C. 2004. Formation and stability of nano-emulsions. *Advances in Colloid and Interface Science,* 108-109**,** 303-318. Available: https://doi.org/10.1016/j.cis.2003.10.023
TAHA, A., HU, T., ZHANG, Z., BAKRY, A. M., KHALIFA, I., PAN, S. & HU, H. 2018. Effect of different oils and ultrasound emulsification conditions on the physicochemical properties of emulsions stabilized by soy protein isolate. *Ultrasonics Sonochemistry,* 49**,** 283-293. Available: https://doi.org/10.1016/j.ultsonch.2018.08.020
TAKAHASHI, M., UECHI, S., TAKARA, K., ASIKIN, Y. & WADA, K. 2009. Evaluation of an Oral Carrier System in Rats: Bioavailability and Antioxidant Properties of Liposome-Encapsulated Curcumin. *Journal of Agricultural and Food Chemistry,* 57**,** 9141-9146. Available: 10.1021/jf9013923
TAKASHIMA, A. 2006. GSK-3 is essential in the pathogenesis of Alzheimer's disease. *J Alzheimers Dis,* 9**,** 309-17. Available: 10.3233/jad-2006-9s335
TAKIZAWA, C., GEMMELL, E., KENWORTHY, J. & SPEYER, R. 2016. A Systematic Review of the Prevalence of Oropharyngeal Dysphagia in Stroke, Parkinson's Disease, Alzheimer's Disease, Head Injury, and Pneumonia. *Dysphagia,* 31**,** 434-441. Available: 10.1007/s00455-016-9695-9
TANG, Q., XIE, X., LI, C., ZHEN, B., CAI, X., ZHANG, G., ZHOU, C. & WANG, L. 2019. Medium-chain triglyceride/water Pickering emulsion stabilized by phosphatidylcholine-kaolinite for encapsulation and controlled release of curcumin. *Colloids and Surfaces B: Biointerfaces,* 183**,** 110414. Available: https://doi.org/10.1016/j.colsurfb.2019.110414
THAPA, A., VERNON, B. C., DE LA PEÑA, K., SOLIZ, G., MORENO, H. A., LÓPEZ, G. P. & CHI, E. Y. 2013. Membrane-mediated neuroprotection by curcumin from amyloid-β-peptide-induced toxicity. *Langmuir,* 29**,** 11713-23. Available: 10.1021/la4020459
THOMPSON, A. K. & SINGH, H. 2006. Preparation of Liposomes from Milk Fat Globule Membrane Phospholipids Using a Microfluidizer. *Journal of Dairy Science,* 89**,** 410-419. Available: https://doi.org/10.3168/jds.S0022-0302(06)72105-1
THOTA, R. N., DIAS, C. B., ABBOTT, K. A., ACHARYA, S. H. & GARG, M. L. 2018. Curcumin alleviates postprandial glycaemic response in healthy subjects: A cross-over, randomized controlled study. *Scientific Reports,* 8**,** 13679. Available: 10.1038/s41598-018-32032-x
TIWARI, M. K. & KEPP, K. P. 2016. β-Amyloid pathogenesis: Chemical properties versus cellular levels. *Alzheimer's & Dementia,* 12**,** 184-194.

TØNNESEN H.H., K. J., AND MOSTAD A. 1982. Studies on curcumin and curcuminoids XXXIX. Photophysical properties of bisdemethoxycurcumin. *Acta Chem. Scand,* 36**,** 475-479.
TØNNESEN, H. H., MÁSSON, M. & LOFTSSON, T. 2002. Studies of curcumin and curcuminoids. XXVII. Cyclodextrin complexation: solubility, chemical and photochemical stability. *International Journal of Pharmaceutics,* 244**,** 127-135. Available: https://doi.org/10.1016/S0378-5173(02)00323-X
TRUJILLO-ESTRADA, L., SANCHEZ-MEJIAS, E., SANCHEZ-VARO, R., GARCIA-LEON, J. A., NUÑEZ-DIAZ, C., DAVILA, J. C., VITORICA, J., LAFERLA, F. M., MORENO-GONZALEZ, I., GUTIERREZ, A. & BAGLIETTO-VARGAS, D. 2022. Animal and Cellular Models of Alzheimer's Disease: Progress, Promise, and Future Approaches. *The Neuroscientist,* 28**,** 572-593. Available: 10.1177/10738584211001753
TULLY, A., ROCHE, H., DOYLE, R., FALLON, C., BRUCE, I., LAWLOR, B., COAKLEY, D. & GIBNEY, M. 2003. Low serum cholesteryl ester-docosahexaenoic acid levels in Alzheimer's disease: a case–control study. *British Journal of Nutrition,* 89**,** 483-489.
UAUY DAGACH-IMBARACK, R. E. & DANGOUR, A. D. 2006. Nutrition in brain development and aging: Role of essential fatty acids.
UAUY, R. & DANGOUR, A. D. 2006. Nutrition in brain development and aging: role of essential fatty acids. *Nutrition reviews,* 64**,** S24-S33.
ULLAH, F., ASGAROV, R., VENIGALLA, M., LIANG, H., NIEDERMAYER, G., MÜNCH, G. & GYENGESI, E. 2020a. Effects of a solid lipid curcumin particle formulation on chronic activation of microglia and astroglia in the GFAP-IL6 mouse model. *Scientific Reports,* 10**,** 2365. Available: 10.1038/s41598-020-58838-2
ULLAH, F., LIANG, H., NIEDERMAYER, G., MÜNCH, G. & GYENGESI, E. 2020b. Evaluation of Phytosomal Curcumin as an Anti-inflammatory Agent for Chronic Glial Activation in the GFAP-IL6 Mouse Model. *Frontiers in neuroscience,* 14**,** 170-170. Available: 10.3389/fnins.2020.00170
UNNO, K., TAGUCHI, K., HASE, T., MEGURO, S. & NAKAMURA, Y. 2022. Coffee Polyphenol, Chlorogenic Acid, Suppresses Brain Aging and Its Effects Are Enhanced by Milk Fat Globule Membrane Components. *International Journal of Molecular Sciences,* 23**,** 5832.
VAN DEN BRINK, A. C., BROUWER-BROLSMA, E. M., BERENDSEN, A. A. M. & VAN DE REST, O. 2019. The Mediterranean, Dietary Approaches to Stop Hypertension (DASH), and Mediterranean-DASH Intervention for Neurodegenerative Delay (MIND) Diets Are Associated with Less Cognitive Decline and a Lower Risk of Alzheimer's Disease-A Review. *Adv Nutr,* 10**,** 1040-1065. Available: 10.1093/advances/nmz054
VAREED, S. K., KAKARALA, M., RUFFIN, M. T., CROWELL, J. A., NORMOLLE, D. P., DJURIC, Z. & BRENNER, D. E. 2008. Pharmacokinetics of curcumin conjugate metabolites in healthy human subjects. *Cancer Epidemiol Biomarkers Prev,* 17**,** 1411-7. Available: 10.1158/1055-9965.Epi-07-2693
VASILEVA, L. V., SARACHEVA, K. E., IVANOVSKA, M. V., PETROVA, A. P., MARCHEV, A. S., GEORGIEV, M. I., MURDJEVA, M. A. & GETOVA, D. P. 2018. Antidepressant-like effect of salidroside and curcumin on the immunoreactivity of rats subjected to a chronic mild stress model. *Food Chem Toxicol,* 121**,** 604-611. Available: 10.1016/j.fct.2018.09.065

VENKATESAN, P. & RAO, M. 2000. Structure-activity relationships for the inhibition of lipid peroxidation and the scavenging of free radicals by synthetic symmetrical curcumin analogues. *Journal of pharmacy and pharmacology,* 52**,** 1123-1128.
VERGER, R. 1984. *Pancreatic lipase*, Elsevier Amsterdam.
VERHEY, F. R. J. 2009. Alois Alzheimer (1864–1915). *Journal of Neurology,* 256**,** 502-503. Available: 10.1007/s00415-009-0003-6
VERMA, K., TARAFDAR, A., MISHRA, V., DILBAGHI, N., KONDEPUDI, K. K. & BADGUJAR, P. C. 2021. Nanoencapsulated curcumin emulsion utilizing milk cream as a potential vehicle by microfluidization: Bioaccessibility, cytotoxicity and physico-functional properties. *Food Research International,* 148**,** 110611. Available: https://doi.org/10.1016/j.foodres.2021.110611
VILLARINO, B. J., DY, L. M. & LIZADA, M. C. C. 2007. Descriptive sensory evaluation of virgin coconut oil and refined, bleached and deodorized coconut oil. *LWT - Food Science and Technology,* 40**,** 193-199. Available: https://doi.org/10.1016/j.lwt.2005.11.007
VON ARNIM, C. A. F., GOLA, U. & BIESALSKI, H. K. 2010. More than the sum of its parts? Nutrition in Alzheimer's disease. *Nutrition,* 26**,** 694-700. Available: http://dx.doi.org/10.1016/j.nut.2009.11.009
WADE, T. & BEATTIE, J. K. 1997. Electroacoustic determination of size and zeta potential of fat globules in milk and cream emulsions. *Colloids and Surfaces B: Biointerfaces,* 10**,** 73-85.
WAHLSTROM, B. & BLENNOW, G. 1978. A study on the fate of curcumin in the rat. *Acta Pharmacol Toxicol (Copenh),* 43. Available: 10.1111/j.1600-0773.1978.tb02240.x
WAHLSTRÖM, B. & BLENNOW, G. 1978. A study on the fate of curcumin in the rat. *Acta pharmacologica et toxicologica,* 43**,** 86-92.
WALLACE, T. C. 2019. Health Effects of Coconut Oil—A Narrative Review of Current Evidence. *Journal of the American College of Nutrition,* 38**,** 97-107. Available: 10.1080/07315724.2018.1497562
WALSTRA, P., WALSTRA, P., WOUTERS, J., GEURTS, T. 2005. *Dairy Science and Technology.*, CRC Press. Available: https://doi.org/10.1201/9781420028010
WANG, J. & PANTOPOULOS, K. 2005. The pathway for IRP2 degradation involving 2-oxoglutarate-dependent oxygenase (s) does not require the E3 ubiquitin ligase activity of pVHL. *Biochimica et Biophysica Acta (BBA)-Molecular Cell Research,* 1743**,** 79-85.
WANG, X., JIANG, Y., WANG, Y. W., HUANG, M. T., HO, C. T. & HUANG, Q. 2008. Enhancing anti-inflammation activity of curcumin through O/W nanoemulsions. *Food Chem,* 108**,** 419-24. Available: 10.1016/j.foodchem.2007.10.086
WANG, Y., QIN, X. & PAUDEL, H. K. 2017. Amyloid β peptide promotes lysosomal degradation of clusterin via sortilin in hippocampal primary neurons. *Neurobiology of Disease,* 103**,** 78-88. Available: https://doi.org/10.1016/j.nbd.2017.04.003
WANG, Y.-J., PAN, M.-H., CHENG, A.-L., LIN, L.-I., HO, Y.-S., HSIEH, C.-Y. & LIN, J.-K. 1997. Stability of curcumin in buffer solutions and characterization of its degradation products. *Journal of Pharmaceutical and Biomedical Analysis,* 15**,** 1867-1876. Available: https://doi.org/10.1016/S0731-7085(96)02024-9
WASSALL, S. R., BRZUSTOWICZ, M. R., SHAIKH, S. R., CHEREZOV, V., CAFFREY, M. & STILLWELL, W. 2004. Order from disorder, corralling cholesterol with chaotic lipids: the role of polyunsaturated lipids in membrane raft formation. *Chemistry and Physics of Lipids,* 132**,** 79-88.

WEI, Q. Y., CHEN, W. F., ZHOU, B., YANG, L. & LIU, Z. L. 2006. Inhibition of lipid peroxidation and protein oxidation in rat liver mitochondria by curcumin and its analogues. *Biochim Biophys Acta,* 1760**,** 70-7. Available: 10.1016/j.bbagen.2005.09.008
WEIR, M. A., WALSH, M., CUERDEN, M. S., SONTROP, J. M., CHAMBERS, L. C. & GARG, A. X. 2018. Micro-Particle Curcumin for the Treatment of Chronic Kidney Disease-1: Study Protocol for a Multicenter Clinical Trial. *Can J Kidney Health Dis,* 5**,** 2054358118813088. Available: 10.1177/2054358118813088
WEISBRODT, N. 2001. Swallowing. *Gastrointestinal Physiology, 6th Edition, LR Johnson, Editor***,** 27-35.
WICKHAM, M., GARROOD, M., LENEY, J., WILSON, P. D. & FILLERY-TRAVIS, A. 1998. Modification of a phospholipid stabilized emulsion interface by bile salt: effect on pancreatic lipase activity. *Journal of Lipid Research,* 39**,** 623-632.
WIT, N. D., DERRIEN, M., BOSCH-VERMEULEN, H., OOSTERINK, E., KESHTKAR, S., DUVAL, C., BOSCH, J. D. V.-V. D., KLEEREBEZEM, M., MÜLLER, M. & MEER, R. V. D. 2012. Saturated fat stimulates obesity and hepatic steatosis and affects gut microbiota composition by an enhanced overflow of dietary fat to the distal intestine. *American Journal of Physiology-Gastrointestinal and Liver Physiology,* 303**,** G589-G599. Available: 10.1152/ajpgi.00488.2011
WOLTERS, F. J., TINGA, L. M., DHANA, K., KOUDSTAAL, P. J., HOFMAN, A., BOS, D., FRANCO, O. H. & IKRAM, M. A. 2019. Life Expectancy With and Without Dementia: A Population-Based Study of Dementia Burden and Preventive Potential. *American Journal of Epidemiology,* 188**,** 372-381. Available: 10.1093/aje/kwy234
YALLAPU, M. M., JAGGI, M. & CHAUHAN, S. C. 2012. Curcumin nanoformulations: a future nanomedicine for cancer. *Drug Discovery Today,* 17**,** 71-80. Available: https://doi.org/10.1016/j.drudis.2011.09.009
YAN, Y.-D., KIM, J. A., KWAK, M. K., YOO, B. K., YONG, C. S. & CHOI, H.-G. 2011. Enhanced Oral Bioavailability of Curcumin via a Solid Lipid-Based Self-Emulsifying Drug Delivery System Using a Spray-Drying Technique. *Biological and Pharmaceutical Bulletin,* 34**,** 1179-1186. Available: 10.1248/bpb.34.1179
YANG, F., LIM, G. P., BEGUM, A. N., UBEDA, O. J., SIMMONS, M. R., AMBEGAOKAR, S. S., CHEN, P. P., KAYED, R., GLABE, C. G. & FRAUTSCHY, S. A. 2005. Curcumin inhibits formation of amyloid β oligomers and fibrils, binds plaques, and reduces amyloid in vivo. *Journal of Biological Chemistry,* 280**,** 5892-5901.
YANG, K.-Y., LIN, L.-C., TSENG, T.-Y., WANG, S.-C. & TSAI, T.-H. 2007. Oral bioavailability of curcumin in rat and the herbal analysis from Curcuma longa by LC–MS/MS. *Journal of chromatography B,* 853**,** 183-189.
YARZA, R., VELA, S., SOLAS, M. & RAMIREZ, M. J. 2016. c-Jun N-terminal Kinase (JNK) Signaling as a Therapeutic Target for Alzheimer's Disease. *Frontiers in Pharmacology,* 6. Available: 10.3389/fphar.2015.00321
YE, A. 2008. Interfacial composition and stability of emulsions made with mixtures of commercial sodium caseinate and whey protein concentrate. *Food Chemistry,* 110**,** 946-952.
YEHUDA, S., RABINOVITZ, S., CARASSO, R. & MOSTOFSKY, D. 2000. Mixture of essential fatty acids rehabilitates stress effects on learning, and cortisol and cholesterol level. *Int J Neurosci,* 101**,** 73-87.
YEHUDA, S., RABINOVITZ, S., CARASSO, R. L. & MOSTOFSKY, D. I. 2002. The role of polyunsaturated fatty acids in restoring the aging neuronal membrane. *Neurobiology of Aging,* 23**,** 843-853. Available: 10.1016/S0197-4580(02)00074-X

YEHUDA, S., RABINOVITZ, S. & MOSTOFSKY, D. 2005a. Essential fatty acids and the brain: from infancy to aging. *Neurobiology of aging,* 26**,** 98-102.
YEHUDA, S., RABINOVITZ, S. & MOSTOFSKY, D. I. 1998. Modulation of learning and neuronal membrane composition in the rat by essential fatty acid preparation: time-course analysis. *Neurochemical research,* 23**,** 627-634.
YEHUDA, S., RABINOVITZ, S. & MOSTOFSKY, D. I. 2005b. Essential fatty acids and the brain: From infancy to aging. *Neurobiology of Aging,* 26**,** S98-S102. Available: 10.1016/j.neurobiolaging.2005.09.013
YOON, A. J., WU, H., PAN, R. D., TETER, B., CIPOLLA, J., CHANG, E., AVILA, L. Z., BASAK, S. K., SRIVATSAN, E. S., WANG, M. B., COLE, G. M., FRAUTSCHY, S. A., HAMPTON, P. D. & FAULL, K. F. 2020. A sensitive LC-MS assay using derivatization with boron trifluoride to quantify curcuminoids in biological samples. *Anal Biochem,* 596**,** 113636. Available: 10.1016/j.ab.2020.113636
YOUNG, S., BASIANA, E. & NITIN, N. 2018. Effects of interfacial composition on the stability of emulsion and encapsulated bioactives after thermal and high pressure processing. *Journal of Food Engineering,* 231**,** 22-29. Available: https://doi.org/10.1016/j.jfoodeng.2018.02.022
YU, H. & HUANG, Q. 2010. Enhanced in vitro anti-cancer activity of curcumin encapsulated in hydrophobically modified starch. *Food Chemistry,* 119**,** 669-674.
YU, J. E., KIM, M., POKHAREL, S., KIM, J., CHOI, I., CHOE, N.-H. & NAHM, S.-S. 2013. Potential use of adult bovine serum obtained during the slaughtering process as a biological reagent. *Animal Cells and Systems,* 17**,** 106-112. Available: 10.1080/19768354.2013.772073
YUAN, X., XIAO, J., LIU, X., MCCLEMENTS, D. J., CAO, Y. & XIAO, H. 2019. The gastrointestinal behavior of emulsifiers used to formulate excipient emulsions impact the bioavailability of β-carotene from spinach. *Food Chemistry,* 278**,** 811-819. Available: https://doi.org/10.1016/j.foodchem.2018.11.135
YUEN, A. W., SANDER, J. W., FLUEGEL, D., PATSALOS, P. N., BELL, G. S., JOHNSON, T. & KOEPP, M. J. 2005. Omega-3 fatty acid supplementation in patients with chronic epilepsy: a randomized trial. *Epilepsy & Behavior,* 7**,** 253-258.
ZHU, X., RAINA, A. K., LEE, H.-G., CASADESUS, G., SMITH, M. A. & PERRY, G. 2004. Oxidative stress signalling in Alzheimer's disease. *Brain research,* 1000**,** 32-39.
ZHU, X., SVENDSEN, C., JAEPELT, K. B., MOUGHAN, P. J. & RUTHERFURD, S. M. 2011. A comparison of selected methods for determining eicosapentaenoic acid and docosahexaenoic acid in cereal-based foods. *Food Chemistry,* 125**,** 1320-1327. Available: https://doi.org/10.1016/j.foodchem.2010.09.105
ZOU, L., ZHENG, B., ZHANG, R., ZHANG, Z., LIU, W., LIU, W., ZHANG, G., XIAO, H. & MCCLEMENTS, D. 2016. *Influence of Lipid Phase Composition of Excipient Emulsions on Curcumin Solubility, Stability, and Bioaccessibility*. Available: 10.1007/s11483-016-9432-9

Appendixes

Chapter 4

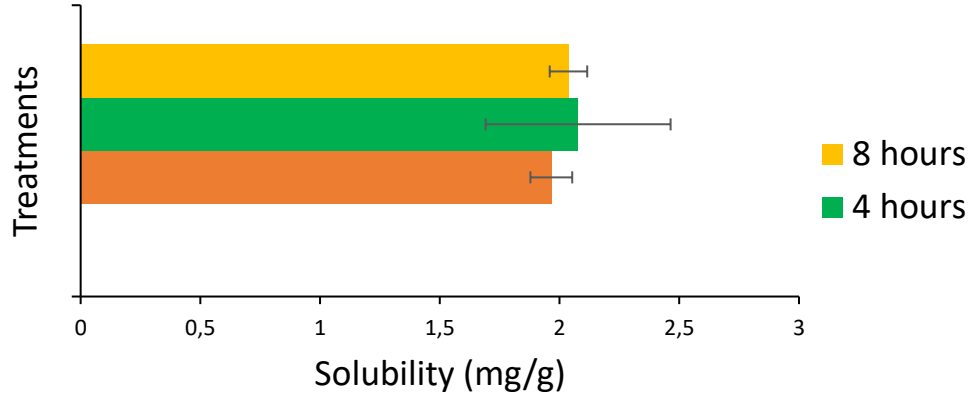

Figure A4.1. Solubility of curcumin in coconut oil after two, four and eight hours at 60°C. A calibration curve in methanol (1 to 16 mg/g) was used to calculate the concentrations after readings at 425nm in spectrophotometer.

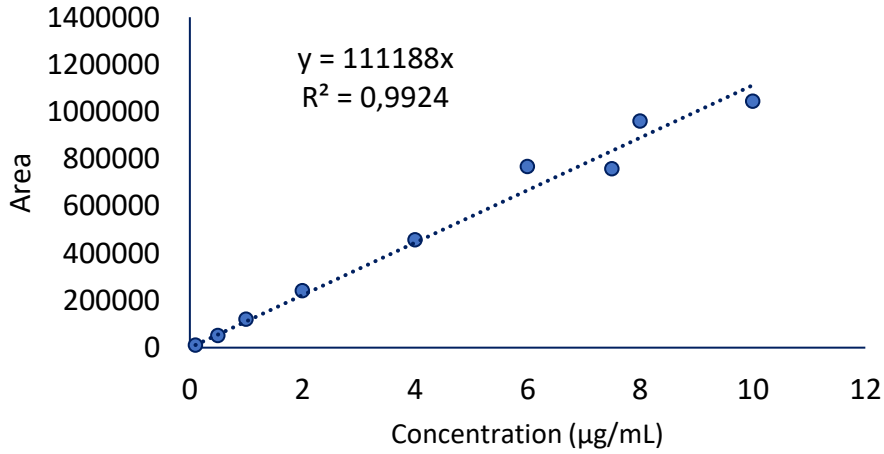

Figure A4.2. Calibration curve for curcumin in methanol. Concentrations in standard curves varied from 0.1µg/mL to 10 µg/mL. Concentration of curcumin was plotted against area of curcumin. Each timepoint had at least 4 readings. A linear trendline was applied and the obtained equation used to calculate concentration of curcumin in emulsions and digesta.

Table A4.3. Calibration data points for phospholipids in methanol. Calibration curve was generated by the software. Equation was used for calculation of phospholipids in emulsions, digested materials and ream and aqueous phase.

R^2	0.9969	0.99892	0.99809	0.99892	0.99391	0.99822	0.99851
	Observed µg/mL						
	PE	PC	SM	PS	PI - 260	LPE	LPC
Cal 13	0.241	0.210	0.230	0.019	0.031	0.040	0.027
Cal 12	0.329	0.345	0.302	0.023	0.066	0.071	0.045
Cal 11	0.636	0.728	0.615	0.041	0.105	0.079	0.083
Cal 10	1.679	1.473	1.202	0.086	0.242	0.214	0.169
Cal 9	3.639	3.159	2.887	0.156	0.442	0.406	0.306
Cal 8	7.453	7.662	6.190	0.323	1.040	0.758	0.636
Cal 7	13.460	16.160	13.530	0.626	2.087	1.716	1.406
Cal 6	23.940	29.910	27.020	1.369	3.199	3.339	2.517
Cal 5	39.330	46.350	48.140	3.572	6.244	6.170	4.974
Cal 4	55.900	65.530	78.180	9.825	10.320	11.210	9.787
Cal 3	79.740	83.290	113.900	21.390	17.510	19.900	17.600
Cal 2	107.400	100.900	139.400	41.290	21.840	31.710	29.340
Cal 1	139.200	114.900	154.100	65.760	36.640	49.260	46.750

Calibration points were obtained by serial dilution of standard starting from 500ng/mL. PE=Phosphatidylethanolamine, PC=Phosphatidylcholine, SM=Sphingomyelin, PS=Phosphatidylserine, PI=phosphatidylinositol, LPE- Lyso-Phosphatidylethanolamine, LPC- Lyso-Phosphatidylcholine. Asterix (*) indicate significant interactions between oil and emulsifier in the absorbed concentration of phospholipid (cream phase).

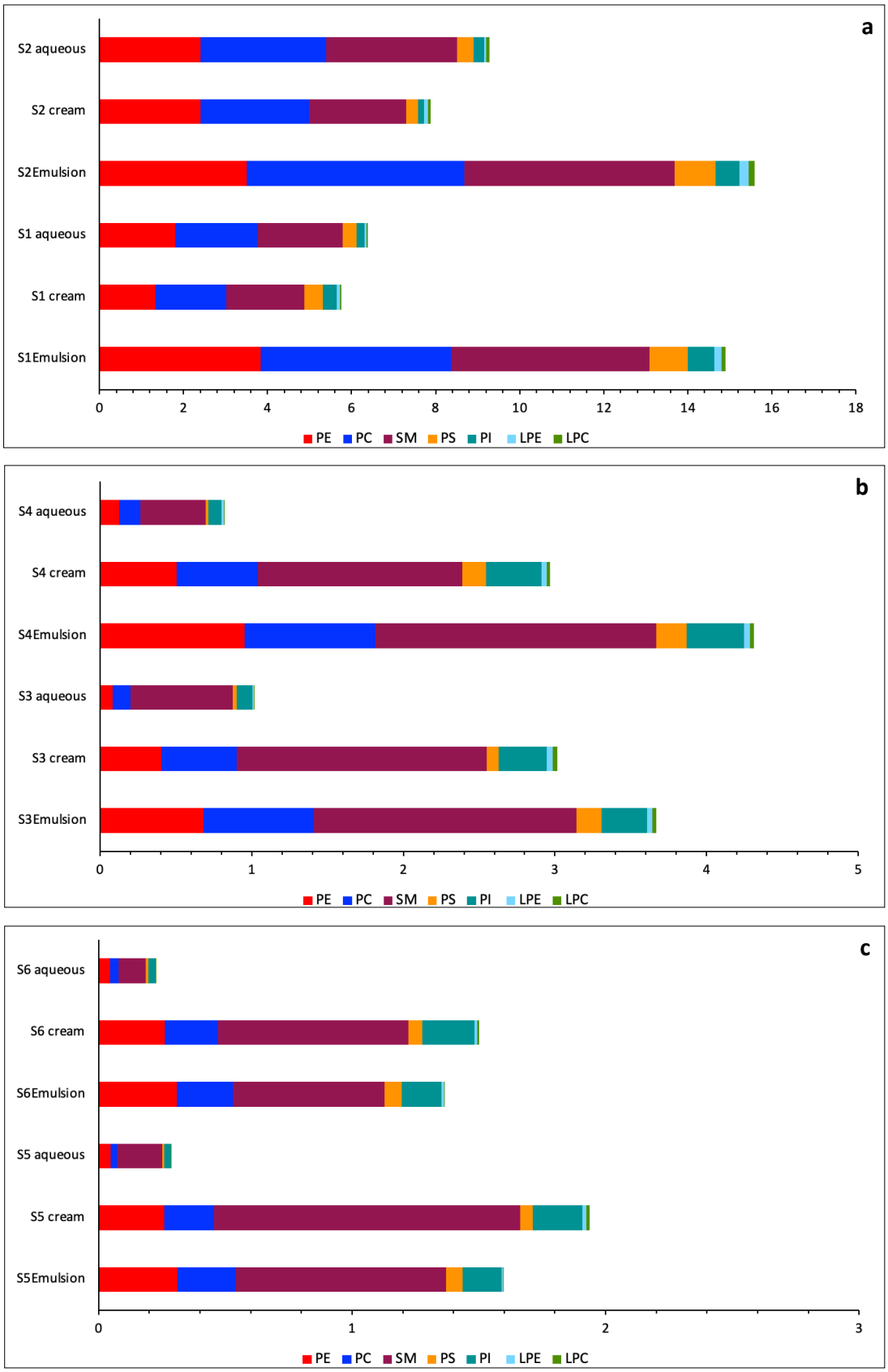

Figure A4.4. Total phospholipid distribution by class of freshly prepared emulsion systems and their respective cream and aqueous phase a) **S1**, 5% w/w MFGM1, 20% w/w coconut oil and **S2**, 5% w/w MFGM1, 10% w/w coconut oil, 10% w/w fish oil; b) **S3**, 3% w/w MFGM2, 20% w/w coconut oil and **S4**, 3% w/w MFGM2, 10% w/w coconut oil, 10% w/w fish oil; c) **S5**, 3% w/w MFGM3, 20% w/w coconut oil and **S6**, 3% w/w MFGM3, 10% w/w coconut oil, 10% w/w fish oil).

Chapter 6

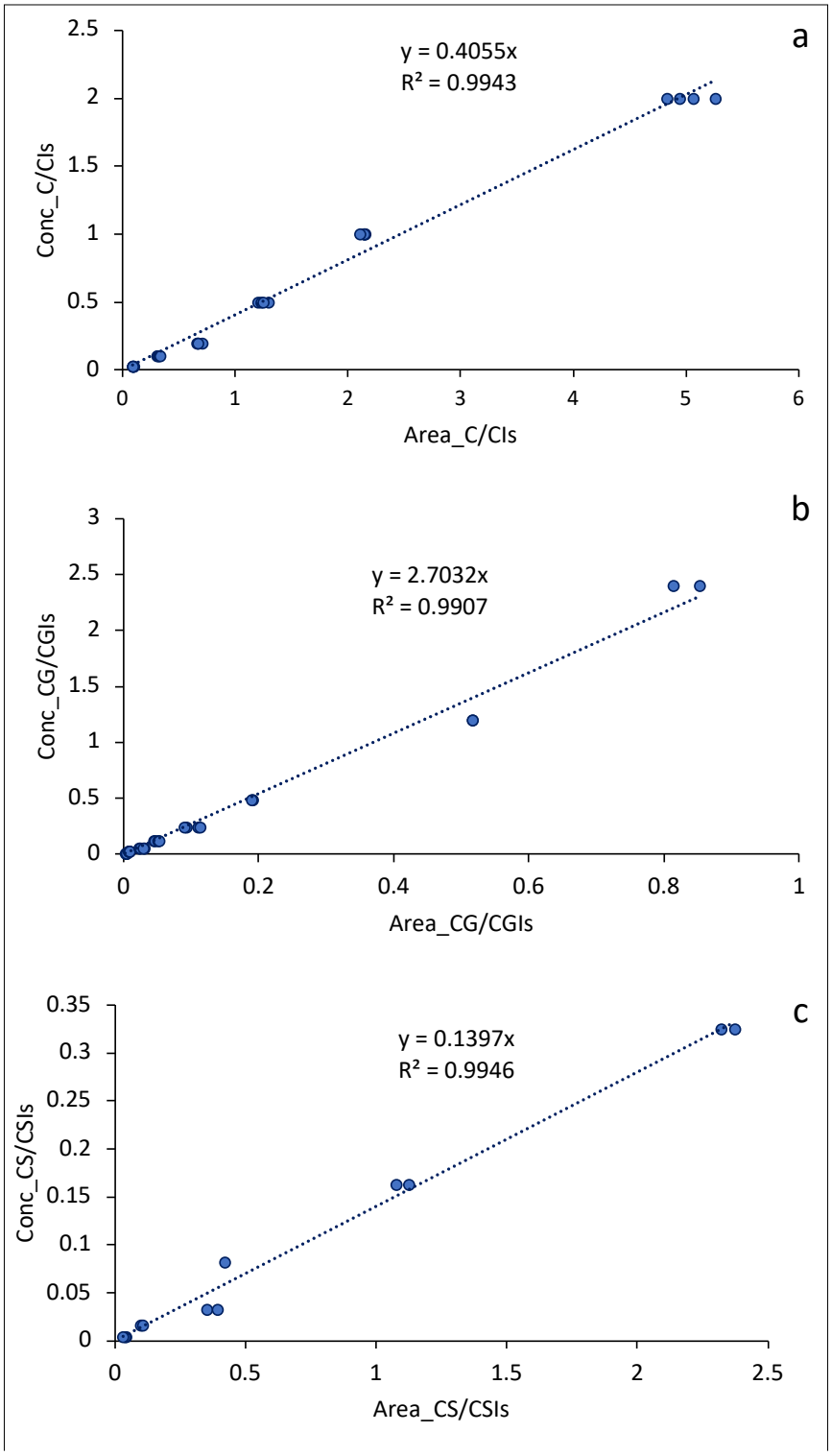

Figure A6.1. Calibration curve for curcumin (a), curcumin glucuronide (b) and curcumin sulfate (c) in rat plasma. Concentrations in standard curves varied from 0.126ng/mL to 50ng/mL. Concentration of compound was divided by its internal standard and plotted against area of compound divided by area of its internal standard. Each timepoint had 4 readings and outliers were removed from curves. A linear trendline was applied and the obtained equation used to calculate concentration of specific compounds in rat's plasma.

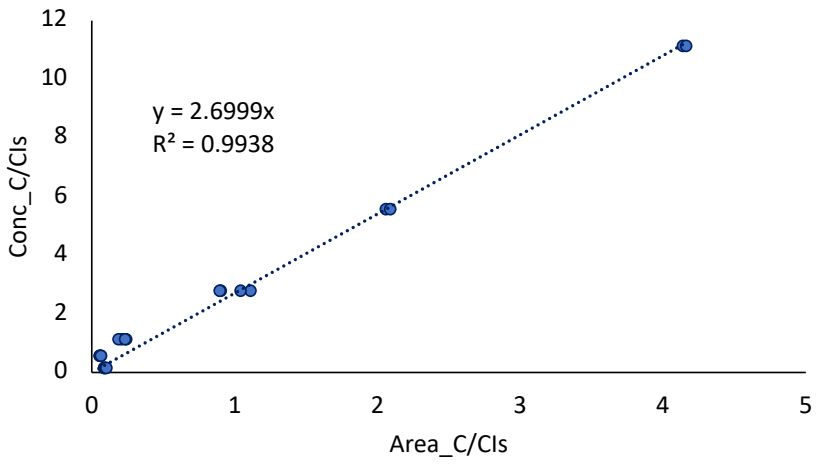

Figure A6.2. Calibration curve for curcumin in rat brain. Concentrations in standard curves varied from 0.125ng/mL to 10ng/mL. Concentration of curcumin was divided by its internal standard and plotted against area of curcumin divided by area of its internal standard. Each timepoint had 4 readings and outliers were removed from curves. A linear trendline was applied and the obtained equation used to calculate concentration of curcumin in rat's brain.